UNIVERSITAT POLITÈCNICA DE CATALUNYA
BARCELONATECH

Departament de Teoria del Senyal
i Comunicacions

Distributed Demand-Side Optimization in the Smart Grid

Ph.D. Thesis Dissertation

by

Italo Atzeni

Submitted to the Universitat Politècnica de Catalunya – Barcelona Tech
in partial fulfillment of the requirements for the degree of

DOCTOR OF PHILOSOPHY

Supervised by Prof. Javier Rodríguez Fonollosa and Dr. Luis García Ordóñez

Barcelona, June 2014

Ai miei genitori,

Summary

The modern power grid is facing major challenges in the transition to a low-carbon energy sector. The growing energy demand and environmental concerns require carefully revisiting how electricity is generated, transmitted, and consumed, with an eye to the integration of renewable energy sources. The envisioned smart grid is expected to address such issues by introducing advanced information, control, and communication technologies into the energy infrastructure. In this context, demand-side management (DSM) makes the end users responsible for improving the efficiency, reliability and sustainability of the power system: this opens up unprecedented possibilities for optimizing the energy usage and cost at different levels of the network.

The design of DSM techniques has been extensively discussed in the literature in the last decade, although the performance of these methods has been scarcely investigated from the analytical point of view. In this thesis, we consider the demand-side of the electrical network as a multiuser system composed of coupled active consumers with DSM capabilities and we propose a general framework for analyzing and solving demand-side management problems. Since centralized solution methods are too demanding in most practical applications due to their inherent computational complexity and communication overhead, we focus on developing efficient distributed algorithms, with particular emphasis on crucial issues such as convergence speed, information exchange, scalability, and privacy. In this respect, we provide a rigorous theoretical analysis of the conditions ensuring the existence of optimal solutions and the convergence of the proposed algorithms.

Among the plethora of DSM methods, energy consumption scheduling (ECS) programs allow to modify the user's demand profile by rescheduling flexible loads to off-peak hours. On the other hand, incorporating dispatchable distributed generation (DG) and distributed storage (DS) into the demand-side of the network has been shown to be equally successful in diminishing the

peak-to-average ratio of the demand curve, plus overcoming the limitations in terms users' inconvenience introduced by ECS. Quite surprisingly, while the literature has mostly concentrated on ECS techniques, DSM approaches based on dispatchable DG and DS have not attracted the deserved attention despite their load-shaping potential and their capacity to facilitate the integration of renewable sources. In this dissertation, we fill this gap and devise accurate DSM models to study the impact of dispatchable DG and DS at the level of the end users and on the whole electricity infrastructure.

With this objective in mind, we tackle several DSM scenarios, starting from a deterministic day-ahead optimization with local constraints and culminating with a stochastic day-ahead optimization combined with real-time adjustments under both local and global requirements. Each task is complemented by defining appropriate network and pricing models that enable the implementation of the DSM paradigm in realistic energy market environments. In this regard, we design both user-oriented and holistic-based DSM optimization frameworks, which are respectively applicable to competitive and externally regulated market scenarios. Numerical results are reported to corroborate the presented distributed schemes. On the one hand, the users' electricity expenditures are consistently reduced, which encourages their active and voluntary participation in the proposed DSM programs; on the other hand, this results in a lower generation costs and enhances the robustness of the whole grid.

Resum

La xarxa elèctrica moderna s'enfronta a enormes reptes en la transició cap a un sector energètic de baixa generació de carboni. La creixent demanda d'energia i les preocupacions ambientals requereixen revisar acuradament com es genera, transmet, i consumeix l'electricitat, amb l'objectiu de la integració de les fonts d'energia renovables. S'espera que el concepte de smart grid pugui abordar aquestes qüestions mitjançant la introducció d'informació avançada, control i tecnologies de la comunicació en la infraestructura energètica. En aquest context, el concepte de gestió de la demanda (DSM) fa que els usuaris finals siguin responsables de millorar l'eficiència, la fiabilitat i la sostenibilitat del sistema de potència obrint possibilitats sense precedents per a l'optimització de l'ús i el cost de l'energia en els diferents nivells de la xarxa.

El disseny de tècniques de DSM s'ha debatut àmpliament en la literatura durant l'última dècada, tot i que el rendiment d'aquests mètodes ha estat poc investigat des del punt de vista analític. En aquesta tesi es considera la demanda de la xarxa elèctrica com un sistema multiusuari format per consumidors actius amb capacitats de DSM i es proposa un marc general per analitzar i resoldre problemes de gestió. Donat que els mètodes de solució centralitzats són excessivament exigents per a aplicacions práctiques per la seva complexitat computacional i al inherent sobrecost de comunicació, ens centrem en el desenvolupament d'algorismes distribuïts, amb especial èmfasi en temes crucials com la velocitat de convergència, l'intercanvi d'informació, l'escalabilitat i la privacitat. En aquest sentit, oferim un rigorós anàlisi teòric de les condicions que garanteixen l'existència de solucions òptimes i la convergència dels algorismes proposats.

Entre la gran quantitat de mètodes de DSM, els programes de programació del consum d'energia (ECS) permeten modificar el perfil de la demanda dels usuaris a través de la reprogramació de càrregues flexibles durant hores de baix consum. D'altra banda, la incorporació de generació distribuïda (DG) i d'emmagatzematge distribuït (DS) ha demostrat ser igualment

eficaç disminuint la relació entre potència de pic i mitja de la corba de demanda, evitant els inconvenients introduïts pel ECS als usuaris. Sorprenentment, si bè que la literatura s'ha concentrat sobretot en les tècniques de ECS, les tècniques de DSM basades en DG i DS no han atret l'atenció merescuda malgrat el seu potencial de conformació de la càrrega i la seva capacitat de facilitar la integració de les fonts renovables. En aquesta tesi, omplim aquest buit i elaborem models precisos de DSM per estudiar l'impacte de DG i DS a nivell dels usuaris finals i de tota la infraestructura elèctrica .

Tenint present aquest objectiu, fem front a diversos escenaris de DSM, partint d'una optimització sobre les previsions amb un dia d'antelació (day-ahead). Es considera des del cas determinista amb restriccions locals fins al cas estocàstic combinat amb ajustos en temps real i amb restriccions locals i globals. Cada tasca es complementa amb la definició de models de xarxa i de tarifació apropiats que permetin la posada en pràctica del paradigma de DSM en entorns realistes del mercat energètic. En aquest sentit vam dissenyar marcs d'optimització de DSM globals i orientats als usuaris, que són respectivament aplicables a situacions de mercat competitives i regulades externament. Els resultats numèrics reportats corroboren els esquemes distribuïts presentats. D'una banda, les despeses d'electricitat dels usuaris es redueixen de forma consistent, el que fomenta la seva participació activa en els programes de DSM proposats; per una altra banda, aquesta optimització resulta en un cost de generació inferior i millora la robustesa de tota la xarxa.

Resumen

La red eléctrica moderna se enfrenta a enormes retos en la transición hacia un sector energético de baja generación de carbono. La creciente demanda de energía y las preocupaciones ambientales requieren revisar cuidadosamente cómo se genera, transmite y consume la electricidad, con vista a la integración de las fuentes de energía renovable. Se espera que el concepto de smart grid pueda abordar estas cuestiones mediante la introducción de información avanzada, control y tecnologías de la comunicación en la infraestructura energética. En este contexto, el concepto de gestión de la demanda (DSM) hace que los usuarios finales sean responsables de mejorar la eficiencia, la fiabilidad y la sostenibilidad del sistema de potencia abriéndose posibilidades sin precedentes para la optimización del uso y el coste de la energía en los diferentes niveles de la red.

El diseño de técnicas de DSM se ha debatido ampliamente en la literatura en la última década, aunque el rendimiento de estos métodos ha sido poco investigado desde el punto de vista analítico. En esta tesis se considera la demanda de la red eléctrica como un sistema multiusuario compuesto por consumidores activos con capacidades de DSM y se propone un marco general para analizar y resolver problemas de gestión de demanda. Dado que los métodos de solución centralizados son excesivamente exigentes para aplicaciones prácticas debido a su complejidad computacional y al inherente sobrecoste de comunicación, nos centramos en el desarrollo de algoritmos distribuidos, con especial énfasis en temas cruciales como la velocidad de convergencia, el intercambio de información, la escalabilidad y la privacidad. En este sentido, ofrecemos un riguroso análisis teórico de las condiciones que garantizan la existencia de soluciones óptimas y la convergencia de los algoritmos propuestos.

Entre la gran cantidad de métodos de DSM, los programas de programación del consumo de energía (ECS) permiten modificar el perfil de la demanda de los usuarios a través de la

reprogramación de cargas flexibles durante horas de bajo consumo. Por otro lado, la incorporación de generación distribuida (DG) y de almacenamiento distribuido (DS) ha demostrado ser igualmente eficaz disminuyendo la relación entre potencia de pico y media de la curva de demanda, evitando los inconvenientes introducidos por el ECS a los usuarios. Sorprendentemente, mientras que la literatura se ha concentrado sobre todo en las técnicas de ECS, los programas de DSM basados en DG y DS no han atraído la atención merecida a pesar de su potencial de conformación de la carga y su capacidad de facilitar la integración de las fuentes renovables. En esta tesis, llenamos este vacío y elaboramos modelos precisos de DSM para estudiar el impacto de DG y DS a nivel de los usuarios finales y de toda la infraestructura eléctrica.

Teniendo presente este objetivo, hacemos frente a varios escenarios de DSM, a partir de una optimización sobre las previsiones con un día de antelación (day-ahead). Se considera desde el caso determinista con restricciones locales hasta el caso estocástico combinado con ajustes en tiempo real y con restricciones locales y globales. Cada tarea se complementa con la definición de modelos de red y de tarificación apropiados que permitan la puesta en práctica del paradigma de DSM en entornos realistas del mercado energético. En este sentido diseñamos marcos de optimización de DSM globales y orientados a los usuarios, que son respectivamente aplicables a situaciones de mercado competitivas y reguladas externamente. Los resultados numéricos reportados corroboran los esquemas distribuidos presentados. Por un lado, los gastos de electricidad de los usuarios se reducen de forma consistente, lo que fomenta su participación activa en los programas de DSM propuestos; por otra parte, esta optimización resulta en un coste de generación inferior y mejora la robustez de toda la red.

Acknowledgements

So many times during the last four years I've wished I had one of those boring, ordinary jobs that you don't have to think about outside of the regular working hours. Nonetheless, this is exactly what I wanted to avoid when I decided to pursue a PhD degree. For this reason, I'd like to express my deepest gratitude to my supervisor Prof. Javier R. Fonollosa for giving me this life-changing opportunity and for encouraging me all the way through it: I really appreciate your precious guidance and the confidence you have constantly shown in me. Likewise, I'd like to thank Dr. Luis G. Ordóñez for taking me under his wing (literally) with great patience and dedication: to you I owe most of the things that I've learned during these years. A special mention goes to Prof. Daniel P. Palomar and Prof. Gesualdo Scutari, with whom I've had the pleasure to collaborate and from whom I've acquired crucial technical skills. Besides, I thank Dani for the rewarding and pleasant experience at the Hong Kong University of Science and Technology and for treating me like another member of his group. From these four people, I've gained not only invaluable knowledge and expertise, but also inspiration to remain in the academic field.

To all the great people that I've met at the UPC, especially Prof. Alba Pagès Zamora (who gave me my first teaching opportunity), Silvana, Adriano, Luis, Toni, and my fellow Hongkonger Maria: thank you all for the pleasant company and advice in every situation.

Thanks to my dear friends scattered around the world, always making jokes about me not having a "real" job, without whom I would have surely graduated earlier. To the people who made Barcelona even more beautiful and enjoyable, especially Claudio, Farina, Grzegorz, Laura, Ashley, Isa, Fedele, and the huge FC Michael Collins family: you all owe me countless hours of sleep and perhaps a new liver. A special recognition to my mates from Cagliari ("oh, ma quando scendi?") for your distant yet unconditional support (bomba!): Ale, Dani, Foche, Franca, Garau, Gianlu, Il Buon, Ila, La Bionda, Luga, Margy, Mariadda, Mastro, Michael, Piojo, Scucca, Scucco,

Ste, Vale, Vanuel, Varca, Varco, and my dearest flatmate Varta (in strict alphabetical order). And of course I could not forget my Erasmus family, especially Pino, Sarah, Domingo, and Neri. I'd also like to mention Pizzeria N.A.P. for giving me a weekly taste of home, and Bateras Beat Sardegna for filling my neighbors' ears with hours of drumming exercises.

Thanks Roby for your patience and unconditional love, for all the visits, and for the tons of food you have smuggled through the route Cagliari-Barcelona. Last but not least, I thank my family: my mom for being my best mentor since 1984 and for giving me confidence even in the darkest moments of this experience, Plutone (I wish you'd called me more often), Giorgio, and my grandma for always thinking of me as a genius. I'll never be one, but at least I'll soon be a doctor.

The work of this thesis was supported in part by the Catalan Government (FI-DGR2011 AGAUR) and by the European Union (FP7-SME-2012-1-315007).

Contents

Acronyms and Abbreviations

cdf	cumulative density function.
cf.	(from Latin *confer*) compare.
DA	Day-Ahead.
DDPA	Distributed Dynamic Pricing Algorithm.
DG	Distributed Generation.
DS	Distributed Storage.
DSM	Demand-Side Management.
ECS	Energy Consumption Scheduling..
e.g.	(from Latin *exempli gratia*) for example.
GNE	Generalized Nash Equilibrium.
GNEP	Generalized Nash Equilibrium Problem.
HA	Home Appliances.
i.e.	(from Latin *id est*) that is.
NE	Nash Equilibrium.
NEP	Nash Equilibrium Problem.
PAR	Peak-to-Average Ratio.
PDA	Proximal Decomposition Algorithm.
pdf	probability density function
QVI	Quasi-Variational Inequality.
RES	Renewable Energy Source.
RT	Real-Time.
SM	Smart Meter.
VI	Variational Inequality.

1

Introduction

1.1 The Smart Grid

The *Smart Grid* is the envisioned electrical network that integrates advanced information, control, and communication technologies into the current grid infrastructure in order to guarantee the optimized usage of its capacity. The smart grid aims at improving the interaction between all participants in the electricity industry (providers, transmission lines, substations, distribution networks, and consumers) by means of smart metering and bidirectional communications, encouraging active participation by all of them. These advances result in a power system that is more secure and efficient, that ensures low losses and high quality of supply, and that facilitates the integration of renewable energy sources [1, 2].

Today's electrical grid is a complex network comprising several subsystems, which can be conveniently divided into *supply-side* and *demand-side*. Typically, the supply-side consists of a few hundred generators interconnected by a transmission network and serving several hundred substations. The demand-side starts from each substation downwards, where the distribution network has a simple topology and connects to a large number of consumers in a treelike structure [3]. Since generators are not usually located close to the consumers, the transmission/distribution of the electricity entails considerable capital investments and often yields significant energy losses [4].

The smart grid concept, with distributed generation as one of its key elements, is expected to reduce the distance between energy production and consumption, transforming the traditional electrical network into a much more decentralized power system [5–7]. This becomes even more relevant in light of the increasing penetration of small-scale power generators, individually owned renewable resources (such as solar panels and wind turbines), and electric vehicles, which gives

rise to irregularly distributed energy sources. In this context, those who were once just electricity consumers become buyers/sellers establishing a bidirectional power flow with the distribution network.

A tangible consequence of distributed generation and of the related new distribution infrastructure is the advent of microgrids, which are localized, self-sufficient groups of electricity generators, storage devices, and loads that are able to disconnect from the rest of the electrical network. This practice, referred to as "islanding mode", allows to isolate any disturbance in the outer transmission/distribution grid. Indeed, the intentional islanding of bounded network sectors has the potential to improve the local reliability of the electricity supply with respect to that provided by the power system as a whole [8,9]. Despite increasing the system flexibility and reducing losses, such transformation sensibly complicates the power flow network constraints: this calls for the investigation of smarter energy distribution and delivery methods [4].

A fundamental principle of any power system is that electricity consumption and production must be precisely balanced at all times, for any mismatch between the two can cause grid instability and severe voltage fluctuation, producing power outages and blackouts. In the conventional electrical network, it has always been the responsibility of the supply-side to follow the load demanded by the consumers. For this reason, the generation and transmission capacity is sized to meet peak demand that only occurs sporadically. Besides, this state of things favors fast-ramping, dispatchable generation, mostly relying on fossil fuels. Undeniably, the so-called peaking generators, which operate only during peak demand, account for a large portion of the energy cost and carbon emissions [10]. In this respect, renewable energy sources will play an increasingly crucial role to achieve a more sustainable energy network.

Integrating massive amounts of renewable production into the bulk power grid poses great challenges for generation planning and system stability [11]. Therefore, under the smart grid paradigm, the demand is encouraged to follow the available production to accommodate the intermittent nature of the renewable resources. This represent an important breakthrough in the future electrical network. On this matter, demand-side management (DSM) refers to the plethora of initiatives intended to modify the timing and the amount of the energy load demand [12]. DSM introduces advanced mechanisms for encouraging the end users to individually manage their consumption schedules in a way that is beneficial for the whole grid. With smart meters embedding intelligence into the demand-side and with the deployment of enhanced DSM methods, the demand-side becomes the main actor in the network optimization process.

Traditionally, residential customers have always paid a fixed price per unit of electricity, which is meant to represent an average cost of power generation over a given time interval regardless of the actual generation cost. In this context, the end-users are shielded from making short-term market decisions, since their actions are not affected by, and do not affect, the energy prices. In

contrast, under price-based DSM programs, the retail prices are connected with the generation cost and vary according to the availability of energy supplies. The concept of dynamic pricing involves price signals that are constantly delivered to the consumers as economic incentives to modify their demand and alleviate the pressure on the grid, with the reward of lowering their bill [12].

The electricity market is also experiencing significant changes towards deregulation and competition with the aim of improving economic efficiency [13]. In such context, providers and consumers compete to exchange energy at a price set by the market, as a result of the interaction among all of them, while maximizing their own profit/benefit. Obviously, the complexity of the market mechanisms regulating the energy trading among competing agents increases notably under the smart grid paradigm. This is due to the difficulty of balancing demand and supply in the presence of decentralized generation and while dealing with the uncertainty induced by the renewable supply.

Addressing these challenges for the smart grid involves technology that leverages a number of emerging signal processing techniques [14]. The smart grid concept has been recognized as "*a major initiative related to the field of energy with significant signal processing content*" which requires expertise in the fields of communication, sensing, optimization, and machine learning [15]. Indeed, there are many areas where signal processing research can contribute to pave the way for a greener and more efficient energy grid.

1.2 State of the Art

Not surprisingly, all these premises are arousing the interest of the signal processing community. It is hardly possible here to even summarize the huge amount of research that has been done in the field of signal processing applied to smart grids. In fact, this topic has gained so much popularity in the past 10 years to deserve dedicated journals and conferences, and even to claim a relevant spot in the major existing publications in signal processing (cf. [16, 17]) and communications (cf. [18–24]).

The first publications were mainly focused on the communication and control aspects of the smart grid. Undoubtedly, the smart communication infrastructure is the primary ingredient of the future power system since it allows to collect and exchange information (e.g., about energy prices and network state) to guarantee the efficient trading and dispatch of electricity [25, 26]. The large-scale deployment of smart meters, which provide an interface between customers and providers, requires ad-hoc machine-to-machine transmission schemes that ensure quality of service, security, and privacy, and that can adapt to the ever-changing topology of the network [27]. In this regard, power line communication has been intensively investigated since it exploits the connections provided by the existing energy grid and greatly reduces the implementation

cost [28]. Nonetheless, advanced information and communication technologies are only enablers of the envisioned power system and, more importantly, they are not the sole aspects that can benefit from the contribution of the signal processing community.

The smart grid is expected to provide real-time, system-wide situation awareness, and advances in state estimation via enhanced sensing and telemetry will play an important role in attaining this goal. Responsive and robust monitoring techniques are essential to perform various important control and planning tasks such as optimizing power flows, analyzing contingencies, and determining necessary corrective actions against possible failures [14, 29]. However, the process of acquiring and transmitting massive volumes of information across the network often produces noisy or corrupted data: this could be due to several reasons including sensor miscalibration or outright damages, as well as communication errors caused by noise, network congestion/outages, and malicious attacks. Automated analysis and bad data detection are thus instrumental to operate the grid reliably [30, 31], especially in light of the anticipated "big data" challenge that will inevitably pervade the energy industry [32].

Maintaining the reliability of the grid and meeting its operational requirements are crucial tasks that are further complicated by the uncertainty associated with renewable energy generation, load demand, and energy prices. Of particular interest is the role of statistical signal processing and machine learning in modeling and forecasting such time-varying factors [33]. For instance, decision-making in the day-ahead energy market is characterized by a certain degree of uncertainty in both demand- and supply-side. Therefore, some level of risk aversion or robust optimization is desirable in order to control the variability of the loss/dissatisfaction of the market agents [34, Ch. 4.2], [35, 36].

In the following, we focus our attention on state-of-the-art DSM methods; then, we briefly review the optimization techniques that are employed in this thesis to carry out the proposed DSM programs.

1.2.1 Demand-Side Management

Demand-side management aims at ensuring that the demand-side users behave responsively to the available (possibly renewable) energy production and, more generally, to the current state of the power grid. The basic principle behind DSM is that energy-aware decisions made locally at the demand-side will inevitably be beneficial at a global level in terms of reliability of the whole infrastructure and overall energy costs. Some primitive forms of DSM have been considered since the early 1980s [37] and have evolved over the past decades thanks to the activities of researchers, power utilities, and governments designed to change the time pattern and the magnitude of the load demand.

A well-consolidated DSM approach is *direct load control*, through which the utilities can force residential subscribers to decrease their consumption by remotely controlling the operations of certain appliances (see, e.g., [38, 39]). However, this sort of programs involve a rather passive role of the subscribers and have serious privacy and scalability implications [40]. In fact, there are social and legal barriers to overcome as the customer must explicitly authorize the energy provider to actuate directly over his household appliances. Furthermore, such centralized schemes typically rely on large-scale algorithms that entail high computational complexity and substantial communication overhead. In this respect, devising distributed and scalable methods, which imply a more active role of the end users, is of paramount importance for the successful deployment of DSM.

The smart grid paradigm promises to introduce more advanced mechanisms that permit and encourage the active and voluntary participation of the demand-side towards a distributed optimization of the electrical infrastructure. To this end, the smart meter surpasses the classical metering and billing role and allows to manage the user's energy demand by taking into account different factors such as user convenience, grid capacity, and sustainable energy production, and to actuate accordingly on his own intelligent appliances, generators, storage devices, etc. [5, 33]. Among all, advanced smart metering enables the implementation of *dynamic pricing*, which provides the demand-side with the economic incentives for a responsible energy consumption.

The generation costs at the supply-side suffer continuous variations in order to satisfy the irregular demand over the day. Despite this, most subscribers are still charged flat-rate retail prices for electricity, which do not reflect the actual wholesale prices. Furthermore, the fluctuation between the so-called off-peak and peak hours not only induces high costs to the providers, but also has a negative impact on the stability of the power grid [41]. The principle of dynamic pricing is to charge the users based not only on "how much" but also on "when" electricity is consumed, encouraging them to decrease the peak-to-average ratio (PAR) by shifting their usage to off-peak hours. Properly designed dynamic pricing mechanisms are expected to [42]: i) flatten the load demand curve, which enhances the robustness of the whole network and reduces the need of peaking power plants; ii) lower generation costs, which decreases the wholesale prices and increases the suppliers' profit; iii) reduce the users' electricity expenditures. The plethora of initiatives whereby demand-side users respond to dynamic pricing signals is often referred to as *demand response* [43].[1]

There are three main ways through which the active subscribers can exploit the incentives given by the dynamic pricing paradigm and achieve a more flattened demand, namely: i) *dispatchable distributed energy generation* (DG), ii) *distributed energy storage* (DS), and iii) *energy*

[1] Note that, in this thesis, we group together the connected areas of DSM and demand response due to the close relationship between the two.

consumption scheduling (ECS).

i) Distributed energy resources can be classified depending on the nature of their output as non-dispatchable (intermittent) or dispatchable (controllable) [44, Ch. 7.1]. Non-dispatchable, renewable sources are strictly dependent on the weather conditions: such devices as solar panels and wind turbines generate electricity at their maximum capacity whenever possible (since they only have fixed costs) and, therefore, cannot serve the purpose of providing energy at will. To the contrary, dispatchable sources as, e.g., internal combustion engines, gas turbines, and fuel cells, can be required to supply a constant amount of power for a certain time interval. Precisely, one can employ dispatchable DG to diminish his demand from the grid whenever is convenient [45].

ii) Fast-response energy storage allows to manage the grid imbalances caused by volatile sources and enables demand shifting in order to shave off the peak in the load demand [12,43]. Traditionally, energy storage has been a concern of the suppliers, which use large chemical batteries to put aside the energy in excess from their solar and wind farms. However, centralized storage of massive amounts of energy is still highly expensive and inefficient, whereas smaller-scale DS is becoming a more attractive and viable option [46, 47]. Electric vehicles will play an important role in increasing the DS capacity of the smart grid although, on the other hand, they also introduce further uncertainty in the dynamics of energy consumption. A large body of the DSM literature is devoted to the optimization of the charging/discharging schedule of electric vehicles in terms of customer comfort and grid stability; see, e.g., [48–50] for more details on this topic.

iii) Perhaps the most popular DSM approach in the smart grid literature is ECS (cf. [51–54]): in this kind of methods, the user's appliances are usually divided into flexible, i.e., with soft scheduling constraint (such as dishwasher, clothes dryer, electric vehicles, etc.) and inflexible, i.e., with strict scheduling constraint (such as refrigerator, lighting, heating, etc.). The purpose of ECS is thus to modify the individual demand profiles by scheduling flexible loads to off-peak hours, which calls for intelligent and responsive appliances. The implementation of ECS techniques has been shown to be successful in diminishing the PAR of the load curve; however, since the users' inconvenience must be taken into account (e.g., the rescheduling of activities results in lost services for industrial customers [55]), ECS presents flexibility limitations that can be overcome by incorporating dispatchable DG and DS into the demand-side of the network.

By the aforementioned initiatives, the demand-side users locally pursue the minimization of their electricity bill while maintaining certain standards of comfort. In particular, the optimal DG, DS, or ECS strategies are calculated automatically by their smart meter, which responds to the dynamic pricing schemes established by the market regulator. In this scenario, the users will tend to generate, discharge their batteries, and reschedule flexible loads when the energy is most expensive, which generally occurs during hours of peak load or shortage of renewable

energy.

The short-term electricity market[2] consists mainly of a day-ahead market, which produces financially binding schedules for energy demand and supply before the operating day, and a real-time market, used to balance day-ahead and real-time energy requirements [34, Ch. 1.2]. Accordingly, DSM finds concrete applications to optimize the subscribers' demand profiles at both temporal scales [54, 56]. Day-ahead DSM allow the supply-side to know in advance the amount of energy to be provided to the demand-side along the time period of analysis and to plan its production accordingly. On the other hand, by applying real-time DSM techniques, it is possible to take into consideration the uncertainties induced by the unpredictable behavior of renewable energy sources, contingencies in the supply-side, and the randomness of the users' consumption [57].

1.2.2 Optimization Techniques

Optimization methods have become ubiquitous in power systems and, particularly, in DSM. The optimization of the demand-side has been traditionally formulated from the selfish point of view of the end user, who is interested in maximizing his own welfare regardless of the others' (other subscribers, utilities, etc.) [51,58]: in this context, the resulting strategies that are individually optimal may not be socially optimal in terms of, e.g., minimum PAR of the energy demand curve or minimum total energy cost. Nonetheless, from a social fairness perspective, it is desirable to utilize the load shaping capacity of the individual subscribers in a way that attains some measure of global welfare [59–61]. These two alternatives are suitable for competitive and externally regulated market scenarios, respectively.

Most problems of practical interest can be properly formulated as constrained optimization problems. In some cases, possibly after some mathematical manipulations, such problems can be expressed in convex form. Convex optimization problems arise quite frequently in practical applications and their importance stems from the fact that powerful analytical and algorithmic tools are available for their study and solution (as, for example, the well-known interior-point method). These solution methods are so efficient and reliable that they can be embedded in a computer-aided design or analysis tool. Some prominent references to this topic, from both mathematical and algorithmic perspectives, are [62–64].

In this dissertation, we attack the demand-side optimization problem from two different perspectives, namely: a user-oriented optimization, and a holistic-based design. Therefore, in the following, we first discuss noncooperative game theory (and the more general framework of variational inequality theory); then, we introduce a very recent method for the distributed

[2] Medium- and long-term electricity trading between producers and retailers/consumers, which take place through futures markets and bilateral contracts [34, Ch. 1.2], are not the focus of this thesis.

optimization of nonconvex sum-utility functions (see also Section 2.1.2). Both these frameworks are somehow related to convex optimization.

Noncooperative Game Theory and Variational Inequality

Game theory is a field of applied mathematics that describes and analyzes scenarios with interactive decisions. A game can be represented as a set of coupled optimization problems relying on two basic assumptions: i) the decision makers (called players) are rational, i.e., they pursue well defined exogenous objectives; ii) the players act strategically, i.e., they take into account their knowledge or expectations of the other players' behavior [65]. Game theoretical approaches provide meaningful models for many applications where the interaction among several agents is by no means negligible and centralized approaches are not suitable.

Game theory has strong potential for addressing several emerging issues in the smart grid, given its heterogeneous and large-scale nature. This promising view is corroborated by the recent results and advances in game theoretical approaches applied to communications and networking problems (e.g., in cognitive radio systems [66] as well as in resource allocation [67] and power control [68, 69] in wireless networks). Indeed, as a result of the deregulation of the energy market, there has been recently a growing interest in using games to model the interaction among smart grid participants: an overview on this topic is given in [70] (see also [71]). In particular, the essence of DSM revolves naturally around the interactions between various entities with specific objectives. Under the umbrella of DSM techniques, real-time and day-ahead ECS problems have been widely studied in literature using game theoretical frameworks (for example in [51, 58, 72, 73]).

Noncooperative game theory is a broad branch of game theory where the players act selfishly to optimize their own well-being. In this thesis, we deal with two categories of noncooperative game theoretical problems: the first is the class of Nash equilibrium problems (NEPs), where the interaction among players takes place at the level of objective functions only; the second is the class of generalized NEPs (GNEPs), where each strategy set, i.e., the spectrum of the choices available to each player, also depends on the actions taken by his rivals [74]. Although GNEPs have a wider range of applicability (essentially, any case where the players share a limited, common resource), they are much harder problems than ordinary NEPs. This is due to the coupling in the strategy sets, which prevents the application of well-known decomposition methods available for NEPs and sensibly complicates the design of distributed algorithms for their solution. We refer to [75] for a detailed discussion on this topic.

The variational inequality (VI) problem constitutes a very general class of problems in nonlinear analysis, which encompasses convex optimization and bears strong connections to game theory. The VI framework proves suitable for investigating and solving various equilibrium mod-

els even when classical game theory may fail. Formulating a noncooperative game as a VI problem allows to easily study existence, uniqueness, and stability of the solutions and, more importantly, it leads quite naturally to the derivation of implementable solution algorithms along with their convergence properties [76]. We refer the interested reader to [74, 77–79] for a comprehensive treatment of the subject.

As stated above, the concept of GNEP extends the classical NEP setting by assuming that each player's strategy set can depend on the rivals' strategies. In its full generality, GNEPs are almost intractable and also the VI approach is of no great help. However, for the special class of GNEPs with jointly convex shared constraints, some solutions (termed as variational solutions) can be studied and calculated relatively easily by using a VI approach [74, 75]. In the specific, variational solutions can be interpreted as the solution of a NEP with pricing.

Nonconvex Sum-Utility Optimization

In some contexts, instead of adopting a noncooperative approach, it is meaningful to optimize the "social function" given by the sum of the users' individual objective functions. Since centralized solution methods are too demanding in most applications, the main difficulty of this formulation lies in performing the optimization in a distributed fashion with limited signaling among the users. When the social problem is a sum-separable convex programming, many distributed methods, e.g., based on primal and dual decomposition techniques [80, 81], have been proposed.

Very recent results in [82, 83] allow to deal with the more frequent and difficult case in which the social function is nonconvex. Traditionally, optimization problems of this form have been tackled by using gradient-based algorithms, which solve a sequence of convex problems by convexifying the whole social function: because of that, they generally suffer from slow convergence. By exploiting any degree of convexity that might be present in the sum-utility function, it is possible to obtain decomposition methods that converge to stationary points of the nonconvex social problem, resulting in the parallel solution of convex subproblems (one for each user). Since such a procedure preserves some structure of the original objective function, it is expected to be faster than classical gradient algorithms for nonconvex sum-utility problems.

1.3 Thesis Structure

In order to maximize the dissemination of results, a thesis by publication was chosen. Table 1.1 reports the list, in logical order, of the journal papers that compose the main body of thesis, along with the conference papers that complement them. The PhD candidate was the first author of all the presented papers: work planning, state of the art, methodology, analysis, and conclusions

for each paper were performed entirely by the PhD candidate with the recommendations of his advisors and coauthors. All the presented papers were written during the candidate's PhD period.

Chapter		Reference
3	[84]	I. Atzeni, L. G. Ordóñez, G. Scutari, D. P. Palomar, and J. R. Fonollosa, "Demand-side management via distributed energy generation and storage optimization," *IEEE Trans. on Smart Grid*, vol. 4, no. 2, pp. 866–876, June 2013.
4	[85]	I. Atzeni, L. G. Ordóñez, G. Scutari, D. P. Palomar, and J. R. Fonollosa, "Noncooperative and cooperative optimization of distributed energy generation and storage in the demand-side of the smart grid," *IEEE Trans. Signal Process.*, vol. 61, no. 10, pp. 2454–2472, May 2013.
	[86]	I. Atzeni, L. G. Ordóñez, G. Scutari, D. P. Palomar, and J. R. Fonollosa, "Day-ahead bidding strategies for demand-side expected cost minimization," in *IEEE Int. Conf. Smart Grid Comm. (SmartGridComm)*, pp. 91–96, Nov. 2012.
	[87]	I. Atzeni, L. G. Ordóñez, G. Scutari, D. P. Palomar, and J. R. Fonollosa, "Cooperative day-ahead bidding strategies for demand-side expected cost minimization," in *IEEE Int. Conf. Acoust., Speech, Signal Process. (ICASSP)*, pp. 5224–5228, May 2013.
5	[88]	I. Atzeni, L. G. Ordóñez, G. Scutari, D. P. Palomar, and J. R. Fonollosa, "Noncooperative day-ahead bidding strategies for demand-side expected cost minimization: A GNEP approach," *IEEE Trans. Signal Process.*, vol. 62, no. 9, pp. 2397–2412, May 2014.

Table 1.1: List of papers related to this thesis.

1.3.1 Chapters Outline

The thesis is structured around the presented papers, with each journal paper representing a self-contained chapter of the main body, i.e., Chapters 3, 4, and 5. The rest of the dissertation is organized as follows; Figure 1.1 highlights the connection between the different papers and chapters.

Chapter 2: Contribution

In Chapter 2, we provide a comprehensive summary of the theoretical results of this thesis. First of all, we illustrate an overall smart grid model that accommodates generalized DSM methods, and on which we build the proposed frameworks for dispatchable DG and DS optimization; furthermore, we formally introduce the optimization techniques that are used throughout the thesis. Then:

i) We present a deterministic day-ahead DSM framework where the users know in advance

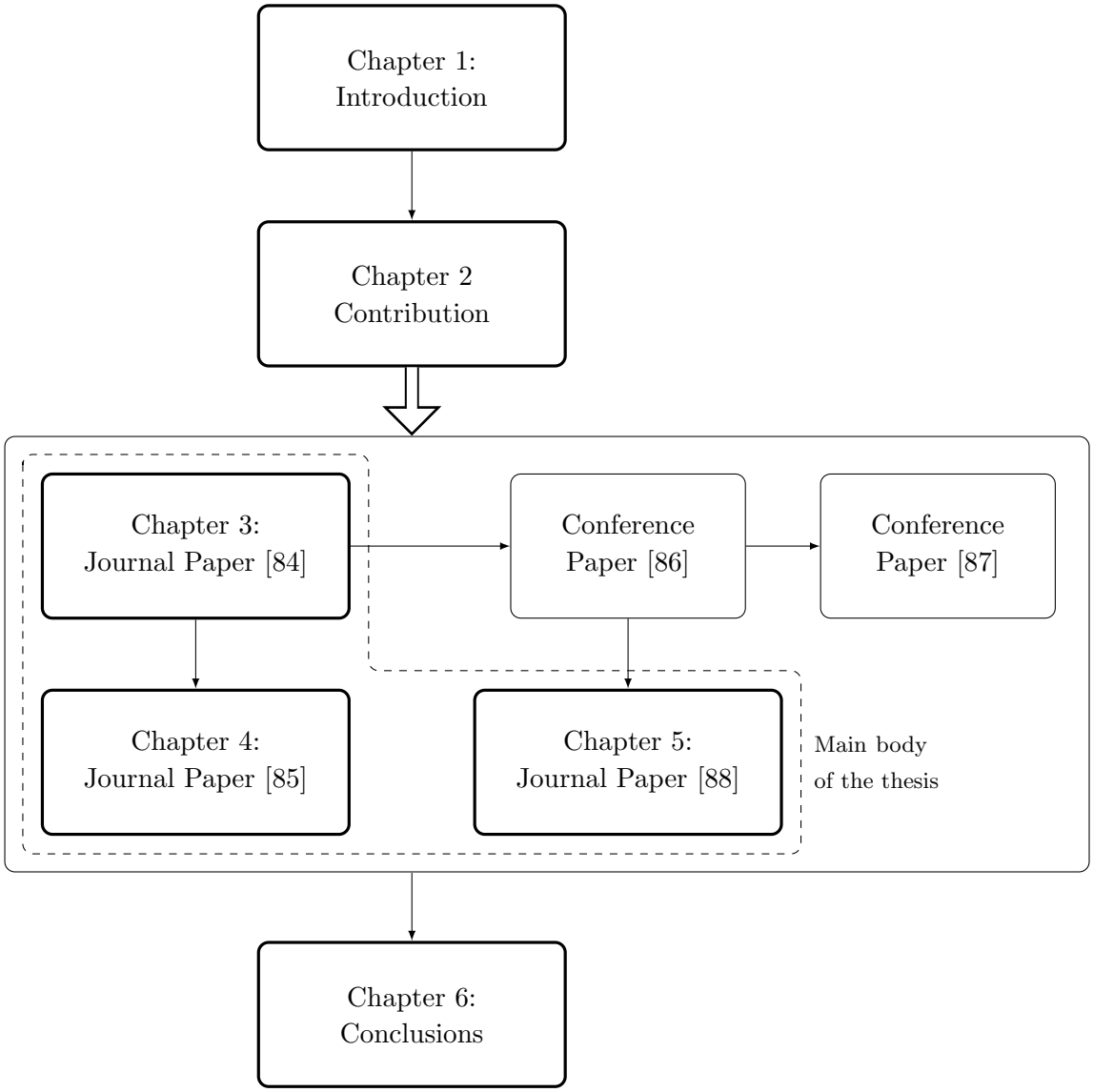

Figure 1.1: Chapters outline.

their energy consumption needs and commit to follow strictly the resulting day-ahead demand pattern in real-time. For this scenario, we tackle the DSM problem from both noncooperative and cooperative perspectives. The extensive description of these topics is given in Chapter 3 (cf. [84]) and in Chapter 4 (cf. [85]).

ii) We describe a stochastic DSM framework where the users' energy consumption needs is subject to uncertainty; then, in real-time, the users are allowed to adopt a different demand pattern under a penalty system that discourages deviations with respect to the day-ahead schedule. For this scenario, a noncooperative approach that accommodates global constraints is used. The detailed discussion is given in Chapter 5 (cf. [88]).

Chapter 3: Journal Paper [84]

Chapter 3 presents the first attempt to devise a day-ahead optimization framework where selfish demand-side users know in advance their consumption needs and aim at minimizing their monetary expense by adopting DSM strategies based on dispatchable DG and DS. We can summarize the content of this chapter as follows:

i) We present an accurate demand-side model that constitutes a guideline for representing realistic DSM scenarios where dispatchable DG and DS are employed.
ii) We formulate the demand-side optimization design as a NEP and, considering a standard quadratic energy cost function, we establish that the existence of (multiple, yet equivalent) Nash equilibria is guaranteed upon the fulfillment of local requirements by the users.
iii) We propose a distributed and iterative algorithm with synchronous update that is ensured to converge to one of the aforementioned solutions under very mild conditions and that requires only the knowledge of aggregate load of the demand-side, thus preserving the users' privacy and limiting the information exchange.
iv) Numerical results show substantial savings achieved by the users and lower PAR of the aggregate demand curve, which paves the way for a more extensive deployment of dispatchable DG and DS under the DSM paradigm.

Chapter 4: Journal Paper [85]

Chapter 4 addresses a more advanced study of the day-ahead optimization described in Chapter 3. More specifically:

i) The pricing model used is completely general and includes that of Chapter 3 as a special case; hence, the existence of optimal solutions and the convergence of the proposed algorithms not only depend on local conditions at the user level but also restrain the choice of the grid cost function.
ii) We attack the demand-side optimization problem from both user-oriented and holistic-based perspectives: in the former case, we optimize each user individually by formulating the optimization design as a NEP, whose solution analysis is addressed building on the theory of variational inequalities; in the latter case, we focus instead on the joint optimization of the demand-side, allowing some cooperation among the users.
iii) For both formulations, we design distributed and iterative algorithm providing the optimal DG and DS strategies of the users: for the first scenario, we propose a noncooperative scheme with asynchronous update, whereas for the second we build on decomposition methods based on partial linearizations to perform the parallel and distributed optimization of nonconvex sum-utility functions.
iv) Interestingly, the overall results produced by the noncooperative and the cooperative ap-

proaches happen to be equivalent in the case under exam, despite their different (sufficient) convergence conditions, strategy update, and convergence speed that make them appealing in different situations.

Chapter 5: Journal Paper [88]

In Chapter 5, we propose a stochastic day-ahead DSM optimization where the users do not have perfect knowledge of their real-time consumption needs, which makes the scenario described in the previous chapters considerably more realistic. The main contribution of this chapter is summarized below:

i) The day-ahead optimization consists of a bidding process and, in real-time, the deviations with respect to the day-ahead negotiated loads are penalized: therefore, the users estimate their consumption and optimize their bidding, dispatchable DG, and DS strategies with the objective of minimizing their individual expected monetary expense (taking into account the aforementioned real-time penalty charges).

ii) By considering a competitive market environment with global constraints on the aggregate bidding strategy of the users, the above bidding process is formulated as a GNEP, and we derive the conditions guaranteeing the existence of variational solutions.

iii) We build on the game theoretical pricing-based interpretation of a GNEP to design distributed and iterative algorithms that converge to the variational solutions under some technical conditions, while preserving the users' privacy and with limited information exchange; notably, the proposed scheme can also accommodate ECS methods.

iv) We devise a complementary DSM procedure that allows the users to perform unilateral adjustments on their DG and DS strategies so as to reduce the impact of their real-time deviations with respect to the day-ahead schedule.

v) Simulations on realistic scenarios show that the proposed day-ahead DSM method consistently diminishes the users' expected monetary expenses while fulfilling the global constraints, whereas the real-time adjustments reduce both the average value and the variance of the user's real-time monetary expense.

Chapter 6: Conclusions

Chapter 6 concludes by summarizing the results of this PhD thesis and presenting some future research lines.

2

Contribution

In this chapter, we summarize the overall contribution of this dissertation. Since Chapters 3, 4, and 5 are self-contained publications that do not always share the same notation, here we adopt a general notation (yet different from that of the aforementioned chapters) in order to provide a comprehensive view of the proposed models and algorithms. The main characteristics of the distributed schemes presented in this thesis are provided in Table 2.1.

Chapter	Reference	Pricing System	Noncoop./Coop.	Constraints	Alg. Update
3	[84]	DA	Noncooperative	Local	Synchronous
4	[85]	DA (with generalized cost function)	Noncooperative Cooperative	Local	Asynchronous Parallel
	[86]	DA with RT penalties	Noncooperative	Local	Asynchronous
	[87]	DA with RT penalties	Cooperative	Local	Parallel
5	[88]	DA with RT penalties + RT adjustments	Noncooperative	Local & Global	Asynchronous

Table 2.1: Distributed algorithms proposed in the main body of the thesis (DA: day-ahead, RT: real-time).

2.1 Preliminaries

2.1.1 Smart Grid Model

The smart grid model adopted in this thesis can be schematized as follows (see Figures 4.1–4.2):

i) Supply-side: energy producers and providers;
ii) Central unit: regulation authority that coordinates the demand-side bidding process;
iii) Demand-side: end users.

Since our aim is to propose novel DSM methods, we focus our attention on the demand-side of the smart grid, whereas the supply-side and the central unit are modeled as simple as possible.

Demand-side users, whose associated set is denoted by $\mathcal{D}$, are divided into *passive* and *active* users. Passive users $\mathcal{P} \subset \mathcal{D}$ are basically energy consumers and resemble traditional demand-side users, whereas active users $\mathcal{N} \triangleq \mathcal{D} \backslash \mathcal{P}$, with $N \triangleq |\mathcal{N}|$, indicate those consumers participating in the demand-side bidding process, i.e., reacting to changes in the energy price by modifying their demand profile. In our model, each active user is connected not only to the bidirectional power distribution infrastructure, but also to a communication infrastructure that enables two-way communication between his smart meter and the central unit.

Let us consider a time horizon of one day divided into H time-slots, with $h = 1, \dots, H$. Demand-side users $\mathcal{D}$ are characterized in the first instance by the *per-slot energy consumption* $e_n(h)$ defined as the energy needed by user $n \in \mathcal{D}$ to supply his appliances at time-slot h: this term also accounts for eventual renewable energy sources that the user may have. On the other hand, the *per-slot energy load* $l_n(h)$ gives the energy flow between user n and the distribution grid at time-slot h. For passive users $n \in \mathcal{P}$, we have that $l_n(h) = e_n(h)$, whereas this relationship does not necessarily hold for active users $\mathcal{N}$, who can modify their demand profile by applying DSM techniques.

In Section 2.2, we examine a preliminary scenario where $e_n(h)$ is deterministic: then, the users perform a day-ahead optimization whose resulting demand pattern coincides with the real-time load $l_n(h)$. Subsequently, in Section 2.3, we deal with a more realistic scenario that models $e_n(h)$ as a random variable: therefore, the demand pattern resulting from the day-ahead optimization does not necessarily coincide with the real-time load $l_n(h)$, and the difference between the two is penalized; for this reason, a stochastic day-ahead optimization is performed and real-time adjustments of the day-ahead strategies are allowed.

2.1.2 Optimization Framework

We consider the demand-side as a multiuser system composed of N coupled users, i.e., the active users $\mathcal{N}$. We start by providing some preliminary definitions. For each active user $n \in \mathcal{N}$, $\Omega_n \subseteq \mathbb{R}^{\omega_n H}$ denotes the strategy set, with ω_n representing the number of dimensions of the user's per-slot DSM strategy; user n's objective function is given by $\mathsf{f}_n(\mathbf{x}_n, \mathbf{x}_{-n})$ and depends on all users' strategies, which are described by the vector $\mathbf{x} \triangleq \big(\mathbf{x}_n\big)_{n=1}^{N}$, where $\mathbf{x}_n \triangleq \big(\mathbf{x}_n(h)\big)_{h=1}^{H}$ defines the strategy vector of user n and $\mathbf{x}_{-n} \triangleq (\mathbf{x}_m)_{m \in \mathcal{N} \backslash \{n\}}$ denotes the vector of all active users' strategy profiles except that of user n; the joint strategy set is denoted by $\Omega \triangleq \prod_{n \in \mathcal{N}} \Omega_n \subseteq \mathbb{R}^{\omega H}$,

with $\omega \triangleq \sum_{n\in\mathcal{N}} \omega_n$, and $\Omega_{-n} \triangleq \prod_{m\in\mathcal{N}\setminus\{n\}} \Omega_m$. We call a vector $\mathbf{x}$ feasible if $\mathbf{x}_n \in \Omega_n$, $\forall n \in \mathcal{N}$. Moreover, unless specified otherwise, each user n's strategy set Ω_n is independent of the other users' actions.

In this thesis, we express the demand-side optimization using three different formulations (introduced in Section 1.2.2), namely:

A1) A Nash equilibrium problem (NEP), where each user $n \in \mathcal{N}$ is a player who aims at choosing $\mathbf{x}_n \in \Omega_n$ that minimizes his objective function $\mathsf{f}_n(\mathbf{x}_n, \mathbf{x}_{-n})$, given the other players' strategies $\mathbf{x}_{-n}$:

$$\begin{array}{ll} \min\limits_{\mathbf{x}_n} & \mathsf{f}_n(\mathbf{x}_n, \mathbf{x}_{-n}) \\ \text{s.t.} & \mathbf{x}_n \in \Omega_n \end{array} \quad \forall n \in \mathcal{N}. \tag{2.1}$$

A Nash equilibrium (NE), or simply a solution of the NEP, is a feasible point $\mathbf{x}^\star$ such that $\mathsf{f}_n(\mathbf{x}_n^\star, \mathbf{x}_{-n}^\star) \leq \mathsf{f}_n(\mathbf{x}_n, \mathbf{x}_{-n}^\star)$, $\forall \mathbf{x}_n \in \Omega_n$, $\forall n \in \mathcal{N}$.

A2) A generalized NEP (GNEP), where the strategy set Ω_n of each user $n \in \mathcal{N}$ depends of the other users' actions: we denote by $\Omega_n(\mathbf{x}_{-n})$ the strategy set of user n when the other users choose $\mathbf{x}_{-n}$. Here, each user n is a player who aims at choosing $\mathbf{x}_n \in \Omega_n(\mathbf{x}_{-n})$ that minimizes his objective function $\mathsf{f}_n(\mathbf{x}_n, \mathbf{x}_{-n})$, given the other players' strategies $\mathbf{x}_{-n}$:

$$\begin{array}{ll} \min\limits_{\mathbf{x}_n} & \mathsf{f}_n(\mathbf{x}_n, \mathbf{x}_{-n}) \\ \text{s.t.} & \mathbf{x}_n \in \Omega_n(\mathbf{x}_{-n}) \end{array} \quad \forall n \in \mathcal{N}. \tag{2.2}$$

A generalized Nash equilibrium (GNE), or simply a solution of the GNEP, is a feasible point $\mathbf{x}^\star$ such that $\mathsf{f}_n(\mathbf{x}_n^\star, \mathbf{x}_{-n}^\star) \leq \mathsf{f}_n(\mathbf{x}_n, \mathbf{x}_{-n}^\star)$, $\forall \mathbf{x}_n \in \Omega_n(\mathbf{x}_{-n})$, $\forall n \in \mathcal{N}$.

B) A sum-utility optimization problem, where the users $\mathcal{N}$ aim at optimizing the social function given by the sum of their individual objective functions:

$$\begin{array}{ll} \min\limits_{\{\mathbf{x}_n\}} & U(\mathbf{x}) = \sum\limits_{n\in\mathcal{N}} \mathsf{f}_n(\mathbf{x}_n, \mathbf{x}_{-n}) \\ \text{s.t.} & \mathbf{x}_n \in \Omega_n, \quad \forall n \in \mathcal{N}. \end{array} \tag{2.3}$$

A stationary solution of the above sum-utility problem is a feasible point $\mathbf{x}^\star$ such that $\nabla_{\mathbf{x}} \sum_{n\in\mathcal{N}} \mathsf{f}_n(\mathbf{x}_n, \mathbf{x}_{-n}) = \mathbf{0}$.

In order to study the problems A1 and A2, they will be reformulated as (partitioned) VI problems, whose formal definition is provided next.

Definition 2.1 ([74, Def. 4.2])**.** Let $\mathbf{F}(\mathbf{x}) : \Omega \to \mathbb{R}^{\omega H}$ be a vector-valued function defined as $\mathbf{F}(\mathbf{x}) = \big(\mathbf{F}_n(\mathbf{x}_n, \mathbf{x}_{-n})\big)_{n=1}^N$, where $\mathbf{F}_n(\mathbf{x}_n, \mathbf{x}_{-n}) : \Omega_n \to \mathbb{R}^{\omega_n H}$ is the nth component block function of $\mathbf{F}(\mathbf{x})$, $\mathbf{x} = \big(\mathbf{x}_n\big)_{n=1}^N$, and $\Omega = \prod_{n\in\mathcal{N}} \Omega_n$. Then, the VI problem, denoted by $\mathrm{VI}(\Omega, \mathbf{F})$, consists

in finding $\mathbf{x}^\star \in \Omega$ such that

$$(\mathbf{x} - \mathbf{x}^\star)^{\mathrm{T}} \mathbf{F}(\mathbf{x}^\star) \geq 0, \qquad \forall \mathbf{x} \in \Omega. \tag{2.4}$$

2.2 Day-Ahead DSM

Day-ahead DSM is of paramount importance since it provides the supply-side with an estimation of the amount of energy to be delivered to the demand-side during the time period of analysis, so that energy suppliers can plan their production accordingly. In this section, we design a noncooperative and a cooperative DSM optimization frameworks that apply to deterministic day-ahead pricing models: in doing so, we summarize the theoretical analysis and algorithms of Chapter 4, which includes the subject of Chapter 3 as a spacial case. Here, we work under the following assumptions:

i) The per-slot energy consumption $e_n(h)$ is deterministic, i.e., each demand-side user knows exactly, and in advance, his energy requirements for each time-slot in the upcoming day;
ii) Active users $\mathcal{N}$ commit to follow strictly the demand pattern resulting from the day-ahead optimization, i.e., the per-slot energy load $l_n(h)$ is determined in the day-ahead and remains unchanged in real-time.

Lastly, we introduce the transformation vector $\boldsymbol{\delta} \in \mathbb{R}^{\omega_n}$ defined such that $\boldsymbol{\delta}^{\mathrm{T}} \mathbf{x}_n(h) = l_n(h)$.

2.2.1 Energy Cost and Pricing Model

Typically, during the day-ahead market, the different energy generators in the supply-side (each of them characterized by a specific price curve) submit their production offers; likewise, consumers and retailers submit their consumption bids. This process determines the energy prices, i.e., the locational marginal prices [89], and the traded quantities [34, Ch. 1.2]. Since we are particularly interested in the demand-side of the network, we can abstract this procedure by considering a single price curve resulting from aggregating the individual curves of each generator in the supply-side; this is a well-established procedure in the smart grid literature.

With this objective in mind, let us first define the *per-slot energy load* at time-slot h as

$$L(h) \triangleq \sum_{n \in \mathcal{D}} l_n(h) = L^{(\mathcal{P})}(h) + \sum_{n \in \mathcal{N}} \boldsymbol{\delta}^{\mathrm{T}} \mathbf{x}_n(h) \tag{2.5}$$

where $L^{(\mathcal{P})}(h) = \sum_{n \in \mathcal{P}} l_n(h)$ is the per-slot aggregate energy consumption associated with the passive users. Throughout Section 2.2, the per-slot aggregate energy load in (2.5) is fixed in the day-ahead and remains unchanged in real-time, and we work under the hypothesis that it is always guaranteed by the supply-side.

Given the per-slot aggregate energy load $L(h)$, let us define the *grid cost function per unit of*

energy $C_h\big(L(h)\big)$ at time-slot h. Then, $C_h\big(L(h)\big)l_n(h)$ represents the amount of money paid by user n to purchase the energy load $l_n(h)$ from the grid (if $l_n(h) > 0$) or, eventually, received to sell the energy load $l_n(h)$ to the grid (if $l_n(h) < 0$) at time-slot h. Observe that $C_h(\cdot)$ can represent either the actual energy cost (as a result of energy generation, transmission, and distribution costs among other issues) or simply a pricing function designed to incentivize load shifting by the end users. In any case, $C_h(\cdot)$ varies across the day according to the energy demand and to the availability of intermittent sources. Observe that, throughout Section 2.2, we keep the pricing model general, whereas in Chapter 3 we analyze a particular pricing model where the grid cost function per unit of energy is linear.

On the other hand, we denote by $W_n(\mathbf{x}_n(h))$ the *DSM cost function*, i.e., the cost incurred by user n to shape his consumption $e_n(h)$ into the energy load $l_n(h)$ via DSM programs. For instance, this can represent the monetary cost of operating a fuel generator or a storage device, as well as the discomfort created by the rescheduling of appliances or by a voluntary decrease in the energy consumption.

Finally, we can write the objective function of each active user $n \in \mathcal{N}$ as

$$\mathsf{f}_n(\mathbf{x}_n, \mathbf{l}_{-n}) \triangleq \sum_{h=1}^{H} \Big(C_h\big(\boldsymbol{\delta}^{\mathrm{T}}\mathbf{x}_n(h) + l_{-n}(h)\big)\boldsymbol{\delta}^{\mathrm{T}}\mathbf{x}_n + W_n\big(\mathbf{x}_n(h)\big)\Big) \tag{2.6}$$

where $\mathbf{l}_{-n} \triangleq \big(l_{-n}(h)\big)_{h=1}^{H}$ is the aggregate energy load vector of the other users, with

$$l_{-n}(h) \triangleq L(h) - l_n(h) = L^{(\mathcal{P})}(h) + \sum_{m \in \mathcal{N}\setminus\{n\}} \boldsymbol{\delta}^{\mathrm{T}}\mathbf{x}_m(h). \tag{2.7}$$

Note that, since the above objective function only depends on the aggregate energy loads, the users are not required to know the individual strategies (and not even the individual energy loads) of the others, which preserve the users' privacy.

2.2.2 DSM Model

In our smart grid model, active users $\mathcal{N}$ adopt dispatchable DG and DS. In this regard, $g_n(h) \geq 0$ represents the *per-slot energy production* at time-slot h. Likewise, $s_n(h)$ denotes the *per-slot energy storage* at each time-slot h: we have that $s_n(h) > 0$ when the storage device is to be charged (implying an additional energy consumption), $s_n(h) < 0$ when the storage device is to be discharged (resulting in a reduction of the energy consumption), and $s_n(h) = 0$ when the storage device is inactive. In this context, the resulting per-slot strategy and per-slot energy

load of user $n \in \mathcal{N}$ are given by

$$\mathbf{x}_n(h) \triangleq \big(e_n(h), g_n(h), s_n(h)\big) \tag{2.8}$$

$$l_n(h) \triangleq e_n(h) - g_n(h) + s_n(h) \tag{2.9}$$

with $\boldsymbol{\delta} \triangleq (1, -1, 1)$. The DSM cost function $W_n(\mathbf{x}_n)$ indicates the fuel cost for the dispatchable generator, whereas we assume that the storage device implies no variable costs: therefore, we refer to the objective function $\mathsf{f}_n(\mathbf{x}_n, \mathbf{l}_{-n})$ in (2.6) as *cumulative monetary expense*. Lastly, the strategy set Ω_n includes all the feasible dispatchable DG and DS strategies that user n can adopt. The constraints regarding dispatchable DG and DS are illustrated in detail in Sections 3.2 and 4.2; for the purpose of the discussion in this chapter, it is sufficient to mention that such constraints yield compact and convex strategy sets Ω_n.

2.2.3 Noncooperative Day-Ahead DSM

Here, following Approach A1 described in Section 2.1.2, we model our DSM procedure as a NEP. Each active user is a player who competes against the others by choosing the dispatchable DG and DS strategies (included in the strategy vector $\mathbf{x}_n$) that minimize his cumulative monetary expense $\mathsf{f}_n(\mathbf{x}_n, \mathbf{l}_{-n})$ defined in (2.6), subject to the local constraints Ω_n (cf. (2.1)):

$$\begin{aligned} \min_{\mathbf{x}_n} \quad & \mathsf{f}_n(\mathbf{x}_n, \mathbf{l}_{-n}) \\ \text{s.t.} \quad & \mathbf{x}_n \in \Omega_n \end{aligned} \qquad \forall n \in \mathcal{N}. \tag{2.10}$$

The formal definition of the NEP is the following: $\mathscr{G} = \langle \Omega, \mathbf{f} \rangle$, with $\Omega \triangleq \prod_{n \in \mathcal{N}} \Omega_n$ and $\mathbf{f} \triangleq \big(\mathsf{f}_n(\mathbf{x}_n, \mathbf{l}_{-n})\big)_{n=1}^N$.

In order to analyze the existence of the Nash equilibria as well as the convergence of distributed algorithms while keeping the pricing model general, it is very convenient to reformulate the NEP as a partitioned VI problem $\mathrm{VI}(\Omega, \mathbf{F})$, which was formally defined in Definition 2.1. The equivalence between the game theoretical and the VI formulation is established in the following lemma.

Lemma 2.1 ([74, Prop. 4.1])**.** *Given the NEP $\mathscr{G} = \langle \Omega, \mathbf{f} \rangle$, suppose that, for each $n \in \mathcal{N}$, the following hold:*

(a) *The strategy set Ω_n is closed and convex;*

(b) *For every feasible $\mathbf{l}_{-n}$ (i.e., such that $\mathbf{x}_{-n} \in \Omega_{-n}$), the objective function $\mathsf{f}_n(\mathbf{x}_n, \mathbf{l}_{-n})$ is convex and twice continuously differentiable in $\mathbf{x}_n \in \Omega_n$.*

Let $\mathbf{F}(\mathbf{x}) \triangleq \big(\nabla_{\mathbf{x}_n} \mathsf{f}_n(\mathbf{x}_n, \tilde{\mathbf{l}}_{-n})\big)_{n=1}^N$. Then, the NEP is equivalent to the VI problem $\mathrm{VI}(\Omega, \mathbf{F})$.

Assuming that Lemma 2.1 holds, we can formulate the NEP $\mathscr{G}$ as the VI problem $\mathrm{VI}(\Omega, \mathbf{F})$.

Sufficient conditions that guarantee the existence of the Nash equilibria of the NEP $\mathscr{G}$, i.e., of the solutions of the VI problem $\mathrm{VI}(\Omega_{\mathbf{x}}, \mathbf{F})$, are derived in the next theorem.

Theorem 2.1. *Given the NEP $\mathscr{G} = \langle \Omega, \mathbf{f} \rangle$, suppose that the following hold:*

(a) *The strategy set Ω_n is compact and convex, for each $n \in \mathcal{N}$;*

(b) *The grid cost functions per unit of energy $\left\{C_h(\cdot)\right\}_{h=1}^{H}$ are increasing and convex and satisfy*

$$C_h'(\cdot) \geq \frac{1}{2}\zeta^{(\min)} C_h''(\cdot) \tag{2.11}$$

where $\zeta^{(\min)}$ denotes the maximum amount of energy that can be sold to the grid by any single user $n \in \mathcal{N}$ at any time-slot;

(c) *The DSM function $W_n(\cdot)$ is convex and twice continuously differentiable, for each $n \in \mathcal{N}$.*

Then, the NEP has a nonempty and compact solution set.

The conditions in Theorem 2.1 are very mild and always satisfied in practice; we refer to Remark 4.1 in Section 4.3.2 for more details. Furthermore, their fulfillment also implies the accomplishment of Lemma 2.1 (whose requirements are less stringent than those of Theorem 2.1).

Theorem 2.1 guarantees the existence of a solution of the NEP $\mathscr{G}$, but not the uniqueness. Interestingly, all Nash equilibria for this problem happen to have the same quality in terms of optimal values of the players' objective functions (cf. Proposition 4.1 in Section 4.3.2).

Distributed Algorithm

We are now interested in designing distributed algorithms to compute one of the (equivalent) solutions of the NEP $\mathscr{G}$. We focus on the class of *totally asynchronous* best-response algorithms, where some users may update their strategies more frequently than others and they may even use outdated information about the strategy profiles adopted by the other users. A synchronous user-oriented scheme, which is based on a particular pricing model with linear grid cost functions per unit of energy, is presented in Chapter 3 and is included in the following as a special case. Let $\mathscr{T}_n \subseteq \mathscr{T} \subseteq \{0, 1, 2, \ldots\}$ be the set of times at which user $n \in \mathcal{N}$ updates his own strategy $\mathbf{x}_n$, denoted by $\mathbf{x}_n^{(i)}$ at the ith iteration. We use $t_n(i)$ to denote the most recent time at which the strategy of user n is perceived by the central unit at the ith iteration. We assume that some standard conditions in asynchronous convergence theory (see (A1)–(A3) in Section 4.3.3), which are fulfilled in any practical implementation, hold for $\mathscr{T}_n$ and $t_n(i)$, $\forall n \in \mathcal{N}$. According to the asynchronous scheduling, each user updates his strategy by minimizing his cumulative monetary expense, given the most recently available value of the aggregate energy load vector of the other

users $\mathbf{l}_{-n}^{(\mathbf{t}(i))} \triangleq \big(l_{-n}^{(\mathbf{t}(i))}(h)\big)_{h=1}^{H}$, with

$$l_{-n}^{(\mathbf{t}(i))}(h) \triangleq L^{(\mathcal{P})}(h) + \sum_{m\in\mathcal{N}\setminus\{n\}} l_{m}^{(t_m(i))}(h). \tag{2.12}$$

Since all Nash equilibria are equivalent (in the sense of Proposition 4.1), we focus on proximal-based best-response algorithms, which are guaranteed to converge to one of the Nash equilibria even in the presence of multiple solutions. We then obtain Algorithm 2.1 below, whose convergence conditions are expressed by Theorem 2.2. We refer to Section 4.3.3 for a detailed discussion of the algorithm.

Algorithm 2.1 Asynchronous Proximal Decomposition Algorithm (PDA)

`Data` : Set $i = 0$ and the initial centroid $\big(\bar{\mathbf{x}}_n\big)_{n=1}^{N} = \mathbf{0}$. Given $\big\{C_h(\cdot)\big\}_{h=1}^{H}$, $\big\{\rho^{(i)}\big\}_{i=0}^{\infty}$, $\tau > 0$, and any feasible starting point $\mathbf{x}^{(0)} = \big(\mathbf{x}_n^{(0)}\big)_{n=1}^{N}$:

`(S.1)` : `If` a suitable termination criterion is satisfied: `STOP`.

`(S.2)` : `For` $n \in \mathcal{N}$, each user computes $\mathbf{x}_n^{(i+1)}$ as

$$\mathbf{x}_n^{(i+1)} = \begin{cases} \mathbf{x}_n^{\star} \in \underset{\mathbf{x}_n\in\Omega_n}{\operatorname{argmin}} \Big\{ \mathsf{f}_n\big(\mathbf{x}_n, \mathbf{l}_{-n}^{(\mathbf{t}(i))}\big) + \dfrac{\tau}{2}\|\mathbf{x}_n - \bar{\mathbf{x}}_n\|^2 \Big\}, & \text{if } i \in \mathscr{T}_n \\ \mathbf{x}_n^{(i)}, & \text{otherwise} \end{cases}$$

`End`

`(S.3)` : `If` the NE is reached, then each user $n \in \mathcal{N}$ sets $\mathbf{x}_n^{(i+1)} \leftarrow (1-\rho^{(i)})\bar{\mathbf{x}}_n + \rho^{(i)}\mathbf{x}_n^{(i+1)}$ and updates his centroid: $\bar{\mathbf{x}}_n = \mathbf{x}_n^{(i+1)}$.

`(S.4)` : $i \leftarrow i+1$; `Go to (S.1)`.

Theorem 2.2. *Given the NEP $\mathscr{G} = \langle \Omega, \mathbf{f}\rangle$, suppose that the conditions of Theorem* 2.1 *and the following hold:*

(a) *The grid cost functions per unit of energy $\big\{C_h(\cdot)\big\}_{h=1}^{H}$ are increasing and convex and additionally satisfy*

$$C_h'(\cdot) \geq N\big(\zeta^{(\min)} + \zeta^{(\max)}\big) C_h''(\cdot) \tag{2.13}$$

where N is the number of active users and where $\zeta^{(\min)}$ and $\zeta^{(\max)}$ denote the maximum amount of energy that can be sold to or both from the grid by any single user $n \in \mathcal{N}$ at any time-slot, respectively;

(b) *The regularization parameter τ satisfies*

$$\tau > 2(N-1)\max_h C_h'(L^{(\max)}) + 2L^{(\max)} \max_h \Big(\max_{L^{(\min)}\leq x\leq L^{(\max)}} C_h''(x) \Big) \tag{2.14}$$

where $L^{(\min)}$ and $L^{(\max)}$ are the minimum and maximum aggregate energy load allowed by the grid infrastructure, respectively;

(c) $\rho^{(i)}$ *is chosen so that* $\{\rho^{(i)}\} \subset [R_m, R_M]$, *with* $0 < R_m < R_M < 2$.

Then, any sequence $\{\mathbf{x}_n^{(i)}\}_{i=1}^{\infty}$ *generated by Algorithm* 2.1 *converges to a Nash equilibrium of the NEP.*

Condition (2.13) in Theorem 2.2(a) provides a guideline to choose the grid cost functions per unit of energy $\{C_h(\cdot)\}_{h=1}^{H}$, and can be also understood as a tradeoff between the minimum demand generated by the passive users and that coming from the active users (see Remark 4.3 in Section 4.3.3). On the other hand, the regularization parameter τ determines the tradeoff between the convergence stability and the convergence speed [76]. The peculiarity of the expression of τ provided in (2.14) is that it can be calculated by the central unit a priori without interfering with the privacy of the users (see Remark 4.4 in Section 4.3.3); the same consideration holds for the values of τ derived in Theorem 2.3 (cf. (2.21)) and in Theorem 2.5 (cf. (2.42)).

2.2.4 Cooperative Day-Ahead DSM

In contrast to the noncooperative approach A1 adopted in Section 2.2.3, we now follow Approach B described in Section 2.1.2 (cf. (2.3)) and consider an alternative DSM technique, in which demand-side users collaborate to minimize the aggregate cumulative monetary expense of the demand-side.

Let us write the aggregate cumulative monetary expense of the passive users $\mathcal{P}$ as

$$U^{(\mathcal{P})}(\mathbf{x}) \triangleq \sum_{h=1}^{H} C_h\Big(\sum_{n\in\mathcal{N}} \boldsymbol{\delta}^{\mathrm{T}}\mathbf{x}_n(h) + L^{(\mathcal{P})}(h)\Big)L^{(\mathcal{P})}(h) \tag{2.15}$$

which indirectly depends on the strategies adopted by the active users $\mathcal{N}$ through the grid cost function per unit of energy $C_h(\cdot)$. We aim at solving the following social problem (c.f. (2.3))

$$\begin{aligned} \min_{\{\mathbf{x}_n\}} \quad & U(\mathbf{x}) \triangleq \sum_{n\in\mathcal{N}} \mathsf{f}_n^{(\mathcal{D})}(\mathbf{x}_n, \mathbf{l}_{-n}) \\ \text{s.t.} \quad & \mathbf{x}_n \in \Omega_n, \quad \forall n \in \mathcal{N}. \end{aligned} \tag{2.16}$$

where $\mathsf{f}_n^{(\mathcal{D})}(\mathbf{x}_n, \mathbf{l}_{-n})$ is defined so as to distribute the term $U^{(\mathcal{P})}(\mathbf{x})$ in (2.15) among the active users $\mathcal{N}$, i.e.,

$$\mathsf{f}_n^{(\mathcal{D})}(\mathbf{x}_n, \mathbf{l}_{-n}) \triangleq \mathsf{f}_n(\mathbf{x}_n, \mathbf{l}_{-n}) + \frac{1}{N}U^{(\mathcal{P})}(\mathbf{x}) \tag{2.17}$$

with the individual cumulative expense $\mathsf{f}_n(\mathbf{x}_n, \mathbf{l}_{-n})$ given by (2.6). In fact, the common term (equal for all users) $U^{(\mathcal{P})}(\mathbf{x})$ is a transferable utility and can be arbitrarily shared among the active users (e.g., as in (2.17)) without affecting the optimal value of the social function $U^{(\mathcal{D})}(\mathbf{x})$.

Distributed Algorithm

Instead of tackling problem (2.3) via classical gradient-based schemes, we build on the framework recently proposed in [82, 83]: since each $\mathsf{f}_n^{(\mathcal{D})}(\mathbf{x}_n, \mathbf{l}_{-n})$ is convex for any feasible $\mathbf{l}_{-n}$ (under the settings of Theorem 2.1), one can linearize only the nonconvex part, i.e., $\sum_{m\in\mathcal{N}\setminus\{n\}} \mathsf{f}_m^{(\mathcal{D})}(\mathbf{x})$, and solve the sequence of resulting optimization problems. Such a procedure preserves some structure of the original objective function and, therefore, it is expected to be faster than classical gradient-based schemes. A formal description of the algorithm is given next.

Let us preliminary define $\mathbf{x}^{(i)} \triangleq \big(\mathbf{x}_n^{(i)}\big)_{n=1}^N$ as the joint strategy vector at iteration i and the resulting aggregate load as

$$L^{(i)}(h) \triangleq L^{(\mathcal{P})}(h) + \sum_{n\in\mathcal{N}} \boldsymbol{\delta}^{\mathrm{T}} \mathbf{x}_n^{(i)}(h) \tag{2.18}$$

where $\mathbf{x}_n^{(i)}(h)$ represents the per-slot strategy of active user n at iteration i. We can then introduce the best-response mapping $\Omega \ni \mathbf{x}^{(i)} \to \widehat{\mathbf{x}}_\tau(\mathbf{x}^{(i)}) = \big(\widehat{\mathbf{x}}_{\tau,n}(\mathbf{x}^{(i)})\big)_{n=1}^N$, where we have defined

$$\widehat{\mathbf{x}}_{\tau,n}(\mathbf{x}^{(i)}) \triangleq \operatorname*{argmin}_{\mathbf{x}_n\in\Omega_n} \Big\{ \mathsf{f}_n^{(\mathcal{D})}\big(\mathbf{x}_n, \mathbf{l}_{-n}^{(i)}\big) + \boldsymbol{\pi}_n(\mathbf{l}_{-n}^{(i)})^{\mathrm{T}} \mathbf{x}_n + \frac{\tau}{2}\|\mathbf{x}_n - \mathbf{x}_n^{(i)}\|^2 \Big\} \tag{2.19}$$

and

$$\boldsymbol{\pi}_n(\mathbf{l}_{-n}^{(i)}) \triangleq \sum_{m\in\mathcal{N}\setminus\{n\}} \nabla_{\mathbf{x}_n} \mathsf{f}_m(\mathbf{x}_m, \mathbf{l}_{-m}^{(i)}). \tag{2.20}$$

Note that each individual mapping in (2.19) is strongly convex under Theorem 2.1 and, therefore, has a unique solution; (2.19) is thus well-defined. The proposed algorithm solving the social problem in (2.16) is formally described in Algorithm 2.2 below, whose convergence conditions are given in Theorem 2.3. We refer to Section 4.4.1 for a detailed discussion of the algorithm.

Algorithm 2.2 Distributed Dynamic Pricing Algorithm (DDPA)

`Data` : Set $i = 0$. Given $\big\{C_h(\cdot)\big\}_{h=1}^H$, $\big\{L^{(\mathcal{P})}(h)/N\big\}_{h=1}^H$, $\tau > 0$, and any feasible starting point $\mathbf{x}^{(0)} = \big(\mathbf{x}_n^{(0)}\big)_{n=1}^N$:

`(S.1)` : `If` a suitable termination criterion is satisfied: `STOP`.

`(S.2)` : `For` $n \in \mathcal{N}$, each user computes $\mathbf{x}_n^{(i+1)}$ as

$$\mathbf{x}_n^{(i+1)} = \operatorname*{argmin}_{\mathbf{x}_n\in\Omega_n} \Big\{ \mathsf{f}_n^{(\mathcal{D})}\big(\mathbf{x}_n, \mathbf{l}_{-n}^{(i)}\big) + \boldsymbol{\pi}_n(\mathbf{l}_{-n}^{(i)})^{\mathrm{T}} \mathbf{x}_n + \frac{\tau}{2}\|\mathbf{x}_n - \mathbf{x}_n^{(i)}\|^2 \Big\}$$

`End`

`(S.3)` : $i \leftarrow i + 1$; `Go to (S.1)`.

Theorem 2.3. *Given the social problem* (2.16)*, suppose that the conditions of Theorem* 2.1 *hold*

and that the regularization parameter τ *satisfies*

$$\tau \geq \max_{h} \left((N+1) C_h'(L^{(\max)}) + \max_{L^{(\min)} \leq x \leq L^{(\max)}} \left(C_h''(x) x \right) \right) \tag{2.21}$$

where N *is the number of active users and where* $L^{(\min)}$ *and* $L^{(\max)}$ *are the minimum and maximum aggregate energy load allowed by the grid infrastructure, respectively. Then, either Algorithm* 2.2 *converges in a finite number of iterations to a stationary solution of* (2.16) *or every limit point of the sequence* $\left\{ \mathbf{x}^{(i)} \right\}_{i=1}^{\infty}$ *is a stationary solution of* (2.16).

Algorithm 2.2 is guaranteed to converge whenever a solution to the social problem (2.16) exists: therefore, its convergence conditions are consistently milder than those required by the noncooperative approach based on Algorithm 2.1 and, most importantly, it does not impose any limitation on the number of active users (which means better scalability). In addition, Algorithm 2.2 is not incentive compatible, in the sense that demand-side users need to reach an agreement in following the best-response protocol (2.19). For these reasons, the proposed method needs to be coordinated by an external regulator in order to promote the cooperative optimization of demand-side users. Lastly, Algorithm 2.2 differs from Algorithm 2.1 in the synchronous (parallel) update of the users' strategies.

2.2.5 DSM Implementation

Summarizing, the proposed day-ahead demand-side optimization based on Algorithms 2.1 and 2.2 works as follows. At the beginning of the optimization process, τ is computed, respectively as in (2.14) or (2.21), and broadcast to each user $n \in \mathcal{N}$, together with the grid cost functions per unit of energy $\left\{ C_h(\cdot) \right\}_{h=1}^{H}$ and, only for Algorithm 2.2, the terms related to the transferable utility $\left\{ L^{(\mathcal{P})}(h)/N \right\}_{h=1}^{H}$. Then, at each iteration i, we have that:

1) In Algorithm 2.1, any active user who wants to update his strategy solves his own (regularized) optimization problem based on the most recent values of the aggregate energy loads $\left\{ L^{(\mathbf{t}^{(i)})}(h) \right\}_{h=1}^{H}$, which are calculated by the central unit referring to the (possibly outdated) individual demands, and communicates his new load to the central unit. When an equilibrium in the inner loop is reached, the central unit proceeds to the next iteration.
2) In Algorithm 2.2, all active users simultaneously update their strategies by solving their own optimization problems in (2.19) based on the aggregate energy loads $\left\{ L^{(i)}(h) \right\}_{h=1}^{H}$, which are calculated by the central unit summing up the individual demands. Then, active users provide their new energy loads to the central unit.

This process is iterated until a suitable termination criterion imposed by the central unit is satisfied.

2.3 Day-Ahead DSM with Real-Time Penalty Charges

Pure day-ahead approaches as those presented in Section 2.2 prove incapable of accommodating real-time fluctuations from the expected energy consumption by the demand-side users, as well as the randomness of their renewable sources. On top of that, additional costs are incurred by the supply-side when the consumption schedule is not correctly predicted by the users, and are transferred to the demand-side in the form of penalty charges. In this section, we design a non-cooperative DSM optimization framework that applies to stochastic day-ahead and real-time pricing models and that accommodates global constraints: in doing so, we summarize the theoretical analysis and algorithms of Chapter 5, which includes [86] as a special case; a cooperative method applied to an equivalent stochastic day-ahead pricing model and that neglects the global constraints is illustrated in [87]. Here, we work under the following assumptions:

i) The per-slot energy consumption $e_n(h)$ is modeled as a random variable whose pdf $f_{e_n(h)}(\cdot)$ is known by the corresponding demand-side user n.
ii) Active users $\mathcal{N}$ can deviate in real-time, although subject to penalty charges, from the demand pattern resulting from the day-ahead optimization.

Therefore, we distinguish between the *per-slot bid energy load* $\tilde{l}_n(h)$, which gives the day-ahead demand pattern, and the (real-time) per-slot energy load $l_n(h)$. Lastly, we introduce the transformation vector $\boldsymbol{\delta} \in \mathbb{R}^{\omega_n}$ defined such that $\boldsymbol{\delta}^{\mathrm{T}} \mathbf{x}_n(h) = \tilde{l}_n(h)$.

2.3.1 Energy Cost and Pricing Model

In addition to the per-slot aggregate energy load $L(h)$ in (2.5), we further define the *per-slot aggregate bid energy load* at time-slot h as

$$\tilde{L}(h) \triangleq \hat{L}^{(\mathcal{P})}(h) + \sum_{n \in \mathcal{N}} \boldsymbol{\delta}^{\mathrm{T}} \mathbf{x}_n(h) \tag{2.22}$$

where $\hat{L}^{(\mathcal{P})}(h)$ is the predicted per-slot aggregate energy consumption associated with the passive users. Throughout Section 2.3, $\tilde{L}(h)$ is determined in the day-ahead and may differ from the real-time aggregate energy demand, which is given by $L(h)$; we work under the hypothesis that the latter is always guaranteed by the supply-side.

To achieve a realistic smart grid model, the per-slot aggregate bid energy load in (2.22) must satisfy the following global constraint:

$$L^{(\min)}(h) \leq \tilde{L}(h) \leq L^{(\max)}(h), \qquad \forall h \tag{2.23}$$

where $L^{(\min)}(h) > 0$ (resp. $L^{(\max)}(h) > 0$) denotes the minimum (resp. the maximum) per-slot aggregate energy allowed by the grid infrastructure. In particular, a real-time aggregate demand lower than $L^{(\min)}(h)$ may imply additional costs for the supply-side if this requires turning off

some base load power plant. On the other hand, $L^{(\max)}(h)$ can be interpreted as the upper bound on the per-slot aggregate bid energy load that allows to satisfy the real-time aggregate demand with a certain outage probability. Alternatively, these boundaries can be chosen to guarantee a certain PAR of the real-time aggregate load with high probability.

In the same way as in Section 2.2.1, given the per-slot aggregate bid energy load $\tilde{L}(h)$, let us define the *grid cost function per unit of energy* $C_h\big(\tilde{L}(h)\big)$ at time-slot h, which remains fixed during the day period. In particular, we adopt a linear cost function per unit of energy:

$$C_h\big(\tilde{L}(h)\big) = K_h \tilde{L}(h). \tag{2.24}$$

The overall variable costs to supply the amount $\tilde{L}(h)$ are then given by $C_h\big(\tilde{L}(h)\big)\tilde{L}(h) = K_h \tilde{L}^2(h)$, which corresponds to the quadratic grid cost function widely used in the smart grid literature. In general, the grid coefficients $K_h > 0$ are different at each time-slot h, since the energy production varies across the day period according to the aggregate energy demand and to the availability of intermittent energy sources.

Each active user $n \in \mathcal{N}$ participates in a day-ahead demand-side bidding process during which he derives his per-slot bid energy load $\tilde{l}_n(h)$ for all h in the day period. If the user attains to his day-ahead bid $\tilde{l}_n(h)$, he simply pays $K_h \tilde{L}(h) \tilde{l}_n(h)$; nonetheless, he can possibly deviate from such strategy in real time by purchasing/selling a different amount of energy $l_n(h)$, for which he pays/perceives $K_h \hat{L}(h) l_n(h)$, while incurring in the penalties given by $\vartheta_h\big(l_n(h) - \tilde{l}_n(h)\big)$, where the penalty function $\vartheta_h(\cdot)$ is defined as

$$\vartheta_h(x) \triangleq \alpha_h (x)^+ + \beta_h (-x)^+ \tag{2.25}$$

with $(x)^+ = \max(x, 0)$, and where $\alpha_h, \beta_h \in (0, 1]$ are the penalty parameters for exceeding and for falling behind $\hat{l}_n(h)$, respectively. The parameters $\big\{\alpha_h, \beta_h\big\}_{h=1}^{H}$ are established before the day-ahead bidding process with the objective of discouraging real-time deviations from the bid loads, either upwards or downwards, giving incentives for a more accurate demand prediction: for instance, the central unit would choose $\alpha_h > \beta_h$ during hours of high expected consumption, and $\alpha_h < \beta_h$ during hours of low expected consumption.

The *cumulative monetary expense* incurred by user $n \in \mathcal{N}$ for exchanging the energy loads $\big\{l_n(h)\big\}_{h=1}^{H}$ with the grid can be expressed as

$$\mathsf{p}_n(\mathbf{x}_n, \tilde{\mathbf{l}}_{-n}) \triangleq \sum_{h=1}^{H} \Big(K_h\big(\boldsymbol{\delta}_n^{\mathrm{T}} \mathbf{x}_n(h) + \tilde{l}_{-n}(h)\big)\Big(l_n(h) + \vartheta_h\big(l_n(h) - \boldsymbol{\delta}_n^{\mathrm{T}} \mathbf{x}_n(h)\big)\Big) + W_n\big(\mathbf{x}_n(h)\big)\Big) \tag{2.26}$$

where $\tilde{\mathbf{l}}_{-n} \triangleq \big(\tilde{l}_{-n}(h)\big)_{h=1}^{H}$ is the aggregate bid energy load vector of the other users, with

$$\tilde{l}_{-n}(h) \triangleq \tilde{L}(h) - \tilde{l}_n(h) = \hat{L}^{(\mathcal{P})}(h) + \sum_{m \in \mathcal{N} \setminus \{n\}} \boldsymbol{\delta}^{\mathrm{T}} \mathbf{x}_m(h) \tag{2.27}$$

and where $W_n(\mathbf{x}_n(h))$ denotes the DSM cost function introduced in Section 2.2.1.

2.3.2 DSM Model

Let us denote by $\tilde{e}_n(h)$ the *per-slot bid energy consumption*, i.e., the day-ahead amount of energy (to be optimized) that user $n \in \mathcal{N}$ commits to consume at time-slot h, which is bounded as

$$\chi_n^{(\min)}(h) \leq \tilde{e}_n(h) \leq \chi_n^{(\max)}(h), \qquad \forall h \tag{2.28}$$

where $\chi_n^{(\min)}(h)$ and $\chi_n^{(\max)}(h)$ denote the minimum and maximum per-slot bid energy consumption at h, respectively. In addition, as in Section 2.2.2, active users $\mathcal{N}$ optimize their dispatchable DG and DS strategies, with $g_n(h)$ and $s_n(h)$ representing the per-slot energy production and the per-slot energy storage at time-slot h, respectively. In this context, the resulting per-slot strategy, per-slot energy load, and per-slot bid energy load of user $n \in \mathcal{N}$ are given by

$$\mathbf{x}_n(h) \triangleq \big(\tilde{e}_n(h), g_n(h), s_n(h)\big) \tag{2.29}$$

$$l_n(h) \triangleq e_n(h) - g_n(h) + s_n(h) \tag{2.30}$$

$$\tilde{l}_n(h) \triangleq \tilde{e}_n(h) - g_n(h) + s_n(h) \tag{2.31}$$

with $\boldsymbol{\delta} \triangleq (1, -1, 1)$. Again, the DSM cost function $W_n(\mathbf{x}_n)$ simply indicates the fuel cost for the dispatchable generator. We use $\bar{\Omega}_n$ to indicate the set of local constraints regulating user n's bidding (c.f. (2.28), dispatchable DG, and DS strategies. The constraints regarding dispatchable DG and DS are illustrated in detail in Sections 3.2 and 4.2; for the purpose of the discussion in this chapter, it is sufficient to mention that they are compact and convex in $\mathbf{x}_n$.

In our DSM procedure, the active users individually optimize their bidding, dispatchable DG, and DS strategies at two different time granularities, i.e., day-ahead and real-time.

1) *Day-ahead optimization* (c.f. Section 2.3.3). In the day-ahead bidding process, the users' goal is to minimize their individual expected cumulative expense over the day period

$$\mathsf{f}_n(\mathbf{x}_n, \tilde{\mathbf{l}}_{-n}) \triangleq \mathsf{E}\big\{\mathsf{p}_n(\mathbf{x}_n, \tilde{\mathbf{l}}_{-n})\big\} \tag{2.32}$$

with $\mathsf{p}_n(\mathbf{x}_n, \tilde{\mathbf{l}}_{-n})$ defined in (2.26), subject to the local and global constraints given by $\Omega_n(\mathbf{l}_{-n})$. Note that, like (2.6) in Section 2.2, the objective function (2.32) only depends on the aggregate energy loads and, hence, the users are not required to know the individual strategies of the others (and not even their individual energy loads), which preserve the users'

privacy.

2) *Real-time optimization* (c.f. Section 2.3.4). As the energy dispatch approaches, active users have more reliable information about their energy needs, which can be exploited to alleviate the impact of the day-ahead uncertainty. Hence, they can adjust their dispatchable DG and DS strategies in real-time so as to reduce the deviation of the real-time strategy with respect to the bid energy load, i.e., $\left|l_n(h) - \tilde{l}_n(h)\right|$, and minimize their expected expense for the rest of the day period.

After performing the day-ahead and the real-time optimization, the active users are finally billed according to (2.26).

2.3.3 Noncooperative Day-Ahead DSM for Expected Cost Minimization

Here, following Approach A2 described in Section 2.1.2, we model our DSM procedure as a GNEP. First of all, let us introduce some preliminary definitions. Let us rewrite the global constraint in (2.23) in the form of shared constraints $\mathbf{q}(\mathbf{x}) \leq \mathbf{0}$, where $\mathbf{q}(\mathbf{x}) \triangleq (\mathbf{q}^{(\min)}(\mathbf{x}), \mathbf{q}^{(\max)}(\mathbf{x})) : \mathbb{R}^{3HN} \to \mathbb{R}^{2H}$ with $\mathbf{x} \triangleq \big(\mathbf{x}_n\big)_{n=1}^{N}$ and

$$\mathbf{q}^{(\min)}(\mathbf{x}) \triangleq \Big(L^{(\min)}(h) - \sum_{n\in\mathcal{N}} \boldsymbol{\delta}^{\mathrm{T}}\mathbf{x}_n(h) - \hat{L}^{(\mathcal{P})}(h)\Big)_{h=1}^{H} \tag{2.33}$$

$$\mathbf{q}^{(\max)}(\mathbf{x}) \triangleq \Big(\sum_{n\in\mathcal{N}} \boldsymbol{\delta}^{\mathrm{T}}\mathbf{x}_n(h) + \hat{L}^{(\mathcal{P})}(h) - L^{(\max)}(h)\Big)_{h=1}^{H}. \tag{2.34}$$

Note that $\mathbf{q}(\mathbf{x})$ is convex on $\prod_{n\in\mathcal{N}} \bar{\Omega}_{\mathbf{x}_n}$. The strategy set of user $n \in \mathcal{N}$ can be then expressed as

$$\Omega_n(\tilde{\mathbf{l}}_{-n}) \triangleq \big\{\mathbf{x}_n \in \bar{\Omega}_n : \mathbf{q}(\mathbf{x}_n, \tilde{\mathbf{l}}_{-n}) \leq \mathbf{0}\big\} \tag{2.35}$$

whereas the joint strategy set is given by

$$\Omega \triangleq \big\{\mathbf{x} \in \mathbb{R}^{3HN} : \mathbf{x}_n \in \bar{\Omega}_n, \forall n \in \mathcal{N} \text{ and } \mathbf{q}(\mathbf{x}) \leq \mathbf{0}\big\}. \tag{2.36}$$

Hence, each active user is a player who competes against the others by choosing the bidding, dispatchable DG, and DS (included in the strategy vector $\mathbf{x}_n$) that minimize his cumulative monetary expense $\mathsf{f}_n(\mathbf{x}_n, \mathbf{l}_{-n})$ defined in (2.32), subject to the local and global constraints in $\Omega_n(\mathbf{l}_{-n})$ (cf. (2.2)):

$$\begin{aligned} \min_{\mathbf{x}_n} \quad & \mathsf{f}_n(\mathbf{x}_n, \tilde{\mathbf{l}}_{-n}) \\ \text{s.t.} \quad & \mathbf{x}_n \in \Omega_n(\tilde{\mathbf{l}}_{-n}) \end{aligned} \qquad \forall n \in \mathcal{N}. \tag{2.37}$$

The formal definition of the GNEP is the following: $\mathscr{G} = \langle \Omega, \mathbf{f} \rangle$, with $\Omega \triangleq \prod_{n\in\mathcal{N}} \Omega_n(\tilde{\mathbf{l}}_{-n})$ and $\mathbf{f} \triangleq \big(\mathsf{f}_n(\mathbf{x}_n, \tilde{\mathbf{l}}_{-n})\big)_{n=1}^{N}$.

GNEPs with shared constraints such as (2.37) are difficult problems to solve. They can

be formulated as quasi-variational inequality (QVI) problems [77]; however, in spite of some interesting and promising recent advancements (see, e.g., [90,91]), no efficient numerical methods based on the QVI reformulation have been developed yet. Nevertheless, for this type of GNEPs, some VI techniques can still be employed [74]: indeed, a solution of the GNEP can be computed by solving a suitably defined VI problem, as stated in the next lemma.

Lemma 2.2 ([74, Prop. 4.2])**.** *Given the GNEP* $\mathscr{G} = \langle \Omega, \mathbf{f} \rangle$*, suppose that the following hold:*

(a) *The strategy set* Ω_n *is closed and convex, for each* $n \in \mathcal{N}$*;*

(b) *For every feasible* $\tilde{\mathbf{l}}_{-n}$ *(i.e., such that* $\mathbf{x}_{-n} \in \Omega_{-n}$*), the objective function* $\mathsf{f}_n(\mathbf{x}_n, \tilde{\mathbf{l}}_{-n})$ *is convex and twice continuously differentiable in* $\mathbf{x}_n \in \Omega_n$*, for each* $n \in \mathcal{N}$*;*

(c) *The coupling constraint* $\mathbf{q}(\mathbf{x})$ *is continuously differentiable and jointly convex in* $\mathbf{x} \in \Omega$*.*

Let $\mathbf{F}(\mathbf{x}) \triangleq \left(\nabla_{\mathbf{x}_n} \mathsf{f}_n(\mathbf{x}_n, \tilde{\mathbf{l}}_{-n})\right)_{n=1}^{N}$*. Then, every solution of the* $\mathrm{VI}(\Omega, \mathbf{F})$ *is a solution of the GNEP.*

Note that, when passing from the GNEP (2.37) to the associated VI, not all the GNEP's solutions are preserved: in fact, Lemma 2.2 does not state that any solution of the GNEP is also a solution of the VI. The solutions of the GNEP that are also solutions of the $\mathrm{VI}(\Theta_{\mathbf{x}}, \mathbf{F})$ are termed as *variational solutions* [74] and enjoy some remarkable properties that make them particularly appealing in many applications. Among all, they can be interpreted as the solutions of a NEP with pricing, as detailed next.

Consider the following augmented NEP with $N+1$ players, in which the "new" $(N+1)$-th player (at the same level of the other N players) controls the price variable $\boldsymbol{\lambda} \in \mathbb{R}_{+}^{2H}$:

$$\begin{aligned} \min_{\mathbf{x}_n} \quad & \mathsf{f}_n(\mathbf{x}_n, \tilde{\mathbf{l}}_{-n}) + \boldsymbol{\lambda}^{\mathrm{T}} \mathbf{q}(\mathbf{x}_n, \tilde{\mathbf{l}}_{-n}) \\ & \qquad\qquad\qquad\qquad\qquad\qquad \forall n \in \mathcal{N} \\ \text{s.t.} \quad & \mathbf{x}_n \in \Omega_n \\ \min_{\boldsymbol{\lambda} \geq \mathbf{0}} \quad & -\boldsymbol{\lambda}^{\mathrm{T}} \mathbf{q}(\mathbf{x}). \end{aligned} \tag{2.38}$$

We can interpret $\boldsymbol{\lambda}$ as the overprices applied to force the users to satisfy the shared constraints $\mathbf{q}(\mathbf{x})$. Indeed, when $\mathbf{q}(\mathbf{x}) \leq \mathbf{0}$, the optimal price will be $\boldsymbol{\lambda} = \mathbf{0}$ (there is no need to punish the users if the constraints are already satisfied).

We can now establish the connection between the $\mathrm{VI}(\Omega, \mathbf{F})$ and the augmented NEP (2.38) [74, Lem. 4.4].

Lemma 2.3 ([74, Prop. 4.4])**.** *Under the setting of Lemma* 2.2*,* $(\mathbf{x}^\star, \boldsymbol{\lambda}^\star)$ *is a Nash equilibrium of the NEP* (2.38) *if and only if* $\mathbf{x}^\star$ *is a solution of the* $\mathrm{VI}(\Omega, \mathbf{F})$*, i.e., a variational solution of the GNEP* $\mathscr{G} = \langle \Omega, \mathbf{f} \rangle$*, and* $\boldsymbol{\lambda}^\star$ *is the multiplier associated with the shared constraints* $\mathbf{q}(\mathbf{x}^\star) \leq \mathbf{0}$ *in* Ω*.*

Based on Lemma 2.3, we are now able to analyze and compute the variational solutions of

the GNEP (2.37) as solutions of the augmented NEP (2.38).

Theorem 2.4. *Given the GNEP $\mathscr{G} = \langle \Omega, \mathbf{f} \rangle$, suppose that, for each $n \in \mathcal{N}$, the following hold:*

(a) *The strategy set Ω_n is compact and convex;*

(b) *$\chi_n^{(\min)}(h)$ and $\chi_n^{(\max)}(h)$ in (2.28) are chosen such that the pdf of the per-slot energy consumption satisfies*

$$f_{e_n(h)}(x) \geq \frac{1}{(\alpha_h + \beta_h) L^{(\min)}(h)} \frac{\left(\alpha_h + 1\right)^2}{2} \tag{2.39}$$

$\forall x \in \left[\chi_n^{(\min)}(h), \chi_n^{(\max)}(h)\right]$.

(c) *The DSM function $W_n(\cdot)$ is convex and twice continuously differentiable, for each $n \in \mathcal{N}$.*

Then, the GNEP has variational solutions.

The conditions (a) and (c) in Theorem 2.4 are very mild and always satisfied in practice. Regarding condition (b), when the distribution of $e_n(h)$ is unimodal, condition (2.39) limits the displacement of $\tilde{e}_n(h)$ around the mode of $e_n(h)$ in order to ensure the convexity of the objective function $\mathsf{f}_n(\mathbf{x}_n, \tilde{\mathbf{l}}_{-n})$; on the contrary, when the distribution of $e_n(h)$ is multimodal, $\chi_n^{(\min)}(h)$ and $\chi_n^{(\max)}(h)$ must be carefully selected to guarantee the convexity of $\mathsf{f}_n(\mathbf{x}_n, \tilde{\mathbf{l}}_{-n})$ (see Appendix 5.B.2). These considerations also apply to condition (a.2) in Theorem 2.5. Lastly, the fulfillment of the conditions in Theorem 2.4 also implies the accomplishment Lemma 2.2 (whose requirements are less stringent than those in Theorem 2.4).

Distributed Algorithm

Now, we build on the game theoretical pricing-based interpretation (2.38) (c.f. Lemma 2.3) to design distributed algorithms that converge to a variational solution of the GNEP $\mathscr{G}$. As in Section 2.2.3, we focus on the class of totally asynchronous best-response algorithms. Recalling the definitions of $\mathscr{T}_n$ and $t_n(i)$, and assuming that conditions (A1)–(A3) in Section 4.3.3 hold for $\mathscr{T}_n$ and $t_n(i)$, $\forall n \in \mathcal{N}$, each user updates his strategy by minimizing his cumulative monetary expense, given the most recently available value of the aggregate bid energy load vector of the other users $\tilde{\mathbf{l}}_{-n}^{(\mathbf{t}(i))} \triangleq \left(\tilde{l}_{-n}^{(\mathbf{t}(i))}(h)\right)_{h=1}^{H}$, with

$$l_{-n}^{(\mathbf{t}(i))}(h) \triangleq \hat{L}^{(\mathcal{P})}(h) + \sum_{m \in \mathcal{N} \setminus \{n\}} \tilde{l}_m^{(t_m(i))}(h). \tag{2.40}$$

We can compute the variational solutions of the GNEP (2.37) by solving the augmented NEP (2.38). This can be done using the recent framework in [76], which leads to the asynchronous proximal decomposition algorithm (PDA) described in Algorithm 2.3, and whose convergence conditions are given in Theorem 2.4. We refer to Section 5.4.2 for a detailed discussion of the algorithm.

Algorithm 2.3 Asynchronous PDA with Coupling Constraints

`Data` : Set $i=0$ and the initial centroids $\big(\bar{\mathbf{x}}_n\big)_{n=1}^N = \mathbf{0}$ and $\bar{\boldsymbol{\lambda}} = \mathbf{0}$. Given $\big\{K_h, \alpha_h, \beta_h\big\}_{h=1}^H$, $\big\{\rho^{(i)}\big\}_{i=0}^\infty$, $\tau > 0$, and any feasible starting point $\mathbf{z}^{(0)} \triangleq \big(\big(\mathbf{x}_n^{(0)}\big)_{n=1}^N, \boldsymbol{\lambda}^{(0)}\big)$ with $\boldsymbol{\lambda}^{(0)} \geq \mathbf{0}$:

`(S.1)` : `If` a suitable termination criterion is satisfied: `STOP`.

`(S.2)` : `For` $n \in \mathcal{N}$, each user computes $\mathbf{x}_n^{(i+1)}$ as

$$\mathbf{x}_n^{(i+1)} = \begin{cases} \mathbf{x}_n^\star \in \underset{\mathbf{x}_n \in \Omega_{\mathbf{x}_n}}{\operatorname{argmin}} \Big\{ \mathsf{f}_n\big(\mathbf{x}_n, \tilde{\mathbf{l}}_{-n}^{(\mathbf{t}(i))}\big) + (\boldsymbol{\lambda}^{(i)})^{\mathrm{T}} \mathbf{q}\big(\mathbf{x}_n, \tilde{\mathbf{l}}_{-n}^{(\mathbf{t}(i))}\big) + \dfrac{\tau}{2}\|\mathbf{x}_n - \bar{\mathbf{x}}_n\|^2 \Big\}, & \text{if } i \in \mathscr{T}_n \\ \mathbf{x}_n^{(i)}, & \text{otherwise} \end{cases}$$

`End`

The central unit computes $\boldsymbol{\lambda}^{(i+1)}$ as

$$\boldsymbol{\lambda}^{(i+1)} = \boldsymbol{\lambda}^\star \in \underset{\boldsymbol{\lambda} \geq \mathbf{0}}{\operatorname{argmin}} \Big\{ -\boldsymbol{\lambda}^{\mathrm{T}} \mathbf{q}(\mathbf{x}) + \frac{\tau}{2}\|\boldsymbol{\lambda} - \bar{\boldsymbol{\lambda}}\|^2 \Big\}$$

`(S.3)` : `If` the NE is reached, then each user $n \in \mathcal{N}$ sets $\mathbf{x}_n^{(i+1)} \leftarrow (1-\rho^{(i)})\bar{\mathbf{x}}_n + \rho^{(i)}\mathbf{x}_n^{(i+1)}$ and updates his centroid: $\bar{\mathbf{x}}_n = \mathbf{x}_n^{(i+1)}$; likewise, the central unit sets $\boldsymbol{\lambda}^{(i+1)} \leftarrow (1-\rho^{(i)})\bar{\boldsymbol{\lambda}} + \rho^{(i)}\boldsymbol{\lambda}^{(i+1)}$ and updates the centroid: $\bar{\boldsymbol{\lambda}} = \boldsymbol{\lambda}^{(i+1)}$.

`(S.4)` : $i \leftarrow i+1$; `Go to (S.1)`.

Theorem 2.5. *Given the GNEP* $\mathscr{G} = \big\langle \Omega, \mathbf{f} \big\rangle$*, suppose that the following hold:*

(a.1) *Conditions* (a) *and* (c) *in Theorem* 2.4 *are satisfied;*

(a.2) $\chi_n^{(\min)}(h)$ *and* $\chi_n^{(\max)}(h)$ *in* (2.28) *are chosen such that the pdf of the per-slot energy consumption satisfies*

$$f_{e_n(h)}(x) \geq \frac{1}{(\alpha_h + \beta_h) L^{(\min)}(h)} \Big(\frac{(\alpha_h+1)^2}{4} + N\big(\max(\alpha_h, \beta_h) + \alpha_h + \beta_h \big) \Big) \tag{2.41}$$

$\forall x \in \big[\chi_n^{(\min)}(h), \chi_n^{(\max)}(h)\big]$*, for each* $n \in \mathcal{N}$*;*

(a.3) *The penalty parameters are such that* $\alpha_h + \beta_h \leq 1, \forall h$*;*

(b) *The regularization parameter* τ *satisfies*

$$\tau > \frac{3}{2}(N-1) \max_h K_h + \sqrt{\frac{9}{4}(N-1)^2 \max_h K_h^2 + 3HN} \tag{2.42}$$

(c) $\{\rho^{(i)}\} \subset [R_m, R_M]$*, with* $0 < R_m < R_M < 2$.

Then, any sequence $\big\{(\mathbf{x}^{(i)}, \boldsymbol{\lambda}^{(i)})\big\}_{i=1}^\infty$ *generated by Algorithm* 2.3 *converges to a variational solution of the GNEP.*

Note that, if we omit the global constraint (2.23), the GNEP (2.37) reduces to a classical NEP, where the coupling among the players occurs only at the level of the objective functions (as addressed in [86]). Of course, the framework and algorithm proposed in the present paper

contain this formulation as special case.

2.3.4 Real-Time Adjustments

After the day-ahead bidding process, the per-slot aggregate bid energy loads $\{\tilde{L}(h)\}_{h=1}^{H}$ are fixed as a result of Algorithm 2.3 and, consequently, so are the energy prices per unit of energy. Then, active users are charged in real-time based on such prices, while the differences between their actual energy requirements and the negotiated day-ahead amounts are penalized as in (2.26). However, at this point, it is reasonable to assert that the users know their energy consumption $e_n(h)$ for the upcoming time-slot with much less uncertainty than during the day-ahead bidding process. In this setting, at each h, one can exploit this reduced uncertainty to independently adjust his dispatchable DG and DS strategies $\{g_n(t), s_n(t)\}_{t=h}^{H}$ so as to minimize his expected expense for the remaining time-slots $t = h, \ldots, H$. At the same time, we can guarantee the physical constraints on the user's individual distribution infrastructure given by

$$-l_n^{(\min)} \leq l_n(h) \leq l_n^{(\max)}, \qquad \forall h \tag{2.43}$$

where $l_n^{(\min)} \geq 0$ and $l_n^{(\max)} > 0$ are the outgoing and the incoming capacities of user n's energy link, respectively. For modeling simplicity, we assume that, right before each time-slot h, each user $n \in \mathcal{N}$ has perfect knowledge of $e_n(h)$. Nonetheless, he still needs to satisfy the requirements on his dispatchable DG and DS strategies: in this regard, if the strategies over different time-slots are coupled (see, e.g., the constraints in Table 5.1 in Section 5.6), the user has to take into account the strategies adopted in the previous time-slots.

Let us provide some preliminary definitions. We denote by $\mathbf{y}_n(h) \triangleq \big(g_n(h), s_n(h)\big)$ the real-time strategy for each time-slot h, and we introduce the transformation vector $\boldsymbol{\delta}_{s-g} \triangleq (-1, 1)$ such that $\boldsymbol{\delta}_{s-g}^{\mathrm{T}} \mathbf{y}_n(h) = -g_n(h) + s_n(h)$. Moreover, $\Theta_n^{(\mathsf{DG})}$ and $\Theta_n^{(\mathsf{DS})}$ denote the dispatchable DG and DS strategy sets, respectively, such that such strategies are feasible if $\big(g_n(h)\big)_{h=1}^{H} \in \Theta_n^{(\mathsf{DG})}$ and $\big(s_n(h)\big)_{h=1}^{H} \in \Theta_n^{(\mathsf{DS})}$. Lastly, $\big(g_n^{\star}(t)\big)_{t=1}^{h-1}$ and $\big(s_n^{\star}(t)\big)_{t=1}^{h-1}$ express the dispatchable DG and DS strategies already fixed in the past time-slots $t = 1, \ldots, h-1$. Then, we define $\Theta_{n,h}$ as the real-time strategy set for user $n \in \mathcal{N}$ at h:

$$\begin{aligned}\Theta_{n,h} \triangleq \Big\{ &\big(\mathbf{y}_n(t)\big)_{t=h}^{H} \in \mathbb{R}^{2(H-h+1)} : \big(\big(g_n^{\star}(t)\big)_{t=1}^{h-1}, \big(g_n(t)\big)_{t=h}^{H}\big) \in \Theta_n^{(\mathsf{DG})}, \\ &\big(\big(s_n^{\star}(t)\big)_{t=1}^{h-1}, \big(s_n(t)\big)_{t=h}^{H}\big) \in \Theta_n^{(\mathsf{DS})}, \text{ and } -l_n^{(\min)} \leq e_n(h) + \boldsymbol{\delta}_{s-g}^{\mathrm{T}} \mathbf{y}_n(h) \leq l_n^{(\max)}, \forall h \Big\}\end{aligned} \tag{2.44}$$

The price paid by user $n \in \mathcal{N}$ for purchasing energy from the grid at time-slot h (conditioned on the per-slot bid energy load $\tilde{l}_n(h)$ resulting from the day-ahead optimization) is given by

$$\mathsf{p}_{n,h}\big(\mathbf{y}_n(h) \mid \tilde{l}_n(h)\big) \triangleq \mathsf{p}_h\big(e_n(h) + \boldsymbol{\delta}_{s-g}^{\mathrm{T}} \mathbf{y}_n(h) + \vartheta_h\big(e_n(h) + \boldsymbol{\delta}_{s-g}^{\mathrm{T}} \mathbf{y}_n(h) - \tilde{l}_n(h)\big)\big) + W_n\big(\mathbf{y}_n(h)\big) \tag{2.45}$$

with $\mathsf{p}_h \triangleq K_h \tilde{L}(h)$ and $\vartheta_h(x)$ defined in (2.25). Likewise, the expected expense for each time-slot $t = h+1, \ldots, H$ is

$$\mathsf{f}_{n,t}\big(\mathbf{y}_n(t) \mid \tilde{l}_n(t)\big) \triangleq \mathsf{p}_t \mathsf{E}\big\{e_n(t) + \boldsymbol{\delta}_{s-g}^{\mathrm{T}} \mathbf{y}_n(t) + \vartheta_t\big(e_n(t) + \boldsymbol{\delta}_{s-g}^{\mathrm{T}} \mathbf{y}_n(t) - \tilde{l}_n(t)\big)\big\} + W_n\big(\mathbf{y}_n(t)\big). \quad (2.46)$$

Therefore, at each time-slot h, each user $n \in \mathcal{N}$ uses the value of $e_n(h)$ and the reduced uncertainty about $\big\{e_n(t)\big\}_{t=h+1}^{H}$ to solve

$$\begin{aligned} \min_{\{\mathbf{y}_n(t)\}_{t=h}^{H}} \quad & \mathsf{p}_{n,h}\big(\mathbf{y}_n(h) \mid \tilde{l}_n(h)\big) + \sum_{t=h+1}^{H} \mathsf{f}_{n,t}\big(\mathbf{y}_n(t) \mid \tilde{l}_n(t)\big) \\ \text{s.t.} \quad & \big(\mathbf{y}_n(t)\big)_{t=h}^{H} \in \Theta_{n,h}. \end{aligned} \quad (2.47)$$

It is straightforward to observe that $\mathsf{p}_{n,h}\big(\mathbf{y}_n(h) \mid \tilde{l}_n(h)\big)$ in (2.45) and $\mathsf{f}_{n,h}\big(\mathbf{y}_n(h) \mid \tilde{l}_n(h)\big)$ in (2.46) are both convex in $\mathbf{y}_n(h)$ under Theorem 2.5. Since the dispatchable DG and DS strategy sets are known to be convex, the optimization problem (2.47) is convex in $\big(\mathbf{y}_n(t)\big)_{t=h}^{H}$ and can be solved using efficient convex optimization techniques [62, Ch. 11].

2.3.5 DSM Implementation

Summarizing, the proposed demand-side optimization based on Algorithm 2.3 works as follows. At the beginning of the day-ahead optimization process, τ is computed as in (2.42) and broadcast to each user $n \in \mathcal{N}$, together with the grid coefficients and the penalty parameters $\big\{K_h, \alpha_h, \beta_h\big\}_{h=1}^{H}$. Then, at each iteration i, any active user who wants to update his strategy solves his own (regularized) augmented optimization problem given $\boldsymbol{\lambda}^{(i)}$ and based on the most recent values of the aggregate bid energy loads $\big\{\tilde{L}^{(\mathbf{t}(i))}(h)\big\}_{h=1}^{H}$, which are calculated by the central unit referring to the (possibly outdated) individual demands, and communicates his new load to the central unit. At the same time, the central unit updates the price variable $\boldsymbol{\lambda}$ and broadcasts it to the demand-side. When an equilibrium in the inner loop is reached, the central unit proceeds to the next iteration. This process is iterated until a suitable termination criterion imposed by the central unit is satisfied. In real-time, given the aggregate bid energy loads $\big\{\tilde{L}(h)\big\}_{h=1}^{H}$ (fixed in the day-ahead), at each time-slot h, active users can exploit the reduced uncertainty about their energy requirements and adjust their DG and DS strategies $\big\{g_n(h), s_n(h)\big\}_{h=1}^{H}$ so as to minimize the impact of the real-time penalties.

3

Demand-Side Management via Distributed Energy Generation and Storage Optimization

Abstract—Demand-side management, together with the integration of distributed energy generation and storage, are considered increasingly essential elements for implementing the smart grid concept and balancing massive energy production from renewable sources. We focus on a smart grid in which the demand-side comprises traditional users as well as users owning some kind of distributed energy sources and/or energy storage devices. By means of a day-ahead optimization process regulated by an independent central unit, the latter users intend to reduce their monetary energy expense by producing or storing energy rather than just purchasing their energy needs from the grid. In this paper, we formulate the resulting grid optimization problem as a noncooperative game and analyze the existence of optimal strategies. Furthermore, we present a distributed algorithm to be run on the users' smart meters, which provides the optimal production and/or storage strategies, while preserving the privacy of the users and minimizing the required signaling with the central unit. Finally, the proposed day-ahead optimization is tested in a realistic situation.

Index Terms—Demand-Side Management, Distributed Energy Generation, Distributed Energy Storage, Game Theory, Proximal Decomposition Algorithm, Smart Grid.

This chapter is an exact reproduction of [84] with the exception of pagination.

3.1 Introduction

Smart grids have an essential role in the process of transforming the functionalities of the present energy grid in order to provide a user-oriented service and guarantee high security, quality, and economic efficiency of the electricity supply in a market environment. In addition, smart grids are expected to be a key enabler in the transition to a low-carbon energy sector, ensuring the efficient and sustainable use of natural resources [92]. The production from renewable sources as, for instance, wind and photovoltaic units is, however, intermittent in nature and there is often no correlation between the production and the local consumption. Furthermore, since large amounts of variable generation from renewable sources are not fully forecastable, there is an increasing need for flexible, dispatchable, fast-ramping energy generation for balancing variations in load and contingencies such as the loss of transmission or generation assets. Similar problems arise at a market level, since national and local balances between supply and demand are more complicated to manage with high levels of renewable energy generation [93].

In this regard, the concepts of demand-side management (DSM), distributed energy generation (DG), and distributed energy storage (DS) are recognized as main facilitators for the smart grid deployment, since the challenges caused by the integration of renewable energy sources can be minimized when dispatchable DG and DS are incorporated into the demand-side of the electricity network and innovative DSM methods are simultaneously implemented. Indeed, the combination of DG, DS, and DSM techniques results in a system of diverse generation sources supplying energy across the grid to a large set of demand-side users with possibilities for improved energy efficiency, local generation, and controllable loads. Demand-side management refers to the different initiatives intended to modify the time pattern and magnitude of the demand, introducing advanced mechanisms for encouraging the demand-side to participate actively in the network optimization process [94]. Therefore, demand-side users are equipped with a control device, commonly known as smart meter, which communicates with the supply-side and manages their energy demand.

In this paper, we propose a DSM method consisting in a day-ahead optimization process. We focus on those demand-side users, possibly owning DG and DS devices, whose energy consumption is greater than their energy production capabilities. The main objective of these end users is to reduce their monetary expense during the time period of analysis by producing and/or storing energy rather than just purchasing their energy needs from the grid.

Considering the selfish nature of the users, a game theoretical approach is particularly suitable in order to calculate their optimal production and storage strategies. For this reason, we model the day-ahead optimization problem as a noncooperative Nash game and we analyze the existence of the solutions, which correspond to the well-known concept of Nash equilibria, when a practical pricing model (cf. [51, 58]) is applied. Finally, we present a distributed and iterative

scheme based on the proximal decomposition algorithm that converges to the Nash equilibria with minimum information exchange while safeguarding the privacy of the users.

The rest of the paper is structured as follows. In Section 3.2 we describe the overall structure of our smart grid and, specifically, we introduce the production and storage models, as well as the energy cost and pricing model. Section 3.3 formulates the optimization problem as a noncooperative game and solves it by means of a specific distributed algorithm. In addition, we derive sufficient conditions for the existence of a solution, as well as for the convergence of the proposed algorithm. In Section 3.4 we show some illustrative numerical results obtained through experimental evaluations. Finally, we provide some concluding remarks in Section 3.5.

3.2 Smart Grid Model

The goal of this section is to present the overall smart grid model, describe the different types of users belonging to demand-side of the network, and introduce the adopted energy cost and pricing mechanism.

The modern power grid is a complex network comprising several subsystems (power plants, transmission lines, substations, distribution grids, and consumers), which can be conveniently divided into [3, 57, 95]:

(i) *Supply-side*: it includes the utilities (energy producers and providers) and the energy transmission network;
(ii) *Central unit*: it is the regulation authority that coordinates the grid optimization process;
(iii) *Demand-side*: it incorporates the end users (energy consumers), eventually equipped with DG and/or DS, and the energy distribution network.

Since in this paper we propose a DSM mechanism, we focus our attention only on the demand-side of the smart grid, which is described in detail in Section 3.2.1, whereas the supply-side and the central unit are modeled as plainly as possible.

3.2.1 Demand-Side Model

Demand-side users are characterized in the first instance by their individual *per-slot energy consumption profile* $e_n(h)$, defined as the energy needed by user $n \in \mathcal{D}$ to supply his appliances at time-slot h. Accordingly, we also introduce the *energy consumption scheduling vector* $\mathbf{e}_n$, which gathers the energy consumption profiles for the H time-slots in which the time period of analysis is divided, i.e., $\mathbf{e}_n \triangleq \big(e_n(h)\big)_{h=1}^{H}$.

Our model classifies the set of all demand-side users $\mathcal{D}$, with cardinality $|\mathcal{D}| = P + N$, into the set of P *passive* users, denoted by $\mathcal{P} \subset \mathcal{D}$, and the set of N *active* users, denoted by

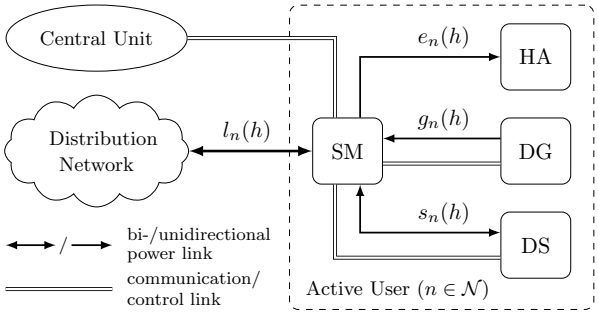

Figure 3.1: Connection scheme between the smart grid and one active user consisting of: smart meter (SM), home appliances (HA), distributed energy generation (DG), and distributed energy storage (DS).

$\mathcal{D} \supset \mathcal{N} \triangleq \mathcal{D} \backslash \mathcal{P}$. Passive users are basically energy consumers and resemble traditional demand-side users, whereas active users participate in the optimization process, i.e., they react to changes in the cost per unit of energy by modifying their demand. Each active user is connected not only to the bidirectional power distribution grid, but also to a communication infrastructure that enables two-way communication between his smart meter and the central unit (as shown in Figure 3.1). The main objective of each active user is to optimize his day-ahead strategy while fulfilling his energy requirements during the time period of analysis, $\mathbf{e}_n$. This strategy depends in the first instance on the equipment owned by user $n \in \mathcal{N}$, e.g., energy sources (see Section 3.2.2) and/or storage devices (see Section 3.2.3), but is also strongly related to the strategy followed by the rest of the active users $\mathcal{N} \backslash \{n\}$ (see Section 3.2.4) and to the aggregate energy consumption of the passive users connected to the grid.

Active users include two broad categories: dispatchable energy producers and energy storers. For convenience, we use $\mathcal{G} \subseteq \mathcal{N}$ to denote the subset of users possessing some dispatchable energy source. For users $n \in \mathcal{G}$, $g_n(h) \geq 0$ represents the *per-slot energy production profile* at time-slot h. Likewise, we introduce $\mathcal{S} \subseteq \mathcal{N}$ as the subset of users owning some energy storage device. Users $n \in \mathcal{S}$ are characterized by the *per-slot energy storage profile* $s_n(h)$ at time-slot h: $s_n(h) > 0$ when the storage device is to be charged (i.e., an additional energy consumption), $s_n(h) < 0$ when the storage device is to be discharged (i.e., a reduction of the energy consumption), and $s_n(h) = 0$ when the device is inactive. It is worth remarking that $\mathcal{G} \cup \mathcal{S} = \mathcal{N}$, but we also contemplate active users being both dispatchable producers and storers, i.e., $\mathcal{G} \cap \mathcal{S} \neq \emptyset$.

Finally, we define the *per-slot energy load profile* as

$$l_n(h) \triangleq \begin{cases} e_n(h), & \text{if } n \in \mathcal{P} \\ e_n(h) - g_n(h) + s_n(h), & \text{if } n \in \mathcal{N} \end{cases} \tag{3.1}$$

which expresses the energy flow between user n and the distribution grid at time-slot h, where $l_n(h) > 0$ if the energy flows from the grid to user n and $l_n(h) < 0$ otherwise, as shown in Figure 3.1.

3.2.2 Energy Production Model

Energy producers can generate energy either to power their own appliances, to charge a storage device, or to sell it to the grid during peak hours. Let us first characterize energy producers depending upon the type of DG they employ [96].

Non-dispatchable energy producers $\mathcal{G}_{\mathrm{R}} \subset \mathcal{D}$ using, e.g., renewable resources of intermittent nature such as solar panels or wind turbines. Having only fixed costs, they generate electricity at their maximum available power, which implies no strategy regarding energy production. Consequently, for users $n \in \mathcal{G}_{\mathrm{R}}$, we include non-dispatchable generation within the per-slot energy consumption profile $e_n(h)$. Hence, they may have $e_n(h) < 0$ when this energy production is greater than their energy consumption at a given time-slot h. Note that any demand-side user can belong to $\mathcal{G}_{\mathrm{R}}$ regardless of his condition of passive or active participant in the optimization process.

Dispatchable energy producers $\mathcal{G} \subseteq \mathcal{N}$ using, e.g., internal combustion engines, gas turbines, or fuel cells. These energy producers, beside fixed costs, have also variable production costs (e.g., the fuel cost) and, therefore, they are interested in optimizing their energy production strategies. In consequence, we introduce the *production cost function* $W_n\big(g_n(h)\big)$, which gives the variable production costs for generating the amount of energy $g_n(h)$ at time-slot h, with $W_n(0) = 0$.

Let us now introduce our model for dispatchable energy producers. Let $g_n^{(\max)}$ be the *maximum energy production capability* for user $n \in \mathcal{G}$ over a time-slot. Then, the per-slot energy production profile is bounded as

$$0 \leq g_n(h) \leq g_n^{(\max)}. \tag{3.2}$$

For the sake of simplicity, we consider dispatchable energy sources with a fixed instantaneous output power level, which are operated during fractions of a time slot. Hence, $g_n^{(\max)}$ represents the amount of energy produced when user n's energy source operates during 100% of a time-slot. Additionally, the cumulative energy production must satisfy

$$\sum_{h=1}^{H} g_n(h) \leq \gamma_n^{(\max)} \tag{3.3}$$

where $0 < \gamma_n^{(\max)} \leq H g_n^{(\max)}$represents the maximum amount of energy that user $n \in \mathcal{G}$ can generate during the time period of analysis (e.g., to prevent over-usage). Then, introducing $\mathbf{g}_n \triangleq \big(g_n(h)\big)_{h=1}^{H}$ as the *energy production scheduling vector*, we define the strategy set $\Omega_{\mathbf{g}_n}$ for dispatchable energy producers $n \in \mathcal{G}$, including constraints (3.2) and (3.3), as

$$\Omega_{\mathbf{g}_n} \triangleq \big\{\mathbf{g}_n \in \mathbb{R}_+^H : \mathbf{g}_n \preceq g_n^{(\max)}\mathbf{1}_H, \mathbf{1}_H^{\mathrm{T}}\mathbf{g}_n \leq \gamma_n^{(\max)}\big\} \tag{3.4}$$

where the operator $\preceq$ for vectors is defined componentwise, and $\mathbf{1}_H$ is the H-dimensional unit

vector.

3.2.3 Energy Storage Model

In our model, storage devices (see, e.g., [96,97] for an overview on storage technologies) of users $n \in \mathcal{S}$ are characterized by: *charging efficiency*, *discharging efficiency*, *leakage rate*, *capacity*, and *maximum charging rate*. If we express the per-slot energy storage profile as $s_n(h) \triangleq s_n^{(+)}(h) - s_n^{(-)}(h)$, where $s_n^{(+)}(h), s_n^{(-)}(h) \geq 0$ are the *per-slot energy charging profile* and the *per-slot energy discharging profile*, respectively, the charging and discharging efficiencies $0 < \beta_n^{(+)} \leq 1$ and $\beta_n^{(-)} \geq 1$ take into account the conversion losses of the storage device. For instance, if $s_n^{(+)}(h)$ is taken from the grid to be stored on the device, only $\beta_n^{(+)} s_n^{(+)}(h)$ is effectively charged; on the other hand, in order to obtain $s_n^{(-)}(h)$ from the device, $\beta_n^{(-)} s_n^{(-)}(h)$ is to be discharged. The leakage rate $0 < \alpha_n \leq 1$ models the decrease in the energy level with the passage of time: if $q_n(h)$ denotes the *charge level* at the end of time-slot h, then it reduces to $\alpha_n q_n(h)$ at the end of time-slot $h+1$. The capacity c_n indicates how much energy the storage device can accumulate. Lastly, the maximum charging rate $s_n^{(\max)}$ is the maximum energy that can be stored during a single time-slot.

Let us introduce the vectors $\mathbf{s}_n(h) \triangleq \left(s_n^{(+)}(h), s_n^{(-)}(h)\right)^{\mathrm{T}}$ and $\boldsymbol{\beta}_n \triangleq (\beta_n^{(+)}, -\beta_n^{(-)})^{\mathrm{T}}$: the charge level $q_n(h)$ is given by

$$q_n(h) \triangleq \alpha_n q_n(h-1) + \boldsymbol{\beta}_n^{\mathrm{T}} \mathbf{s}_n(h) \tag{3.5}$$

where $q_n(h-1)$ is the charge level at the previous time-slot, which gets reduced by a factor α_n during time-slot h, and $\boldsymbol{\beta}_n^{\mathrm{T}} \mathbf{s}_n(h)$ is the energy charged or discharged at h.[1] Since $q_n(h)$ is bounded above by c_n and below by 0, $\mathbf{s}_n(h)$ satisfies

$$-\alpha_n q_n(h-1) \leq \boldsymbol{\beta}_n^{\mathrm{T}} \mathbf{s}_n(h) \leq c_n - \alpha_n q_n(h-1). \tag{3.6}$$

Moreover, since the maximum charging rate cannot be surpassed, we also have that

$$\boldsymbol{\beta}_n^{\mathrm{T}} \mathbf{s}_n(h) \leq s_n^{(\max)}. \tag{3.7}$$

Additionally, it is convenient to include a constraint on the desired charge level at the end of the time period of analysis. The choice of the optimal $q_n(H)$ requires, however, the knowledge of the energy cost at time-slot $H+1$, while the optimization process addressed in this paper only takes in consideration one isolated time period of analysis. In any case, it is reasonable to expect the storage device going through an integer number of cycles of charging to discharging that are opposite to the daily energy demand fluctuation [47]. This implies that the final charge

[1] Although we do not impose charging and discharging operations to be mutually exclusive, the optimal storage strategies obtained in Section 3.3 satisfy $s_n^{(+)}(h) s_n^{(-)}(h) = 0$, $\forall h$, whenever $\beta_n^{(+)} < 1$ and $\beta_n^{(-)} > 1$.

level $q_n(H)$ must be approximately the same as the *initial charge level* $q_n(0)$, i.e., the charge level of user $n \in \mathcal{S}$ at the beginning of time-slot $h = 1$. Hence, we have that

$$\big|q_n(H) - q_n(0)\big| \leq \epsilon_n \tag{3.8}$$

where ϵ_n is a sufficiently small positive constant.

Now, we can relate $q_n(h)$ to the initial charge level and to the energy storage profiles at the previous time-slots as

$$q_n(h) = \alpha_n^h q_n(0) + \sum_{t=1}^{h} \alpha_n^{(h-t)} \boldsymbol{\beta}_n^{\mathrm{T}} \mathbf{s}_n(t). \tag{3.9}$$

Given the above expression, and introducing the *energy storage scheduling vector* $\mathbf{s}_n \triangleq \big(\big(s_n^{(+)}(h)\big)_{h=1}^{H}, \big(s_n^{(-)}(h)\big)_{h=1}^{H}\big)$, we define the strategy set for energy storers $n \in \mathcal{S}$ as $\Omega_{\mathbf{s}_n}$, which combines constraints (3.6), (3.7), and (3.8):

$$\begin{aligned}\Omega_{\mathbf{s}_n} \triangleq \big\{\mathbf{s}_n \in \mathbb{R}_+^{2H} : \boldsymbol{\Delta}_{\beta,n}\mathbf{s}_n \preceq s_n^{(\max)}\mathbf{1}_H, -q_n(0)\mathbf{b}_n \preceq \mathbf{A}_n\boldsymbol{\Delta}_{\beta,n}\mathbf{s}_n \preceq c_n\mathbf{1}_H - q_n(0)\mathbf{b}_n,\\ (1-\alpha_n^H)q_n(0) - \epsilon_n \leq \mathbf{a}_n^{\mathrm{T}}\boldsymbol{\Delta}_{\beta,n}\mathbf{s}_n \leq (1-\alpha_n^H)q_n(0) + \epsilon_n\big\}\end{aligned} \tag{3.10}$$

where $\boldsymbol{\Delta}_{\beta,n} \triangleq (\beta_n^{(+)}\mathbf{I}_H \ -\beta_n^{(-)}\mathbf{I}_H)$, $\mathbf{A}_n$ is a H-dimensional lower triangular matrix with elements $[\mathbf{A}_n]_{i,j} \triangleq \alpha_n^{(i-j)}$, and $\mathbf{a}_n$ and $\mathbf{b}_n$ are H-dimensional vectors defined respectively as $[\mathbf{a}_n]_i \triangleq \alpha_n^{(H-i)}$ and $[\mathbf{b}_n]_i = \alpha_n^i$.

Finally, it is important to remark that the optimization process analysis and the algorithm presented in Section 3.3 hold for any production and storage models resulting in a compact and convex strategy set as the ones in (3.4) and (3.10).

After analyzing all possible types of users in the demand-side, we summarize their strategy sets in Table 3.1.

3.2.4 Energy Cost and Pricing Model

This section describes the cost model on which depends the price of energy. Let us define the *aggregate per-slot energy load* at time-slot h as

$$0 < L(h) \triangleq L^{(\mathcal{P})}(h) + \sum_{n \in \mathcal{N}} l_n(h) \tag{3.11}$$

where $L^{(\mathcal{P})}(h) \triangleq \sum_{n\in\mathcal{P}} e_n(h)$ is the aggregate per-slot energy consumption associated with the passive users connected to the grid. Since we are not interested in analyzing overload conditions, throughout the paper we assume that $L(h) < L^{(\max)}$ at each time-slot h, where $L^{(\max)}$ denotes the maximum aggregate energy load that the grid can take before experiencing a blackout.

Let us define the *grid cost function* $C_h\big(L(h)\big)$ indicating the price fixed by the supply-side

	User subset	Strategy set
$\mathcal{P}$	$\mathcal{P}\backslash\mathcal{G}_{\mathrm{R}}$ $\mathcal{G}_{\mathrm{R}}\backslash(\mathcal{N}\cap\mathcal{G}_{\mathrm{R}})$	No strategy
$\mathcal{N}$	$\mathcal{G}\backslash(\mathcal{G}\cap\mathcal{S})=\mathcal{N}_{\mathcal{G}\backslash\mathcal{S}}$ $\mathcal{S}\backslash(\mathcal{G}\cap\mathcal{S})=\mathcal{N}_{\mathcal{S}\backslash\mathcal{G}}$ $\mathcal{G}\cap\mathcal{S}=\mathcal{N}_{\mathcal{G}\cap\mathcal{S}}$	$\mathbf{g}_n\in\Omega_{\mathbf{g}_n}$ $\mathbf{s}_n\in\Omega_{\mathbf{s}_n}$ $(\mathbf{g}_n,\mathbf{s}_n)\in(\Omega_{\mathbf{g}_n}\times\Omega_{\mathbf{s}_n})$

Table 3.1: Different types of demand-side users and corresponding strategy sets.

to provide the aggregate per-slot energy load $L(h)$ at time-slot h. Then, $C_h\big(L(h)\big)\big(l_n(h)/L(h)\big)$ represents the amount of money paid by user n to purchase the energy load $l_n(h)$ from the grid (if $l_n(h)>0$) or received to sell the energy load $l_n(h)$ to the grid (if $l_n(h)<0$) at time-slot h. We adopt the quadratic grid cost function widely used in the smart grid literature (e.g., in [51, 58]):

$$C_h\big(L(h)\big)=K_hL^2(h) \tag{3.12}$$

with $\big\{K_h\big\}_{h=1}^{H}>0$. In general, the grid coefficients K_h are different at each time-slot h, since the energy production varies along the time period of analysis according to the energy demand and to the availability of intermittent energy sources.

Finally, let $f_n(\mathbf{g}_n,\mathbf{s}_n)$ denote the *cumulative expense* over the time period of analysis, which represents the cumulative monetary expense incurred by user $n\in\mathcal{N}$ for obtaining the desired amount of energy over the time period of analysis:

$$f_n(\mathbf{g}_n,\mathbf{s}_n)\triangleq\sum_{h=1}^{H}\Big(K_hL(h)\big(e_n(h)-g_n(h)+s_n(h)\big)+W_n\big(g_n(h)\big)\Big). \tag{3.13}$$

Note that, in general, the amount of money paid/received by user n to purchase/sell the same amount of energy from/to the grid is different during distinct time-slots due to the fact that the grid cost function and the aggregate per-slot energy load are variable along the day. A summary of the principal variables introduced throughout Section 3.2, along with the corresponding domains, is reported in Table 3.2.

3.3 Day-Ahead Optimization Problem

Once defined the overall model, in this section we focus on analyzing the proposed day-ahead optimization problem.

First, the grid energy prices for the time period of analysis, i.e., the grid coefficients $\big\{K_h\big\}_{h=1}^{H}$,

Symbol	Domain	
$l_n(h)$	$l_n(h) \geq 0$	if $n \in \mathcal{P} \backslash \mathcal{G}_{\mathrm{R}}$
	possibly negative	if $n \in \mathcal{N} \cup \mathcal{G}_{\mathrm{R}}$
$e_n(h)$	$e_n(h) \geq 0$	if $n \in \mathcal{N} \backslash \mathcal{G}_{\mathrm{R}}$
	possibly negative	if $n \in \mathcal{G}_{\mathrm{R}}$
$g_n(h)$	$g_n(h) \geq 0$	
$s_n(h)$	$s_n(h) > 0$	if charging
	$s_n(h) < 0$	if discharging
$L(h)$	$0 < L(h) < L^{(\max)}$	

Table 3.2: List of important symbols and corresponding domains.

are fixed by the supply-side in the day-ahead market-clearing process [3, 47, 57]. Then, each active demand-side user reacts to the prices provided by the central unit through iteratively adjusting his generation and storage strategies $\mathbf{g}_n$ and $\mathbf{s}_n$ and, thus, his day-ahead energy demand $\big\{l_n(h)\big\}_{h=1}^{H}$, with the final objective of minimizing his cumulative expense throughout the time period of analysis $f_n(\mathbf{g}_n, \mathbf{s}_n)$, given the aggregate energy loads $\big\{L(h)\big\}_{h=1}^{H}$.

By participating in the day-ahead optimization process, demand-side users commit to follow strictly the resulting consumption pattern. Here, we suppose that users know exactly their energy requirements at each time-slot in the time period of analysis in advance and we neglect any real-time fluctuation of such demand (for an overview on real-time pricing mechanisms, we refer to [57, 94]). Additionally, we assume that energy supply follows demand precisely (cf. [95]).

One could consider to solve the previous optimization problem in a centralized fashion, with the central unit imposing every active user how much energy he must produce, charge, and discharge at each time-slot. However, this represents a quite invasive solution, since it requires each user to provide detailed information about his energy production and/or storage capabilities. Indeed, these privacy issues may discourage the demand-side users to subscribe to the optimization process. Besides, a centralized approach is not scalable and cannot account for an unpredictably increasing number of participants. In consequence, we are interested instead in a *fully distributed* solution and, hence, a game theoretical approach is remarkably suitable to accommodate our optimization problem (see [98] for an overview on game theory applied on smart grids).

3.3.1 Game Theoretical Formulation

Game theory is a field of applied mathematics that describes and analyzes scenarios with interactive decisions [65]. Here, we model the optimization process as a (noncooperative) Nash game.

Each active user is a player who competes against the others by choosing, given the aggregate energy load at each iteration, the production and storage strategies $\mathbf{g}_n$ and $\mathbf{s}_n$ that minimize his payoff function, i.e., his cumulative expense over the time period of analysis. Since these individual strategies impact the grid energy price of all users, this leads to a coupled problem where the desired solution is an equilibrium point where all users are unilaterally satisfied.

First, let us define the strategy vector and the corresponding per-slot strategy profile of a generic user $n \in \mathcal{N}$ as

$$\mathbf{x}_n \triangleq (\mathbf{g}_n, \mathbf{s}_n) \tag{3.14}$$

$$\mathbf{x}_n(h) \triangleq \big(g_n(h), \mathbf{s}_n(h)\big)^{\mathrm{T}}. \tag{3.15}$$

For convenience, we divide the users participating actively in the optimization in three main groups (see Table 3.1 for details):

(i) *Dispatchable energy producers*: $\mathcal{N}_{\mathcal{G}\setminus\mathcal{S}} \triangleq \mathcal{G}\setminus(\mathcal{G}\cap\mathcal{S})$, for whom $\mathbf{g}_n \in \Omega_{\mathbf{g}_n}$ and $\mathbf{s}_n = \mathbf{0}$;
(ii) *Energy storers*: $\mathcal{N}_{\mathcal{S}\setminus\mathcal{G}} \triangleq \mathcal{S}\setminus(\mathcal{G}\cap\mathcal{S})$, for whom $\mathbf{s}_n \in \Omega_{\mathbf{s}_n}$ and $\mathbf{g}_n = \mathbf{0}$;
(iii) *Dispatchable energy producers-storers*: $\mathcal{N}_{\mathcal{G}\cap\mathcal{S}} \triangleq \mathcal{G}\cap\mathcal{S}$, for whom $\mathbf{g}_n \in \Omega_{\mathbf{g}_n}$ and $\mathbf{s}_n \in \Omega_{\mathbf{s}_n}$.

Taking into account the strategy sets $\Omega_{\mathbf{g}_n}$ and $\Omega_{\mathbf{s}_n}$ introduced in Sections 3.2.2 and 3.2.3, respectively, we can now characterize the corresponding strategy set as

$$\Omega_{\mathbf{x}_n} \triangleq \begin{cases} \mathbf{g}_n \in \Omega_{\mathbf{g}_n},\ \mathbf{s}_n = \mathbf{0}, & \text{if } n \in \mathcal{N}_{\mathcal{G}\setminus\mathcal{S}} \\ \mathbf{g}_n = \mathbf{0},\ \mathbf{s}_n \in \Omega_{\mathbf{s}_n}, & \text{if } n \in \mathcal{N}_{\mathcal{S}\setminus\mathcal{G}} \\ \mathbf{g}_n \in \Omega_{\mathbf{g}_n},\ \mathbf{s}_n \in \Omega_{\mathbf{s}_n}, & \text{if } n \in \mathcal{N}_{\mathcal{G}\cap\mathcal{S}} \end{cases}. \tag{3.16}$$

It is worth pointing out that the strategy sets $\Omega_{\mathbf{x}_n}$ are decoupled.[2] Bearing in mind the pricing model given in (3.13), the payoff function of user n is given by

$$f_n\big(\mathbf{x}_n, \mathbf{l}_{-n}\big) \triangleq \sum_{h=1}^{H} \Big(K_h\big(l_{-n}(h) + e_n(h) + \boldsymbol{\delta}^{\mathrm{T}}\mathbf{x}_n(h)\big)\big(e_n(h) + \boldsymbol{\delta}^{\mathrm{T}}\mathbf{x}_n(h)\big) + W_n\big(\boldsymbol{\delta}_g^{\mathrm{T}}\mathbf{x}_n(h)\big)\Big) \tag{3.17}$$

where $\mathbf{l}_{-n} \triangleq \big(l_{-n}(h)\big)_{h=1}^{H}$, with $l_{-n}(h) \triangleq L^{(\mathcal{P})}(h) + \sum_{m\in\mathcal{N}\setminus\{n\}} l_m(h)$ being the aggregate per-slot energy load of the other players $m \in \mathcal{N}\setminus\{n\}$ at time-slot h, and where we have introduced the auxiliary vectors $\boldsymbol{\delta} \triangleq (-1, 1, -1)^{\mathrm{T}}$ and $\boldsymbol{\delta}_g \triangleq (1, 0, 0)^{\mathrm{T}}$.

We can now formally define the game among the active users as $\mathscr{G} = \langle \Omega_{\mathbf{x}}, \mathbf{f}\rangle$, with $\Omega_{\mathbf{x}} \triangleq \prod_{n=1}^{N} \Omega_{\mathbf{x}_n}$ and $\mathbf{f} \triangleq \big(f_n(\mathbf{x}_n, \mathbf{l}_{-n})\big)_{n=1}^{N}$. The final objective of each player $n \in \mathcal{N}$, is to choose his own strategy $\mathbf{x}_n \in \Omega_{\mathbf{x}_n}$ in order to minimize his payoff function $f_n(\mathbf{x}_n, \mathbf{l}_{-n})$, given the aggregate

[2] Due to space limitation, we neglect any physical coupling between the strategy sets of the users $\Omega_{\mathbf{x}_n}$ (we refer to [74, Sec. 4.3] for details).

energy load vector of the other players $\mathbf{l}_{-n}$:

$$\begin{aligned} \min_{\mathbf{x}_n} \quad & f_n(\mathbf{x}_n, \mathbf{l}_{-n}) \\ \text{s.t.} \quad & \mathbf{x}_n \in \Omega_{\mathbf{x}_n} \end{aligned} \qquad \forall n \in \mathcal{N}. \tag{3.18}$$

Then, the solution of the game $\mathscr{G} = \langle \Omega_{\mathbf{x}}, \mathbf{f} \rangle$ corresponds to the well-known concept of Nash equilibrium, which is a feasible strategy profile $\mathbf{x}^\star \triangleq \left(\mathbf{x}_n^\star\right)_{n=1}^N$ with the property that no single player n can profitably deviate from his strategy $\mathbf{x}_n^\star$, if all other players act according to their optimal strategies [65].

3.3.2 Analysis of Nash Equilibria

The objective of this section is to study the existence of the Nash equilibria of the game $\mathscr{G} = \langle \Omega_{\mathbf{x}}, \mathbf{f} \rangle$ in (3.18), with $\Omega_{\mathbf{x}_n}$ given in (3.16). Sufficient conditions to guarantee the existence of such Nash equilibria are derived in the next theorem.

Theorem 3.1. *Given the game $\mathscr{G} = \langle \Omega_{\mathbf{x}}, \mathbf{f} \rangle$ in (3.18), suppose that the production cost function $W_n(x)$ is convex in $0 \leq x \leq g_n^{(\max)}$, $\forall n \in \mathcal{G}$. Then, the following hold:*

(a) The game has a nonempty and compact solution set;

(b) The payoff function of each player is constant over the solution set of the game, i.e., all Nash equilibria yield the same values of the payoff functions.

Proof (a) The game $\mathscr{G} = \langle \Omega_{\mathbf{x}}, \mathbf{f} \rangle$ has a nonempty and compact solution set if [74, Th. 4.1(a)]: (i) the individual strategy sets $\Omega_{\mathbf{x}_n}$ in (3.16) are compact and convex; (ii) the payoff functions $f_n(\mathbf{x}_n, \mathbf{l}_{-n})$ in (3.17) are convex for any feasible $\mathbf{l}_{-n}$. The first condition is immediately satisfied since the sets $\Omega_{\mathbf{x}_n}$, i.e., (3.4) and (3.10), are defined as sets of linear inequalities, i.e., polyhedrons [62, Sec. 2.2.4], and they thus form compact and convex sets. Hence, we only need to verify the second condition. The payoff function $f_n(\mathbf{x}_n, \mathbf{l}_{-n})$ is convex if its Hessian matrix $\mathbf{H}(f_n)$, with block elements

$$\begin{aligned} \nabla^2_{\mathbf{x}_n(h_1)\mathbf{x}_n(h_1)} f_n(\mathbf{x}_n, \mathbf{l}_{-n}) &= 2K_h \boldsymbol{\delta}\boldsymbol{\delta}^{\mathrm{T}} + \boldsymbol{\delta}_g \boldsymbol{\delta}_g^{\mathrm{T}} W_n''\left(\boldsymbol{\delta}_g^{\mathrm{T}} \mathbf{x}_n(h)\right) \\ \nabla^2_{\mathbf{x}_n(h_1)\mathbf{x}_n(h_2)} f_n(\mathbf{x}_n, \mathbf{l}_{-n}) &= \mathbf{0}_3, \qquad\qquad h_1 \neq h_2 \end{aligned} \tag{3.19}$$

with $\mathbf{0}_a$ denoting the a-dimensional zero matrix, is positive semidefinite. Since $\left\{K_h\right\}_{h=1}^H > 0$ and the matrix $\boldsymbol{\delta}\boldsymbol{\delta}^{\mathrm{T}}$ has nonnegative eigenvalues, $\mathbf{H}(f_n)$ is guaranteed to be positive semidefinite if $W_n(x)$ is convex, i.e., if $W_n''(x) \geq 0$. Nevertheless, $f_n(\mathbf{x}_n, \mathbf{l}_{-n})$ must be convex $\forall n \in \mathcal{N}$ and, therefore, this constraint must hold $\forall n \in \mathcal{G}$. □

Proof (b) Although the Nash equilibrium is not unique, all Nash equilibria happen to have the same quality. In fact, consider a generic user $n \in \mathcal{N}_{\mathcal{G}\cap\mathcal{S}}$: given two optimal strategy vectors $\mathbf{x}_{1,n}^\star \neq$

$\mathbf{x}^{\star}_{2,n}$, with $\mathbf{x}^{\star}_{1,n} \triangleq (\mathbf{g}_{1,n}, \mathbf{s}_{1,n})$ and $\mathbf{x}^{\star}_{2,n} \triangleq (\mathbf{g}_{2,n}, \mathbf{s}_{2,n})$, we have that $f_n\big(\mathbf{x}^{\star}_{1,n}, \mathbf{l}_{-n}\big) = f_n\big(\mathbf{x}^{\star}_{2,n}, \mathbf{l}_{-n}\big)$ if the following $H+2$ conditions hold:

$$\sum_{h=1}^{H} W_n\big(g_{1,n}(h)\big) = \sum_{h=1}^{H} W_n\big(g_{2,n}(h)\big) \tag{3.20}$$

$$s_{1,n}(h) - g_{1,n}(h) = s_{2,n}(h) - g_{2,n}(h), \qquad \forall h \tag{3.21}$$

$$\sum_{h=1}^{H} \alpha_n^{(H-h)} \boldsymbol{\beta}_n^{\mathrm{T}} \mathbf{s}_{1,n}(h) = \sum_{h=1}^{H} \alpha_n^{(H-h)} \boldsymbol{\beta}_n^{\mathrm{T}} \mathbf{s}_{2,n}(h) \tag{3.22}$$

where the equality in (3.22) comes from the constraint in (3.8). Hence, being $\mathbf{x}_n \in \mathbb{R}^{3H}$ and $H > 1$, it follows that user $n \in \mathcal{N}_{\mathcal{G}\cap\mathcal{S}}$ can choose among infinitely many optimal strategy vectors $\mathbf{x}^{\star}_n$, each of them giving the same value of $f_n\big(\mathbf{x}^{\star}_n, \mathbf{l}_{-n}\big)$. Furthermore, since $\mathbf{x}^{\star}_n$ produces the same $\big\{l^{\star}_n(h)\big\}_{h=1}^{H}$, $\forall n \in \mathcal{N}$, the aggregate loads $\big\{L^{\star}(h)\big\}_{h=1}^{H}$, with $L^{\star}(h) \triangleq L^{\mathcal{P}} + \sum_{n\in\mathcal{N}}^{H} l^{\star}_n(h)$, are not affected by the multiplicity of the Nash equilibria. Hence, any $\mathbf{x}^{\star} = \big(\mathbf{x}^{\star}_n\big)_{n=1}^{N}$ yields the same values of the payoff functions $\big\{f_n\big(\mathbf{x}^{\star}_n, \mathbf{l}_{-n}\big)\big\}_{n\in\mathcal{N}}$. □

Remark 3.1. The convexity of $W_n(\cdot)$ required by Theorem 3.1 simply implies that the production cost function does not tend to saturate as the per-slot energy production profile increases, which is a very reasonable assumption.

3.3.3 Computation of Nash Equilibria

Once we have established the conditions under which the Nash equilibria of the game $\mathscr{G} = \langle \Omega_{\mathbf{x}}, \mathbf{f} \rangle$ exist, we are interested in obtaining a suitable distributed algorithm to compute one of these equilibria with minimum information exchange among the users. Since in a Nash game every player tries to minimize his own objective function, a natural approach is to consider an *iterative* algorithm where, at every iteration i, each individual user n updates his strategy by minimizing his payoff function

$$f_n(\mathbf{x}_n, \mathbf{l}^{(i)}_{-n}) \triangleq \sum_{h=1}^{H} \Big(K_h\big(l^{(i)}_{-n}(h) + e_n(h) + \boldsymbol{\delta}^{\mathrm{T}}\mathbf{x}_n(h)\big)\big(e_n(h) + \boldsymbol{\delta}^{\mathrm{T}}\mathbf{x}_n(h)\big) + W_n\big(\boldsymbol{\delta}_g^{\mathrm{T}}\mathbf{x}_n(h)\big)\Big) \tag{3.23}$$

referring to the value of the aggregate energy load vector of the other users calculated at the iteration i, i.e., $\mathbf{l}^{(i)}_{-n} \triangleq \big(l^{(i)}_{-n}(h)\big)_{h=1}^{H}$, with $l^{(i)}_{-n} \triangleq L^{(\mathcal{P})}(h) + \sum_{m\in\mathcal{N}\setminus\{n\}} l^{(i)}_m(h)$.

Recall that, in the game (3.18), the coupling between users lies at the level of the payoff functions $f_n(\mathbf{x}_n, \mathbf{l}_{-n})$, whereas the feasible sets $\Omega_{\mathbf{x}_n}$ are decoupled. Distributed algorithms based on the individual best-responses of the players [74, Alg. 4.1] represent an extremely flexible and easy-to-implement solution. The conditions ensuring the convergence of these algorithms, however, may not be easy to fulfill: in fact, following [74, Th. 4.2], it is not difficult to show that their convergence cannot be guaranteed in our case if the users are allowed to simultaneously

adopt production and storage strategies.

To overcome this issue, we consider a distributed algorithm based on the proximal decomposition [74, Alg. 4.2], which is guaranteed to converge under milder conditions on the system specifications and some additional constraints on the parameters of the algorithm that we provide next in Theorem 3.2. Given $\mathbf{x}^{(i)} \triangleq \left(\mathbf{x}_n^{(i)}\right)_{n=1}^N \in \Omega_{\mathbf{x}}$, consider the regularized game

$$\begin{aligned} \min_{\mathbf{x}_n} \quad & f_n(\mathbf{x}_n, \mathbf{l}_{-n}) + \frac{\tau}{2}\|\mathbf{x}_n - \mathbf{x}_n^{(i)}\|^2 \\ \text{s.t.} \quad & \mathbf{x}_n \in \Omega_{\mathbf{x}_n} \end{aligned} \qquad \forall n \in \mathcal{N}. \tag{3.24}$$

which, for a sufficiently large regularization parameter $\tau > 0$, has a unique solution that can be computed in a distributed way using the best-response algorithm [74, Cor. 4.1]. Furthermore, the sequence generated by a proper averaging of the solution of the regularized game (3.24) and $\mathbf{x}^{(i)}$ converges to a solution of the game (3.18) (we refer to [74, Ch. 4.2.4.2] for details). This idea is formalized in Algorithm 3.1.

Algorithm 3.1 Proximal Decomposition Algorithm

`Data` : Set i=0 and the initial centroid $\left(\bar{\mathbf{x}}_n^{(0)}\right)_{n=1}^N = \mathbf{0}$. Given $\left\{K_h\right\}_{h=1}^H$, any feasible starting point $\mathbf{x}^{(0)} = \left(\mathbf{x}_n^{(0)}\right)_{n=1}^N$, and $\tau > 0$:

`(S.1)` : `If` a suitable termination criterion is satisfied: `STOP`.

`(S.2)` : `For` $n \in \mathcal{N}$, each user computes $\mathbf{x}_n^{(i+1)}$ as

$$\mathbf{x}_n^{(i+1)} \in \underset{\mathbf{x}_n \in \Omega_{\mathbf{x}_n}}{\operatorname{argmin}} \left\{ f_n(\mathbf{x}_n, \mathbf{l}_{-n}^{(i)}) + \frac{\tau}{2}\|\mathbf{x}_n - \bar{\mathbf{x}}_n\|^2 \right\} \tag{3.25}$$

`End`

`(S.3)` : `If` the NE has been reached, each user $n \in \mathcal{N}$ updates his centroid: $\bar{\mathbf{x}}_n = \mathbf{x}_n^{(i+1)}$.

`(S.4)` : $i \leftarrow i + 1$; `Go to (S.1)`.

Next theorem provides sufficient conditions for the convergence of Algorithm 3.1 to a solution of the game $\mathscr{G} = \langle \Omega_{\mathbf{x}}, \mathbf{f} \rangle$.

Theorem 3.2. *Given the game $\mathscr{G} = \langle \Omega_{\mathbf{x}}, \mathbf{f} \rangle$ in (3.18), suppose that the following conditions hold:*

(a) *The production cost function $W_n(x)$ is convex in $0 \le x \le g_n^{(\max)}$, $\forall n \in \mathcal{G}$;*

(b) *The regularization parameter τ satisfies*

$$\tau > 3(N-1) \max_h K_h. \tag{3.26}$$

Then, any sequence $\left\{\mathbf{x}_n^{(i)}\right\}_{i=1}^{\infty}$ generated by Algorithm 3.1 converges to a Nash equilibrium of the game.

Proof Algorithm 3.1 is an instance of the proximal decomposition algorithm, which is pre-

sented in [74, Alg. 4.2] for the variational inequality problem. Next, we rewrite the convergence conditions exploiting the equivalence between game theory and variational inequality (see [74, Ch. 4.2] for details). Given $f_n(\mathbf{x}_n, \mathbf{l}_{-n})$ defined as in (3.17), Algorithm 3.1 converges if the following two conditions are satisfied: (i) the Jacobian $\mathbf{J}(\mathbf{x})$ of $\big(\nabla_{\mathbf{x}_n} f_n(\mathbf{x}_n, \mathbf{l}_{-n})\big)_{n=1}^{N}$ is positive semidefinite $\forall \mathbf{x} \in \Omega_{\mathbf{x}}$ [74, Th. 4.3]; (ii) the $N \times N$ matrix $\boldsymbol{\Upsilon}_{\mathrm{F},\tau} \triangleq \boldsymbol{\Upsilon}_{\mathrm{F}} + \tau \mathbf{I}_N$, with

$$[\boldsymbol{\Upsilon}_{\mathrm{F}}]_{nm} \triangleq \begin{cases} \upsilon_n^{(\min)}, & \text{if } n = m \\ -\upsilon_{nm}^{(\max)}, & \text{if } n \neq m \end{cases} \tag{3.27}$$

is a P-matrix [74, Cor. 4.1], where we have introduced

$$\upsilon_n^{(\min)} \triangleq \min_{\mathbf{x} \in \Omega_{\mathbf{x}}} \lambda_{\min}\big\{\mathbf{J}_{nn}(\mathbf{x})\big\} \tag{3.28}$$

$$\upsilon_{nm}^{(\max)} \triangleq \max_{\mathbf{x} \in \Omega_{\mathbf{x}}} \big\|\mathbf{J}_{nm}(\mathbf{x})\big\| \tag{3.29}$$

with $\lambda_{\min}\{\cdot\}$ denoting the smallest eigenvalue of the matrix argument. We can write the block elements of $\mathbf{J}(\mathbf{x})$ as

$$\mathbf{J}_{nn}(\mathbf{x}) \triangleq 2\boldsymbol{\Delta}^{\mathrm{T}}\mathbf{K}\boldsymbol{\Delta} + \boldsymbol{\Delta}_g^{\mathrm{T}}\mathbf{D}_{W_n''}(\mathbf{x}_n)\boldsymbol{\Delta}_g \tag{3.30}$$

$$\mathbf{J}_{nm}(\mathbf{x}) \triangleq \boldsymbol{\Delta}^{\mathrm{T}}\mathbf{K}\boldsymbol{\Delta}, \qquad n \neq m \tag{3.31}$$

where we have introduced the H-dimensional diagonal matrices $\mathbf{D}_{W_n''}(\mathbf{x}_n) \triangleq \mathrm{Diag}\big(W_n''(\boldsymbol{\delta}_g^{\mathrm{T}}\mathbf{x}_n(1)), \ldots, W_n''(\boldsymbol{\delta}_g^{\mathrm{T}}\mathbf{x}_n(H))\big)$ and $\mathbf{K} \triangleq \mathrm{Diag}(K_1, \ldots, K_H)$, and the auxiliary matrices $\boldsymbol{\Delta} \triangleq (-\mathbf{I}_H \ \mathbf{I}_H \ -\mathbf{I}_H)$ and $\boldsymbol{\Delta}_g \triangleq (-\mathbf{I}_H \ \mathbf{0}_H \ \mathbf{0}_H)$.

We show next that conditions (a) and (b) in Theorem 3.2 imply (i) and (ii), respectively. Since $\big\{K_h\big\}_{h=1}^{H} > 0$, the terms in (3.31) are positive semidefinite. On the other hand, the positive semidefiniteness of the diagonal terms in (3.30), and thereby the inequality $\mathbf{J}(\mathbf{x}) \succeq 0$, is also guaranteed if $W_n''(x) \geq 0, \forall n \in \mathcal{G}$, as required by Theorem 3.2(a). On the other hand, considering $\mathbf{J}_{nn}(\mathbf{x})$ and $\mathbf{J}_{nm}(\mathbf{x})$ in (3.30)–(3.31), we have that $\upsilon_n^{(\min)} \geq 0$ and $\upsilon_{nm}^{(\max)} \leq 3 \max_h K_h$. Then, it follows from [74, Prop 4.3] that, if τ is chosen as in Theorem 3.2(b), the matrix $\boldsymbol{\Upsilon}_{\mathrm{F},\tau}$ is a P-matrix, which completes the proof. □

Finally, we can describe the proposed day-ahead optimization as follows. At the beginning of the optimization process, τ is computed as in Theorem 3.2(b) and broadcast to each user $n \in \mathcal{N}$, together with the grid coefficients $\big\{K_h\big\}_{h=1}^{H}$. Then, at each iteration i, the central unit broadcasts a synchronization signal and all users update their centroid $\bar{\mathbf{x}}_n$ simultaneously. Within each iteration, each active user computes his strategy by solving his own optimization problem in (3.25) referring to the aggregate energy load vector of the other users $\mathbf{l}_{-n}^{(i-1)}$, until equilibrium in the inner loop in `(S.2)` is reached. Indeed, user n receives the aggregate energy loads $\big\{L(h)\big\}_{h=1}^{H}$, which are calculated by the central unit summing up the individual demands provided by all

users, and he obtains $\mathbf{l}_{-n}^{(i-1)}$ by subtracting his own energy loads at the previous iteration $i-1$. Lastly, as indicated in `(S.1)` of Algorithm 3.1, the central unit finalizes the whole process when some termination criterion is met as, for instance, when the relative modification in the energy loads of all users between two consecutive iterations is sufficiently small: $\|\mathbf{l}^{(i)}-\mathbf{l}^{(i-1)}\|_2/\|\mathbf{l}^{(i)}\|_2 \leq \varepsilon$, where $\mathbf{l}^{(i)} \triangleq \big(\big(l_n^{(i)}(h)\big)_{h=1}^{H}\big)_{n=1}^{N}$. Note that the individual strategies are not revealed among the users in any case, and only the aggregate energy load, which is determined at the central unit adding the individual day-ahead energy demands, is communicated by the central unit to each active user.

3.4 Simulation Results

In this section, we provide some numerical results that illustrate the performance of the proposed day-ahead DSM mechanism based on the proximal decomposition algorithm described in Algorithm 3.1. Two different cases of analysis are examined: Case 1 delineates the overall results of our optimization process, examines the convergence of Algorithm 3.1, and compares the benefits achieved by the different types of active users, showing that they all have substantially reduced their monetary expense by adopting distributed energy generation and/or storage; Case 2 evaluates the day-ahead optimization process with different percentages of active users.

We test the performance of Algorithm 3.1 within a smart grid of 1000 demand-side users, considering a time period of analysis of one day divided in $H = 24$ time-slots of one hour each. Each demand-side user $n \in \mathcal{D}$ has a random energy consumption curve with daily average of $\sum_{h=1}^{24} e_n(h) = 12$ kWh [99], where higher consumption occurs more likely during day-time hours, i.e., from 08:00 to 24:00, than during night-time hours, i.e., from 00:00 to 08:00, reaching its peak between 17:00 and 23:00. Setting $L^{(\max)} = N \times 3$ kWh, we use the quadratic grid cost function introduced in (3.12), with

$$C_h\big(L(h)\big) = K_h L^2(h) = \begin{cases} K_{\text{night}} L^2(h), & \text{for } h = 1,\ldots,8 \\ K_{\text{day}} L^2(h), & \text{for } h = 9,\ldots,24 \end{cases} \tag{3.32}$$

where $K_{\text{day}} = 1.5 K_{\text{night}}$ as in [51], and whose values are chosen in order to obtain an initial average price per kWh of 0.1412 £/kWh [100]. Besides, we suppose that dispatchable energy producers $n \in \mathcal{G}$ have a linear production cost function, resembling that of a combustion engine (e.g., a biomass generator [101]) working in the linear region, given by

$$W_n(x) = \eta_n x, \qquad \eta_n > 0,\ \forall n \in \mathcal{G}. \tag{3.33}$$

For the sake of simplicity, we assume that all dispatchable energy producers adopt a generator characterized by the linear production cost function in (3.33), with $\eta_n = 0.039$ £/kWh [102].

Furthermore, we arbitrarily set $g_n^{(\max)} = 0.4$ kW and $\gamma_n^{(\max)} = 0.8 g_n^{(\max)} \times 24$ h, $\forall n \in \mathcal{G}$. Likewise, we suppose that all energy storers use the same type of storage device, e.g., a lithium-ion battery [103] with $\alpha_n = \sqrt[24]{0.9}$ (which corresponds to a leakage rate of 0.9 over the 24 hours), $\beta_n^{(+)} = 0.9$, $\beta_n^{(-)} = 1.1$, $c_n = 4$ kWh (same value used in [47]), $s_n^{(\max)} = 0.125 c_n$/h, $q_n(0) = 0.25 c_n$, and $\epsilon_n = 0$, $\forall n \in \mathcal{S}$.

3.4.1 Case 1: Overall Performance

In this first case of analysis, we consider a smart grid comprising $N = 180$ active users, where $n = \{1, \ldots, 60\} \in \mathcal{N}_{\mathcal{G} \cap \mathcal{S}}$, $n = \{61, \ldots, 120\} \in \mathcal{N}_{\mathcal{S} \setminus \mathcal{G}}$, $n = \{121, \ldots, 180\} \in \mathcal{N}_{\mathcal{G} \setminus \mathcal{S}}$, respectively, and $P = 820$ passive users $n = \{181, \ldots, 1000\} \in \mathcal{P}$; this corresponds to having 18% of active users equally distributed among dispatchable energy producers, energy storers, and dispatchable energy producers-storers. Moreover, we arbitrarily set the daily energy consumption for each demand-side user ranging between 8 kWh and 16 kWh. Figure 3.2(a) shows the aggregate energy consumption $\sum_{n \in \mathcal{D}} e_n(h)$ together with the aggregate load $L(h)$ at each hour h resulting from Algorithm 3.1, while Figure 3.2(b) delineates the aggregate per-slot energy production $\sum_{n \in \mathcal{G}} g_n(h)$ and storage $\sum_{n \in \mathcal{S}} s_n(h)$ at each hour h. As expected, energy storers charge their battery at the valley of the energy cost, resulting in a substantially more flattened demand curve. Contrarily, they discharge it at peak hours, shaving off the peak of the load. Likewise, dispatchable producers generate little energy during night-time hours, when they rather purchase it from the grid.

The average grid price per kWh reduces to 0.1234 £/kWh (i.e., 12.6% less). Considering the individual energy production cost for users $n \in \mathcal{G}$, the overall price further decreases to 0.1171 £/kWh. The comparison between the initial and the final grid price at each hour h is illustrated in Figure 3.2(c). Moreover, the total expense $\sum_{n \in \mathcal{D}} f_n(\mathbf{g}_n, \mathbf{s}_n)$ reduces from 1704 £ to 1426 £ (i.e., 16.3% less). Finally, the peak-to-average ratio (PAR), calculated as $\text{PAR} \triangleq \big(H \max_h L(h)\big) / \big(\sum_{h=1}^{H} L(h)\big)$ decreases from 1.5223 to 1.3129 (i.e., 13.8% less) resulting in a generally flattened demand curve.

Figure 3.3(a) plots the termination criterion $\|\mathbf{l}^{(i)} - \mathbf{l}^{(i-1)}\|_2 / \|\mathbf{l}^{(i)}\|_2 \leq 10^{-2}$ that finalizes Algorithm 3.1, over the first 10 iterations. With the above setup, convergence is reached after $i = 8$ iterations. However, Figure 3.3(b) shows that active users approximately converge to their final value of the payoff function $f_n(\mathbf{g}_n, \mathbf{s}_n)$ after just $i = 2$ iterations, although they keep adjusting their strategies until the termination criterion is met. Furthermore, from Figure 3.3(b) it is straightforward to conclude that active users with more degrees of freedom (i.e, storage/production equipment) obtain better saving percentages, although the employment of DG and DS benefits all users in the network. In particular, the average savings obtained for each subset of active users are: 1.0539 £ (i.e., 61.4% less) for $n \in \mathcal{N}_{\mathcal{G} \cap \mathcal{S}}$, 0.8562 £ (i.e., 50.1% less)

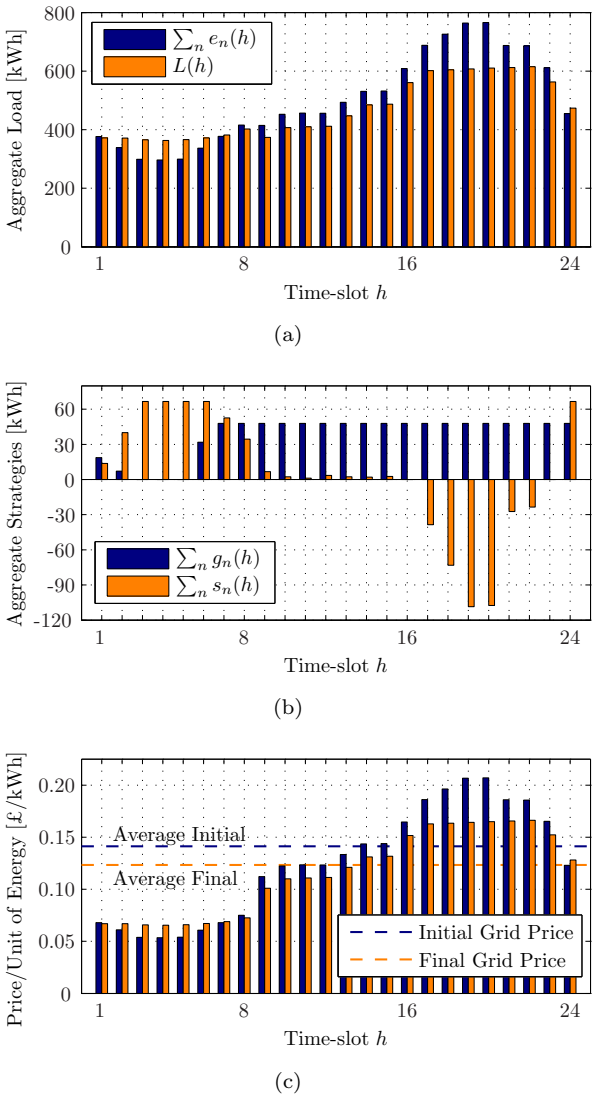

Figure 3.2: Case 1: (a) Aggregate per-slot initial consumption and energy loads resulting from Algorithm 3.1; (b) aggregate per-slot energy production and storage; (c) initial and final grid prices per unit of energy.

for $n \in \mathcal{N}_{\mathcal{G}\setminus\mathcal{S}}$, and 0.3766 £ (i.e., 22.2% less) for $n \in \mathcal{N}_{\mathcal{S}\setminus\mathcal{G}}$. On the other hand, passive users $n \in \mathcal{P}$ save on average 0.1718 £ (i.e., 10.1% less) each. Evidently, the saving for users $n \in \mathcal{N}$ is greater than for users $n \in \mathcal{P}$, i.e., all demand-side users are incentivized to directly adopt DG and/or DS. Moreover, using both dispatchable energy sources and storage devices allows users to further decrease their individual cumulative expenses.

3.4.2 Case 2: Comparison Between Different Percentages of Active Users

In this second case of analysis, we compare the benefits given by the day-ahead optimization process addressed in this paper with different percentages of active users, uniformly distributed among dispatchable energy producers, energy storers, and dispatchable energy producers-storers:

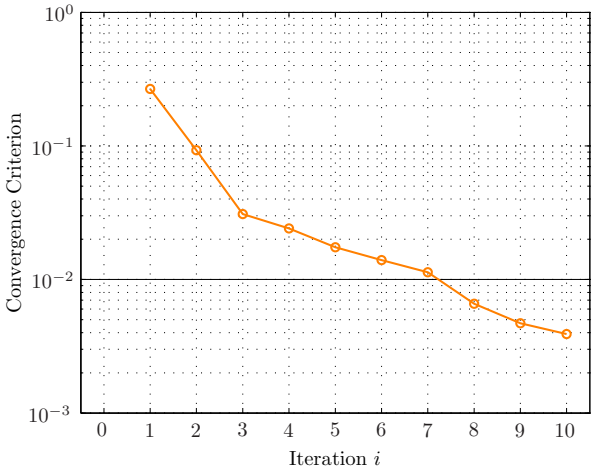

(a)

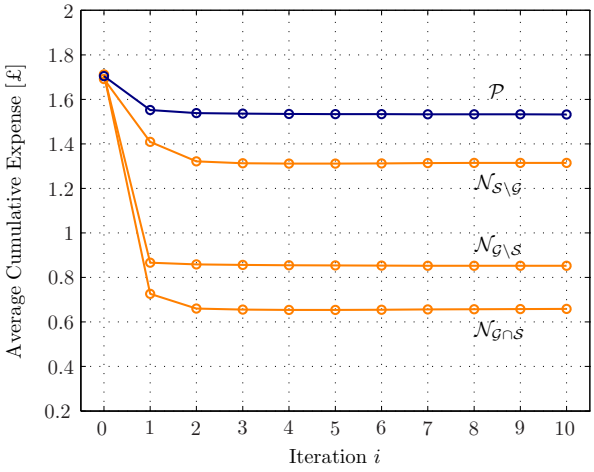

(b)

Figure 3.3: Case 1: (a) Convergence of Algorithm 3.1 with termination criterion $\|\mathbf{l}^{(i)} - \mathbf{l}^{(i-1)}\|_2 / \|\mathbf{l}^{(i)}\|_2 \leq 10^{-2}$; (b) average cumulative expense over the time period of analysis for each subset of active users, at each iteration i.

$n = \{1, \ldots, N/3\} \in \mathcal{N}_{\mathcal{G}\cap\mathcal{S}}$, $n = \{N/3+1, \ldots, 2N/3\} \in \mathcal{N}_{\mathcal{S}\setminus\mathcal{G}}$, $n = \{2N/3+1, \ldots, N\} \in \mathcal{N}_{\mathcal{G}\setminus\mathcal{S}}$, and $P = 1000 - N$, with $N = 60$, $N = 120$, and $N = 240$, which correspond to having 6%, 12%, and 24% of active users, respectively. We assign each demand-side user $n \in \mathcal{D}$ the same energy consumption curve, with daily average of $\sum_{h=1}^{24} e_n(h) = 12$ kWh.

Figure 3.4 compares the aggregate loads $L(h)$ and the final grid prices resulting from Algorithm 3.1 at each hour h for the aforementioned percentages of active users. From Figure 3.4(a) we can see that, as N increases, the increment in the overall production and storage capacity of the grid allows the demand curve to be progressively more flattened, raising the load during valley hours and shaving off the peak of the consumption. In the specific, the PAR decreases from its initial value 1.5253 to 1.4202 (i.e., 6.9% less) with $N = 60$, to 1.3591 (i.e., 10.9% less)

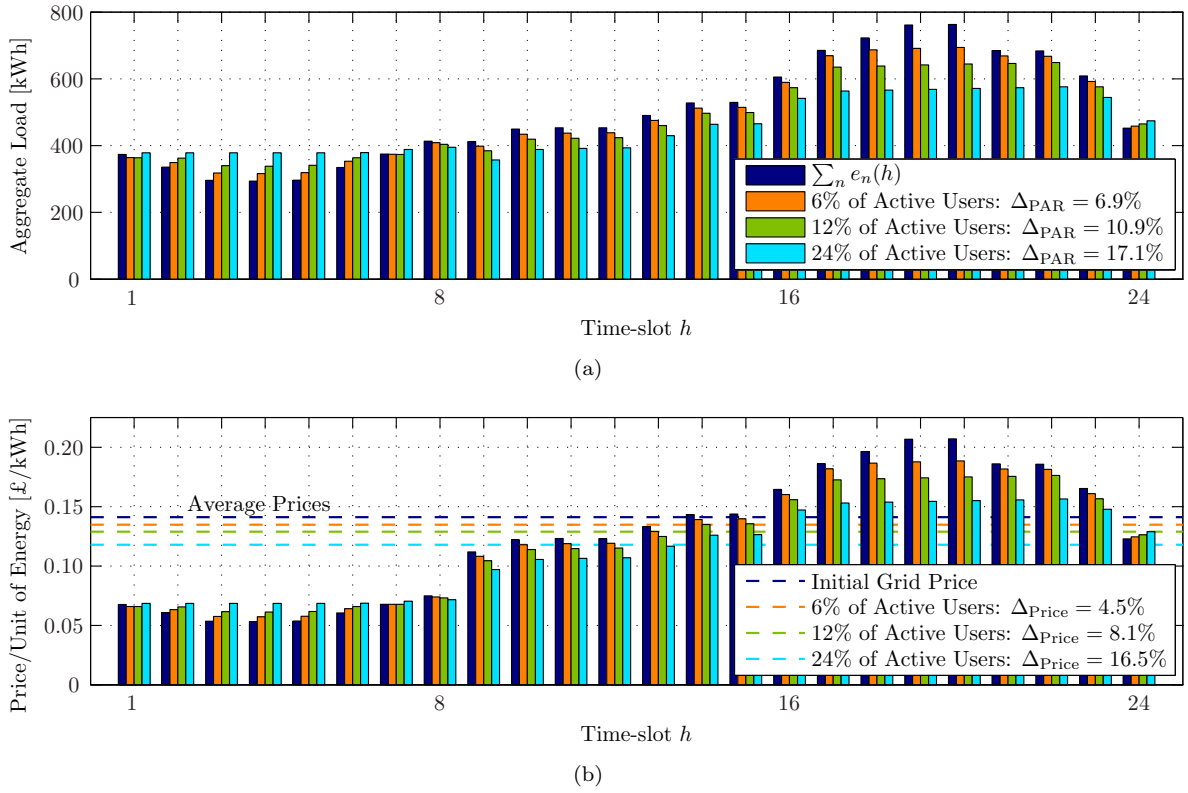

Figure 3.4: Case 2: (a) Aggregate per-slot energy loads (Δ_{PAR}= decrease in the PAR); (b) initial and final grid prices (Δ_{Price}= decrease in the grid price).

with $N = 120$, and to 1.2653 (i.e., 17.1% less) with $N = 240$. Likewise, the price curve in Figure 3.4(b) follows a similar trend, producing a more uniform price per unit of energy throughout the 24 hours. In particular, the average grid price per kWh reduces to 0.1349 £/kWh (i.e., 4.5% less) with $N = 60$, to 0.1298 £/kWh (i.e., 8.1% less) with $N = 120$, and to 0.1179 £/kWh (i.e., 16.5% less) with $N = 240$.

3.5 Conclusions

In this paper, we propose a general grid model that accommodates distributed energy production and storage. In particular, we formulate the day-ahead grid optimization problem, whereby each active user on the demand-side selfishly minimizes his cumulative monetary expense for buying/producing his energy needs, using a game theoretical approach, and we study the existence of the Nash equilibria. We describe a distributed and iterative algorithm based on the proximal decomposition, which allows to compute the optimal strategies of the users with minimum information exchange between the central unit and the demand-side of the network. Simulations on a realistic situation employing practical cost functions show that the demand curve resulting from optimization is sensibly flattened, reducing the need for carbon-intensive and expensive

peaking power plants. Finally, it is worth mentioning that the approach presented here, being directly applicable to end users like households and small businesses, can also be extended to larger contexts, such as small communities or cities. In fact, flattening the energy demand along time is clearly beneficial at any layer or scale of the energy grid.

4

Noncooperative and Cooperative Optimization of Distributed Energy Generation and Storage in the Demand-Side of the Smart Grid

Abstract—The electric energy distribution infrastructure is undergoing a startling technological evolution with the development of the smart grid concept, which allows more interaction between the supply- and the demand-side of the network and results in a great optimization potential. In this paper, we focus on a smart grid in which the demand-side comprises traditional users as well as users owning some kind of distributed energy source and/or energy storage device. By means of a day-ahead demand-side management mechanism regulated through an independent central unit, the latter users are interested in reducing their monetary expense by producing or storing energy rather than just purchasing their energy needs from the grid. Using a general energy pricing model, we tackle the grid optimization design from two different perspectives: a user-oriented optimization and an holistic-based design. In the former case, we optimize each user individually by formulating the grid optimization problem as a noncooperative game, whose solution analysis is addressed building on the theory of variational inequalities. In the latter case, we focus instead on the joint optimization of the whole system, allowing some cooperation among the users. For both formulations, we devise distributed and iterative algorithms providing the optimal production/storage strategies of the users, along with their convergence properties. Among all, the proposed algorithms preserve the users' privacy and require very limited signaling with the central unit.

Index Terms—Demand-Side Management, Distributed Pricing Algorithm, Game Theory, Proximal Decomposition Algorithm, Smart Grid, Variational Inequality.

This chapter is an exact reproduction of [85] with the exception of pagination.

4.1 Introduction

The term *"smart grid"* refers to a manifold of concepts, solutions, and products. Still, no internationally unified definition for smart grids has been adopted [5]. Energy regulators describe the smart grid as an electricity network that can cost-efficiently integrate all users connected to it—generators, consumers, and those who do both—in order to ensure economically-efficient, sustainable power systems with low losses, high levels of quality and security of supply, and improved safety [1]. The smart grids task force set up by the European Commission goes one step beyond and includes smart metering and bidirectional communication capabilities as inherent parts of smart grids [92]. Indeed, smart metering and the related smart communication infrastructure provide information to the different grid users (distribution system operators, retailers, service-providers, and end users) and allow interactions among all of them. This opens up unprecedented possibilities for optimizing the energy grid and energy usage at different network levels.

Not surprisingly, these premises are arousing the interest of the signal processing community. Indeed, the smart grid concept has been recognized as "*a major initiative related to the field of energy with significant signal processing content*" which requires expertise in the fields of communication, sensing, analysis, and actuation [15]. The first publications are mainly focused on the communication aspects of the smart grid. However, these technologies are only an enabler of the envisioned smart grid and, most importantly, they are not the sole aspects that can benefit from the contribution of the signal processing community.[1]

Recently, there has been a growing interest in adopting cooperative and noncooperative game theory to model the interaction among the smart grid users (see [70, 71] for an overview on this topic). In particular, real-time and day-ahead energy consumption scheduling (ECS) techniques, common demand-side management (DSM) procedures that intend to modify the demand profile by shifting energy consumption to off-peak hours, have been recently studied in literature using game theoretical approaches (see, e.g., [51, 58, 72, 73]). However, since the users' inconvenience[2] must be taken into account, ECS presents limitations in terms of flexibility that can be overcome by incorporating distributed generation (DG) and distributed storage (DS) in the demand-side of the network.

In this paper, we propose a DSM method consisting in a day-ahead optimization process that corresponds to energy production and energy storage scheduling rather than shifting energy consumption as in ECS techniques. We associate to each demand-side user, possibly owning a

[1] As evidence in support of this statement, the IEEE Signal Processing Magazine published a special issue entitled "Signal Processing Techniques for the Smart Grid" [16] during the reviewing process of the present paper.

[2] Note that ECS implies no monetary cost for the residential customer, but this is not the case for the industrial customer, for whom the rescheduling of activities may result in monetary loss [55].

DG and/or a DS device, an energy consumption vector containing his energy requirements for each time-slot in which the time period of analysis is divided. Here, we assume that this vector is set a priori by each user according to his needs or as the result of an ECS algorithm. In doing so, we suppose that, by participating in the day-ahead optimization process, demand-side users commit to follow strictly the resulting consumption pattern.[3] The main objective of these end users is to reduce their monetary expense during the time period of analysis by producing or storing energy rather than just purchasing their energy needs from the grid.

DSM techniques have been traditionally formulated from the selfish point of view of the end users. However, it has been demonstrated that a collaborative approach can be more beneficial for all actors in the energy grid by minimizing, e.g., the peak-to-average ratio (PAR) of the energy demand or the total energy cost [51]. In this paper, we attack the grid optimization problem from two different perspectives, namely: a user-oriented optimization and an holistic-based design. More specifically, in the first approach, we formulate the DSM design as a noncooperative game where the end users act as players with objective functions and optimization variables given by their individual monetary expenses and production/storage strategies, respectively. Building on the variational inequality (VI) framework [74,76,78], we study the existence of a solution for the proposed game, the Nash equilibrium (NE); we obtain sufficient conditions on the energy cost functions guaranteeing the existence of Nash equilibria. Quite interestingly, we prove that all the solutions are equivalent, in the sense that the optimal value of the players' objective function is constant over the set of the Nash equilibria. We then focus on distributed algorithms solving the game; we propose a proximal-based best-response scheme and derive sufficient conditions guaranteeing its convergence to any of the (equivalent) Nash equilibria.

The second method we propose consists in formulating the DSM design as a standard nonlinear optimization problem, where one minimizes the overall expense incurred by the demand-side of the network. This approach is more suitable for "collaborative" contexts, where the users are willing to exchange some (limited) signaling in favor of better performance as, for example, when an energy retailer acts as intermediary between the supply-side and a group of subscribers. To solve the resulting nonconvex optimization problem, we build on the recent results in [82,83] and introduce a distributed dynamic pricing-based algorithm (DDPA) that converges to a stationary solution of the problem.

The proposed algorithms have many desired (complementary) features, which make them applicable to alternative scenarios. For instance, the DDPA i) requires essentially the same signaling as the PDA (which is based on a noncooperative approach), ii) is proved to converge under very mild assumptions (always satisfied in practice), and iii) has fast convergence speed (considerably

[3] We refer to [86] for an extended grid model that allows real-time deviations with respect to the negotiated demand, and where the day-ahead energy requirements follow from a bidding process based on the individual consumption statistics.

faster than the scheme presented in [51]). However, despite having the same communication cost as the PDA, the DDPA is not incentive compatible, implying that its best-response update must be imposed as a protocol to the demand-side users, in order to avoid selfish deviations from it. The PDA, instead, can be implemented by selfish users; moreover, quite surprisingly, numerical results show that it yields the same performance as the DDPA (at least for the scenarios simulated in this paper), but its convergence conditions are more stringent than those of the DDPA. Lastly, the PDA is based on a totally asynchronous update of the users' strategies, as opposed to the DDPA and the synchronous user-oriented DSM method presented in [84].

Notably, both approaches addressed in this paper are valid for a general energy pricing model, which includes the energy pricing used in [84] as a special case. Furthermore, they equivalently allow to achieve a generally flattened energy demand curve, from which both demand- and supply-side benefit in terms of reduced energy cost and CO_2 emissions, as well as overall power plants and capital cost requirements [5].

The rest of the paper is structured as follows. In Section 4.2, we introduce the smart grid, the production, and the storage models, as well as the energy cost and pricing model. Section 4.3 formulates the grid optimization problem as a Nash game; we then derive sufficient conditions for the existence of a solution, propose a distributed algorithm solving the game, and study its convergence. In Section 4.4, we present an holistic-based optimization of the system and devise an efficient, distributed algorithm for computing its solutions. Section 4.5 shows some experiments, whereas Section 4.6 draws the conclusions.

4.2 Smart Grid Model

The modern electric grid is a complex network comprising several subsystems, which, for our purposes, can be conveniently divided into [3, 57, 95] (see Figure 4.1):

(i) *Supply-side*: it incorporates the utilities (energy producers) and the energy transmission network;
(ii) *Central unit*: it is the regulation authority that coordinates the grid optimization process. It serves both as independent system operator, by maintaining the reliability of a control area and optimally matching energy supply and demand, and as market operator, by fixing the energy price in the day-ahead market;
(iii) *Demand-side*: it includes the end users (energy consumers), possibly equipped with DG and/or DS, energy retailers, and the energy distribution network.

Since in this paper we are designing a DSM mechanism, we focus in particular on the end users, whereas the supply-side of the smart grid and the central unit are modeled as plainly as possible.

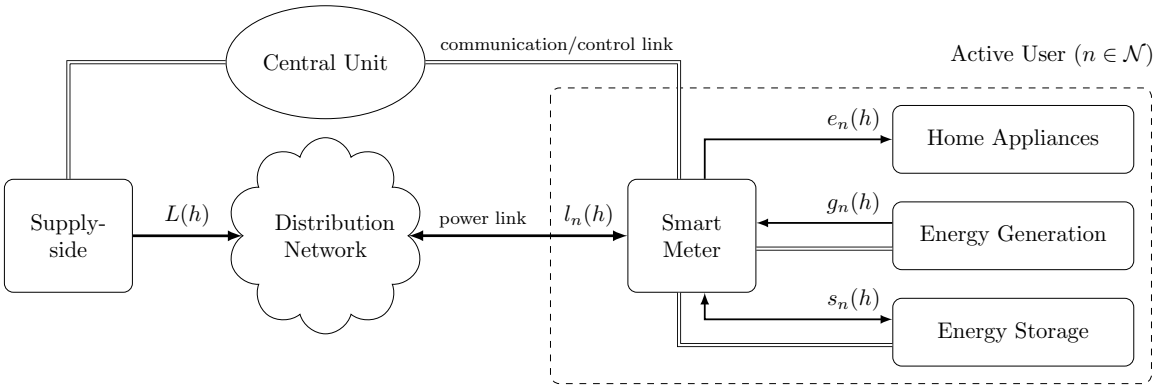

Figure 4.1: Connection scheme between one end user and the smart grid.

4.2.1 Demand-Side Model

Demand-side users, whose associated set is denoted by $\mathcal{D}$, are characterized in the first instance by their individual *per-slot energy consumption profile* $e_n(h)$, defined as the energy needed by user $n \in \mathcal{D}$ to supply his appliances at time-slot h. Accordingly, we also introduce the *energy consumption vector* $\mathbf{e}_n$, which gathers the energy consumption profiles for the H time-slots in which the time period of analysis is divided, i.e., $\mathbf{e}_n \triangleq \big(e_n(h)\big)_{h=1}^{H}$. We assume that demand-side users know exactly their energy requirements at each time-slot in the time period of analysis in advance. A stochastic formulation that deals with the uncertainty induced by the end users' energy consumption and renewable generation is addressed in [86].

Our demand-side model distinguishes between *passive* and *active* users. Passive users are basically energy consumers and resemble traditional demand-side users, whereas active users denote those consumers participating in the optimization process, i.e., reacting to changes in the cost per unit of energy by modifying their demand. Hence, each active user is connected not only to the bidirectional power distribution grid, but also to a communication infrastructure that enables two-way communication between his smart meter and the central unit, as shown in Figure 4.1. For convenience, we group the P passive users in the set $\mathcal{P} \subset \mathcal{D}$ and the N active users in the set $\supset \mathcal{N} \triangleq \mathcal{D} \backslash \mathcal{P}$.

Furthermore, active users include two broad categories: dispatchable energy producers and energy storers. We use $\mathcal{G} \subseteq \mathcal{N}$ to denote the subset of users possessing some dispatchable energy generator. For users $n \in \mathcal{G}$, $g_n(h) \geq 0$ represents the *per-slot energy production profile* at time-slot h, to which corresponds the *energy production scheduling vector* $\mathbf{g}_n \triangleq \big(g_n(h)\big)_{h=1}^{H}$. Likewise, we introduce $\mathcal{S} \subseteq \mathcal{N}$ as the subset of users owning some energy storage device. Users $n \in \mathcal{S}$ are characterized by the *per-slot energy storage profile* $s_n(h)$ at each time-slot h: $s_n(h) > 0$ when the storage device is to be charged (implying an additional energy consumption), $s_n(h) < 0$ when the storage device is to be discharged (resulting in a reduction of the energy consumption), and

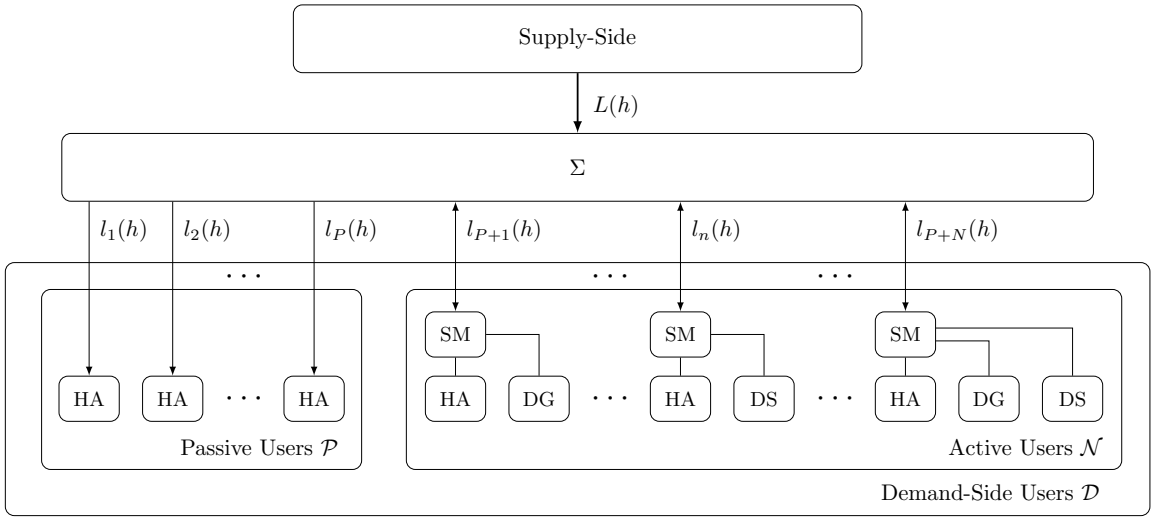

Figure 4.2: Supply-side model and demand-side model including the sets of passive users $\mathcal{P}$ and active users $\mathcal{N}$.

$s_n(h) = 0$ when the storage device is inactive. The per-slot energy storage profiles are gathered in the *energy storage scheduling vector* $\mathbf{s}_n \triangleq \big(s_n(h)\big)_{h=1}^{H}$. It is worth remarking that $\mathcal{G} \cup \mathcal{S} = \mathcal{N}$, but we also contemplate the possibility of some active users being both dispatchable energy producers and storers, i.e., $\mathcal{G} \cap \mathcal{S} \neq \emptyset$, as shown in Figure 4.2.

Finally, let us introduce the *per-slot energy load profile* as

$$l_n(h) \triangleq \begin{cases} e_n(h), & \text{if } n \in \mathcal{P} \\ e_n(h) - g_n(h) + s_n(h), & \text{if } n \in \mathcal{N} \end{cases} \tag{4.1}$$

which gives the energy flow between user n and the grid at time-slot h, as shown schematically in Figure 4.1. Observe that $l_n(h) > 0$ if the energy flows from the grid to user n and $l_n(h) < 0$ otherwise. Due to physical constraints on the user's individual grid infrastructure, the per-slot energy load profile is bounded as

$$-\, l_n^{(\min)} \leq l_n(h) \leq l_n^{(\max)} \tag{4.2}$$

where $l_n^{(\min)} \geq 0$ and $l_n^{(\max)} > 0$ are the outgoing and the incoming capacities of user n's energy link, respectively. These capacities are negotiated between the users and the energy provider and are thus known to the central unit for each user $n \in \mathcal{D}$. The energy load profiles and capacities for the different demand-side users are provided in Table 4.1.

4.2.2 Energy Production Model

Let us first characterize energy producers depending upon the type of DG they employ, as done in [84].

Non-dispatchable DG, $\mathcal{G}_{\mathrm{R}} \subset \mathcal{D}$, e.g, renewable resources of intermittent nature such as solar panels and wind turbines. These energy producers generate electricity at their maximum capacity whenever possible since they only have fixed costs and, therefore, they do not adopt any strategy regarding energy production. For convenience, we consider that the per-slot energy consumption profile $e_n(h)$ already takes into account the non-dispatchable energy production of each user $n \in \mathcal{G}_{\mathrm{R}}$. Hence, for this type of users, we can have $e_n(h) \leq 0$ when the non-dispatchable energy production is greater than the energy consumption at a given time-slot h. Observe that any demand-side user can belong to $\mathcal{G}_{\mathrm{R}}$ without modifying his condition of passive or active participant in the day-ahead optimization process.

Dispatchable DG, $\mathcal{G} \subseteq \mathcal{N}$, e.g., internal combustion engines, gas turbines, or fuel cells, to be operated mostly during high demand hours in order to lower the peak in the load curve. These energy producers, beside fixed costs, have also variable production costs (due to, e.g., the fuel) and they are thus interested in optimizing their energy production strategies. We introduce accordingly the *production cost function* $W_n\big(g_n(h)\big)$, which gives the variable production costs for generating the amount of energy $g_n(h)$ at time-slot h, with $W_n(0) = 0$.

In the following, we provide, as an example, the dispatchable production model adopted in [84]. It is important to remark, however, that the optimization process analysis and algorithms provided in Sections 4.3 and 4.4 hold for any production model resulting in a compact and convex strategy set. Dispatchable energy producers $n \in \mathcal{G}$ are characterized in [84] by their *maximum energy production capability* $g_n^{(\max)}$ and their capacity factor requirements, i.e., the minimum and maximum amount of energy generated during the time period of analysis, $\gamma_n^{(\min)}$ and $\gamma_n^{(\max)}$, so as to remain efficient. The strategy set $\Omega_{\mathbf{g}_n}$ for dispatchable energy producers $n \in \mathcal{G}$ is consequently defined as (see [84, Sec. II-B] for details)

$$\Omega_{\mathbf{g}_n} \triangleq \left\{\mathbf{g}_n \in \mathbb{R}_+^H : \mathbf{g}_n \preceq g_n^{(\max)}\mathbf{1}_H, \gamma_n^{(\min)} \leq \mathbf{1}_H^{\mathrm{T}}\mathbf{g}_n \leq \gamma_n^{(\max)}\right\} \tag{4.3}$$

where the operator $\preceq$ for vectors is defined componentwise, and $\mathbf{1}_H$ denotes the H-dimensional unit vector.

4.2.3 Energy Storage Model

Let us present, for illustration purposes, a simplified version of the energy storage model introduced in [84]. Nonetheless, as pointed out in the previous section for dispatchable energy producers, any storage model resulting in a compact and convex strategy set renders the results in Sections 4.3 and 4.4 still valid.

We characterize storage devices by three attributes: *leakage rate*, *capacity*, and *maximum*

charging rate.[4] The leakage rate $0 < \alpha_n \leq 1$ models the decrease in the energy level of the storage device with the passage of time: let $q_n(h)$ denote the *charge level* at time-slot h, indicating the amount of energy contained in the storage device of user $n \in \mathcal{S}$ at the end of time-slot h, then $q_n(h)$ gets reduced to $\alpha_n q_n(h)$ at the end of time-slot $h+1$. The capacity c_n denotes the maximum amount of energy that the storage device can accumulate. Lastly, the maximum charging rate $s_n^{(\max)}$ represents the maximum amount of energy that can be charged into the device during a time-slot. Observe that charging and discharging are mutually exclusive operations during the same time-slot, which results from the leakage of the storage device. Additionally, it is convenient to include a constraint on the desired charge level at the end of the time period of analysis $q_n(H)$. Following the discussion in [84, Sec. II-C], we impose that

$$|q_n(H) - q_n(0)| \leq \epsilon_n \tag{4.4}$$

where $q_n(0)$ denotes the *initial charge level* and ϵ_n is a sufficiently small constant. Finally, we can define the strategy set $\Omega_{\mathbf{s}_n}$ for energy storers $n \in \mathcal{S}$ as (see [84, Sec. II-C] for details)

$$\begin{aligned}\Omega_{\mathbf{s}_n} \triangleq \big\{\mathbf{s}_n \in \mathbb{R}^H : \mathbf{s}_n \preceq s_n^{(\max)}\mathbf{1}_H, -q_n(0)\mathbf{b}_n \preceq \mathbf{A}_n\mathbf{s}_n \preceq c_n\mathbf{1}_H - q_n(0)\mathbf{b}_n,\\ (1-\alpha_n^H)q_n(0) - \epsilon_n \leq \mathbf{a}_n^{\mathrm{T}}\mathbf{s}_n \leq (1-\alpha_n^H)q_n(0) + \epsilon_n\big\}\end{aligned} \tag{4.5}$$

where $\mathbf{A}_n$ is a $H \times H$ lower triangular matrix with elements $[\mathbf{A}_n]_{i,j} \triangleq \alpha_n^{(i-j)}$, and $\mathbf{a}_n$ and $\mathbf{b}_n$ are H-dimensional vectors with elements $[\mathbf{a}_n]_i \triangleq \alpha_n^{(H-i)}$ and $[\mathbf{b}_n]_i \triangleq \alpha_n^i$, respectively.

Now that we have gone through all possible types of users in the demand-side, we summarize their main characteristics in Table 4.1.

4.2.4 Energy Cost and Pricing Model

This section describes the cost model on which depends the price of energy. Let us first define the *aggregate per-slot energy load* at time-slot h as

$$L(h) \triangleq L^{(\mathcal{P})}(h) + \sum_{n \in \mathcal{N}} l_n(h), \qquad h = 1, \ldots, H. \tag{4.6}$$

where $L^{(\mathcal{P})}(h) \triangleq \sum_{n \in \mathcal{P}} e_n(h)$ is the aggregate per-slot energy consumption associated with the passive users connected to the grid. Then, we can model the supply-side as a single utility that provides, at each time-slot h, a one-way energy flow $L(h)$ through the transmission grid to the demand-side (see Figures 4.1 and 4.2). We work under the hypothesis that the aggregate energy

[4] The storage model in [84] also takes into account charging and discharging efficiencies, which are not considered here for clarity of presentation.

User subset		Energy load profile	Outg. capacity	Strategy set
$\mathcal{P}$	$\mathcal{P}\backslash\mathcal{G}_{\mathrm{R}}$	$l_n(h) = e_n(h)$	$l_n^{(\min)} = 0$	No strategy
	$\mathcal{G}_{\mathrm{R}}\backslash(\mathcal{N}\cap\mathcal{G}_{\mathrm{R}})$		$l_n^{(\min)} \geq 0$	
$\mathcal{N}$	$\mathcal{G}\backslash(\mathcal{G}\cap\mathcal{S}) = \mathcal{N}_{\mathcal{G}\backslash\mathcal{S}}$	$l_n(h) = e_n(h) - g_n(h)$	$l_n^{(\min)} \geq 0$	$\mathbf{g}_n \in \Omega_{\mathbf{g}_n}$
	$\mathcal{S}\backslash(\mathcal{G}\cap\mathcal{S}) = \mathcal{N}_{\mathcal{S}\backslash\mathcal{G}}$	$l_n(h) = e_n(h) + s_n(h)$		$\mathbf{s}_n \in \Omega_{\mathbf{s}_n}$
	$\mathcal{G}\cap\mathcal{S} = \mathcal{N}_{\mathcal{G}\cap\mathcal{S}}$	$l_n(h) = e_n(h) - g_n(h) + s_n(h)$		$(\mathbf{g}_n, \mathbf{s}_n) \in (\Omega_{\mathbf{g}_n} \times \Omega_{\mathbf{s}_n})$

Table 4.1: Characteristics of the different types of demand-side users.

demand is always guaranteed by the supply-side[5] and satisfies

$$L^{(\min)} \leq L(h) \leq L^{(\max)} \tag{4.7}$$

where $L^{(\min)} > 0$ is the *minimum aggregate energy load* throughout the grid, and $L^{(\max)} > 0$ is the *maximum aggregate energy load* that the grid can take before experiencing a blackout. Observe that both $L^{(\min)}$ and $L^{(\max)}$ are known to the central unit based on the actual grid infrastructure and on the available load statistics. A summary of the principal variables introduced throughout Section 4.2, along with their main characteristics, is reported in Table 4.2.

Given the aggregate per-slot energy load $L(h)$, let us now define the *cost per unit of energy* $C_h\big(L(h)\big)$ as the price for a unit of energy at time-slot h resulting from the day-ahead market [3, 43, 47]. Then, $C_h\big(L(h)\big)l_n(h)$ represents the amount of money paid by user n to purchase the energy load $l_n(h)$ from the grid (if $l_n(h) > 0$) or received to sell the energy load $l_n(h)$ to the grid (if $l_n(h) < 0$) at time-slot h. Observe that $C_h(\cdot)$ can represent either the actual energy cost (as a result of energy generation, transmission, and distribution costs among other issues) or simply a pricing function designed to incentivize load-shifting by the end users [51]. In any case, $C_h(\cdot)$ is generally different at each time-slot h, since the energy production changes along the time period of analysis according to the energy demand and to the availability of intermittent sources. For instance, the energy price can be less during the night compared to the day time (as in the practical test case in Section 4.5). Equivalent pricing models are given in [51, 51, 84].

We now have all the elements to introduce the cumulative expense of each group of users in the demand-side of the network. Let $p_n^{(\mathcal{N})}$ denote the *individual cumulative expense* over the time period of analysis for user n, representing the cumulative monetary expense incurred by

[5] The day-ahead optimization allows the supply-side to know in advance the amount of energy to be delivered to the demand-side over the upcoming time period of analysis in order to plan its production accordingly [86, 104].

Symbol	Definition	Domain	
$l_n(h)$	Per-slot energy load profile	$0 \leq l_n(h) \leq l_n^{(\max)}$	$n \in \mathcal{P} \backslash \mathcal{G}_{\mathrm{R}}$
		$-l_n^{(\min)} \leq l_n(h) \leq l_n^{(\max)}$	$n \in \mathcal{N} \cup \mathcal{G}_{\mathrm{R}}$
$e_n(h)$	Per-slot energy consumption profile	$e_n(h) \geq 0$	$n \in \mathcal{D} \backslash \mathcal{G}_{\mathrm{R}}$
		possibly negative	$n \in \mathcal{G}_{\mathrm{R}}$
$g_n(h)$	Per-slot energy production profile	$g_n(h) \geq 0$	$n \in \mathcal{G}$
$s_n(h)$	Per-slot energy storage profile	$s_n(h) > 0$	$n \in \mathcal{S}$ (charging)
		$s_n(h) < 0$	$n \in \mathcal{S}$ (discharging)
$L(h)$	Aggregate per-slot energy load	$L^{(\min)} \leq L(h) \leq L^{(\max)}$	

Table 4.2: List of important symbols with corresponding definitions and domain.

user $n \in \mathcal{N}$ for obtaining the desired amount of energy in the time period of analysis:

$$p_n^{(\mathcal{N})} \triangleq \sum_{h=1}^{H} \Big(C_h\big(L(h)\big)\big(e_n(h) - g_n(h) + s_n(h)\big) + W_n\big(g_n(h)\big)\Big) \tag{4.8}$$

where we have included the individual production costs $\big\{W_n\big(g_n(h)\big)\big\}_{h=1}^{H}$. Note that, in general, the amount of money paid/received by user n to purchase/sell the same amount of energy from/to the grid is different during distinct time-slots due to the fact that the grid cost function and the aggregate per-slot energy load vary along the day. Likewise, the aggregate cumulative expense incurred by the passive users is given by

$$p^{(\mathcal{P})} \triangleq \sum_{h=1}^{H} C_h\big(L(h)\big) L^{(\mathcal{P})}(h) \tag{4.9}$$

which indirectly depends on the strategies of the active users through the cost per unit of energy at each time-slot $C_h\big(L(h)\big)$. Lastly, we introduce the *aggregate cumulative expense* $p^{(\mathcal{D})}$, which expresses the overall grid expense over the time period of analysis, and which is related to the individual cumulative expenses of the active users in (4.8) and to the aggregate cumulative expense of the passive users in (4.9) as

$$p^{(\mathcal{D})} \triangleq \sum_{h=1}^{H} \Big(C_h\big(L(h)\big)\Big(\sum_{n\in\mathcal{N}} l_n(h) + L^{(\mathcal{P})}(h)\Big) + \sum_{n\in\mathcal{G}} W_n\big(g_n(h)\big)\Big) = \sum_{n\in\mathcal{N}} p_n^{(\mathcal{N})} + p^{(\mathcal{P})}. \tag{4.10}$$

4.2.5 Introduction to the DSM Approaches

In the rest of the paper, we focus on the optimization problems posed by our DSM mechanisms, through which active users determine in advance their generation/storage strategies for the

upcoming time period of analysis (corresponding usually to a day [105]). Once the grid cost functions $\{C_h(\cdot)\}_{h=1}^{H}$ are fixed in the day-ahead market, active users react to the prices provided by the central unit by iteratively adjusting their generation and storage strategies, $\mathbf{g}_n$ and $\mathbf{s}_n$, and, thus, their day-ahead energy demands $\{l_n(h)\}_{h=1}^{H}$, given the aggregate energy loads $\{L(h)\}_{h=1}^{H}$. The final objective of the active users is either i) to individually minimize their individual cumulative expense over the time period of analysis in (4.8) (see Section 4.3), or ii) to jointly minimize the aggregate cumulative expense of all demand-side users in (4.10) (see Section 4.4). In the first method, active users act selfishly to reduce their cumulative monetary expenses without consulting or coordinating with each other. Despite the flexibility of this approach, the second solution may be more desirable from the point of view of both the individual users and the supply-side, since it takes into account the overall production costs and results in a more efficient demand-side energy consumption.

One could consider to solve the aforementioned optimization problems in a centralized fashion, with the central unit imposing every single user how much energy he must produce, charge, and discharge at each time-slot. Nonetheless, such solution requires every user to provide detailed information about his energy production and/or storage capabilities and this could lead to privacy issues. Besides, a centralized approach is not scalable and cannot account for an unpredictably increasing number of participants. In consequence, we adopt *fully distributed* solutions for both DSM techniques in Sections 4.3 and 4.4, respectively.

4.3 Noncooperative DSM Approach

In this section, we focus on the optimization problem posed by the noncooperative DSM mechanism through which active demand-side users aim at individually minimizing their individual cumulative expense over the time period of analysis introduced in (4.8).

For convenience, let us first distinguish three main groups among the users participating actively in the optimization (see Table 4.1 for details):

(i) *Dispatchable energy producers*: $\mathcal{N}_{\mathcal{G}\setminus\mathcal{S}} \triangleq \mathcal{G}\setminus(\mathcal{G}\cap\mathcal{S})$, for whom $\mathbf{g}_n \in \Omega_{\mathbf{g}_n}$ and $\mathbf{s}_n = \mathbf{0}$;

(ii) *Energy storers*: $\mathcal{N}_{\mathcal{S}\setminus\mathcal{G}} \triangleq \mathcal{S}\setminus(\mathcal{G}\cap\mathcal{S})$, for whom $\mathbf{s}_n \in \Omega_{\mathbf{s}_n}$ and $\mathbf{g}_n = \mathbf{0}$;

(iii) *Dispatchable energy producers-storers*: $\mathcal{N}_{\mathcal{G}\cap\mathcal{S}} \triangleq \mathcal{G}\cap\mathcal{S}$, for whom $\mathbf{g}_n \in \Omega_{\mathbf{g}_n}$ and $\mathbf{s}_n \in \Omega_{\mathbf{s}_n}$.

Then, we can define the strategy vector and the per-slot strategy profile of a generic active user $n \in \mathcal{N}$ as

$$\mathbf{x}_n \triangleq \begin{cases} \mathbf{g}_n, & \text{if } n \in \mathcal{N}_{\mathcal{G}\setminus\mathcal{S}} \\ \mathbf{s}_n, & \text{if } n \in \mathcal{N}_{\mathcal{S}\setminus\mathcal{G}} \\ (\mathbf{g}_n, \mathbf{s}_n), & \text{if } n \in \mathcal{N}_{\mathcal{G}\cap\mathcal{S}} \end{cases}, \qquad \mathbf{x}_n(h) \triangleq \begin{cases} g_n(h), & \text{if } n \in \mathcal{N}_{\mathcal{G}\setminus\mathcal{S}} \\ s_n(h), & \text{if } n \in \mathcal{N}_{\mathcal{S}\setminus\mathcal{G}} \\ \big(g_n(h), s_n(h)\big)^{\mathrm{T}}, & \text{if } n \in \mathcal{N}_{\mathcal{G}\cap\mathcal{S}} \end{cases}. \tag{4.11}$$

In addition, taking into account the limitations on the link capacity given in (4.2), we denote

the corresponding strategy set by

$$\Omega_{\mathbf{x}_n} \triangleq \begin{cases} \big\{\mathbf{x}_n \in \Omega_{\mathbf{g}_n} : \boldsymbol{\Delta}_n \mathbf{x}_n \succeq -l_n^{(\min)} \mathbf{1}_H - \mathbf{e}_n\big\}, & \text{if } n \in \mathcal{N}_{\mathcal{G}\setminus\mathcal{S}} \\ \big\{\mathbf{x}_n \in \Omega_{\mathbf{s}_n} : -l_n^{(\min)} \mathbf{1}_H - \mathbf{e}_n \preceq \boldsymbol{\Delta}_n \mathbf{x}_n \preceq l_n^{(\max)} \mathbf{1}_H - \mathbf{e}_n\big\}, & \text{if } n \in \mathcal{N}_{\mathcal{S}\setminus\mathcal{G}} \\ \big\{\boldsymbol{\Delta}_{g,n}\mathbf{x}_n \in \Omega_{\mathbf{g}_n}, \boldsymbol{\Delta}_{s,n}\mathbf{x}_n \in \Omega_{\mathbf{s}_n} : \\ \qquad\qquad -l_n^{(\min)} \mathbf{1}_H - \mathbf{e}_n \preceq \boldsymbol{\Delta}_n \mathbf{x}_n \preceq l_n^{(\max)} \mathbf{1}_H - \mathbf{e}_n\big\}, & \text{if } n \in \mathcal{N}_{\mathcal{G}\cap\mathcal{S}} \end{cases} \tag{4.12}$$

with dimension $\omega_{\mathbf{x}_n} \triangleq H\boldsymbol{\delta}_n^{\mathrm{T}}\boldsymbol{\delta}_n$, where we have introduced the auxiliary variables $\boldsymbol{\Delta}_n \triangleq \boldsymbol{\delta}_n^{\mathrm{T}} \otimes \mathbf{I}_H$, $\boldsymbol{\Delta}_{g,n} \triangleq \boldsymbol{\delta}_{g,n}^{\mathrm{T}} \otimes \mathbf{I}_H$, with

$$\boldsymbol{\delta}_n \triangleq \begin{cases} -1, & \text{if } n \in \mathcal{N}_{\mathcal{G}\setminus\mathcal{S}} \\ 1, & \text{if } n \in \mathcal{N}_{\mathcal{S}\setminus\mathcal{G}} \\ (-1,1)^{\mathrm{T}}, & \text{if } n \in \mathcal{N}_{\mathcal{G}\cap\mathcal{S}} \end{cases}, \qquad \boldsymbol{\delta}_{g,n} \triangleq \begin{cases} 1, & \text{if } n \in \mathcal{N}_{\mathcal{G}\setminus\mathcal{S}} \\ 0, & \text{if } n \in \mathcal{N}_{\mathcal{S}\setminus\mathcal{G}} \\ (1,0)^{\mathrm{T}}, & \text{if } n \in \mathcal{N}_{\mathcal{G}\cap\mathcal{S}} \end{cases} \tag{4.13}$$

and $\boldsymbol{\Delta}_{s,n} \triangleq (\mathbf{0}_H^{\mathrm{T}} \otimes \mathbf{0}_H \ \mathbf{I}_H)$, with $\mathbf{0}_H$ denoting the H-dimensional zero vector. Furthermore, let $\mathbf{x}_{-n} \triangleq \big(\mathbf{x}_m\big)_{n\neq m=1}^{N}$ be the vector including the strategies of the other users $m \in \mathcal{N}\setminus\{n\}$. Bearing in mind the individual cumulative expense given in (4.8), the objective function of user n is given by

$$f_n(\mathbf{x}_n, \mathbf{x}_{-n}) \triangleq (\mathbf{e}_n + \boldsymbol{\Delta}_n \mathbf{x}_n)^{\mathrm{T}} \mathbf{c}(\mathbf{x}) + \mathbf{1}_H^{\mathrm{T}} \mathbf{w}_n(\boldsymbol{\Delta}_{g,n}\mathbf{x}_n) \tag{4.14}$$

with $\mathbf{x} \triangleq \big(\mathbf{x}_n\big)_{n=1}^{N}$ being the joint strategy vector and the vector functions $\mathbf{c}(\cdot)$ and $\mathbf{w}_n(\cdot)$ given by

$$\mathbf{c}(\mathbf{x}) \triangleq \Big(C_h\big(L^{(\mathcal{P})}(h) + \sum_{m\in\mathcal{N}} \big(e_m(h) + \boldsymbol{\delta}_m^{\mathrm{T}}\mathbf{x}_m(h)\big)\big)\Big)_{h=1}^{H} \tag{4.15}$$

$$\mathbf{w}_n(\boldsymbol{\Delta}_{g,n}\mathbf{x}_n) \triangleq \Big(W_n\big(\boldsymbol{\delta}_{g,n}^{\mathrm{T}}\mathbf{x}_n(h)\big)\Big)_{h=1}^{H}. \tag{4.16}$$

4.3.1 Game Theoretical and VI Formulation

Here, we model our DSM procedure as a (noncooperative) Nash game. Each active user is a player who competes against the others by choosing the production and storage strategies $\mathbf{g}_n$ and $\mathbf{s}_n$ that minimize his objective function $f_n(\mathbf{x}_n, \mathbf{x}_{-n})$ in (4.14), i.e., his cumulative expense over the time period of analysis. The formal definition of the game is the following: $\mathscr{G} = \langle \Omega_{\mathbf{x}}, \mathbf{f} \rangle$, where $\Omega_{\mathbf{x}} \triangleq \prod_{n=1}^{N} \Omega_{\mathbf{x}_n}$ is the $\omega_{\mathbf{x}}$-dimensional joint strategy set, $\omega_{\mathbf{x}} \triangleq H \sum_{n\in\mathcal{N}} (\boldsymbol{\delta}_n^{\mathrm{T}}\boldsymbol{\delta}_n)$, and $\mathbf{f} \triangleq \big(f_n(\mathbf{x}_n, \mathbf{x}_{-n})\big)_{n=1}^{N}$ is the vector of the objective functions. Each player $n \in \mathcal{N}$ aims at solving the following optimization problem, given $\mathbf{x}_{-n}$:

$$\begin{aligned} \min_{\mathbf{x}_n} \quad & f_n(\mathbf{x}_n, \mathbf{x}_{-n}) \\ \text{s.t.} \quad & \mathbf{x}_n \in \Omega_{\mathbf{x}_n} \end{aligned} \qquad \forall n \in \mathcal{N}. \tag{4.17}$$

Note that the dependence of the objective function in (4.14) on $\mathbf{x}_{-n}$ lies within the argument of the cost functions $C_h(\cdot)$ in (4.15), since $L(h) = \sum_{m\in\mathcal{N}\setminus\{n\}} \big(e_m(h)+\boldsymbol{\delta}_m^{\mathrm{T}}\mathbf{x}_m(h)\big)+e_n(h)+\boldsymbol{\delta}_n^{\mathrm{T}}\mathbf{x}_n(h)$. The solution of the game $\mathscr{G} = \langle \Omega_{\mathbf{x}}, \mathbf{f}\rangle$ is given by the well-known concept of Nash equilibrium, which is a feasible strategy profile $\mathbf{x}^\star$ with the property that no single player n can unilaterally deviate from his strategy $\mathbf{x}_n^\star$, if all other players act according to $\mathbf{x}_{-n}^\star$ [65], i.e.,

$$f_n(\mathbf{x}_n^\star, \mathbf{x}_{-n}^\star) \leq f_n(\mathbf{x}_n, \mathbf{x}_{-n}^\star), \qquad \forall \mathbf{x}_n \in \Omega_{\mathbf{x}_n},\ \forall n \in \mathcal{N}. \tag{4.18}$$

Variational inequality theory provides a general framework for investigating and solving various optimization problems and equilibrium models, even when classical game theory may fail. Throughout this and the next section, we refer extensively to [74]. For a detailed description of the subject, we refer the interested reader also to [76,78,79,106] and to [77] for a comprehensive treatment of VIs.

In order to analyze the existence of the Nash equilibria as well as the convergence of distributed algorithms while keeping the pricing model general, it is very convenient to reformulate the game as a partitioned VI problem, which is formally defined next.

Definition 4.1 ([77, Def. 1.1.1]). *Let* $\mathbf{F}(\mathbf{x}) : \Omega_{\mathbf{x}} \to \mathbb{R}^{\omega_{\mathbf{x}}}$ *be a vector-valued function defined as* $\mathbf{F}(\mathbf{x}) \triangleq \big(\mathbf{F}_n(\mathbf{x}_n, \mathbf{x}_{-n})\big)_{n=1}^N$, *where* $\mathbf{F}_n(\mathbf{x}_n, \mathbf{x}_{-n}) : \Omega_{\mathbf{x}_n} \to \mathbb{R}^{\omega_{\mathbf{x}_n}}$ *is the* n*th component block function of* $\mathbf{F}(\mathbf{x})$, $\mathbf{x} \triangleq \big(\mathbf{x}_n\big)_{n=1}^N$, *and* $\Omega_{\mathbf{x}} = \prod_{n=1}^N \Omega_{\mathbf{x}_n}$. *Then, the VI problem, denoted by* $\mathrm{VI}(\Omega_{\mathbf{x}}, \mathbf{F})$, *consists in finding* $\mathbf{x}^\star \in \Omega_{\mathbf{x}}$ *such that*

$$(\mathbf{x} - \mathbf{x}^\star)^{\mathrm{T}}\mathbf{F}(\mathbf{x}^\star) \geq 0, \qquad \forall \mathbf{x} \in \Omega_{\mathbf{x}}. \tag{4.19}$$

The equivalence between the game theoretical and the VI formulation is established in the following lemma.

Lemma 4.1 ([74, Prop. 4.1], [77, Prop. 1.4.2]). *The Game* $\mathscr{G} = \langle \Omega_{\mathbf{x}}, \mathbf{f}\rangle$ *is equivalent to the VI problem* $\mathrm{VI}(\Omega_{\mathbf{x}}, \mathbf{F})$, *with* $\mathbf{F}(\mathbf{x}) \triangleq \big(\nabla_{\mathbf{x}_n} f_n(\mathbf{x}_n, \mathbf{x}_{-n})\big)_{n=1}^N$, *if:*

(a) *The strategy sets* $\Omega_{\mathbf{x}_n}$ *are closed and convex;*
(b) *For every fixed* $\mathbf{x}_{-n} \in \Omega_{\mathbf{x}_{-n}} \triangleq \prod_{m\in\mathcal{N}\setminus\{n\}} \Omega_{\mathbf{x}_m}$, *the objective function* $f_n(\mathbf{x}_n, \mathbf{x}_{-n})$ *is convex and twice continuously differentiable on* $\Omega_{\mathbf{x}_n}$.

Since the individual strategy sets $\Omega_{\mathbf{x}_n}$ in (4.12) are nonempty polyhedra [62, Sec. 2.2.4], Lemma 4.1(a) is readily satisfied. On the other hand, Lemma 4.1(b) is satisfied if and only if the gradient of $f_n(\,\cdot\,, \mathbf{x}_{-n})$, $\mathbf{F}_n(\,\cdot\,, \mathbf{x}_{-n}) \triangleq \nabla_{\mathbf{x}_n} f_n(\,\cdot\,, \mathbf{x}_{-n})$, is monotone on $\Omega_{\mathbf{x}_n}$ for any given

$\mathbf{x}_{-n} \in \Omega_{\mathbf{x}_{-n}}$ [79],[6] where

$$\mathbf{F}_n(\mathbf{x}_n, \mathbf{x}_{-n}) \triangleq \nabla_{\mathbf{x}_n} f_n(\mathbf{x}_n, \mathbf{x}_{-n}) = \boldsymbol{\Delta}_n^{\mathrm{T}} \mathbf{c}(\mathbf{x}) + \boldsymbol{\Delta}_n^{\mathrm{T}} \mathbf{D}_{\mathbf{c}'}(\mathbf{x})(\mathbf{e}_n + \boldsymbol{\Delta}_n \mathbf{x}_n) + \boldsymbol{\Delta}_{g,n}^{\mathrm{T}} \mathbf{w}_n'(\boldsymbol{\Delta}_{g,n} \mathbf{x}_n) \quad (4.20)$$

with $\mathbf{D}_{\mathbf{c}'}(\mathbf{x}) \triangleq \mathrm{Diag}\big(\mathbf{c}'(\mathbf{x})\big)$. This requirement is accomplished under the conditions of Theorem 4.1 given in the next section.

Assuming that Lemma 1 holds, we can formulate the game $\mathscr{G} = \langle \Omega_{\mathbf{x}}, \mathbf{f} \rangle$ as the VI problem $\mathrm{VI}(\Omega_{\mathbf{x}}, \mathbf{F})$, where the vector function $\mathbf{F}(\mathbf{x})$ is

$$\mathbf{F}(\mathbf{x}) = \big(\nabla_{\mathbf{x}_n} f_n(\mathbf{x}_n, \mathbf{x}_{-n})\big)_{n=1}^N = \boldsymbol{\Delta}^{\mathrm{T}}\big(\mathbf{1}_N \otimes \mathbf{c}(\mathbf{x})\big) + \boldsymbol{\Delta}^{\mathrm{T}}\big(\mathbf{I}_N \otimes \mathbf{D}_{\mathbf{c}'}(\mathbf{x})\big)\big(\mathbf{e} + \boldsymbol{\Delta}\mathbf{x}\big) + \boldsymbol{\Delta}_g^{\mathrm{T}} \mathbf{w}'(\mathbf{x}) \quad (4.21)$$

with $\boldsymbol{\Delta} \triangleq \mathrm{Diag}\big(\boldsymbol{\Delta}_1, \ldots, \boldsymbol{\Delta}_N\big)$, $\boldsymbol{\Delta}_g \triangleq \mathrm{Diag}\big(\boldsymbol{\Delta}_{g,1}, \ldots, \boldsymbol{\Delta}_{g,N}\big)$, $\mathbf{e} \triangleq \big(\mathbf{e}_n\big)_{n=1}^N$, and $\mathbf{w}'(\mathbf{x}) \triangleq \big(\mathbf{w}_n'(\boldsymbol{\Delta}_{g,n}\mathbf{x}_n)\big)_{n=1}^N$.

4.3.2 Nash Equilibria Analysis

Sufficient conditions on the grid cost functions per unit of energy and on the production cost functions that guarantee the existence of the Nash equilibria of the game $\mathscr{G} = \langle \Omega_{\mathbf{x}}, \mathbf{f} \rangle$, i.e., of the solutions of the VI problem $\mathrm{VI}(\Omega_{\mathbf{x}}, \mathbf{F})$, are derived in the next theorem.

Theorem 4.1. *Given the game $\mathscr{G} = \langle \Omega_{\mathbf{x}}, \mathbf{f} \rangle$, suppose that the following conditions hold:*

(a) *The grid cost functions per unit of energy $\big\{C_h(x)\big\}_{h=1}^H$ are increasing and convex on $[L^{(\min)}, L^{(\max)}]$, and satisfy*

$$C_h'(x) \geq \frac{1}{2}\zeta^{(\min)} C_h''(x), \qquad \forall x \in [L^{(\min)}, L^{(\max)}] \quad (4.22)$$

where $\zeta^{(\min)} \triangleq \max_n l_n^{(\min)}$ denotes the maximum amount of energy that can be sold to the grid by any single user $n \in \mathcal{N}$ at any time-slot;

(b) *The production cost function $W_n(x)$ is convex on $[0, g_n^{(\max)}]$, $\forall n \in \mathcal{G}$.*

Then, the game has a nonempty and compact solution set.

Proof. See Appendix 4.A.1.

Remark 4.1. Observe that any realistic grid cost function $C_h(\cdot)$ is increasing as required by Theorem 4.1(a) (see, e.g., the power price function in [107]). Actually, for non-strictly increasing $C_h(\cdot)$, a game-theoretical approach may not even be necessary since the individual optimization problems could possibly be decoupled (see details in Example 1.1(a)). The convexity of $C_h(\cdot)$ in Theorem 4.1(a) and the convexity of $W_n(\cdot)$ in Theorem 4.1(b) simply impose that the grid cost

[6] We say that $\mathbf{F}_n(\mathbf{x}_n, \mathbf{x}_{-n})$ is monotone on $\Omega_{\mathbf{x}_n}$ when $(\mathbf{x}_n - \mathbf{y}_n)^{\mathrm{T}}\big(\mathbf{F}_n(\mathbf{x}_n, \mathbf{x}_{-n}) - \mathbf{F}_n(\mathbf{y}_n, \mathbf{x}_{-n})\big) \geq 0$, $\forall \mathbf{x}_n, \mathbf{y}_n \in \Omega_{\mathbf{x}_n}$, for every fixed $\mathbf{x}_{-n} \in \Omega_{\mathbf{x}_{-n}}$ [74, Def. 4.3(i)].

per unit of energy and the production cost function do not tend to saturate as the aggregate energy load and the per-slot energy production profile, respectively, increase, which is a very reasonable assumption. Still, the condition in (4.22) has to be verified case by case, although it is not difficult to be fulfilled (see Example 1.1(d)).

Example 1.1. Suppose, for instance, that the grid cost functions are given by $\left\{C_h(x) = K_h x^a\right\}_{h=1}^{H}$, with $\left\{K_h\right\}_{h=1}^{H} > 0$ and $a \geq 0$. Then:

(a) If $a = 0$, we have that $\left\{C_h'(x)\right\}_{h=1}^{H} = 0$: this means that the cost per unit of energy is constant at each time-slot h, and the resulting optimization problem for users in $\mathcal{N}$ does not depend on the aggregate energy load (and, in consequence, on the strategies of the other users $\mathbf{x}_{-n}$), but only on the energy cost at each time-slot h. In such trivial case, the game-theoretical approach proposed in this paper is not necessary.

(b) If $0 < a < 1$, the grid cost functions are not convex but concave. This is, however, unrealistic, since energy generation becomes less efficient as the aggregate demand increases (in fact, peaking power plants that allow to meet rapidly increasing demand are extremely expensive to operate [108, Sec. 3.9]).

(c) If $a = 1$, the grid cost functions are linear (hence strictly increasing and convex), and condition (4.22) is immediately satisfied since $\left\{C_h''(x)\right\}_{h=1}^{H} = 0$. This particular case is treated in detail in [84].

(d) If $a > 1$, the grid cost functions are strictly increasing and strictly convex and Theorem 4.1 guarantees the existence of the Nash equilibria of the game $\mathscr{G} = \langle \Omega_{\mathbf{x}}, \mathbf{f} \rangle$ in (4.17) whenever

$$a \leq 1 + 2L(h)/\zeta^{(\min)}. \tag{4.23}$$

This is a very mild condition, since the ratio between the aggregate demand $L(h)$ and the maximum energy that can be individually injected into the grid $\zeta^{(\min)}$ can be very large in practice. Alternatively, this condition can be understood as a tradeoff between the minimum demand generated by the passive users and that coming from the active users, as in Remark 4.3.

Theorem 4.1 guarantees the existence of a solution of the game $\mathscr{G} = \langle \Omega_{\mathbf{x}}, \mathbf{f} \rangle$ in (4.17), but not the uniqueness. Interestingly, all Nash equilibria for this problem happen to have the same quality in terms of optimal values of the players' objective functions, as stated in the following proposition.

Proposition 4.1. *Given the game $\mathscr{G} = \langle \Omega_{\mathbf{x}}, \mathbf{f} \rangle$, suppose that the conditions in* Theorem 4.1 *hold; let $\mathrm{NE}_{\mathscr{G}}$ be the set of the Nash equilibria of $\mathscr{G} = \langle \Omega_{\mathbf{x}}, \mathbf{f} \rangle$. Then, the following holds: $f_n(\mathbf{x}^{(1)}) = f_n(\mathbf{x}^{(2)})$, $\forall \mathbf{x}^{(1)}, \mathbf{x}^{(2)} \in \mathrm{NE}_{\mathscr{G}}$ and $\forall n \in \mathcal{N}$.*

Proof. See Appendix 4.A.2.

4.3.3 Proximal Decomposition Algorithm

We focus now on distributed algorithms to compute one of the (equivalent) Nash equilibria (see Proposition 4.1) of the game $\mathscr{G} = \langle \Omega_{\mathbf{x}}, \mathbf{f} \rangle$. We consider the class of *totally asynchronous* algorithms, where some users may update their strategies more frequently than others and they may even use outdated information about the strategy profiles adopted by the other users. This adds more flexibility and robustness with respect to the well-known Jacobi (simultaneous) and Gauss-Seidel (sequential) schemes, as the sequential ECS algorithm proposed in [51]. To provide a formal description of the algorithms, let $\mathscr{T}_n \subseteq \mathscr{T} \subseteq \{0, 1, 2, \ldots\}$ be the set of times at which user $n \in \mathcal{N}$ updates his own strategy $\mathbf{x}_n$, denoted by $\mathbf{x}_n^{(i)}$ at the ith iteration. We use $t_n(i)$ to denote the most recent time at which the strategy of user n is perceived by the central unit at the ith iteration. Each individual user n updates his strategy by minimizing his cumulative expense over the time period of analysis referring to the most recently available value of the per-slot aggregate energy load

$$L^{(\mathbf{t}(i))}(h) = L^{(\mathcal{P})}(h) + \sum_{m \in \mathcal{N}} l_m^{(t_m(i))}(h), \qquad h = 1, \ldots, H \tag{4.24}$$

where $l_n^{(t_n(i))}(h)$ is the energy load of user $n \in \mathcal{N}$ as perceived by the central unit at time $t_n(i)$, which can possibly be outdated when the computation occurs. Finally, to emphasize the dependence of the strategy of user n on the aggregate energy loads of the other users, we rewrite the objective function in (4.14) as

$$f_n\big(\mathbf{x}_n, \big\{L^{(\mathbf{t}(i))}(h)\big\}_{h=1}^{H}\big) = \sum_{h=1}^{H} C_h\big(L^{(\mathbf{t}(i))}(h) + \boldsymbol{\delta}_n^{\mathrm{T}}\big(\mathbf{x}_n(h) - \mathbf{x}_n^{(t_n(i))}(h)\big)\big)\big(e_n(h) + \boldsymbol{\delta}_n^{\mathrm{T}}\mathbf{x}_n(h)\big) + \sum_{h=1}^{H} W_n\big(\boldsymbol{\delta}_{g,n}^{\mathrm{T}}\mathbf{x}_n(h)\big). \tag{4.25}$$

Some standard conditions in asynchronous convergence theory, which are fulfilled in any practical implementation, need to be satisfied by the schedule $\mathscr{T}_n$ and $t_n(i)$, $\forall n \in \mathcal{N}$ [78, Sec. 1.2.2] [109, Ch. 6], namely:

(A1) $0 \leq t_n(i) \leq i$: at any given iteration i, each user n can use only the aggregate energy loads $\big\{L^{(\mathbf{t}(i))}(h)\big\}_{h=1}^{H}$ resulting from the strategies adopted by the other players in the previous iterations;

(A2) $\lim_{k\to\infty} t_n(i_k) = +\infty$, where $\{i_k\}$ is a sequence of elements in $\mathscr{T}_n$ that tends to infinity: for any given iteration index i_k, the values of the components of $\big\{L^{(\mathbf{t}(i))}(h)\big\}_{h=1}^{H}$ generated prior to i_k are not used in the updates of the aggregate energy loads at the iteration i, when i becomes sufficiently larger than i_k;

(A3) $|\mathscr{T}_n| = \infty$: no player fails to update his own strategy as time i goes on.

Since all Nash equilibria are equivalent (in the sense of Proposition 4.1), we focus next on proximal-based best-response algorithms, whose convergence to some of the solutions is guaranteed even in the presence of multiple solutions. According to [74, Alg. 4.2], instead of solving the original game, i.e., the VI problem $\mathrm{VI}(\Omega_{\mathbf{x}}, \mathbf{F})$, one solves a sequence of regularized VI problems, each of them given by $\mathrm{VI}\big(\Omega_{\mathbf{x}}, \mathbf{F} + \tau(\mathbf{I} - \mathbf{x}^{(i)})\big)$, where $\mathbf{I}$ is the identity map (i.e., $\mathbf{I} : \mathbf{x} \to \mathbf{x}$), $\mathbf{x}^{(i)}$ is a fixed real vector, and τ is a positive constant. It can be shown that, under the monotonicity of $\mathbf{F}(\mathbf{x})$ on $\Omega_{\mathbf{x}}$, this regularized problem is strongly monotone and thus has a unique solution [74, Th. 4.1(d)] denoted by $\mathbf{S}_\tau(\mathbf{x}^{(i)})$; such a unique solution is a nonexpansive mapping, meaning that, starting at a given initial point $\mathbf{x}^{(0)} \in \Omega_{\mathbf{x}}$, the sequence generated by a proper averaging of $\mathbf{S}_\tau(\mathbf{x}^{(i)})$ and $\mathbf{x}^{(i)}$ converges to a solution of the $\mathrm{VI}(\Omega_{\mathbf{x}}, \mathbf{F})$, even when this is not unique.[7] Note also that, given $\mathbf{x}^{(i)} = \big(\mathbf{x}_n^{(i)}\big)_{n=1}^N \in \Omega_{\mathbf{x}}$, the solution $\mathbf{S}_\tau(\mathbf{x}^{(i)})$ of the regularized $\mathrm{VI}\big(\Omega_{\mathbf{x}}, \mathbf{F} + \tau(\mathbf{I} - \mathbf{x}^{(i)})\big)$ coincides with the unique Nash equilibrium of the regularized game, where each user n solves the following optimization problem:

$$\begin{aligned} \min_{\mathbf{x}_n} \quad & f_n\big(\mathbf{x}_n, \big\{L^{(\mathbf{t}(i))}(h)\big\}_{h=1}^H\big) + \frac{\tau}{2}\|\mathbf{x}_n - \mathbf{x}_n^{(i)}\|^2 \\ \text{s.t.} \quad & \mathbf{x}_n \in \Omega_{\mathbf{x}_n} \end{aligned} \qquad \forall n \in \mathcal{N}. \tag{4.26}$$

The solution $\mathbf{S}_\tau(\mathbf{x}^{(i)})$ can then be computed in a distributed way with convergence guarantee using any asynchronous best-response algorithm applied to the game (4.26) [74, Cor. 4.1] (see, e.g., [74, Alg. 4.2]). The above scheme is formalized in Algorithm 4.1 below, whose convergence conditions are given in Theorem 4.2.

Algorithm 4.1 Asynchronous Proximal Decomposition Algorithm (PDA)

`Data` : Set $i = 0$ and the initial centroid $\big(\bar{\mathbf{x}}_n\big)_{n=1}^N = \mathbf{0}$. Given $\big\{C_h(\cdot)\big\}_{h=1}^H$, $\big\{\rho^{(i)}\big\}_{i=0}^\infty$, $\tau > 0$, and any feasible starting point $\mathbf{x}^{(0)} = \big(\mathbf{x}_n^{(0)}\big)_{n=1}^N$:

`(S.1)` : `If` a suitable termination criterion is satisfied: `STOP`.

`(S.2)` : `For` $n \in \mathcal{N}$, each user computes $\mathbf{x}_n^{(i+1)}$ as

$$\mathbf{x}_n^{(i+1)} = \begin{cases} \mathbf{x}_n^\star \in \underset{\mathbf{x}_n \in \Omega_{\mathbf{x}_n}}{\operatorname{argmin}} \Big\{ f_n\big(\mathbf{x}_n, \big\{L^{(\mathbf{t}(i))}(h)\big\}_{h=1}^H\big) + \dfrac{\tau}{2}\|\mathbf{x}_n - \bar{\mathbf{x}}_n\|^2 \Big\}, & \text{if } i \in \mathscr{T}_n \\ \mathbf{x}_n^{(i)}, & \text{otherwise} \end{cases}$$

`End`

`(S.3)` : `If` the NE is reached, then each user $n \in \mathcal{N}$ sets $\mathbf{x}_n^{(i+1)} \leftarrow (1 - \rho^{(i)})\bar{\mathbf{x}}_n + \rho^{(i)}\mathbf{x}_n^{(i+1)}$ and updates his centroid: $\bar{\mathbf{x}}_n = \mathbf{x}_n^{(i+1)}$.

`(S.4)` : $i \leftarrow i + 1$; `Go to (S.1)`.

Theorem 4.2. *Given the game $\mathscr{G} = \langle \Omega_{\mathbf{x}}, \mathbf{f} \rangle$, suppose that the conditions of Theorem 4.1 and the following hold:*

[7] Replacing the exact computation of the solution of the regularized VI with an inexact solution does not affect convergence of Algorithm 4.1, as long as the error bound goes to zero as $i \to \infty$ [74, 76, 78].

(a) *The grid cost functions per unit of energy* $\{C_h(x)\}_{h=1}^{H}$ *are strictly increasing and convex in* $L^{(\min)} \leq x \leq L^{(\max)}$*, and additionally satisfy*

$$C_h'(x) \geq N\big(\zeta^{(\min)} + \zeta^{(\max)}\big)C_h''(x), \qquad \forall x \in [L^{(\min)}, L^{(\max)}] \tag{4.27}$$

with N *being the number of active users connected to the grid,* $\zeta^{(\min)} \triangleq \max_{n\in\mathcal{N}} l_n^{(\min)}$ *and* $\zeta^{(\max)} \triangleq \max_{n\in\mathcal{N}} l_n^{(\max)}$ *denoting the maximum amount of energy that can be sold to or bought from the grid by any single user* $n \in \mathcal{N}$ *at any time-slot, respectively;*

(b) *The regularization parameter* τ *satisfies*

$$\tau > 2(N-1)\max_h C_h'(L^{(\max)}) + 2L^{(\max)}\max_h \Big(\max_{L^{(\min)}\leq x\leq L^{(\max)}} C_h''(x)\Big) \tag{4.28}$$

where $L^{(\max)}$ *is the maximum aggregate energy load allowed by the grid infrastructure;*

(c) $\rho^{(i)}$ *is chosen so that* $\{\rho^{(i)}\} \subset [R_m, R_M]$*, with* $0 < R_m < R_M < 2$ [74, Th. 4.3].

Then, any sequence $\{\mathbf{x}_n^{(i)}\}_{i=1}^{\infty}$ *generated by Algorithm* 4.1 *converges to a Nash equilibrium of the game, for any given updating schedule of the users satisfying assumptions* (A1)–(A3).

Proof. See Appendix 4.A.3.

Remark 4.2 (**on Algorithm 4.1**)**.** Algorithm 4.1 can be seen as an asynchronous algorithm with an occasional update of the individual centroids $\bar{\mathbf{x}}_n$, performed simultaneously $\forall n \in \mathcal{N}$. Nonetheless, it is a double-loop algorithm in nature: in the inner loop, the computation of $\mathbf{S}_\tau(\mathbf{x}^{(i)})$ requires the solution of the regularized game in (4.26) via asynchronous best-response algorithms (such as [74, Alg. 4.2]); in the outer loop, all users $n \in \mathcal{N}$ update their centroid $\bar{\mathbf{x}}_n$ and proceed to solve the inner game again, until an equilibrium is reached. Observe that the update of the centroids is performed locally by the users at the cost of no signaling exchange with the central unit. However, since this update must be simultaneous, some sort of synchronization must be provided by the central unit to the users (see [76] for a detailed discussion on synchronization methods for this class of distributed algorithms). The central unit also checks whether the termination criterion in step `(S.1)` is met, terminating thus the algorithm. Since the central unit only receives the individual energy loads from each user, a practical criterion can be to guarantee that the difference of the users' energy loads between two consecutive iterations is below the prescribed accuracy (c.f. Section 4.5).

Summarizing, the proposed demand-side day-ahead optimization based on Algorithm 4.1 works as follows. At the beginning of the optimization process, τ is computed as in Theorem 4.2(b) and broadcast to each user $n \in \mathcal{N}$, together with the grid cost functions per unit of energy $\{C_h(\cdot)\}_{h=1}^{H}$. Then, in each iteration, any active user who wants to update his strategy solves his own optimization problem in (4.26) based on the most recent values of the aggregate energy loads $\{L^{(\mathbf{t}(i))}(h)\}_{h=1}^{H}$, which are calculated by the central unit referring to the (possibly

outdated) individual demands, and communicates his new load to the central unit. When an equilibrium in the inner loop is reached, the central unit proceeds to the next iteration, and this process is repeated until convergence is reached.

Remark 4.3 (on Theorem 4.2(a)). The interpretation of the condition (4.27) given in Theorem 4.2(a) is twofold. First of all, it provides a guideline to choose the grid cost functions per unit of energy $\{C_h(\cdot)\}_{h=1}^{H}$. Second, it represents a tradeoff between the minimum demand generated by the passive users and that coming from the active users, as explained next. Suppose, for instance, that $C_h(x) = K_h x^a$ with $K_h > 0$ and $a > 1$; then (4.27) actually implies that

$$L^{(\min)} = L^{(\min,\mathcal{P})} + L^{(\min,\mathcal{N})} \geq N(a-1)\big(\zeta^{(\min)} + \zeta^{(\max)}\big) \tag{4.29}$$

where $L^{(\min,\mathcal{P})}$ and $L^{(\min,\mathcal{N})}$ denote the minimum aggregated demand of the passive and the active users, respectively. Observe that $L^{(\min,\mathcal{P})}$ is increasing with the number of passive users in the demand-side, whereas the right-hand side of (4.29) is not affected by it. On the other hand, when we add new active users, the previous condition becomes more restrictive, since the resulting increment of the right-hand side of (4.29) is always greater than the one of the left-hand side (as the individual demand of any active user satisfies $-\zeta^{(\min)} \leq l_n(h) \leq \zeta^{(\max)}$). It turns out that, for any given number of passive users, (4.27) provides an upper bound on the number of active users that can be tolerated in the demand-side of the network.

Remark 4.4 (on Theorem 4.2(b)). From the proof of Theorem 4.2(b), it follows that Algorithm 4.1 can converge under a milder bound on the regularization parameter than the one given in (4.28). However, the peculiarity of the provided expression of τ is that none of the terms in (4.28) depends on the particular energy generation or storage equipment owned by user n, but only on the transmission grid infrastructure. Thus, the regularization parameter can be calculated by the central unit a priori without interfering with the privacy of the users. These considerations apply also to the lower bound of τ provided in (4.35) for Algorithm 4.2.

4.4 Cooperative DSM Approach

In contrast to the noncooperative approach discussed in Section 4.3, we now consider an alternative DSM technique, in which demand-side users collaborate to minimize the aggregate cumulative expense over the time period of analysis introduced in (4.10).

Recalling the definitions of strategy vector, strategy set, and objective function given in (4.11), (4.12), and (4.14), respectively (see Section 4.3), we formulate our DSM optimization problem as

$$\begin{aligned} \min_{\mathbf{x}} \quad & f^{(\mathcal{D})}(\mathbf{x}) = \sum_{n\in\mathcal{N}} f_n^{(\mathcal{D})}(\mathbf{x}_n, \mathbf{x}_{-n}) \\ \text{s.t.} \quad & \mathbf{x}_n \in \Omega_{\mathbf{x}_n}, \qquad \forall n \in \mathcal{N} \end{aligned} \tag{4.30}$$

with

$$f_n^{(\mathcal{D})}(\mathbf{x}_n, \mathbf{x}_{-n}) = f_n(\mathbf{x}_n, \mathbf{x}_{-n}) + \frac{1}{N} p^{(\mathcal{P})}(\mathbf{x}) \tag{4.31}$$

where $f_n(\mathbf{x}_n, \mathbf{x}_{-n})$ represents the individual cumulative expense of user $n \in \mathcal{N}$ defined in (4.14) and where $p^{(\mathcal{P})}(\mathbf{x})$ denotes the aggregate cumulative expense of the passive users defined in (4.9), where we made explicit the dependence on the strategies of the active users. Note that in the objective function $f_n^{(\mathcal{D})}(\mathbf{x})$ there is a common term (equal for all users) $p^{(\mathcal{P})}(\mathbf{x})$, which is the cost associated with the aggregate load of the passive users. This cost is, in fact, a transferable utility and can be distributed among the active users in any arbitrary manner (e.g., as we did in (4.31)) without affecting the optimal value of the social function $f^{(\mathcal{D})}(\mathbf{x})$ in (4.30).

4.4.1 Distributed Dynamic Pricing Algorithm

Traditionally, optimization problems of the form of (4.30) have been tackled by using gradient-based algorithms, which solve a sequence of convex problems by convexifying the whole social function; because of that, they generally suffer from slow convergence. A faster algorithm can be obtained by following the approach recently proposed in [83] (see also [82] for more details): since each $f_n^{(\mathcal{D})}(\mathbf{x}_n, \mathbf{x}_{-n})$ is convex for any feasible $\mathbf{x}_{-n}$ (under the settings of Theorem 4.1), one can convexify only the nonconvex part, i.e., $\sum_{m \in \mathcal{N} \setminus \{n\}} f_m^{(\mathcal{D})}(\mathbf{x})$, and solve the sequence of resulting optimization problems. Since such a procedure preserves some structure of the original objective function, it is expected to be faster than classical gradient-based schemes. A formal description of the algorithm is given next.

Let us preliminary define $\mathbf{x}^{(i)} \triangleq \big(\mathbf{x}_n^{(i)}\big)_{n=1}^N$ as the joint strategy vector at iteration i and the resulting aggregate load as

$$L^{(i)}(h) = L^{(\mathcal{P})}(h) + \sum_{m \in \mathcal{N}} l_m^{(i)}(h), \qquad h = 1, \ldots, H \tag{4.32}$$

where $l_n^{(i)}(h)$ is the energy load of user $n \in \mathcal{N}$ at iteration i. We can then introduce the best-response mapping $\Omega_{\mathbf{x}} \ni \mathbf{x}^{(i)} \to \widehat{\mathbf{x}}_\tau(\mathbf{x}^{(i)}) = \big(\widehat{\mathbf{x}}_{\tau,n}(\mathbf{x}^{(i)})\big)_{n=1}^N$, where we have defined

$$\widehat{\mathbf{x}}_{\tau,n}(\mathbf{x}^{(i)}) = \underset{\mathbf{x}_n \in \Omega_{\mathbf{x}_n}}{\operatorname{argmin}} \Big\{ f_n^{(\mathcal{D})}\big(\mathbf{x}_n, \big\{L^{(i)}(h)\big\}_{h=1}^H\big) + \boldsymbol{\pi}_n\big(\big\{L^{(i)}(h)\big\}_{h=1}^H\big)^{\mathrm{T}} \mathbf{x}_n + \frac{\tau}{2} \|\mathbf{x}_n - \mathbf{x}_n^{(i)}\|^2 \Big\} \tag{4.33}$$

and

$$\boldsymbol{\pi}_n\big(\big\{L^{(i)}(h)\big\}_{h=1}^H\big) = \boldsymbol{\Delta}_n^{\mathrm{T}} \Big(C_h'\big(L^{(i)}(h)\big)\big(L^{(i)}(h) - l_n^{(i)}(h) - \frac{1}{N} L^{(\mathcal{P})}(h)\big)\Big)_{h=1}^H \tag{4.34}$$

where $\boldsymbol{\Delta}_n = \boldsymbol{\delta}_n^{\mathrm{T}} \otimes \mathbf{I}_H$, with $\boldsymbol{\delta}_n$ defined as in (4.13). Note that each individual optimization in (4.33) is strongly convex under Theorem 4.1 and, therefore, has a unique solution (see Appendix 4.B.1 for details); (4.33) is thus well-defined. The proposed algorithm solving the social problem in (4.30) is formally described in Algorithm 4.2 below, whose convergence conditions

are given in Theorem 4.3.

Algorithm 4.2 Distributed Dynamic Pricing Algorithm (DDPA)

`Data` : Set $i = 0$. Given $\{C_h(\cdot)\}_{h=1}^{H}$, $\{L^{(\mathcal{P})}(h)/N\}_{h=1}^{H}$, $\tau > 0$, and any feasible starting point $\mathbf{x}^{(0)} = (\mathbf{x}_n^{(0)})_{n=1}^{N}$:

`(S.1)` : `If` a suitable termination criterion is satisfied: `STOP`.

`(S.2)` : `For` $n \in \mathcal{N}$, each user computes $\mathbf{x}_n^{(i+1)}$ as

$$\mathbf{x}_n^{(i+1)} = \underset{\mathbf{x}_n \in \Omega_{\mathbf{x}_n}}{\operatorname{argmin}} \Big\{ f_n^{(\mathcal{D})}\big(\mathbf{x}_n, \{L^{(i)}(h)\}_{h=1}^{H}\big) + \boldsymbol{\pi}_n\big(\{L^{(i)}(h)\}_{h=1}^{H}\big)^{\mathrm{T}}\mathbf{x}_n + \frac{\tau}{2}\|\mathbf{x}_n - \mathbf{x}_n^{(i)}\|^2 \Big\}$$

`End`

`(S.4)` : $i \leftarrow i + 1$; `Go to (S.1)`.

Theorem 4.3. *Given the social problem* (4.30)*, suppose that the conditions of Theorem* 4.1 *hold and that the regularization parameter* τ *satisfies*

$$\tau \geq \max_{h} \Big((N+1) C_h'(L^{(\max)}) + \max_{L^{(\min)} \leq x \leq L^{(\max)}} \big(C_h''(x)x\big) \Big) \tag{4.35}$$

where N *is the number of active users connected to the grid and* $L^{(\max)}$ *is the maximum aggregate energy load allowed by the grid infrastructure. Then, either Algorithm* 4.2 *converges in a finite number of iterations to a stationary solution of* (4.30) *or every limit point of the sequence* $\{\mathbf{x}^{(i)}\}_{i=1}^{\infty}$ *is a stationary solution of* (4.30)*.*

Proof. See Appendix 4.B.1.

Differently from Algorithm 4.1, Algorithm 4.2 is not incentive compatible, in the sense that demand-side users need to reach an agreement in following the best-response protocol (4.33). In addition, it differs from Algorithm 4.1 mainly in the synchronous update of the users' strategies. However, Algorithm 4.2 converges under consistently milder conditions on the grid cost functions than those of Algorithm 4.1 and, most importantly, it does not impose any limitation on the number of active users with respect to the total number of demand-side users, which means better scalability. Lastly, the signaling required by the two algorithms is essentially the same.

Let us summarize the proposed demand-side day-ahead optimization based on Algorithm 4.2. At the beginning of the optimization process, τ is computed as in (4.35) by the central unit and broadcast to each user $n \in \mathcal{N}$, together with the grid cost functions per unit of energy $\{C_h(\cdot)\}_{h=1}^{H}$ and the terms related to the transferable utility $\{L^{(\mathcal{P})}(h)/N\}_{h=1}^{H}$. Then, at each iteration, all users simultaneously update their strategies by solving their own optimization problems in (4.33) based on the aggregate energy loads $\{L^{(i)}(h)\}_{h=1}^{H}$, which are calculated by the central unit summing up the individual demands. Then, active users provide their new energy loads to the central unit, and this process is iterated until a suitable termination criterion imposed by the

central unit is satisfied.

4.5 Evaluation of the DSM Approaches

4.5.1 Smart Grid Setup

Let us consider a smart grid consisting of 1000 demand-side users $n \in \mathcal{D}$, each one having a random energy consumption curve with average daily energy consumption $\sum_{h=1}^{24} e_n(h) = 12\,\text{kWh}$ [99], and ranging between 8 kWh and 16 kWh. We suppose that higher consumption occurs more likely during day-time hours, i.e., from 08:00 to 24:00, than during night-time hours, i.e., from 00:00 to 08:00, reaching peak demand generally between 17:00 and 23:00. The energy grid cost function per unit of energy is given by

$$C_h\big(L(h)\big) = K_h L^2(h) = \begin{cases} K_{\text{night}} L^2(h), & \text{for } h = 1, \dots, 8 \\ K_{\text{day}} L^2(h), & \text{for } h = 9, \dots, 24 \end{cases} \tag{4.36}$$

where $K_{\text{day}} = 1.5 K_{\text{night}}$ as in [51] and whose values are chosen so as to obtain an initial average price per kWh of 0.1412 £/kWh [100]. Additionally, we consider $\zeta^{(\min)} = 1$ kWh, $\zeta^{(\max)} = 1.5$ kWh, $L^{(\min)} = 300$ kWh, and $L^{(\max)} = 800$ kWh. With this setup, condition (4.22) is immediately satisfied, guaranteeing that the game $\mathscr{G} = \langle \Omega_{\mathbf{x}}, \mathbf{f} \rangle$ has a nonempty and compact set of Nash equilibria. Recalling Theorem 4.2, Algorithm 4.1 is ensured to converge to one of these Nash equilibria for any $L^{(\min)} \geq N\big(\zeta^{(\min)} + \zeta^{(\max)}\big)$, which implies that the number of active users should satisfy $N \leq 120$, and for any $\tau > 4 \max_h K_h N L^{(\max)}$. Lastly, according to Theorem 4.3, Algorithm 4.2 converges to a stationary solution of the social problem in (4.30) for any $\tau \geq \max_h K_h (N+2) L^{(\max)}$.

In the following, we consider $N = 120$ active users, with $|\mathcal{N}_{\mathcal{G}\setminus\mathcal{S}}| = |\mathcal{N}_{\mathcal{S}\setminus\mathcal{G}}| = |\mathcal{N}_{\mathcal{G}\cap\mathcal{S}}| = 40$, and $P = 880$ passive users. This corresponds to having 12% of active users equally distributed among dispatchable energy producers, energy storers, and dispatchable energy producers-storers. For the sake of simplicity, we assume that all dispatchable energy producers and energy storers adopt generators and storage devices with the same features as in [84, Sec. IV]. In particular, all generators employed by users $n \in \mathcal{G}$ are characterized by a linear production cost function, resembling that of a combustion engine (e.g., a biomass generator [101]) working in the linear region:

$$W_n(x) = \eta_n x \tag{4.37}$$

with $\eta_n = 0.039$ £/kWh [102], $g_n^{(\max)} = 0.4$ kW, $\gamma_n^{(\min)} = 0$ kWh, and $\gamma_n^{(\max)} = 0.8 g_n^{(\max)} \times 24$ h. Likewise, we suppose that all energy storage devices adopted by users $n \in \mathcal{S}$ present the following

parameters: leakage rate $\alpha_n = \sqrt[24]{0.9}$,[8] capacity $c_n = 4$ kWh (this value is also used in [47] and is equivalent to the capacity of the battery of a small PHEV), maximum charging rate $s_n^{(\max)} = 0.125c_n$/h, $q_n(0) = 0.25c_n$, and $\epsilon_n = 0$.

4.5.2 Simulation Results

In this section, we provide some numerical results in order to illustrate the performance of the proposed noncooperative and cooperative day-ahead DSM mechanisms formalized in Algorithms 4.1 and 4.2, respectively. In doing so, we delineate the overall results and examine the convergence of both schemes, comparing the benefits achieved by the different types of active users. In particular, we show that all active users substantially reduce their monetary expense by adopting distributed energy generation and/or storage.

Interestingly, the overall results produced by the noncooperative and the cooperative approaches happen to be equivalent in our case: beyond any doubt, this constitutes a major strength of Algorithm 4.1. Figure 4.3 illustrates the global results obtained equivalently using Algorithms 4.1 and 4.2. In the specific, Figure 4.3(a) shows, for each hour h, the aggregate per-slot energy consumption $\sum_{n\in\mathcal{D}} e_n(h)$ together with the aggregate per-slot energy load $L(h)$ resulting from both approaches. Likewise, Figure 4.3(b) delineates the aggregate per-slot energy production $\sum_{n\in\mathcal{G}} g_n(h)$ and storage $\sum_{n\in\mathcal{S}} s_n(h)$ at each hour h. As expected, energy storers charge their battery at the valley of the energy cost, resulting in a substantially more flattened demand curve. Contrarily, they discharge it at peak hours, shaving off the peak of the load. For the sake of comparison with ECS techniques [51, 58, 72, 73], our day-ahead DSM optimization with just $|\mathcal{S}| = 80$ energy storers and the adopted storage capacities allows to shift 327 kWh from the peak hours to the valley of the demand curve: this is equivalent to having a shiftable load corresponding to 2.7% of the daily aggregate load among all 1000 demand-side users. On the other hand, dispatchable energy producers generate little energy during night-time hours, when they rather buy it from the grid. The average grid price per kWh reduces to 0.1156 £/kWh (i.e., 20.8% less) and, considering the individual energy production costs for users $n \in \mathcal{G}$, the overall price further decreases to 0.1116 £/kWh. The comparison between the initial and the final grid price at each hour h is illustrated in Figure 4.3(c). Moreover, the aggregate cumulative expense $p^{(\mathcal{D})}$ reduces from £1705 to £1351. Finally, the peak-to-average ratio (PAR), defined as

$$\mathrm{PAR} = \frac{H \max_h L(h)}{\sum_{h=1}^{H} L(h)} \tag{4.38}$$

which expresses the ratio between the peak demand and the average energy demand calculated along the day, decreases from 1.5254 to 1.3337 (i.e., 12.6% less) resulting in a generally flattened

[8] This value of α_n corresponds to having a leakage rate of 0.9 over the 24 hours.

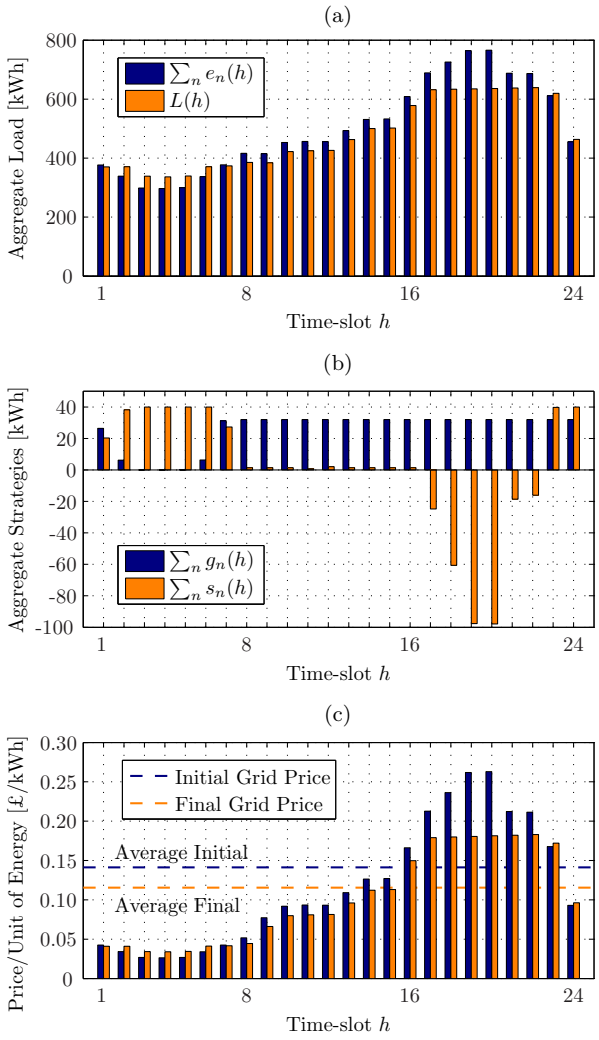

Figure 4.3: (a) Initial aggregate per-slot energy consumption and aggregate per-slot energy load after both DSM optimizations at each h; (b) aggregate per-slot energy production and storage at each h; and (c) initial and final grid price per unit of energy at each h.

demand curve.

We employ $\{\rho^{(i)}\}_{i=0}^{\infty} = 0.8$ for Algorithm 4.1, whereas the termination criterion used to finalize both algorithms is $\|\mathbf{l}^{(i)} - \mathbf{l}^{(i-1)}\|_2 / \|\mathbf{l}^{(i)}\|_2 \leq 10^{-2}$. Figure 4.4(a) plots this measure over the first 10 iterations. With the above setup, Algorithm 4.1 converges after 8 iterations and Algorithm 4.2 after just 2 iterations. In this regard, Figure 4.4(b) shows how the average cumulative expenses over the time period of analysis for each type of active users, as well as that of the passive users, converge to their final value: this further highlights the faster convergence of Algorithm 4.2, since the final values of the objective functions are approximately reached after the first iteration, although active users keep adjusting their production and storage strategies until the above termination criterion is satisfied. From this figure it is also straightforward to conclude that active users with more degrees of freedom (i.e, both generation and storage equipment) ob-

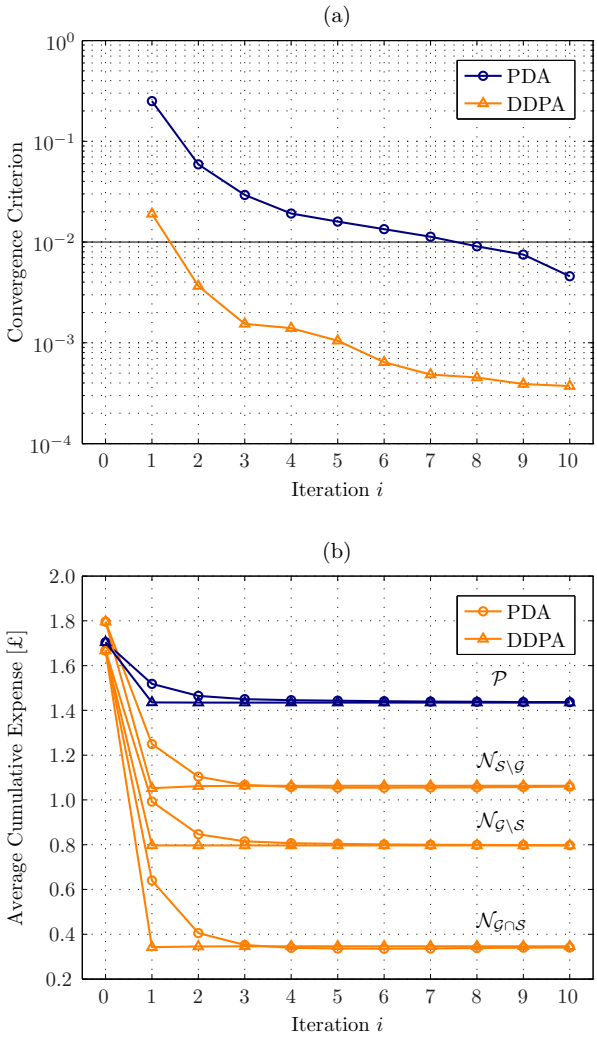

Figure 4.4: (a) Convergence of Algorithm 4.1 (PDA) and Algorithm 4.2 (DDPA) with termination criterion $\|\mathbf{l}^{(i)}-\mathbf{l}^{(i-1)}\|_2/\|\mathbf{l}^{(i)}\|_2 \leq 10^{-2}$; and (b) average cumulative expense over the time period of analysis for each subset of active users, as a function of the iteration i.

tain better saving percentages, although the employment of distributed energy production and storage benefits all users in the smart grid. In particular, the average savings obtained for each subset of active users are: £1.3225 (i.e., 79.3% less) for users $n \in \mathcal{N}_{\mathcal{G}\cap\mathcal{S}}$, £0.8717 (i.e., 52.3% less) for users $n \in \mathcal{N}_{\mathcal{G}\setminus\mathcal{S}}$, and £0.7348 (i.e., 40.9% less) for users $n \in \mathcal{N}_{\mathcal{S}\setminus\mathcal{G}}$. On the other hand, passive users $n \in \mathcal{P}$ save on average £0.2695 (i.e., 15.8% less) each. Evidently, the saving for users $n \in \mathcal{N}$ is greater than for users $n \in \mathcal{P}$, i.e., all demand-side users are incentivized to directly adopt distributed energy generation and/or storage. Moreover, users $n \in \mathcal{N}_{\mathcal{G}\cap\mathcal{S}}$ save more than users $n \in \mathcal{N}_{\mathcal{G}\setminus\mathcal{S}} \cup \mathcal{N}_{\mathcal{S}\setminus\mathcal{G}}$: this means that using both dispatchable energy sources and storage devices allows to further decrease the individual cumulative expense over the time period of analysis.

In Figure 4.5(a) we plot the average cumulative expense over the time period of analysis for

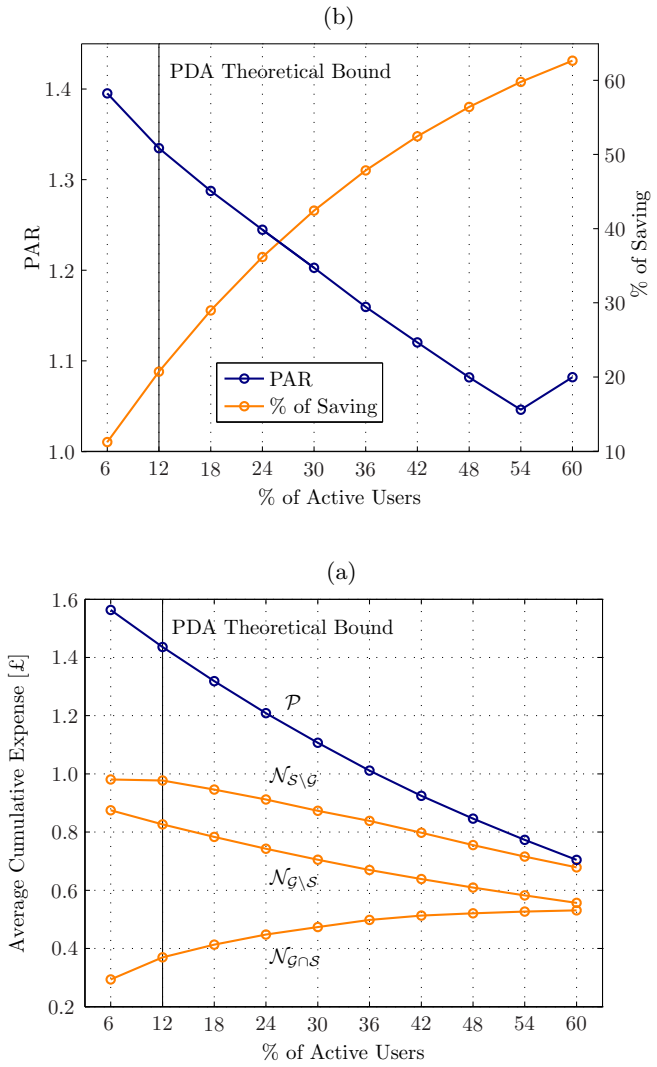

Figure 4.5: (a) Average cumulative expense over the time period of analysis for each subset of users as a function of the percentage of active users; and (b) total percentage saving and PAR as functions of the percentage of active users. The active users are equally distributed among dispatchable energy producers, energy storers, and dispatchable energy producers-storers.

each subset of demand-side users versus different percentages of active users equally distributed among dispatchable energy producers, energy storers, and dispatchable energy producers-storers, with each demand-side user $n \in \mathcal{D}$ having the same consumption curve. Interestingly, Algorithm 4.1 keeps performing equivalently to Algorithm 4.2 even when the theoretical bound on the number of active users, $N > 120$, provided in Theorem 4.2 to ensure its convergence, is not fulfilled. Furthermore, we observe that the average cumulative expense of the active and passive users tend to the same value as the production and storage capacities increase. Besides, as illustrated in Figure 4.5(b), the total saving of all (active and passive) users in the smart grid raises in inverse proportion with the decreasing PAR, which diminishes almost linearly as the percentage of active users increases. Note that, as the PAR approaches 1 with $N = 540$ (54%),

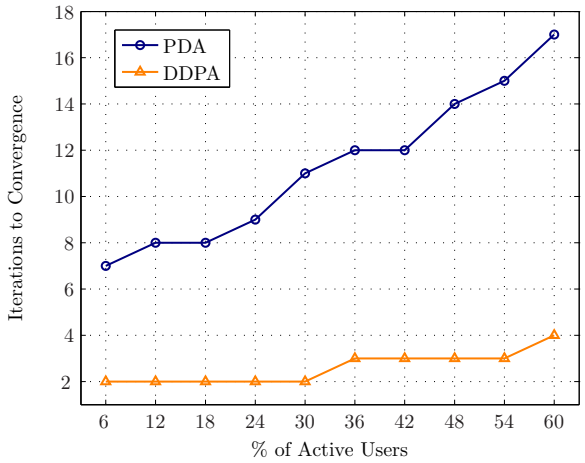

Figure 4.6: Number of iterations required for the convergence of Algorithm 4.1 (PDA) and Algorithm 4.2 (DDPA), with termination criterion $\|\mathbf{l}^{(i)} - \mathbf{l}^{(i-1)}\|_2 / \|\mathbf{l}^{(i)}\|_2 \leq 10^{-2}$, as a function of the percentage of active users.

its value raises unexpectedly when $N = 600$ (60%). This is due to the lower coefficients K_h adopted during $h = 1, \ldots, 8$, as stated in (4.36): in fact, once a perfectly flattened demand curve is achieved, active users naturally keep lowering the aggregate load during the last 16 hours when the price is higher in favor of the first 8 hours during which the price is lower.

Lastly, Figure 4.6 depicts the number of iterations needed for the convergence of Algorithms 4.1 and 4.2 as a function of the percentage of active users, using the same termination criterion $\|\mathbf{l}^{(i)} - \mathbf{l}^{(i-1)}\|_2 / \|\mathbf{l}^{(i)}\|_2 \leq 10^{-2}$. In the first instance, the former always requires several more iterations than the latter, not to mention that each iteration in the proximal decomposition algorithm implies solving a (regularized) Nash game. Moreover, it is evident that the convergence speed of the proximal decomposition algorithm is substantially more related to the number of active participants than that of the distributed dynamic pricing algorithm, which emphasizes the better scalability properties of the latter.

4.6 Conclusions

In this paper, we propose a general grid model that accommodates distributed energy production and storage, and a day-ahead DSM mechanism. In particular, we formulate the resulting grid optimization problem using a noncooperative method and a more classical nonlinear programming approach. In the first case, each active user on the demand-side selfishly minimizes his cumulative monetary expense for buying/producing his energy needs. We use noncooperative game theory and, building on the general framework of variational inequality, we derive (sufficient) conditions on the generalized energy cost functions that guarantee the existence of (multiple, yet equivalent) optimal strategies, as well as the convergence of the proposed asynchronous proximal decomposition algorithm. As for the second approach, we devise a distributed

scheme based on the distributed dynamic pricing algorithm. Both methods allow to compute the optimal strategies of the users in a distributed fashion and with limited information exchange between the central unit and the demand-side of the network. Simulations on a realistic situation employing practical energy cost functions show that, despite their different (sufficient) convergence conditions, the two algorithms achieve equivalent overall results, sensibly flattening the demand curve and reducing the need for carbon-intensive and expensive peaking power plants. Regardless, the two approaches present different characteristics in terms of strategy update and convergence speed that favor the employment of one over the other according to the situation. Finally, it is worth mentioning that the DSM techniques presented in this paper, being directly applicable to end users like households and small businesses, can also be extended to larger contexts, such as small communities or cities, by means of energy aggregators. In fact, flattening the energy demand along time is clearly beneficial at any layer of the energy grid.

4.A Noncooperative DSM Approach

4.A.1 Proof of Theorem 4.1

In this appendix, we derive the conditions on the cost functions per unit of energy $\big\{C_h(\cdot)\big\}_{h=1}^{H}$ and on the production cost functions $\big\{W_n(\cdot)\big\}_{n\in\mathcal{G}}$ that guarantee the existence of the Nash equilibria of the game $\mathscr{G} = \langle \Omega_{\mathbf{x}}, \mathbf{f} \rangle$ in (4.17).

Recalling Lemma 4.1, the VI problem $\mathrm{VI}(\Omega_{\mathbf{x}}, \mathbf{F})$, with $\mathbf{F}(\mathbf{x}) = \big(\nabla_{\mathbf{x}_n} f_n(\mathbf{x}_n, \mathbf{x}_{-n})\big)_{n=1}^{N}$, is equivalent to the game $\mathscr{G} = \langle \Omega_{\mathbf{x}}, \mathbf{f} \rangle$ if the objective function $f_n(\mathbf{x}_n, \mathbf{x}_{-n})$ in (4.14) is convex on $\Omega_{\mathbf{x}_n}$ for any $\mathbf{x}_{-n} \in \Omega_{\mathbf{x}_{-n}}$, $\forall n \in \mathcal{N}$; note that the individual strategy sets $\Omega_{\mathbf{x}_n}$ in (4.12) are closed and convex. The convexity of each objective function is equivalent to the monotonicity of the associated mapping function $\mathbf{F}_n(\mathbf{x}_n, \mathbf{x}_{-n})$ in (4.20) on $\Omega_{\mathbf{x}_n}$, for every given $\mathbf{x}_{-n} \in \Omega_{\mathbf{x}_{-n}}$ [79], i.e.,

$$(\mathbf{x}_n - \mathbf{y}_n)^{\mathrm{T}}\big(\mathbf{F}_n(\mathbf{x}_n, \mathbf{x}_{-n}) - \mathbf{F}_n(\mathbf{y}_n, \mathbf{x}_{-n})\big) \geq 0, \qquad \forall \mathbf{x}_n, \mathbf{y}_n \in \Omega_{\mathbf{x}_n}. \tag{4.39}$$

Next, we derive the conditions for $\mathbf{F}_n(\mathbf{x})$ to satisfy (4.39). We rewrite the left-hand side of (4.39) as

$$
\begin{aligned}
&(\mathbf{x}_n-\mathbf{y}_n)^{\mathrm{T}}\big(\mathbf{F}_n(\mathbf{x}_n,\mathbf{x}_{-n})-\mathbf{F}_n(\mathbf{y}_n,\mathbf{x}_{-n})\big)\\
&\quad=\sum_{h=1}^{H}\Big(C_h\big(L_{-n}(h)+l_{\mathbf{x}_n}(h)\big)+C_h'\big(L_{-n}(h)+l_{\mathbf{x}_n}(h)\big)l_{\mathbf{x}_n}(h)\Big)\big(l_{\mathbf{x}_n}(h)-l_{\mathbf{y}_n}(h)\big) &(4.40)\\
&\qquad-\sum_{h=1}^{H}\Big(C_h\big(L_{-n}(h)+l_{\mathbf{y}_n}(h)\big)+C_h'\big(L_{-n}(h)+l_{\mathbf{y}_n}(h)\big)l_{\mathbf{y}_n}(h)\Big)\big(l_{\mathbf{x}_n}(h)-l_{\mathbf{y}_n}(h)\big) &(4.41)\\
&\qquad+\sum_{h=1}^{H}\Big(W_n'\big(\boldsymbol{\delta}_{g,n}^{\mathrm{T}}\mathbf{x}_n(h)\big)-W_n'\big(\boldsymbol{\delta}_{g,n}^{\mathrm{T}}\mathbf{y}_n(h)\big)\Big)\boldsymbol{\delta}_{g,n}^{\mathrm{T}}\big(\mathbf{x}_n(h)-\mathbf{y}_n(h)\big) &(4.42)
\end{aligned}
$$

where $L_{-n}(h)=L^{(\mathcal{P})}(h)+\sum_{m\in\mathcal{N}\setminus\{n\}}l_m(h)$, $l_{\mathbf{x}_n}(h)=e_n(h)+\boldsymbol{\delta}_n^{\mathrm{T}}\mathbf{x}_n(h)$, and $l_{\mathbf{y}_n}(h)$ is accordingly defined. Observe, then, that the term in (4.42) is nonnegative if $W_n(x)$ is convex, i.e., if $W_n'(x)$ is monotone:

$$W_n''(x)\geq 0,\qquad 0\leq x\leq g_n^{(\max)} \tag{4.43}$$

since, under this condition, each element in the summation is nonnegative itself.

In addition, the sum of the terms in (4.40) and (4.41) is nonnegative if the function $C_h(x)+C_h'(x)\big(x-L_{-n}(h)\big)$ is increasing in $L^{(\min)}\leq x\leq L^{(\max)}$ for any time-slot h or, equivalently, if

$$2C_h'(x)+C_h''(x)\big(x-L_{-n}(h)\big)\geq 0,\qquad L^{(\min)}\leq x\leq L^{(\max)}. \tag{4.44}$$

Assuming that for any time-slot h the grid cost function $C_h(x)$ is convex, i.e., $C_h''(x)\geq 0$, we can distinguish between two cases:

(i) When $C_h''(x)=0$, the inequality in (4.44) is satisfied if $C_h'(x)\geq 0$, which forces $C_h(x)$ to be increasing;

(ii) When $C_h''(x)>0$, it holds that

$$2C_h'(x)+C_h''(x)\big(x-L_{-n}(h)\big)\geq 2C_h'(x)-C_h''(x)l_n^{(\min)}\geq 0 \tag{4.45}$$

where $\max_n l_n^{(\min)}$ represents the maximum amount of energy that can be sold to the grid by any single user $n\in\mathcal{N}$ at any time-slot. Hence, (4.44) is verified if $C_h'(x)>0$, i.e., if $C_h(x)$ is strictly increasing and, additionally, for any time-slot h it holds

$$C_h'(x)\geq\frac{1}{2}l_n^{(\min)}C_h''(x),\qquad L^{(\min)}\leq x\leq L^{(\max)}. \tag{4.46}$$

So far, we have proved that $\mathbf{F}_n(\mathbf{x}_n,\mathbf{x}_{-n})$ is monotone on $\mathbf{x}_n$, for any given $\mathbf{x}_{-n}\in\Omega_{\mathbf{x}_{-n}}$, when the production cost function $W_n(x)$ is convex and the cost functions per unit of energy $\big\{C_h(x)\big\}_{h=1}^{H}$ are increasing and convex and satisfy (4.46). Nevertheless, this must be verified $\forall n\in\mathcal{N}$ and, therefore, constraint (4.46) becomes

$$C_h'(x)\geq\frac{1}{2}\big(\max_{n\in\mathcal{N}}l_n^{(\min)}\big)C_h''(x)=\frac{1}{2}\zeta^{(\min)}C_h''(x) \tag{4.47}$$

whereas the condition on the production cost function in (4.43) must be satisfied $\forall n \in \mathcal{G}$. Now that Lemma 4.1 holds, the solution set of $\mathscr{G} = \langle \Omega_{\mathbf{x}}, \mathbf{f} \rangle$ is nonempty and compact [74, Th. 4.1(a)], since the strategy sets $\Omega_{\mathbf{x}_n}$ are bounded $\forall n \in \mathcal{N}$. This concludes the proof of Theorem 4.1. □

4.A.2 Proof of Proposition 4.1

Theorem 4.1 provides the conditions that guarantee the existence of the Nash equilibria of the game $\mathscr{G} = \langle \Omega_{\mathbf{x}}, \mathbf{f} \rangle$ in (4.17). Although the solution is not unique, all Nash equilibria yield the same values of the objective functions in (4.14). In fact, consider a generic user $n \in \mathcal{N}_{\mathcal{G}\cap\mathcal{S}}$: given two optimal strategy vectors $\mathbf{x}_{1,n}^{\star} \neq \mathbf{x}_{2,n}^{\star}$, with $\mathbf{x}_{1,n}^{\star} \triangleq (\mathbf{g}_{1,n}, \mathbf{s}_{1,n})$ and $\mathbf{x}_{2,n}^{\star} \triangleq (\mathbf{g}_{2,n}, \mathbf{s}_{2,n})$, we have that $f_n\big(\mathbf{x}_{1,n}^{\star}, \mathbf{x}_{-n}\big) = f_n\big(\mathbf{x}_{2,n}^{\star}, \mathbf{x}_{-n}\big)$ if the following $H+2$ conditions hold (see the strategy sets (4.3) and (4.5) for details):

$$\sum_{h=1}^{H} W_n\big(g_{1,n}(h)\big) = \sum_{h=1}^{H} W_n\big(g_{2,n}(h)\big) \tag{4.48}$$

$$s_{1,n}(h) - g_{1,n}(h) = s_{2,n}(h) - g_{2,n}(h), \qquad h = 1, \ldots, H \tag{4.49}$$

$$\sum_{h=1}^{H} \alpha_n^{(H-h)} s_{1,n}(h) = \sum_{h=1}^{H} \alpha_n^{(H-h)} s_{2,n}(h). \tag{4.50}$$

Since in any realistic situation $H > 2$, and being $\mathbf{x}_n \in \mathbb{R}^{2H}$ for $n \in \mathcal{N}_{\mathcal{G}\cap\mathcal{S}}$, it follows that $2H > H+2$, implying that user $n \in \mathcal{N}_{\mathcal{G}\cap\mathcal{S}}$ can choose among infinitely many optimal strategy vectors $\mathbf{x}_n^{\star}$, each of them giving the same value of the objective function $f_n\big(\mathbf{x}_n^{\star}, \mathbf{x}_{-n}\big)$. We can extend the previous considerations to all users: since all $\mathbf{x}_n^{\star}$ produce the same $\big\{l_n^{\star}(h)\big\}_{h=1}^{H}$, $\forall n \in \mathcal{N}$, the aggregate demands $\big\{L^{\star}(h)\big\}_{h=1}^{H}$, with $L^{\star}(h) = L^{\mathcal{P}} + \sum_{n\in\mathcal{N}}^{H} l_n^{\star}(h)$, are not affected by the multiplicity of the Nash equilibria. Hence, any $\mathbf{x}^{\star} = \big(\mathbf{x}_n^{\star}\big)_{n=1}^{N}$ leads to the same values of the objective functions $\big\{f_n\big(\mathbf{x}_n^{\star}, \mathbf{x}_{-n}\big)\big\}_{n\in\mathcal{N}}$. □

4.A.3 Proof of Theorem 4.2

It follows from [74, Th. 4.3] that the sequence generated by the proximal decomposition algorithm described in Algorithm 4.1 converges to a solution of the game $\mathscr{G} = \langle \Omega_{\mathbf{x}}, \mathbf{f} \rangle$ if the following conditions are satisfied: (a) the mapping function $\mathbf{F}(\mathbf{x})$ is monotone on $\Omega_{\mathbf{x}}$; and (b) the regularization parameter τ is such that the mapping $\mathbf{F}(\mathbf{x}) + \tau(\mathbf{I}_N - \mathbf{x}^{(i)})$ is strongly monotone on $\Omega_{\mathbf{x}}$, for any given $\mathbf{x}^{(i)} \in \Omega_{\mathbf{x}}$. Both conditions are proven next in Appendices 4.A.3.1 and 4.A.3.2, respectively.

4.A.3.1 Proof Theorem 4.2(a)

In this appendix, we derive additional conditions on the grid cost functions per unit of energy $\{C_h(\cdot)\}_{h=1}^{H}$ that guarantee the monotonicity of $\mathbf{F}(\mathbf{x}) = \big(\nabla_{\mathbf{x}_n} f_n(\mathbf{x}_n, \mathbf{x}_{-n})\big)_{n=1}^{N}$ on $\Omega_{\mathbf{x}}$, with $f_n(\mathbf{x}_n, \mathbf{x}_{-n})$ defined in (4.14). We assume next that the requirements given by Theorem 4.1 are satisfied.

The mapping $\mathbf{F}(\mathbf{x})$ is monotone on $\Omega_{\mathbf{x}}$ if and only if the Jacobian matrix $\mathsf{J}\mathbf{F}(\mathbf{x})$ satisfies [74, eq. (4.8(i))]

$$\frac{1}{2}\mathbf{z}^{\mathrm{T}}\big(\mathsf{J}\mathbf{F}(\mathbf{x}) + \mathsf{J}\mathbf{F}^{\mathrm{T}}(\mathbf{x})\big)\mathbf{z} \geq 0, \qquad \forall \mathbf{x} \in \Omega_{\mathbf{x}},\ \forall \mathbf{z} \in \mathbb{R}^{\omega_{\mathbf{x}}}. \tag{4.51}$$

Given $\mathbf{F}_n(\mathbf{x}_n, \mathbf{x}_{-n})$ in (4.20), the partial Jacobian matrices of $\mathbf{F}(\mathbf{x})$ are

$$\mathsf{J}_{\mathbf{x}_n}\mathbf{F}_n(\mathbf{x}_n, \mathbf{x}_{-n}) = 2\boldsymbol{\Delta}_n^{\mathrm{T}}\mathbf{D}_{\mathbf{c}'}(\mathbf{x})\boldsymbol{\Delta}_n \tag{4.52}$$

$$+ \boldsymbol{\Delta}_n^{\mathrm{T}}\mathrm{Diag}\big(\mathbf{D}_{\mathbf{c}''}(\mathbf{x})(\mathbf{e}_n + \boldsymbol{\Delta}_n\mathbf{x}_n)\big)\boldsymbol{\Delta}_n + \boldsymbol{\Delta}_{g,n}^{\mathrm{T}}\mathbf{D}_{\mathbf{w}_n''}(\boldsymbol{\Delta}_{g,n}\mathbf{x}_n)\boldsymbol{\Delta}_{g,n} \tag{4.53}$$

$$\mathsf{J}_{\mathbf{x}_m}\mathbf{F}_n(\mathbf{x}_n, \mathbf{x}_{-n}) = \boldsymbol{\Delta}_n^{\mathrm{T}}\mathbf{D}_{\mathbf{c}'}(\mathbf{x})\boldsymbol{\Delta}_m + \boldsymbol{\Delta}_n^{\mathrm{T}}\mathrm{Diag}\big(\mathbf{D}_{\mathbf{c}''}(\mathbf{x})(\mathbf{e}_n + \boldsymbol{\Delta}_n\mathbf{x}_n)\big)\boldsymbol{\Delta}_m, \qquad n \neq m \tag{4.54}$$

where $\mathbf{D}_{\mathbf{c}'}(\mathbf{x}) = \mathrm{Diag}\big(\mathbf{c}'(\mathbf{x})\big)$, $\mathbf{D}_{\mathbf{c}''}(\mathbf{x}) = \mathrm{Diag}\big(\mathbf{c}''(\mathbf{x})\big)$, and $\mathbf{D}_{\mathbf{w}_n''}(\boldsymbol{\Delta}_{g,n}\mathbf{x}_n) = \mathrm{Diag}\big(\mathbf{w}_n''(\boldsymbol{\Delta}_{g,n}\mathbf{x}_n)\big)$ are $H \times H$ diagonal matrices. By defining $\mathbf{J}(\mathbf{x}) = \frac{1}{2}(\mathsf{J}\mathbf{F}(\mathbf{x}) + \mathsf{J}\mathbf{F}^{\mathrm{T}}(\mathbf{x}))$ and decomposing vector $\mathbf{z}$ as $\mathbf{z} = \big(\mathbf{z}_n\big)_{n=1}^{N}$, where $\mathbf{z}_n = \big(z_n(1), \ldots, z_n(\boldsymbol{\delta}_n^{\mathrm{T}}\boldsymbol{\delta}_n H)\big)$, we can rewrite the left-hand side of (4.51) as

$$\mathbf{z}^{\mathrm{T}}\mathbf{J}(\mathbf{x})\mathbf{z} = \sum_{n\in\mathcal{N}}(\boldsymbol{\Delta}_n\mathbf{z}_n)^{\mathrm{T}}\mathbf{D}_{\mathbf{c}'}(\mathbf{x})(\boldsymbol{\Delta}_n\mathbf{z}_n) + \sum_{n\in\mathcal{G}}(\boldsymbol{\Delta}_{g,n}\mathbf{z}_n)^{\mathrm{T}}\mathbf{D}_{\mathbf{w}_n''}(\boldsymbol{\Delta}_{g,n}\mathbf{x}_n)(\boldsymbol{\Delta}_{g,n}\mathbf{z}_n) \tag{4.55}$$

$$+ \sum_{n,m\in\mathcal{N}}(\boldsymbol{\Delta}_n\mathbf{z}_n)^{\mathrm{T}}\Big(\mathbf{D}_{\mathbf{c}'}(\mathbf{x}) + \frac{1}{2}\mathrm{Diag}\big(\mathbf{D}_{\mathbf{c}''}(\mathbf{x})(\mathbf{e}_n + \mathbf{e}_m + \boldsymbol{\Delta}_n\mathbf{x}_n + \boldsymbol{\Delta}_m\mathbf{x}_m)\big)\Big)(\boldsymbol{\Delta}_m\mathbf{z}_m). \tag{4.56}$$

Observing the first term in (4.55), we are already in the position to state that, as long as $\mathcal{N}_{\mathcal{G}\cap\mathcal{S}} \neq \emptyset$, $\mathbf{J}(\mathbf{x})$ cannot even be positive definite: in fact, we can have that $\boldsymbol{\Delta}_n\mathbf{z}_n = \mathbf{0}$ with $\mathbf{z}_n \neq \mathbf{0}$ for $n \in \mathcal{N}_{\mathcal{G}\cap\mathcal{S}}$, whereas we cannot guarantee $W_n(x)$ to be strictly convex (i.e., $W_n''(x) > 0$) for these users.[9] Hence, let us now introduce

$$\tilde{z}_n(h) = [\boldsymbol{\Delta}_n\mathbf{z}_n]_h = \begin{cases} -z_n(h), & \text{if } n \in \mathcal{N}_{\mathcal{G}\setminus\mathcal{S}} \\ z_n(h), & \text{if } n \in \mathcal{N}_{\mathcal{S}\setminus\mathcal{G}} \\ \big(-z_n(h) + z_n(h+H)\big), & \text{if } n \in \mathcal{N}_{\mathcal{G}\cap\mathcal{S}} \end{cases} \tag{4.57}$$

[9] Recall that best-response algorithms such as [74, Alg. 5.1] converge under sufficient conditions that imply the strict monotonicity of $\mathbf{F}(\mathbf{x})$ on $\Omega_{\mathbf{x}}$. It is not difficult to show that such requirement forces $\mathcal{N}_{\mathcal{G}\cap\mathcal{N}} = \emptyset$, which is too restrictive and cannot be guaranteed.

so that we can express the left-hand side of (4.51) as

$$\mathbf{z}^{\mathrm{T}}\mathbf{J}(\mathbf{x})\mathbf{z} = \sum_{h=1}^{H}\sum_{n\in\mathcal{N}} C_h'\big(L(h)\big)\tilde{z}_n^2(h) + \sum_{h=1}^{H}\sum_{n\in\mathcal{G}} W_n''\big(g_n(h)\big)\tilde{z}_n^2(h) \tag{4.58}$$

$$+\sum_{h=1}^{H}\sum_{n\in\mathcal{N}} \Big(C_h'\big(L(h)\big) + C_h''\big(L(h)\big)l_n(h)\Big)\Big(\tilde{z}_n(h)\sum_{m\in\mathcal{N}}\tilde{z}_m(h)\Big). \tag{4.59}$$

Let us now concentrate on the term in (4.56). Note that, under condition (4.22) in Theorem 4.1(a), $C_h'(L(h)) + C_h''(L(h))l_n(h) \geq 0$ at any time-slot h, $\forall n \in \mathcal{N}$. Then, it follows that

$$\begin{aligned}&\Big(C_h'\big(L(h)\big) + C_h''\big(L(h)\big)l_n(h)\Big)\Big(\tilde{z}_n(h)\sum_{m\in\mathcal{N}}\tilde{z}_m(h)\Big)\\ &\qquad\geq \begin{cases}\Big(C_h'\big(L(h)\big) - \zeta^{(\min)}C_h''\big(L(h)\big)\Big)\big|\tilde{z}_n(h)\sum_{m\in\mathcal{N}}\tilde{z}_m(h)\big|, & \text{if } n\in\mathcal{N}^+\\ -\Big(C_h'\big(L(h)\big) + \zeta^{(\max)}C_h''\big(L(h)\big)\Big)\big|\tilde{z}_n(h)\sum_{m\in\mathcal{N}}\tilde{z}_m(h)\big|, & \text{if } n\in\mathcal{N}^-\end{cases}\end{aligned} \tag{4.60}$$

where we have defined $\zeta^{(\min)} = \max_{n\in\mathcal{N}} l_n^{(\min)}$, $\zeta^{(\max)} = \max_{n\in\mathcal{N}} l_n^{(\max)}$, and the sets

$$\mathcal{N}^+ = \Big\{n\in\mathcal{N} : \tilde{z}_n(h)\sum_{m\in\mathcal{N}}\tilde{z}_m(h) \geq 0\Big\}, \qquad \mathcal{N}^- = \Big\{n\in\mathcal{N} : \tilde{z}_n(h)\sum_{m\in\mathcal{N}}\tilde{z}_m(h) < 0\Big\}. \tag{4.61}$$

Then, assuming for instance that $\sum_{m\in\mathcal{N}} z_m(h) \geq 0$ and recalling the inequality in (4.60), we have that

$$\begin{aligned}&\sum_{n\in\mathcal{N}}\Big(C_h'\big(L(h)\big) + C_h''\big(L(h)\big)l_n(h)\Big)\Big(\tilde{z}_n(h)\sum_{m\in\mathcal{N}}\tilde{z}_m(h)\Big)\\ &\qquad\geq \Big(C_h'\big(L(h)\big) - \zeta^{(\min)}C_h''\big(L(h)\big)\Big)\sum_{n\in\mathcal{N}^+}\tilde{z}_n(h)\Big(\sum_{m\in\mathcal{N}}\tilde{z}_m(h)\Big)\\ &\qquad\quad - \Big(C_h'\big(L(h)\big) + \zeta^{(\max)}C_h''\big(L(h)\big)\Big)\sum_{n\in\mathcal{N}^-}\big|\tilde{z}_n(h)\big|\Big(\sum_{m\in\mathcal{N}}\tilde{z}_m(h)\Big) \qquad (4.62)\\ &\qquad\geq -\big(\zeta^{(\min)} + \zeta^{(\max)}\big)C_h''\big(L(h)\big)\Big(\sum_{n\in\mathcal{N}^+}\tilde{z}_n(h)\sum_{m\in\mathcal{N}}\tilde{z}_m(h)\Big) \qquad (4.63)\end{aligned}$$

where in (4.63) we have used

$$\sum_{n\in\mathcal{N}^+}\big|\tilde{z}_n(h)\big| = \sum_{n\in\mathcal{N}^+}\tilde{z}_n(h) \geq \sum_{n\in\mathcal{N}^-}\big|\tilde{z}_n(h)\big| = -\sum_{n\in\mathcal{N}^-}\tilde{z}_n(h). \tag{4.64}$$

On the other hand, when $\sum_{m\in\mathcal{N}}\tilde{z}_m(h) < 0$, we know that

$$\sum_{n\in\mathcal{N}^+}\big|\tilde{z}_n(h)\big| = -\sum_{n\in\mathcal{N}^+}\tilde{z}_n(h) < \sum_{n\in\mathcal{N}^-}\big|\tilde{z}_n(h)\big| = \sum_{n\in\mathcal{N}^-}\tilde{z}_n(h) \tag{4.65}$$

and, following similar steps, we obtain

$$\sum_{n\in\mathcal{N}}\Big(C_h'\big(L(h)\big)+C_h''\big(L(h)\big)l_n(h)\Big)\Big(\tilde{z}_n(h)\sum_{m\in\mathcal{N}}\tilde{z}_m(h)\Big) \\ \geq -\big(\zeta^{(\min)}+\zeta^{(\max)}\big)C_h''\big(L(h)\big)\Big(\sum_{n\in\mathcal{N}^-}\tilde{z}_n(h)\;\Big|\sum_{m\in\mathcal{N}}\tilde{z}_m(h)\Big|\Big). \quad (4.66)$$

Let us consider the lower bound in (4.63): the term in (4.56) satisfies

$$\sum_{h=1}^{H}\sum_{n\in\mathcal{N}}\Big(C_h'\big(L(h)\big)+C_h''\big(L(h)\big)l_n(h)\Big)\Big(\tilde{z}_n(h)\sum_{m\in\mathcal{N}}\tilde{z}_m(h)\Big) \\ \geq -\big(\zeta^{(\min)}+\zeta^{(\max)}\big)\sum_{h=1}^{H}C_h''\big(L(h)\big)\Big(\sum_{n\in\mathcal{N}^+}\tilde{z}_n(h)\sum_{m\in\mathcal{N}}\tilde{z}_m(h)\Big) \quad (4.67)$$

$$\geq -\big(\zeta^{(\min)}+\zeta^{(\max)}\big)\sum_{h=1}^{H}C_h''\big(L(h)\big)\Big(\sum_{n\in\mathcal{N}^+}\tilde{z}_n(h)\Big)^2 \quad (4.68)$$

and, by substituting back in (4.56), it holds that

$$\mathbf{z}^{\mathrm{T}}\mathbf{J}(\mathbf{x})\mathbf{z}\geq\sum_{h=1}^{H}C_h'\big(L(h)\big)\Big(\sum_{n\in\mathcal{N}}\tilde{z}_n^2(h)\Big)+\sum_{h=1}^{H}\sum_{n\in\mathcal{G}}W_n''\big(g_n(h)\big)\tilde{z}_n(h)^2 \\ -\big(\zeta^{(\min)}+\zeta^{(\max)}\big)\sum_{h=1}^{H}C_h''\big(L(h)\big)\Big(\sum_{n\in\mathcal{N}^+}\tilde{z}_n(h)\Big)^2. \quad (4.69)$$

Then, invoking the Cauchy-Schwartz Inequality [110, eq. (3.2.9)]:

$$\sum_{n\in\mathcal{N}^+}\tilde{z}_n^2(h)\geq\frac{1}{|\mathcal{N}^+|}\Big(\sum_{n\in\mathcal{N}^+}\tilde{z}_n(h)\Big)^2\geq\frac{1}{N}\Big(\sum_{n\in\mathcal{N}^+}\tilde{z}_n(h)\Big)^2 \quad (4.70)$$

it follows that

$$\mathbf{z}^{\mathrm{T}}\mathbf{J}(\mathbf{x})\mathbf{z}\geq\sum_{h=1}^{H}\Big(C_h'\big(L(h)\big)-N\big(\zeta^{(\min)}+\zeta^{(\max)}\big)C_h''\big(L(h)\big)\Big)\Big(\sum_{n\in\mathcal{N}^+}\tilde{z}_n^2(h)\Big) \\ +\sum_{h=1}^{H}\Big(C_h'\big(L(h)\big)\sum_{n\in\mathcal{N}^-}\tilde{z}_n^2(h)\Big)+\sum_{h=1}^{H}\sum_{n\in\mathcal{G}}W_n''\big(g_n(h)\big)\tilde{z}_n^2(h) \quad (4.71)$$

$$\geq\sum_{h=1}^{H}\Big(C_h'\big(L(h)\big)-N\big(\zeta^{(\min)}+\zeta^{(\max)}\big)C_h''\big(L(h)\big)\Big)\Big(\sum_{n\in\mathcal{N}}\tilde{z}_n^2(h)\Big). \quad (4.72)$$

The result in (4.72) can be equivalently obtained by considering the lower bound in (4.66), which simply corresponds to swapping $\mathcal{N}^+$ and $\mathcal{N}^-$ in (4.67)–(4.71). Finally, the inequality in (4.51) is satisfied as long as

$$C_h'(x)\geq N\big(\zeta^{(\min)}+\zeta^{(\max)}\big)C_h''(x),\qquad L^{(\min)}\leq x\leq L^{(\max)}. \quad (4.73)$$

Therefore, $\mathbf{F}(\mathbf{x})$ is monotone on $\Omega_{\mathbf{x}}$ if (4.73) is satisfied, and this completes the proof of Theorem 4.2(a). □

4.A.3.2 Proof of Theorem 4.2(b)

Here, we derive the condition on the regularization parameter τ for the convergence of Algorithm 4.1 to one of the Nash Equilibria of the game $\mathscr{G} = \langle \Omega_{\mathbf{x}}, \mathbf{f} \rangle$. By [74, Cor. 4.1], it is sufficient to choose τ large enough such that the matrix $\boldsymbol{\Upsilon}_{\mathrm{F},\tau} = \boldsymbol{\Upsilon}_{\mathrm{F}} + \tau \mathbf{I}_N$ is a P-matrix , where

$$[\boldsymbol{\Upsilon}_{\mathrm{F}}]_{nm} = \begin{cases} \upsilon_n^{(\min)}, & \text{if } n = m \\ -\upsilon_{nm}^{(\max)}, & \text{if } n \neq m \end{cases} \tag{4.74}$$

with

$$\upsilon_n^{(\min)} = \min_{\mathbf{x} \in \Omega_{\mathbf{x}}} \lambda_{\min}\big(\mathsf{J}_{\mathbf{x}_n} \mathbf{F}_n(\mathbf{x}_n, \mathbf{x}_{-n})\big), \qquad \upsilon_{nm}^{(\max)} = \max_{\mathbf{x} \in \Omega_{\mathbf{x}}} \|\mathsf{J}_{\mathbf{x}_m} \mathbf{F}_n(\mathbf{x}_n, \mathbf{x}_{-n})\| \tag{4.75}$$

where $\mathsf{J}_{\mathbf{x}_m} \mathbf{F}_n(\mathbf{x}_n, \mathbf{x}_{-n})$ is the partial Jacobian matrix defined in (4.52)–(4.54), and $\lambda_{\min}\big(\mathsf{J}_{\mathbf{x}_n} \mathbf{F}_n(\mathbf{x}_n, \mathbf{x}_{-n})\big)$ denotes the smallest eigenvalue of $\mathsf{J}_{\mathbf{x}_n} \mathbf{F}_n(\mathbf{x}_n, \mathbf{x}_{-n})$.

In Appendix 4.A.3.1, we have shown that, under the conditions of Theorem 4.1, $\mathbf{F}_n(\mathbf{x}_n, \mathbf{x}_{-n})$ is monotone on $\mathbf{x}_n$, for any given $\mathbf{x}_{-n} \in \Omega_{\mathbf{x}_{-n}}$, implying that $\mathsf{J}_{\mathbf{x}_n} \mathbf{F}_n(\mathbf{x}_n, \mathbf{x}_{-n}) \succeq 0$ [74, eq. (4.8(i))], $\forall \mathbf{x}_n \in \Omega_{\mathbf{x}_n}$, $\forall n \in \mathcal{N}$. Hence, we have that $\upsilon_n^{(\min)} \geq 0$.

Now, let us examine $\upsilon_{nm}^{(\max)}$ for $n \in \mathcal{N}_{\mathcal{G}\setminus\mathcal{S}} \cup \mathcal{N}_{\mathcal{S}\setminus\mathcal{G}}$, for whom $\boldsymbol{\Delta}_n^{\mathrm{T}} \boldsymbol{\Delta}_m = \mathbf{I}_H$ if $n, m \in \mathcal{N}_{\mathcal{G}\setminus\mathcal{S}}$ or if $n, m \in \mathcal{N}_{\mathcal{S}\setminus\mathcal{G}}$ and $\boldsymbol{\Delta}_n^{\mathrm{T}} \boldsymbol{\Delta}_m = -\mathbf{I}_H$ otherwise. Considering the first and worst case, we have:

$$\begin{aligned}
\upsilon_{nm}^{(\max)} &= \max_{\mathbf{x} \in \Omega_{\mathbf{x}}} \|\mathbf{D}_{\mathbf{c}'}(\mathbf{x}) + \mathrm{Diag}\big(\mathbf{D}_{\mathbf{c}''}(\mathbf{x})(\mathbf{e}_n + \boldsymbol{\Delta}_n \mathbf{x}_n)\big)\| && (4.76)\\
&\leq \max_{\mathbf{x} \in \Omega_{\mathbf{x}}} \lambda_{\max}\Big(\mathbf{D}_{\mathbf{c}'}(\mathbf{x}) + \mathrm{Diag}\big(\mathbf{D}_{\mathbf{c}''}(\mathbf{x})(\mathbf{e}_n + \boldsymbol{\Delta}_n \mathbf{x}_n)\big)\Big) && (4.77)\\
&\leq \max_h \Big(\max_{\mathbf{x} \in \Omega_{\mathbf{x}}} C_h'\big(L^{(\mathcal{P})}(h) + \sum_{m \in \mathcal{N}} \big(e_m(h) + \boldsymbol{\delta}_m^{\mathrm{T}} \mathbf{x}_m(h)\big)\big)\Big) \\
&\quad + \max_h \Big(\max_{\mathbf{x} \in \Omega_{\mathbf{x}}} C_h''\big(L^{(\mathcal{P})}(h) + \sum_{m \in \mathcal{N}} \big(e_m(h) + \boldsymbol{\delta}_m^{\mathrm{T}} \mathbf{x}_m(h)\big)\big)\big(e_n(h) + \boldsymbol{\delta}_n^{\mathrm{T}} \mathbf{x}_n(h)\big)\Big) && (4.78)\\
&\leq \max_h C_h'(L^{(\max)}) + l_n^{(\max)} \max_h \Big(\max_{\mathbf{x} \in \Omega_{\mathbf{x}}} C_h''\big(L^{(\mathcal{P})}(h) + \sum_{m \in \mathcal{N}} \big(e_m(h) + \boldsymbol{\delta}_m^{\mathrm{T}} \mathbf{x}_m(h)\big)\big)\Big). && (4.79)
\end{aligned}$$

On the other hand, for $n \in \mathcal{N}_{\mathcal{G}\cap\mathcal{S}}$, we have that, for any $H \times H$ matrix $\mathbf{Q}$, it holds $\boldsymbol{\Delta}_n^{\mathrm{T}} \mathbf{Q} \boldsymbol{\Delta}_n =$

$(2\mathbf{I}_2 - \mathbf{J}_2) \otimes \mathbf{Q}$, where $\mathbf{J}_2$ denotes the 2-dimensional unit matrix, and hence

$$\lambda_{\min}(\boldsymbol{\Delta}_n^{\mathrm{T}}\mathbf{Q}\boldsymbol{\Delta}_n) \triangleq \begin{cases} 2\lambda_{\min}(\mathbf{Q}), & \text{if } \lambda_{\min}(\mathbf{Q}) < 0 \\ 0, & \text{otherwise} \end{cases} \tag{4.80}$$

$$\lambda_{\max}(\boldsymbol{\Delta}_n^{\mathrm{T}}\mathbf{Q}\boldsymbol{\Delta}_n) \triangleq \begin{cases} 2\lambda_{\max}(\mathbf{Q}), & \text{if } \lambda_{\max}(\mathbf{Q}) > 0 \\ 0, & \text{otherwise} \end{cases}. \tag{4.81}$$

Summing up the previous results, we can state that

$$\upsilon_n^{(\min)} \geq 0 \tag{4.82}$$

$$\begin{aligned} \upsilon_{nm}^{(\max)} &\leq 2 \max_h C_h'(L^{(\max)}) \\ &\quad + 2l_n^{(\max)} \max_h \Big(\max_{\mathbf{x}\in\Omega_{\mathbf{x}}} C_h''\big(L^{(\mathcal{P})}(h) + \sum_{m\in\mathcal{N}} \big(e_m(h) + \boldsymbol{\delta}_m^{\mathrm{T}}\mathbf{x}_m(h)\big)\big)\Big) \end{aligned} \tag{4.83}$$

where we have considered the worst case of $\mathcal{N} = \mathcal{N}_{\mathcal{G}\cap\mathcal{S}}$.

Then, $\boldsymbol{\Upsilon}_{\mathrm{F},\tau}$ is a P-matrix if the following condition is fulfilled [74, Prop. 4.3]:

$$\sum_{m\in\mathcal{N}\setminus\{n\}} \left(\frac{\upsilon_{nm}^{(\max)}}{\upsilon_n^{(\min)} + \tau}\right) \tag{4.84}$$

$$\leq \frac{2}{\tau} \sum_{m\in\mathcal{N}\setminus\{n\}} \Big(\max_h C_h'(L^{(\max)}) + l_n^{(\max)} \max_h \Big(\max_{\mathbf{x}\in\Omega_{\mathbf{x}}} C_h''\big(L^{(\mathcal{P})}(h) + \sum_{m\in\mathcal{N}} \big(e_m(h) + \boldsymbol{\delta}_m^{\mathrm{T}}\mathbf{x}_m(h)\big)\big)\Big)\Big) \tag{4.85}$$

$$\leq \frac{2(N-1)}{\tau} \max_h C_h'(L^{(\max)}) + \frac{2L^{(\max)}}{\tau} \max_h \Big(\max_{\mathbf{x}\in\Omega_{\mathbf{x}}} C_h''\big(L^{(\mathcal{P})}(h) + \sum_{m\in\mathcal{N}} \big(e_m(h) + \boldsymbol{\delta}_m^{\mathrm{T}}\mathbf{x}_m(h)\big)\big)\Big) < 1. \tag{4.86}$$

Evidently, the previous inequality is verified for any regularization parameter τ satisfying

$$\tau > 2(N-1) \max_h C_h'(L^{(\max)}) + 2L^{(\max)} \max_h \Big(\max_{\mathbf{x}\in\Omega_{\mathbf{x}}} C_h''\big(L^{(\mathcal{P})}(h) + \sum_{m\in\mathcal{N}} \big(e_m(h) + \boldsymbol{\delta}_m^{\mathrm{T}}\mathbf{x}_m(h)\big)\big)\Big). \tag{4.87}$$

Finally, note that

$$\max_h \Big(\max_{\mathbf{x}\in\Omega_{\mathbf{x}}} C_h''\big(L^{(\mathcal{P})}(h) + \sum_{m\in\mathcal{N}} \big(e_m(h) + \boldsymbol{\delta}_m^{\mathrm{T}}\mathbf{x}_m(h)\big)\big)\Big) \leq \max_h \Big(\max_{L^{(\min)}\leq x\leq L^{(\max)}} C_h''(x)\Big). \tag{4.88}$$

In consequence, we can substitute the term on the left-hand side with the term on the right-hand side of (4.88), maintaining the validity of the inequality in (4.87). This completes the proof of Theorem 4.2(b). □

4.B Cooperative DSM Approach

4.B.1 Proof of Theorem 4.3

By [83, Th. 2], Algorithm 4.2 converges to a stationary solution of the social problem in (4.30) if the following conditions are satisfied: (a) the objective function $f_n^{(\mathcal{D})}(\mathbf{x}_n, \mathbf{x}_{-n})$ in (4.31) is convex on $\Omega_{\mathbf{x}_n}$ for any $\mathbf{x}_{-n} \in \Omega_{\mathbf{x}_{-n}}$, $\forall n \in \mathcal{N}$; and (b) the regularization parameter τ satisfies $\tau \geq L_f/2 - \min_{n\in\mathcal{N}} \big(\upsilon_n^{(\min)}\big)$, where L_f denotes the Lipschitz constant of $\nabla_{\mathbf{x}} f^{(\mathcal{D})}(\mathbf{x})$ on $\Omega_{\mathbf{x}}$ and $\upsilon_n^{(\min)}$ is defined in (4.75). Recall that the individual strategy sets $\Omega_{\mathbf{x}_n}$ in (4.12) are closed and convex and that the set $\Omega_{\mathbf{x}}$ is bounded.

Condition (a) is satisfied under the setting of Theorem 4.1. Therefore, we just need to prove that (4.35) implies condition (b) above. Recalling that $f^{(\mathcal{D})}(\mathbf{x}) = \sum_{n\in\mathcal{N}} f_n^{(\mathcal{D})}(\mathbf{x}_n, \mathbf{x}_{-n})$, with $f_n^{(\mathcal{D})}(\mathbf{x}_n, \mathbf{x}_{-n})$ defined as in (4.31), and the definitions of the partial Jacobian matrices of $\mathbf{F}(\mathbf{x}) = \big(\nabla_{\mathbf{x}_n} f_n(\mathbf{x}_n, \mathbf{x}_{-n})\big)_{n=1}^{N}$ given in (4.52)–(4.54), the previous statement comes readily from the following:

$$
\begin{aligned}
L_f \triangleq \big\|\mathbf{H}(\mathbf{x})\big\|_\infty &= \max_i \sum_j \big|\mathbf{H}_{ij}(\mathbf{x})\big| && (4.89)\\
&\leq \max_h \max_{\mathbf{x}\in\Omega_{\mathbf{x}}} \bigg(\boldsymbol{\delta}_n^{\mathrm{T}} \boldsymbol{\delta}_n \Big(2C_h'\big(L(h)\big) + C_h''\big(L(h)\big)\Big(l_n(h) + \frac{L^{(\mathcal{P})}(h)}{N}\Big)\Big) && (4.90)\\
&\quad + \sum_{m\in\mathcal{N}\setminus\{n\}} \boldsymbol{\delta}_m^{\mathrm{T}} \boldsymbol{\delta}_m \Big(C_h'\big(L(h)\big) + C_h''\big(L(h)\big)\Big(l_m(h) + \frac{L^{(\mathcal{P})}(h)}{N}\Big)\Big)\bigg) && (4.91)\\
&\leq 2 \max_h \max_{\mathbf{x}\in\Omega_{\mathbf{x}}} \Big((N+1) C_h'\big(L(h)\big) + C_h''\big(L(h)\big) L(h)\Big) && (4.92)\\
&\leq 2 \max_h \Big((N+1) C_h'(L^{(\max)}) + \max_{L^{(\min)}\leq x\leq L^{(\max)}} \big(C_h''(x)x\big)\Big) && (4.93)
\end{aligned}
$$

with $\mathbf{H}(\mathbf{x})$ denoting the Hessian of $f^{(\mathcal{D})}(\mathbf{x})$ and $\boldsymbol{\delta}_n$ defined as in (4.13). This concludes the proof of Theorem 4.3.

5

Noncooperative Day-Ahead Bidding Strategies for Demand-Side Expected Cost Minimization with Real-Time Adjustments - A GNEP Approach

Abstract—The envisioned smart grid aims at improving the interaction between the supply- and the demand-side of the electricity network, creating unprecedented possibilities for optimizing the energy usage at different levels of the grid. In this paper, we propose a distributed demand-side management (DSM) method intended for smart grid users with load prediction capabilities, who possibly employ dispatchable energy generation and storage devices. These users participate in the day-ahead market and are interested in deriving the bidding, production, and storage strategies that jointly minimize their expected monetary expense. The resulting day-ahead grid optimization is formulated as a generalized Nash equilibrium problem (GNEP), which includes global constraints that couple the users' strategies. Building on the theory of variational inequalities, we study the main properties of the GNEP and devise a distributed, iterative algorithm converging to the variational solutions of the GNEP. Additionally, users can exploit the reduced uncertainty about their energy consumption and renewable generation at the time of dispatch. We thus present a complementary DSM procedure that allows them to perform some unilateral adjustments on their generation and storage strategies so as to reduce the impact of their real-time deviations with respect to the amount of energy negotiated in the day-ahead. Finally, numerical results in realistic scenarios are reported to corroborate the proposed DSM technique.

Index Terms—Day-Ahead/Real-Time Demand-Side Management, Game Theory, Generalized Nash Equilibrium Problem, Proximal Decomposition Algorithm, Smart Grid, Variational Inequality.

This chapter is an exact reproduction of [88] with the exception of pagination.

5.1 Introduction

The electricity distribution infrastructure is facing a profound transformation with the development of the smart grid concept, which improves the interaction between the supply- and the demand-side of the network by means of demand-side management (DSM) techniques. Indeed, taking advantage of information and communication technologies, DSM methods introduce advanced mechanisms for encouraging the demand-side to participate actively in the network optimization process [12]. Furthermore, DSM, properly integrated with distributed energy generation (DG) and distributed storage (DS), is considered an increasingly essential element for implementing the smart grid paradigm and balancing massive energy production from renewable sources. These concepts allow for an immense opportunity for optimizing the energy grid and energy usage at different levels of the network.

The short-term electricity market[1] consists mainly of a day-ahead market, which produces financially binding schedules for energy supply and demand before the operating day, and a real-time market, used to balance day-ahead and real-time energy requirements [34, Ch. 1.2]. In line with the time granularity of the energy trading process, day-ahead and real-time DSM methods are successfully employed in a complementary fashion in practical situations [105]. In particular, a day-ahead demand-side optimization allows energy users to efficiently manage their electricity consumption and provides the supply-side with an estimation of the amount of energy to be delivered over the upcoming day, so that the production can be planned accordingly [104]. Nonetheless, when the consumption schedule is not correctly predicted by the users, the supply-side incurs additional costs that are transferred to the demand-side in the form of penalty charges [111, 112]. On the other hand, real-time DSM techniques bring the grid optimization process to a finer time scale, allowing to take into consideration possible contingencies in the supply-side and reducing the uncertainties induced by the renewable energy sources and by the randomness of the users' consumption (see, e.g., [57, 94]).

A common DSM procedure is energy consumption scheduling (ECS) [51, 72, 73], which modifies the demand profile by shifting flexible energy consumption to off-peak hours. The implementation of ECS techniques has been shown to be successful in diminishing the peak-to-average ratio (PAR) of the energy demand curve, from which both demand- and supply-side benefit in terms of reduced energy cost, CO_2 emissions, and overall power plants requirements [5]. However, since the users' inconvenience must be taken into account (e.g., the rescheduling of activities results in lost services for industrial customers [55]), ECS presents flexibility limitations that can be overcome by incorporating dispatchable DG and DS into the demand-side of the network. The combined day-ahead optimization of dispatchable DG and DS has been studied in [84,85] assum-

[1] Medium- and long-term electricity trading between producers and retailers/consumers, which take place through futures markets and bilateral contracts [34, Ch. 1.2], are not the focus of the present paper.

ing deterministic consumption profiles. However, this approach cannot accommodate potential real-time deviations from the users' expected energy consumption, neither the randomness of their renewable sources.

Additionally, to achieve a realistic smart grid model, some global requirements, e.g., lower and upper bounds on the aggregate load at specific time intervals [113], must be imposed to comply with the physical constraints of both the supply and the power grid. Besides, the energy price curve, derived by combining the production offers of the individual energy generators in the supply-side of the network, is only valid within a certain range. These limits can be also established so as to force the desired shaping of the aggregate load, e.g., in order to reduce the PAR. By all means, such global constraints result in a coupling between the strategies of the users that has not been addressed in the literature yet.

The main contribution of this paper is to fill the gap in considering the above global grid requirements and to propose a novel DSM method that consists in a day-ahead optimization in the presence of coupling constraints among smart grid users, followed by a real-time optimization. More specifically, the DSM is carried out through (see Fig. 5.2): i) a day-ahead bidding process where demand-side users with DG, DS, and additional load prediction capabilities minimize their expected monetary expense in a competitive market environment; ii) successive real-time adjustments of the generation and storage strategies that exploit the reduced uncertainty about the users' energy consumption at the time of dispatch.

During the day-ahead bidding process, the subscribers' consumption and renewable generation are still uncertain: these quantities are thus modeled as random variables. Based on the corresponding probability distributions, the users individually calculate their bidding, dispatchable production, and storage strategies in a distributed fashion with the objective of minimizing their expected monetary expense. Given the selfish nature of the users and the global requirements on their aggregate load, we formulate the bidding process as a generalized Nash equilibrium problem (GNEP) [74].[2] Building on the variational inequality (VI) framework [74,77,78], we analyze the existence of variational solutions of the GNEP. However, the coupling constraints prevent the application of well-known game theoretical decomposition methods, making the design of distributed algorithms a difficult task. In order to deal with the coupling in a distributed way, we propose a pricing-based, iterative scheme that converges to the variational solutions under some technical conditions. Indeed, this paper is the first attempt towards the solution of such a problem in the smart grid literature. Interestingly, we also show that the proposed framework can be easily adapted to incorporate ECS to the optimization of the bidding strategies.

Once the day-ahead bidding process has taken place, and as the dispatch time approaches, users gain a better knowledge about their energy needs and renewable generation. Based on

[2] A cooperative method applied to the same framework and that neglects the coupling constraints has been addressed in [87].

this coming information, we also devise a real-time method for repeatedly recalculating the production and storage strategies throughout the day period to alleviate the impact of real-time deviations with respect to their day-ahead bid loads.

The problem of deriving the optimal bidding strategies of energy generators and retailers in the sequence of different trading markets has been addressed in a number of works in the power systems literature (a good summary is given in [114]). In such context, the involved agents determine the most profitable combination of buying/selling offers, while dealing with the uncertainty associated with the forecast energy prices [113]. The present paper tackles a substantially different problem: under the smart grid paradigm, energy prices directly depend on the demand-side users' strategies and, therefore, our stochastic formulation rather refers to the uncertainty induced by the end users' energy consumption and renewable generation.

The rest of the paper is structured as follows. Sections 5.2 and 5.3 introduce the overall smart grid framework and the proposed DSM method. Section 5.4 describes the day-ahead DSM approach with coupled strategies of the users. Section 5.5 presents a real-time procedure to adjust the users' production and storage strategies. Section 5.6 illustrates the proposed methods and algorithms through experimental evaluations and comparisons with ECS approaches. Finally, we provide some conclusions in Section 5.7.

Notation. The following notation is used throughout the paper. Lowercase and uppercase boldface denote vectors and matrices, respectively. The operator $\succ$ ($\succeq$) for vectors is defined componentwise, while for matrices it refers to the positive (semi) definiteness property. The matrix $\mathbf{I}_a$ is the a-dimensional identity matrix, while $\mathbf{0}$ is the zero vector. By (a, b) we denote the vertical concatenation of the scalar or vector arguments a and b, $\left(x_a\right)_{a=1}^{A}$ represents the vertical concatenation of scalar or vector arguments x_a ordered according to the index a, and $\{x_a\}_{a\in\mathcal{A}}$ indicates the set of elements x_a with indices $a \in \mathcal{A}$. The operator $\mathrm{Diag}(\cdot)$ results in a diagonal matrix with elements given by the the vector argument or in a block-diagonal of the matrix arguments, whereas $\otimes$ denotes the Kronecker product. Lastly, the operator $(\cdot)^+ \triangleq \max(\cdot, 0)$ extracts the positive part of the scalar argument.

5.2 Smart Grid Model

The modern power grid is a complex network that can be conveniently divided into [3, 57]: i) supply-side (energy producers and providers); ii) central unit (regulation authority that coordinates the proposed demand-side bidding process); iii) demand-side (end users). In this paper, we focus our attention on the demand-side of the smart grid, which is introduced in Section 5.2.1 and further refined in Sections 5.2.2 and 5.3.1, whereas the supply-side and the central unit are modeled as simply as possible.

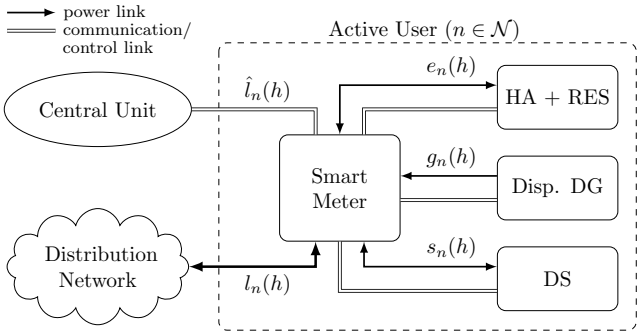

Figure 5.1: Connection scheme between the smart grid and one active user consisting of: home appliances (HA), renewable energy source (RES), dispatchable distributed generation (DG) and distributed storage (DS).

5.2.1 Demand-Side Model

Demand-side users, whose associated set is denoted by $\mathcal{D}$, are characterized in the first place by the individual *per-slot net energy consumption* $e_n(h)$ indicating the energy needed by user $n \in \mathcal{D}$ to supply his appliances at time-slot h in the time period of analysis, which corresponds to a day. This term also accounts for eventual non-dispatchable (renewable) energy resources that the user may have.[3] In order to tackle with the uncertainties related to the future load demands and to the renewable sources, $e_n(h)$ is modeled as a random variable with pdf $f_{e_n(h)}(\cdot)$ and cdf $F_{e_n(h)}(\cdot)$.

Our model distinguishes between *passive* and *active* users. Passive users are basically energy consumers and resemble traditional demand-side users, whereas active users indicate those consumers participating in the demand-side bidding process, i.e., reacting to changes in the cost per unit of energy by modifying their day-ahead bidding strategies. For convenience, we group the P passive users into the set $\mathcal{P} \subset \mathcal{D}$ and the N active users into the set $\mathcal{N} \triangleq \mathcal{D} \backslash \mathcal{P}$. We suppose that each active user can derive his individual load and renewable production statistics from his energy consumption history and data measurements, i.e., we suppose that $f_{e_n(h)}(\cdot)$ and $F_{e_n(h)}(\cdot)$ are known. Furthermore, in order to participate in the optimization process, active users are connected not only to the power distribution grid, but also to a communication infrastructure that enables bidirectional communication between their smart meter and the central unit [12] (see Fig. 5.1). Lastly, we conveniently divide the day period into H time-slots.

5.2.2 Energy Generation and Storage Model

Let us use $\mathcal{G} \subseteq \mathcal{N}$ to denote the subset of users possessing dispatchable DG (e.g., internal combustion engines, gas turbines, or fuel cells). For users $n \in \mathcal{G}$, $g_n(h) \geq 0$ represents the *per-*

[3] Non-dispatchable sources, having only fixed costs, imply no strategy regarding energy production, unlike dispatchable generators (see Section 5.2.2).

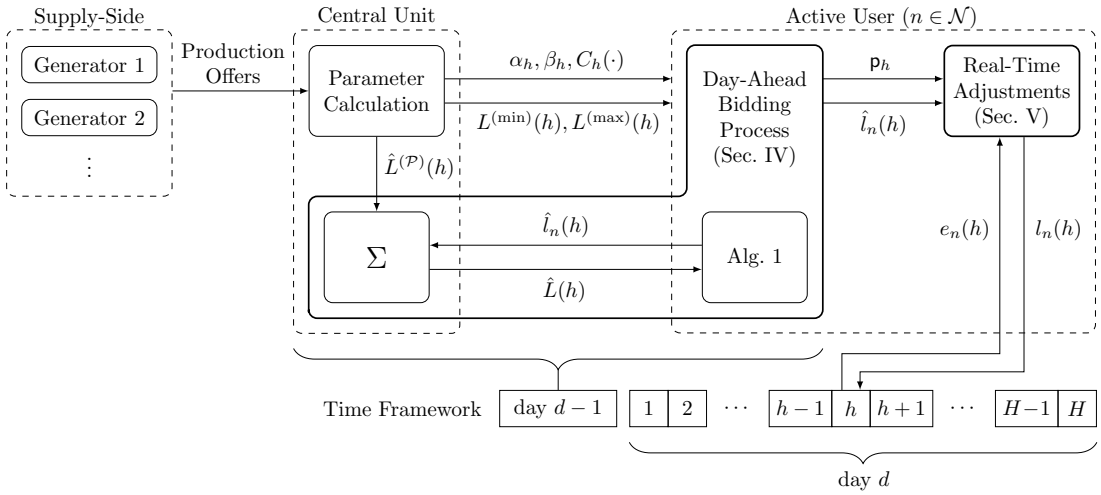

Figure 5.2: Schematic representation of the proposed DSM method, consisting of day-ahead bidding process and real-time adjustments.

slot energy production profile at time-slot h. Introducing the *energy production scheduling vector* $\mathbf{g}_n \triangleq \big(g_n(h)\big)_{h=1}^{H}$, we have that $\mathbf{g}_n \in \Omega_{\mathbf{g}_n}$, where $\Omega_{\mathbf{g}_n}$ is the strategy set for dispatchable energy producer $n \in \mathcal{G}$ (see Section 5.6). Moreover, the *production cost function* $W_n\big(g_n(h)\big)$ gives the variable production costs (e.g., the fuel costs) incurred by user $n \in \mathcal{G}$ for generating the amount of energy $g_n(h)$ at time-slot h, with $W_n(0) = 0$.

Likewise, we use $\mathcal{S} \subseteq \mathcal{N}$ to denote the subset of users owning DS devices. Users $n \in \mathcal{S}$ are characterized by the *per-slot energy storage profile* $s_n(h)$ at time-slot h: we have $s_n(h) > 0$ when the storage device is to be charged, $s_n(h) < 0$ when the storage device is to be discharged, and $s_n(h) = 0$ when the device is inactive. Introducing the *energy storage scheduling vector* $\mathbf{s}_n \triangleq \big(s_n(h)\big)_{h=1}^{H}$, it holds that $\mathbf{s}_n \in \Omega_{\mathbf{s}_n}$, being $\Omega_{\mathbf{s}_n}$ the strategy set for energy storer $n \in \mathcal{S}$ (see Section 5.6).[4]

Let us now introduce the individual *per-slot energy load*

$$l_n(h) \triangleq e_n(h) - g_n(h) + s_n(h) \tag{5.1}$$

which gives the real-time energy flow between user $n \in \mathcal{N}$ and the grid at time-slot h, with $l_n(h) > 0$ when user n purchases energy from the grid and $l_n(h) < 0$ when user n sells energy to the grid, as shown schematically in Fig. 5.1.

[4] Energy storage bears implicit costs related to the intrinsic inefficiency of the storage device, e.g., eventual leakage (see Section 5.6) or non-ideal charging/discharging efficiencies (cf. [84]), rather than direct variable costs as dispatchable generation.

5.3 DSM Model

We are now ready to introduce the proposed demand-side optimization model along with the DSM approach by which active users determine their bidding, production, and storage strategies at two different time granularities (see Fig. 5.2). The procedure described in the following is consistent with the actual functioning of electricity markets (see, e.g., [34, Ch. 1] for more details) allowing multi-round auctions [115].

5.3.1 Energy Load Bidding Model

Let us denote by $\tilde{e}_n(h)$ the *per-slot bid net energy consumption*, i.e., the day-ahead amount of energy (to be optimized) that user $n \in \mathcal{N}$ commits to consume at time-slot h. The corresponding *bidding strategy vector* is $\tilde{\mathbf{e}}_n \triangleq \big(\tilde{e}_n(h)\big)_{h=1}^{H}$, and the bidding strategy set $\Omega_{\tilde{\mathbf{e}}_n}$ can be expressed as

$$\Omega_{\tilde{\mathbf{e}}_n} \triangleq \big\{\tilde{\mathbf{e}}_n \in \mathbb{R}^H : \chi_n^{(\min)}(h) \leq \tilde{e}_n(h) \leq \chi_n^{(\max)}(h), \forall h\big\} \tag{5.2}$$

with $\chi_n^{(\min)}(h)$ and $\chi_n^{(\max)}(h)$ denoting the minimum and maximum per-slot bidding consumption, respectively.

Let us define the *per-slot bid energy load* of user $n \in \mathcal{N}$ as

$$\tilde{l}_n(h) \triangleq \tilde{e}_n(h) - g_n(h) + s_n(h) \tag{5.3}$$

and the strategy vector as $\mathbf{x}_n \triangleq \big(\mathbf{x}_n(h)\big)_{h=1}^{H}$, with

$$\mathbf{x}_n(h) \triangleq \big(\tilde{e}_n(h), g_n(h), s_n(h)\big). \tag{5.4}$$

Taking into account the bidding strategy set $\Omega_{\tilde{\mathbf{e}}_n}$ in (5.2), and the sets $\Omega_{\mathbf{g}_n}$ and $\Omega_{\mathbf{s}_n}$ introduced in Section 5.2.2, the overall strategy set for a generic user $n \in \mathcal{N}$ is given by

$$\Omega_{\mathbf{x}_n} \triangleq \big\{\mathbf{x}_n \in \mathbb{R}^{3H} : \tilde{\mathbf{e}}_n \in \Omega_{\tilde{\mathbf{e}}_n}, \mathbf{g}_n \in \Omega_{\mathbf{g}_n}, \mathbf{s}_n \in \Omega_{\mathbf{s}_n}\big\} \tag{5.5}$$

with $\mathbf{g}_n = \mathbf{0}$ if $n \notin \mathcal{G}$ and $\mathbf{s}_n = \mathbf{0}$ if $n \notin \mathcal{S}$.

5.3.2 Energy Cost and Pricing Model

This section introduces the cost model regulating the energy prices. Typically, during the day-ahead market, the different energy generators in the supply-side (each of them characterized by a specific price curve) submit their production offers; likewise, consumers and retailers submit their consumption bids. This process determines the energy prices and the traded quantities [34, Ch. 1.2]. Since in the present paper we are particularly interested in the demand-side of the network, we can abstract this procedure by considering a single price curve resulting from

aggregating the individual curves of each generator in the supply-side; this is a well-established procedure in the smart grid literature (c.f. [51, 94, 114]).

With this objective in mind, let $C_h(\cdot)$ be the function indicating the *cost per unit of energy* at time-slot h. Within the day-ahead bidding process, demand-side users induce the *per-slot aggregate bid energy load* $\tilde{L}(h)$ and thus determine the price per unit of energy $C_h\big(\tilde{L}(h)\big)$, which remains fixed during the day period. In this paper, we adopt a linear cost function per unit of energy:

$$C_h\big(\tilde{L}(h)\big) = K_h \tilde{L}(h). \tag{5.6}$$

The overall variable costs to supply the amount $\tilde{L}(h)$ are then given by $C_h\big(\tilde{L}(h)\big)\tilde{L}(h) = K_h \tilde{L}^2(h)$, which corresponds to the quadratic grid cost function widely used in the smart grid literature (e.g., in [51,94]). In general, the grid coefficients $K_h > 0$ are different at each time-slot h, since the energy production varies along the day period according to the aggregate energy demand and to the availability of intermittent energy sources.

Let $\hat{L}^{(\mathcal{P})}(h)$ denote the predicted per-slot aggregate energy consumption associated with the passive users: then, the per-slot aggregate bid energy load $\tilde{L}(h)$ can be expressed as

$$\tilde{L}(h) \triangleq \hat{L}^{(\mathcal{P})}(h) + \sum_{n \in \mathcal{N}} \tilde{l}_n(h) \tag{5.7}$$

which depends on the users' strategies through $\tilde{l}_n(h)$ in (5.3), and is subject to the following global constraint.

Constraint 1 (**on the per-slot aggregate bid energy load**)**.** The per-slot aggregate bid energy load in (5.7) must satisfy

$$L^{(\min)}(h) \leq \tilde{L}(h) \leq L^{(\max)}(h), \qquad \forall h \tag{5.8}$$

where $L^{(\min)}(h) > 0$ (resp. $L^{(\max)}(h) > 0$) denotes the minimum (resp. the maximum) per-slot aggregate energy load within which $C_h\big(\tilde{L}(h)\big)$ resembles the energy price curve obtained by aggregating the production costs of the individual energy generators in the supply-side. In particular, a real-time aggregate demand lower than $L^{(\min)}(h)$ may imply additional costs for the supply-side if this requires turning off some base load power plant [113]. On the other hand, $L^{(\max)}(h)$ can be interpreted as the upper bound on the per-slot aggregate bid energy load that allows to satisfy the real-time aggregate demand with a certain outage probability. Alternatively, these boundaries can be chosen to guarantee a certain PAR of the real-time aggregate load with high probability. We suppose that the central unit can set $L^{(\min)}(h)$, $L^{(\max)}(h)$ and predict $\hat{L}^{(\mathcal{P})}(h)$ based on the available past statistics; an overview on load forecasting techniques can be found in [33].

Each active user $n \in \mathcal{N}$ derives his *bid energy load vector* $\tilde{\mathbf{l}}_n \triangleq \big(\tilde{l}_n(h)\big)_{h=1}^{H}$ during the day-ahead demand-side bidding process. At a given time-slot h, if the user attains to his day-ahead bid $\tilde{l}_n(h)$, he simply pays $K_h\tilde{L}(h)\tilde{l}_n(h)$; otherwise, he can possibly deviate from $\tilde{l}_n(h)$ by purchasing/selling a different amount of energy $l_n(h)$, for which he pays/perceives $K_h\tilde{L}(h)l_n(h)$, while incurring in the following penalties:

$$\alpha_h K_h\tilde{L}(h)\big(l_n(h)-\tilde{l}_n(h)\big), \qquad \text{if } l_n(h) > \tilde{l}_n(h) \tag{5.9}$$

$$\beta_h K_h\tilde{L}(h)\big(\tilde{l}_n(h)-l_n(h)\big), \qquad \text{if } l_n(h) < \tilde{l}_n(h) \tag{5.10}$$

where $\alpha_h, \beta_h \in (0,1]$ are the penalty parameters for exceeding and for falling behind the negotiated load $\tilde{l}_n(h)$, respectively.

Given the bid energy loads $\big\{\tilde{l}_n(h)\big\}_{h=1}^{H}$, the *cumulative monetary expense* incurred by user $n \in \mathcal{N}$ for exchanging the energy loads $\big\{l_n(h)\big\}_{h=1}^{H}$ with the grid (including the aforementioned penalties for deviations and taking into account the amount of produced energy $\big\{g_n(h)\big\}_{h=1}^{H}$) can be expressed as[5]

$$\mathsf{p}_n^{(\mathcal{N})}(\tilde{\mathbf{l}}_n, \tilde{\mathbf{l}}_{-n}) \triangleq \sum_{h=1}^{H} K_h\big(\tilde{l}_{-n}(h)+\tilde{l}_n(h)\big)\Big(l_n(h)+\vartheta_h\big(l_n(h)-\tilde{l}_n(h)\big)\Big) + \sum_{h=1}^{H} W_n\big(g_n(h)\big) \tag{5.11}$$

where $\tilde{\mathbf{l}}_{-n} \triangleq \big(\tilde{l}_{-n}(h)\big)_{h=1}^{H}$ is the aggregate bid energy load vector of the other users, with

$$\tilde{l}_{-n}(h) \triangleq \tilde{L}(h) - \tilde{l}_n(h) = \hat{L}^{(\mathcal{P})}(h) + \sum_{m\in\mathcal{N}\setminus\{n\}} \tilde{l}_m(h) \tag{5.12}$$

and where we have introduced the penalty function

$$\vartheta_h(x) \triangleq \alpha_h(x)^+ + \beta_h(-x)^+. \tag{5.13}$$

The penalty parameters $\big\{\alpha_h, \beta_h\big\}_{h=1}^{H}$ are established before the day-ahead bidding process with the objective of discouraging real-time deviations from the bid loads, either upwards or downwards. For instance, the central unit would choose $\alpha_h > \beta_h$ during hours of high expected consumption, and $\alpha_h < \beta_h$ during hours of low expected consumption.

The proposed pricing model does not explicitly deal with the billing of passive users, as our DSM method is not thereby affected. However, in order to encourage demand-side participation in the bidding process, passive users may be penalized with respect to the active ones by applying an overprice to the purchased energy; see Appendix 5.A.1 for more details.

[5] In light of the described penalty system, $L^{(\min)}(h)$ in (5.8) also prevents the active users from intentionally decreasing the aggregate bid energy load $\tilde{L}(h)$ to the level below which the penalties given by α_h are insufficient to compensate for the additional generation costs of the upward real-time deviations.

5.3.3 Proposed DSM Approach

In our DSM procedure, the active users individually optimize their bidding, production, and storage strategies at two different time granularities, i.e., day-ahead and real-time, as illustrated in Fig. 5.2. Before going into the detailed description, let us summarize the temporal sequence of the proposed DSM method.

Day-ahead optimization (c.f. Section 5.4). In the day-ahead bidding process, the users' goal is to minimize their individual expected cumulative expense over the day period

$$\mathsf{f}_n(\mathbf{x}_n, \tilde{\mathbf{l}}_{-n}) \triangleq \mathsf{E}\big\{\mathsf{p}_n^{(\mathcal{N})}(\boldsymbol{\Delta}\mathbf{x}_n, \tilde{\mathbf{l}}_{-n})\big\} \tag{5.14}$$

where $\boldsymbol{\Delta} \triangleq (\mathbf{I}_H \otimes \boldsymbol{\delta})^{\mathrm{T}}$ and $\boldsymbol{\delta} \triangleq (1, -1, 1)$, so that $\boldsymbol{\delta}^{\mathrm{T}}\mathbf{x}_n(h) = \tilde{l}_n(h)$ and $\boldsymbol{\Delta}\mathbf{x}_n = \tilde{\mathbf{l}}_n$. The expected cumulative expense in (5.14) is obtained in closed-form as given in Lemma 5.1, where we have introduced the following notation:

$$\begin{aligned}
\phi_{e_n(h)}\big(\mathbf{x}_n(h)\big) &\triangleq \mathsf{E}\big\{l_n(h) + \vartheta_h\big(l_n(h) - \boldsymbol{\delta}^{\mathrm{T}}\mathbf{x}_n(h)\big)\big\} && (5.15)\\
&= (1+\alpha_h)\bar{e}_n(h) - g_n(h) + s_n(h) - \alpha_h\tilde{e}_n(h)\\
&\quad + (\alpha_h + \beta_h)\big(\tilde{e}_n(h)F_{e_n(h)}\big(\tilde{e}_n(h)\big) - G_{e_n(h)}\big(\tilde{e}_n(h)\big)\big) && (5.16)\\
G_{e_n(h)}(x) &\triangleq \int_{-\infty}^{x} t f_{e_n(h)}(t)dt && (5.17)
\end{aligned}$$

$\bar{e}_n(h) \triangleq \mathsf{E}\{e_n(h)\}$, and $\boldsymbol{\delta}_g \triangleq (0, 1, 0)$.

Lemma 5.1 (**Expected Cumulative Expense**)**.** Given the per-slot bid energy loads $\tilde{\mathbf{l}}_n$, the expected cumulative expense $\mathsf{f}_n(\mathbf{x}_n, \tilde{\mathbf{l}}_{-n})$ in (5.14) is given by

$$\mathsf{f}_n(\mathbf{x}_n, \tilde{\mathbf{l}}_{-n}) = \sum_{h=1}^{H} K_h\big(\tilde{l}_{-n}(h) + \boldsymbol{\delta}^{\mathrm{T}}\mathbf{x}_n(h)\big)\phi_{e_n(h)}\big(\mathbf{x}_n(h)\big) + \sum_{h=1}^{H} W_n\big(\boldsymbol{\delta}_g^{\mathrm{T}}\mathbf{x}_n(h)\big).$$

Proof. See Appendix 5.A.2.

The grid coefficients $\big\{K_h\big\}_{h=1}^{H}$ and the penalty parameters $\big\{\alpha_h, \beta_h\big\}_{h=1}^{H}$ are fixed before the day-ahead bidding process [3, 57] and broadcast to the demand-side users. Then, each active user reacts to the prices $\big\{K_h\tilde{L}(h)\big\}_{h=1}^{H}$ provided by the central unit through iteratively adjusting his per-slot bid energy load vector $\tilde{\mathbf{l}}_n$. Here, his goal is to minimize his expected cumulative expense, subject to both local and global requirements given by $\Omega_{\mathbf{x}_n}$ and Constraint 1, respectively. This optimization problem, however, is not convex and calls for a centralized optimization, which would lead to non-scalable solution algorithms and privacy issues (see [85] for details). For this reason, in this paper we focus on more appealing distributed system designs, as described in Section 5.4.

Real-time optimization (c.f. Section 5.5). Once the day-ahead bidding process finalizes, the

prices per unit of energy $\{K_h\tilde{L}(h)\}_{h=1}^{H}$ remain fixed. However, as the dispatch time-slot approaches, active users have more reliable information about their energy needs. Hence, they can exploit this coming information to adjust their production and storage strategies $\mathbf{g}_n$ and $\mathbf{s}_n$ in real-time. In doing so, they aim at reducing the deviation of the real-time strategy with respect to the bid energy load, i.e., $\left|l_n(h)-\tilde{l}_n(h)\right|$, so as to minimize their expected expense for the rest of the day period.

After performing the day-ahead and the real-time optimization, the active users are finally billed according to (5.11).

5.4 Day-Ahead DSM for Expected Cost Minimization

In this section, we formulate the day-ahead bidding system introduced in Section 5.3 as a generalized Nash equilibria problem (GNEP). To this end, we first introduce some preliminary definitions. Let us rewrite Constraint 1 in the form of shared constraints $\mathbf{q}(\mathbf{x}) \leq \mathbf{0}$, where $\mathbf{q}(\mathbf{x}) \triangleq (\mathbf{q}^{(\min)}(\mathbf{x}), \mathbf{q}^{(\max)}(\mathbf{x})) : \mathbb{R}^{3HN} \to \mathbb{R}^{2H}$ with $\mathbf{x} \triangleq \left(\mathbf{x}_n\right)_{n=1}^{N}$ and

$$\begin{aligned}\mathbf{q}^{(\min)}(\mathbf{x}) &\triangleq \Big(L^{(\min)}(h) - \sum_{n\in\mathcal{N}} \boldsymbol{\delta}^{\mathrm{T}}\mathbf{x}_n(h) - \hat{L}^{(\mathcal{P})}(h)\Big)_{h=1}^{H} \\ \mathbf{q}^{(\max)}(\mathbf{x}) &\triangleq \Big(\sum_{n\in\mathcal{N}} \boldsymbol{\delta}^{\mathrm{T}}\mathbf{x}_n(h) + \hat{L}^{(\mathcal{P})}(h) - L^{(\max)}(h)\Big)_{h=1}^{H}.\end{aligned} \tag{5.18}$$

Note that $\mathbf{q}(\mathbf{x})$ is convex in $\mathbf{x} \in \Omega_{\mathbf{x}} \triangleq \prod_{n\in\mathcal{N}} \Omega_{\mathbf{x}_n}$. The strategy set of user $n \in \mathcal{N}$ can be then expressed as (c.f. (5.5))

$$\Theta_{\mathbf{x}_n}(\tilde{\mathbf{l}}_{-n}) \triangleq \left\{\mathbf{x}_n \in \Omega_{\mathbf{x}_n} : \mathbf{q}(\mathbf{x}_n, \tilde{\mathbf{l}}_{-n}) \leq \mathbf{0}\right\} \tag{5.19}$$

whereas the joint strategy set is given by

$$\Theta_{\mathbf{x}} \triangleq \left\{\mathbf{x} \in \mathbb{R}^{3HN} : \mathbf{x}_n \in \Omega_{\mathbf{x}_n}, \forall n \in \mathcal{N} \text{ and } \mathbf{q}(\mathbf{x}) \leq \mathbf{0}\right\}. \tag{5.20}$$

We formulate the system design as the GNEP $\mathscr{G} = \left\langle \Theta_{\mathbf{x}}, \mathbf{f}\right\rangle$, with $\Theta_{\mathbf{x}}$ given in (5.20), $\mathbf{f} \triangleq \left(\mathsf{f}_n(\mathbf{x}_n, \tilde{\mathbf{l}}_{-n})\right)_{n=1}^{N}$, and $\mathsf{f}_n(\mathbf{x}_n, \tilde{\mathbf{l}}_{-n})$ defined in (5.18). Here, each user is a player who aims at minimizing his expected cumulative expense subject to both individual and global constraints (c.f. (5.19)):

$$\begin{aligned}\min_{\mathbf{x}_n} \quad & \mathsf{f}_n(\mathbf{x}_n, \tilde{\mathbf{l}}_{-n}) \\ \text{s.t.} \quad & \mathbf{x}_n \in \Theta_{\mathbf{x}_n}(\tilde{\mathbf{l}}_{-n})\end{aligned} \qquad \forall n \in \mathcal{N}. \tag{5.21}$$

The GNEP $\mathscr{G} = \left\langle \Theta_{\mathbf{x}}, \mathbf{f}\right\rangle$ is the problem of finding a feasible strategy profile $\mathbf{x}^{\star} \triangleq \left(\mathbf{x}_n^{\star}\right)_{n=1}^{N}$ such that $\mathsf{f}_n(\mathbf{x}_n^{\star}, \tilde{\mathbf{l}}_{-n}^{\star}) \leq \mathsf{f}_n(\mathbf{x}_n, \tilde{\mathbf{l}}_{-n}^{\star})$, $\forall \mathbf{x}_n \in \Theta_{\mathbf{x}_n}(\tilde{\mathbf{l}}_{-n}^{\star})$, for all players $n \in \mathcal{N}$ [79]. The solution of the GNEP is called (generalized) Nash equilibrium. We refer to [74, Sec. 4.3] for a detailed overview

on GNEPs.

5.4.1 Variational Solutions

GNEPs with shared constraints such as (5.21) are difficult problems to solve. They can be formulated as quasi-variational inequality (QVI) problems [77]; however, in spite of some interesting and promising recent advancements (see, e.g., [90,91]), no efficient numerical methods based on the QVI reformulation have been developed yet. Nevertheless, for this type of GNEPs, some VI techniques can still be employed [74].

Definition 5.1 ([77, Def. 1.1.1])**.** *Given the vector-valued function* $\mathbf{F} : \Theta_{\mathbf{x}} \to \mathbb{R}^{3HN}$ *with* $\Theta_{\mathbf{x}}$ *defined in* (5.20)*, the VI problem* $\mathrm{VI}(\Theta_{\mathbf{x}}, \mathbf{F})$ *consists in finding a point* $\mathbf{x}^\star \in \Theta_{\mathbf{x}}$ *such that*

$$(\mathbf{x} - \mathbf{x}^\star)^{\mathrm{T}} \mathbf{F}(\mathbf{x}^\star) \geq 0, \qquad \forall \mathbf{x} \in \Theta_{\mathbf{x}}. \tag{5.22}$$

Indeed a solution of the GNEP can be computed by solving a suitably defined VI problem, as stated in the next lemma, whose proof is based on standard techniques [74, 116, 117]; see Appendix 5.B.1 for more details.

Lemma 5.2. Given the GNEP $\mathscr{G} = \langle \Theta_{\mathbf{x}}, \mathbf{f} \rangle$, suppose that the following conditions are satisfied: for all $n \in \mathcal{N}$,

(a) The strategy sets $\Omega_{\mathbf{g}_n}$ and $\Omega_{\mathbf{s}_n}$ are closed and convex;
(b) The production cost function $W_n(x)$ is convex, $\forall n \in \mathcal{G}$;
(c) $\chi_n^{(\min)}(h)$ and $\chi_n^{(\max)}(h)$ in (5.2) are chosen such that the pdf of the per-slot net energy consumption satisfies

$$f_{e_n(h)}(x) \geq \frac{1}{(\alpha_h + \beta_h) L^{(\min)}(h)} \frac{\left(\alpha_h + 1\right)^2}{2} \tag{5.23}$$

$\forall x \in \left[\chi_n^{(\min)}(h), \chi_n^{(\max)}(h)\right]$.

Let $\mathbf{F}(\mathbf{x}) \triangleq \left(\nabla_{\mathbf{x}_n} \mathsf{f}_n(\mathbf{x}_n, \tilde{\mathbf{l}}_{-n})\right)_{n=1}^N$. Then, every solution of the $\mathrm{VI}(\Theta_{\mathbf{x}}, \mathbf{F})$ is a solution of the GNEP.

Remark 5.1 (on Lemma 5.2). (a) Given $\Omega_{\tilde{\mathbf{e}}_n}$ in (5.2), the closeness and convexity of $\Omega_{\mathbf{g}_n}$ and $\Omega_{\mathbf{s}_n}$ ensure the same properties for the strategy set $\Omega_{\mathbf{x}_n}$ in (5.5). For instance, the dispatchable production and storage models adopted in [84] and evoked in Section 5.6 enjoy such properties. (b) The convexity of $W_n(\cdot)$ simply implies that the production cost function does not tend to saturate as $g_n(h)$ increases [84, Remark 1.1]. (c) When the distribution of $e_n(h)$ is unimodal, condition (5.23) limits the displacement of $\tilde{e}_n(h)$ around the mode of $e_n(h)$ in order to ensure the convexity of the objective function $\mathsf{f}_n(\mathbf{x}_n, \tilde{\mathbf{l}}_{-n})$. On the contrary, when the distribution of $e_n(h)$ is multimodal, $\chi_n^{(\min)}(h)$ and $\chi_n^{(\max)}(h)$ must be carefully selected to guarantee the convexity of

$\mathsf{f}_n(\mathbf{x}_n, \tilde{\mathbf{l}}_{-n})$. A heuristic procedure to deal with such cases is presented in Appendix 5.B.2. These considerations also apply to condition (5.26) given in Theorem 5.1(a.2).

Note that, when passing from the GNEP (5.21) to the associated VI, not all the GNEP's solutions are preserved: Lemma 5.2 in fact does not state that any solution of the GNEP is also a solution of the VI (see [75] for further details and examples). The solutions of the GNEP that are also solutions of the VI($\Theta_{\mathbf{x}}, \mathbf{F}$) are termed as *variational solutions* [74, 75] and enjoy some remarkable properties that make them particularly appealing in many applications. Among all, they can be interpreted as the solutions of a Nash equilibrium problem (NEP) with pricing, as detailed next.

Consider the following augmented NEP with $N+1$ players, in which the "new" $(N+1)$-th player (at the same level of the other N players) controls the price variable $\boldsymbol{\lambda} \in \mathbb{R}_+^{2H}$:

$$\begin{aligned} \min_{\mathbf{x}_n} \quad & \mathsf{f}_n(\mathbf{x}_n, \tilde{\mathbf{l}}_{-n}) + \boldsymbol{\lambda}^{\mathrm{T}} \mathbf{q}(\mathbf{x}_n, \tilde{\mathbf{l}}_{-n}) \\ & \qquad\qquad\qquad\qquad\qquad\qquad \forall n \in \mathcal{N} \\ \text{s.t.} \quad & \mathbf{x}_n \in \Omega_{\mathbf{x}_n} \\ \min_{\boldsymbol{\lambda} \geq \mathbf{0}} \quad & -\boldsymbol{\lambda}^{\mathrm{T}} \mathbf{q}(\mathbf{x}). \end{aligned} \tag{5.24}$$

We can interpret $\boldsymbol{\lambda}$ as the overprices applied to force the users to satisfy the shared constraints $\mathbf{q}(\mathbf{x})$. Indeed, when $\mathbf{q}(\mathbf{x}) \leq \mathbf{0}$, the optimal price will be $\boldsymbol{\lambda} = \mathbf{0}$ (there is no need to punish the users if the constraints are already satisfied).

We can now establish the connection between the VI($\Theta_{\mathbf{x}}, \mathbf{F}$) and the augmented NEP (5.24) [74, Lem. 4.4].

Lemma 5.3. Under the setting of Lemma 5.2, $(\mathbf{x}^\star, \boldsymbol{\lambda}^\star)$ is a Nash equilibrium of the NEP (5.24) if and only if $\mathbf{x}^\star$ is a solution of the VI($\Theta_{\mathbf{x}}, \mathbf{F}$), i.e., a variational solution of the GNEP $\mathscr{G} = \langle \Theta_{\mathbf{x}}, \mathbf{f} \rangle$, and $\boldsymbol{\lambda}^\star$ is the multiplier associated with the shared constraints $\mathbf{q}(\mathbf{x}^\star) \leq \mathbf{0}$ in $\Theta_{\mathbf{x}}$.

Based on Lemma 5.3, we are now able to analyze and compute the variational solutions of the GNEP (5.21) as solutions of the NEP (5.24), building on recent results in [76]. The following is a standard existence result of variational solutions, based on solution analysis of VIs [77].

Lemma 5.4. Given the GNEP $\mathscr{G} = \langle \Theta_{\mathbf{x}}, \mathbf{f} \rangle$, suppose that the conditions in Lemma 5.2 are satisfied and that the strategy sets $\Omega_{\mathbf{g}_n}$ and $\Omega_{\mathbf{s}_n}$ are additionally bounded. Then, the GNEP has variational solutions.

In the next section, we build on the game theoretical pricing-based interpretation (5.24) (c.f. Lemma 5.3) to design distributed algorithms that converge to a variational solution of the GNEP.

5.4.2 Distributed Algorithms

We focus on the class of *totally asynchronous* best-response algorithms, where some users may update their strategies more frequently than others and they may even use outdated information about the strategy profiles adopted by the other users. Let $\mathscr{T}_n \subseteq \mathscr{T} \subseteq \{0,1,2,\ldots\}$ be the set of times at which user $n \in \mathcal{N}$ updates his own strategy $\mathbf{x}_n$, denoted by $\mathbf{x}_n^{(i)}$ at the ith iteration. We use $t_n(i)$ to denote the most recent time at which the strategy of user n is perceived by the central unit at the ith iteration. We assume that some standard conditions in asynchronous convergence theory (see (A1)–(A3) in [85, Sec III-C]), which are fulfilled in any practical implementation, hold for $\mathscr{T}_n$ and $t_n(i)$, $\forall n \in \mathcal{N}$.

According to the asynchronous scheduling, each user updates his strategy by minimizing his cumulative expense over the day period, given the most recently available value of the per-slot aggregate bid energy load

$$\tilde{L}^{(\mathbf{t}(i))}(h) \triangleq \hat{L}^{(\mathcal{P})}(h) + \sum_{m \in \mathcal{N}} \tilde{l}_m^{(t_m(i))}(h) \tag{5.25}$$

that considers the bid energy loads of the other users as perceived by the central unit, which can possibly be outdated when computation occurs. Each user n then obtains $\tilde{\mathbf{l}}_{-n}^{(\mathbf{t}(i))} \triangleq \big(\tilde{l}_{-n}^{(\mathbf{t}(i))}(h)\big)_{h=1}^{H}$, with $\tilde{l}_{-n}^{(\mathbf{t}(i))}(h) \triangleq \tilde{L}^{(\mathbf{t}(i))}(h) - \tilde{l}_n^{(t_n(i))}(h)$.

We can compute the variational solutions of the GNEP (5.21) by solving the augmented NEP (5.24). This can be done using the recent framework in [76], which leads to the asynchronous proximal decomposition algorithm (PDA) described in Algorithm 5.1, and whose convergence conditions are given in Theorem 5.1.

Theorem 5.1. *Given the GNEP* $\mathscr{G} = \big\langle \Theta_{\mathbf{x}}, \mathbf{f} \big\rangle$*, suppose that:*

(a.1) *Conditions* (a)–(b) *in Lemma* 5.2 *are satisfied;*

(a.2) $\chi_n^{(\min)}(h)$ *and* $\chi_n^{(\max)}(h)$ *in* (5.2) *are chosen such that the pdf of the per-slot net energy consumption satisfies*

$$f_{e_n(h)}(x) \geq \frac{1}{(\alpha_h + \beta_h) L^{(\min)}(h)} \Big(\frac{(\alpha_h + 1)^2}{4} + N\big(\max(\alpha_h, \beta_h) + \alpha_h + \beta_h \big) \Big) \tag{5.26}$$

$\forall x \in \big[\chi_n^{(\min)}(h), \chi_n^{(\max)}(h)\big]$*, for all* $n \in \mathcal{N}$*;*

(a.3) *The penalty parameters are such that* $\alpha_h + \beta_h \leq 1, \forall h$*;*

(b) *The regularization parameter* τ *satisfies*

$$\tau > \frac{3}{2}(N-1) \max_h K_h + \sqrt{\frac{9}{4}(N-1)^2 \max_h K_h^2 + 3HN} \tag{5.27}$$

(c) $\{\rho^{(i)}\} \subset [R_m, R_M]$*, with* $0 < R_m < R_M < 2$.

Algorithm 5.1 Asynchronous PDA with Coupling Constraints

`Data` : Set $i=0$ and the initial centroids $\big(\bar{\mathbf{x}}_n\big)_{n=1}^N = \mathbf{0}$ and $\bar{\boldsymbol{\lambda}} = \mathbf{0}$. Given $\big\{K_h, \alpha_h, \beta_h\big\}_{h=1}^H$, $\big\{\rho^{(i)}\big\}_{i=0}^\infty$, $\tau > 0$, and any feasible starting point $\mathbf{z}^{(0)} \triangleq \big(\big(\mathbf{x}_n^{(0)}\big)_{n=1}^N, \boldsymbol{\lambda}^{(0)}\big)$ with $\boldsymbol{\lambda}^{(0)} \geq \mathbf{0}$:

`(S.1)` : `If` a suitable termination criterion is satisfied: `STOP`.

`(S.2)` : `For` $n \in \mathcal{N}$, each user computes $\mathbf{x}_n^{(i+1)}$ as

$$\mathbf{x}_n^{(i+1)} = \begin{cases} \mathbf{x}_n^\star \in \underset{\mathbf{x}_n \in \Omega_{\mathbf{x}_n}}{\operatorname{argmin}} \Big\{ \mathsf{f}_n\big(\mathbf{x}_n, \tilde{\mathbf{l}}_{-n}^{(\mathbf{t}(i))}\big) + (\boldsymbol{\lambda}^{(i)})^{\mathrm{T}} \mathbf{q}\big(\mathbf{x}_n, \tilde{\mathbf{l}}_{-n}^{(\mathbf{t}(i))}\big) + \dfrac{\tau}{2}\|\mathbf{x}_n - \bar{\mathbf{x}}_n\|^2 \Big\}, & \text{if } i \in \mathscr{T}_n \\ \mathbf{x}_n^{(i)}, & \text{otherwise} \end{cases}$$

`End`

The central unit computes $\boldsymbol{\lambda}^{(i+1)}$ as

$$\boldsymbol{\lambda}^{(i+1)} = \boldsymbol{\lambda}^\star \in \underset{\boldsymbol{\lambda} \geq \mathbf{0}}{\operatorname{argmin}} \Big\{ -\boldsymbol{\lambda}^{\mathrm{T}} \mathbf{q}(\mathbf{x}) + \frac{\tau}{2}\|\boldsymbol{\lambda} - \bar{\boldsymbol{\lambda}}\|^2 \Big\}$$

`(S.3)` : `If` the NE is reached, then each user $n \in \mathcal{N}$ sets $\mathbf{x}_n^{(i+1)} \leftarrow (1-\rho^{(i)})\bar{\mathbf{x}}_n + \rho^{(i)}\mathbf{x}_n^{(i+1)}$ and updates his centroid: $\bar{\mathbf{x}}_n = \mathbf{x}_n^{(i+1)}$; likewise, the central unit sets $\boldsymbol{\lambda}^{(i+1)} \leftarrow (1-\rho^{(i)})\bar{\boldsymbol{\lambda}} + \rho^{(i)}\boldsymbol{\lambda}^{(i+1)}$ and updates the centroid: $\bar{\boldsymbol{\lambda}} = \boldsymbol{\lambda}^{(i+1)}$.

`(S.4)` : $i \leftarrow i+1$; `Go to (S.1)`.

Then, any sequence $\big\{(\mathbf{x}^{(i)}, \boldsymbol{\lambda}^{(i)})\big\}_{i=1}^\infty$ *generated by Algorithm* 5.1 *converges to a variational solution of the GNEP.*

Proof. See Appendix 5.B.3.

Remark 5.2 (**on Algorithm 5.1**)**.** Algorithm 5.1 is a double-loop algorithm in nature. The inner loop requires the solution of the regularized game in `(S.3)` via asynchronous best-response algorithms. In the outer loop, all users $n \in \mathcal{N}$ and the central unit, which acts as the $(N+1)$-th player, update the centroids $\{\bar{\mathbf{x}}_n\}_{n\in\mathcal{N}}, \bar{\boldsymbol{\lambda}}$ and proceed to solve the inner game again, until an equilibrium is reached. Observe that the update of $\{\bar{\mathbf{x}}_n\}_{n\in\mathcal{N}}$ is performed locally by the users at the cost of no signaling exchange with the central unit.

Remark 5.3 (**on Theorem 5.1**)**.** The regularization parameter τ determines the trade-off between the convergence stability and the convergence speed [76]. The peculiarity of the expression of τ provided in (5.27) is that it can be calculated by the central unit a priori without interfering with the privacy of the users.

At the beginning of the optimization process, τ is computed as in (5.27) and broadcast, together with the grid coefficients and the penalty parameters $\big\{K_h, \alpha_h, \beta_h\big\}_{h=1}^H$, to the demand-side. At each iteration, any active user can update his strategy by minimizing his objective function (5.18) based on the most recent values of the aggregate bid energy loads $\big\{\tilde{L}^{(\mathbf{t}(i))}(h)\big\}_{h=1}^H$,

which are calculated by the central unit referring to the (possibly outdated) individual demands. At the same time, the central unit updates the price variable $\boldsymbol{\lambda}$ and broadcasts it to the demand-side. When the equilibrium in `(S.3)` is reached, the central unit initiates a new iteration. Observe that it is not necessary to compute the Nash equilibrium in the inner loop exactly; indeed, inexact solutions do not affect the convergence of Algorithm 5.1 as long as the error bound goes to zero as the number of iterations grows [74,78]. This process is repeated until some convergence criterion established by the central unit is fulfilled.

Note that, if we omit Constraint 1, the GNEP (5.21) reduces to a classical NEP, where the coupling among the players occurs only at the level of the objective functions (as addressed in [86]). Of course, the framework and algorithm proposed in the present paper contain this formulation as special case.

5.5 Real-Time Adjustments of the Production and Storage Strategies

In real-time, active users reasonably know the values of their net energy consumption $e_n(h)$ for the upcoming time-slot with much less uncertainty than during the day-ahead bidding process. In this section, we describe how the users can profit from this fact and perform real-time adjustments to the calculated production and storage strategies in order to reduce the impact of the day-ahead uncertainty.

After the day-ahead bidding process, the prices per unit of energy $\left\{\mathsf{p}_h = K_h \tilde{L}(h)\right\}_{h=1}^{H}$ are fixed as a result of the energy bid loads of the active users obtained with Algorithm 5.1. Then, active users are charged in real-time based on such prices, while the differences between their actual energy requirements and the negotiated day-ahead amounts are subject to the penalties described in Section 5.3.2 (c.f. (5.11)). In this setting, at each h, active user $n \in \mathcal{N}$ can exploit the reduced uncertainty about his net energy consumption $e_n(h)$ to independently adjust his production and storage strategies $\left\{g_n(t), s_n(t)\right\}_{t=h}^{H}$ so as to minimize his expected expense for the remaining time-slots $t = h, \ldots, H$. At the same time, we can guarantee the following individual constraints on the per-slot energy load.

Constraint 2 (on the per-slot energy load). Due to physical constraints on the user's individual distribution infrastructure, the per-slot energy load $l_n(h)$ in (5.1) is bounded as

$$-\, l_n^{(\min)} \leq l_n(h) \leq l_n^{(\max)}, \qquad \forall h \tag{5.28}$$

where $l_n^{(\min)} \geq 0$ and $l_n^{(\max)} > 0$ are the outgoing and the incoming capacities of user n's energy link, respectively.

For modeling simplicity, we assume that, right before each time-slot h, each user $n \in \mathcal{N}$ has perfect knowledge of $e_n(h)$. Nonetheless, he still needs to satisfy the requirements given

by his production and storage strategy sets $\Omega_{\mathbf{g}_n}$ and $\Omega_{\mathbf{s}_n}$: in this regard, if the strategies over different time-slots are coupled (see, e.g., the constraints in Table 5.1), the users have to take into account the strategies adopted in the previous time-slots. With this objective in mind, let $\mathbf{y}_n(h) \triangleq \big(g_n(h), s_n(h)\big)$ denote the real-time strategy for each time-slot h, and let $\big(g_n^\star(t)\big)_{t=1}^{h-1}$ and $\big(s_n^\star(t)\big)_{t=1}^{h-1}$ express the production and storage strategies already fixed in the past time-slots $t = 1, \ldots, h-1$. Then, the real-time strategy set for user $n \in \mathcal{N}$ at h is defined as

$$\Omega_{\mathbf{y}_{n,h}} \triangleq \Big\{ \big(\mathbf{y}_n(t)\big)_{t=h}^{H} \in \mathbb{R}^{2(H-h+1)} : \big(\big(g_n^\star(t)\big)_{t=1}^{h-1}, \big(g_n(t)\big)_{t=h}^{H}\big) \in \Omega_{\mathbf{g}_n}, \\ \big(\big(s_n^\star(t)\big)_{t=1}^{h-1}, \big(s_n(t)\big)_{t=h}^{H}\big) \in \Omega_{\mathbf{s}_n}, \text{ and } -l_n^{(\min)} \leq e_n(h) - g_n(h) + s_n(h) \leq l_n^{(\max)}, \forall h \Big\} \quad (5.29)$$

Hence, the price paid by user $n \in \mathcal{N}$ for purchasing energy from the grid at time-slot h (conditioned on the bid load $\tilde{l}_n(h)$) is given by

$$\mathsf{p}_{n,h}^{(\mathcal{N})}\big(\mathbf{y}_n(h) \mid \tilde{l}_n(h)\big) \triangleq \mathsf{p}_h\big(e_n(h) + \boldsymbol{\delta}_{s-g}^{\mathrm{T}}\mathbf{y}_n(h) \\ + \vartheta_h\big(e_n(h) + \boldsymbol{\delta}_{s-g}^{\mathrm{T}}\mathbf{y}_n(h) - \tilde{l}_n(h)\big)\big) + W_n\big(\boldsymbol{\delta}_g^{\mathrm{T}}\mathbf{y}_n(h)\big) \quad (5.30)$$

where $\vartheta_h(x)$ is defined in (5.13), $\boldsymbol{\delta}_{s-g} \triangleq (-1, 1)$, and where we have conveniently redefined $\boldsymbol{\delta}_g \triangleq (1, 0)$. Likewise, the expected expense for each time-slot $t = h+1, \ldots, H$ is

$$\mathsf{f}_{n,t}\big(\mathbf{y}_n(t) \mid \tilde{l}_n(t)\big) \triangleq \mathsf{p}_t\mathsf{E}\big\{e_n(t) + \boldsymbol{\delta}_{s-g}^{\mathrm{T}}\mathbf{y}_n(t) \\ + \vartheta_t\big(e_n(t) + \boldsymbol{\delta}_{s-g}^{\mathrm{T}}\mathbf{y}_n(t) - \tilde{l}_n(t)\big)\big\} + W_n\big(\boldsymbol{\delta}_g^{\mathrm{T}}\mathbf{y}_n(t)\big) \quad (5.31)$$

which can be easily calculated in closed-form using Lemma 5.1. Therefore, at each time-slot h, each user $n \in \mathcal{N}$ uses the value of $e_n(h)$ and the reduced uncertainty about $\big\{e_n(t)\big\}_{t=h+1}^{H}$ to solve

$$\begin{aligned} \min_{\{\mathbf{y}_n(h)\}_{t=h}^{H}} \quad & \mathsf{p}_{n,h}^{(\mathcal{N})}\big(\mathbf{y}_n(h) \mid \tilde{l}_n(h)\big) + \sum_{t=h+1}^{H} \mathsf{f}_{n,t}\big(\mathbf{y}_n(t) \mid \tilde{l}_n(t)\big) \\ \text{s.t.} \quad & \big(\mathbf{y}_n(t)\big)_{t=h}^{H} \in \Omega_{\mathbf{y}_{n,h}}. \end{aligned} \quad (5.32)$$

It is straightforward to observe that $\mathsf{p}_{n,h}^{(\mathcal{N})}\big(\mathbf{y}_n(h) \mid \tilde{l}_n(h)\big)$ in (5.30) and $\mathsf{f}_{n,h}\big(\mathbf{y}_n(h) \mid \tilde{l}_n(h)\big)$ in (5.31) are both convex in $\mathbf{y}_n(h)$, while $W_n(\cdot)$ is convex under the assumptions of Lemma 5.2. Hence, the optimization problem (5.32) is convex in $\big(\mathbf{y}_n(t)\big)_{t=h}^{H}$ and can be solved using efficient convex optimization techniques [62, Ch. 11].

5.6 Numerical Results and Discussions

In this section, we illustrate numerically the performance of the DSM mechanisms described in Sections 5.4 and 5.5.

Constraints	Parameters
$\left\{g_n(h) \leq g_n^{(\max)}\right\}_{h=1}^{H}$	$g_n^{(\max)} = 0.4$ kW
$\sum_{h=1}^{H} g_n(h) \leq \gamma_n^{(\max)}$	$\gamma_n^{(\max)} = 7.2$ kWh
$\left\{s_n(h) \leq \max\left(s_n^{(\max)}, c_n - q_n(h)\right)\right\}_{h=1}^{H}$	$s_n^{(\max)} = 0.5$ kW
	$c_n = 4$ kWh
$\left\{s_n(h) \geq \xi_n q_n(h-1)\right\}_{h=1}^{H}$	$\xi_n = \sqrt[24]{0.9}$
$q_n(0) = q_n(H)$	$q_n(0) = 1$ kWh

Table 5.1: Dispatchable energy generation and storage models adopted in Section 5.6 (also extensively described in [84]).

We consider a smart grid of $N = 100$ active users and $P = 900$ passive users over a day period of $H = 24$ time-slots of one hour each. With the same setup of [86], all demand-side users $n \in \mathcal{D}$ have randomly generated average energy consumption curves with daily average of $\sum_{h=1}^{24} \bar{e}_n(h) = 12$ kWh, with higher consumption during day-time hours (from 08:00 to 24:00) than during night-time hours (from 00:00 to 08:00) and reaching its peak between 16:00 and 24:00. The grid coefficients are chosen such that $\left\{K_h\right\}_{h=1}^{8} = K_{\text{night}}$ and $\left\{K_h\right\}_{h=9}^{24} = K_{\text{day}}$, with $K_{\text{day}} = 1.5K_{\text{night}}$ as in [51, 84–86], so as to obtain an initial price of 0.15 €/kWh when real-time penalties are neglected. Furthermore, we set $\left\{\alpha_h\right\}_{h=1}^{8} = 0.2$ and $\left\{\alpha_h\right\}_{h=9}^{24} = 0.9$, with $\left\{\beta_h = 1 - \alpha_h\right\}_{h=1}^{24}$: this choice penalizes overconsumption during day-time hours and underconsumption during night-time hours.

We model $e_n(h)$ as a normal random variable with mean $\bar{e}_n(h)$ and standard deviation $\sigma_n(h)$, and we choose $\chi_n^{(\min)}(h)$ and $\chi_n^{(\max)}(h)$ to satisfy Theorem 5.1(a.2). For the sake of simplicity, we assume that all active users are subject to the same dispatchable production and storage models summarized in Table 5.1. Here, $g_n^{(\max)}$ denotes the maximum energy production capability and $\gamma_n^{(\max)}$ represents the maximum amount of energy that user can generate during the period of analysis; as for the energy storage model, $s_n^{(\max)}$ indicates the maximum charging rate, ξ_n represents the leakage rate, c_n denotes the storage capacity, and $q_n(h)$ expresses the charge level at time-slot h, with $q_n(0)$ being the initial charge level. Furthermore, all dispatchable generators are characterized by the production cost function $W_n(x) = \eta_n x$, resembling a combustion engine working in the linear region, with $\eta_n = 0.039$ €/kWh.[6] Lastly, we consider Constraint 1 with $\left\{L^{(\min)}(h)\right\}_{h=1}^{H} = 385$ kWh and $\left\{L^{(\max)}(h)\right\}_{h=1}^{H} = 600$ kWh.

[6] The benefit of employing DG and DS is strictly related to the specific parameters of the adopted dispatchable source and storage device. A comparison of the impact produced by DG, DS, and a combination of the two is given in [84, 85]; furthermore, [86] provides some insight on the relative effect of the bidding strategies with respect to DG and DS strategies.

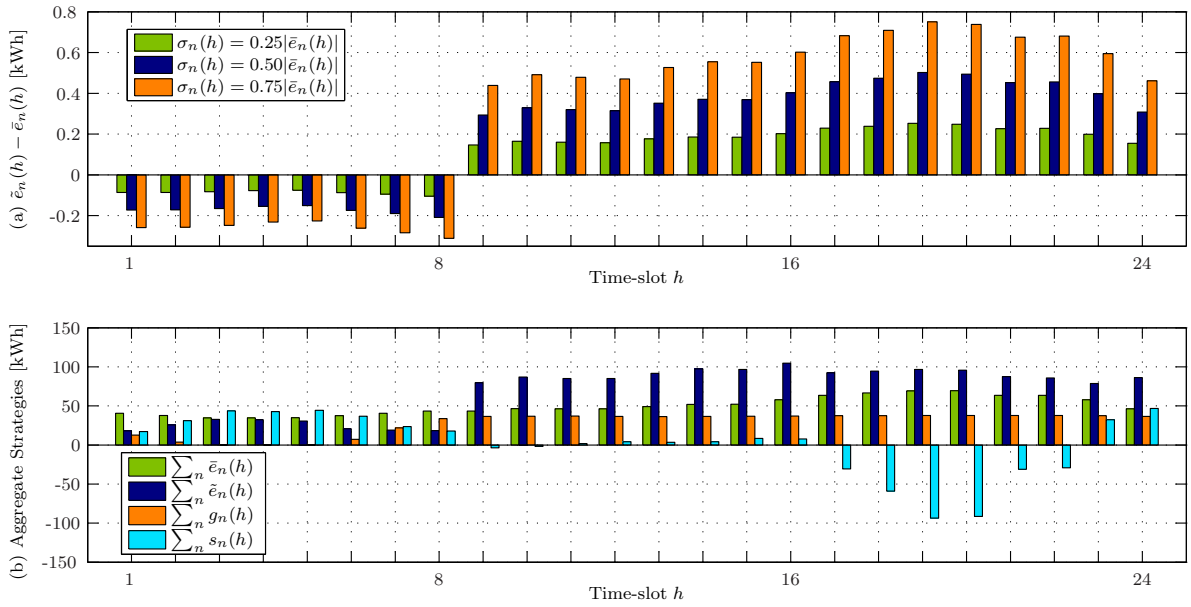

Figure 5.3: Results of Algorithm 5.1: (a) Difference between average consumption and bid consumption for a generic user with three different $\sigma_n(h)$; (b) Aggregated average consumption and bidding, production, and storage strategies.

5.6.1 Day-Ahead DSM for Expected Cost Minimization

Here, we evaluate the performance of the Day-Ahead DSM method proposed in Section 5.4. For Algorithm 5.1, we impose $\|\mathbf{l}^{(i)} - \mathbf{l}^{(i-1)}\|_2 / \|\mathbf{l}^{(i)}\|_2 \leq 10^{-2}$ and the fulfillment of Constraint 1 as termination criteria in `(S.1)`, and $\{\rho^{(i)}\}_{i=0}^{\infty} = 1$.

Let us first analyze the results produced by Algorithm 5.1. Fig. 5.3(a) illustrates the per-slot bid net consumptions $\tilde{e}_n(h)$ with respect to the average per-slot net consumptions $\bar{e}_n(h)$ for a generic active user, using three different standard deviations. Predictably, $\tilde{e}_n(h)$ is greater than $\bar{e}_n(h)$ when $\alpha_h > \beta_h$ since the user is more likely to avoid severe penalties for surpassing the agreed load, and vice versa. Evidently, such displacement becomes greater as the standard deviation (i.e., the uncertainty) increases. Using $\sigma_n(h) = 0.75\big|\bar{e}_n(h)\big|$, Fig. 5.3(b) plots the aggregate bidding, production, and storage strategies obtained from Algorithm 5.1. As expected, the storage devices are charged at the valley of the energy cost and are discharged at peak hours; likewise, the dispatchable production is concentrated during day-time hours when the grid prices are higher.

Now, let us compare Algorithm 5.1 with the PDA in [86, Alg. 2], which is equivalent to the former but only considers local constraints. From Fig. 5.4(a), it is evident that the aggregate load produced by the PDA does not satisfy Constraint 1 during several hours (namely, $h = 3, \ldots, 5, 17, \ldots, 23$). Let us examine the resulting average expected cumulative expense: from Fig. 5.4(b), it is straightforward to see that active users achieve consistent savings using

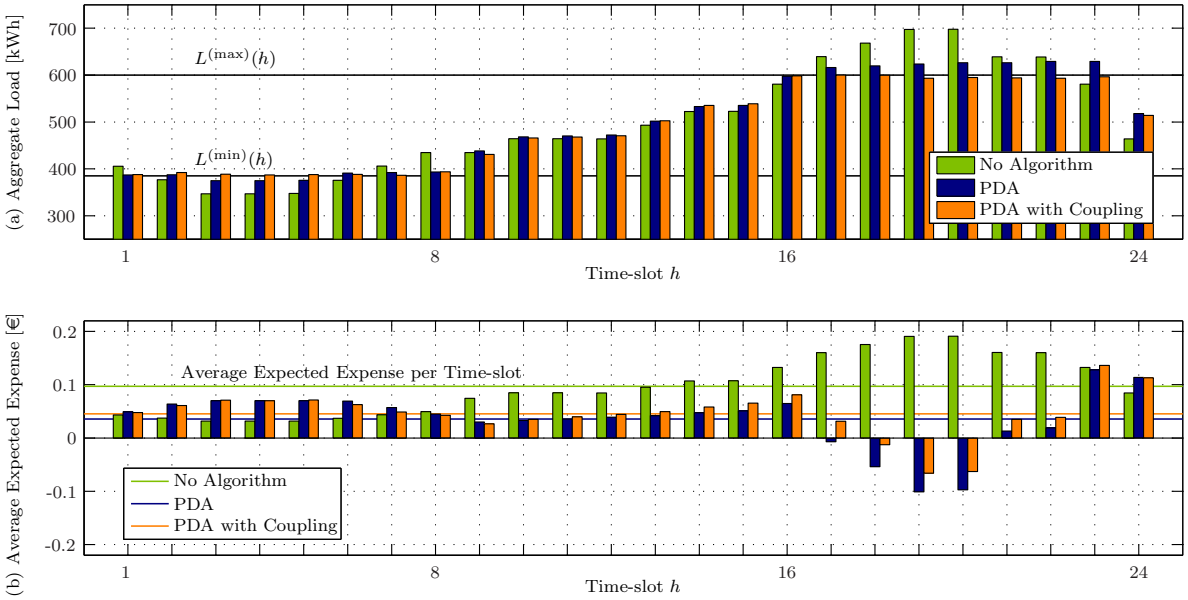

Figure 5.4: Comparison between [86, Alg. 2] (PDA) and Algorithm 5.1 (PDA with Coupling) with $L^{(\min)} = 385$ kWh and $L^{(\max)} = 600$ kWh, $\forall h$: (a) Aggregated bid energy loads; (b) Average per-slot expected expenses.

Algorithm 5.1. In particular, the average expected cumulative expense decreases from the initial value of €2.33 to €1.14 (51.1% less). However, these savings are predictably lower than those produced by [86, Alg. 2] due to the enforcement of Constraint 1. This is shown clearly by Fig. 5.5, which compares the convergence of the two algorithms. The PDA in [86, Alg. 2] converges after just 3 iterations; on the other hand, choosing the starting point $\mathbf{z}^{(0)} = \left(\mathbf{x}^\star, \boldsymbol{\lambda}^{(0)}\right)$, where $\mathbf{x}^\star$ is the optimal strategy profile calculated through [86, Alg. 2],[7] Algorithm 5.1 converges after 29 iterations. In this respect, we can observe as the average expected cumulative expense increases after about 7 iterations as a result of the imposition of Constraint 1.

Comparison with ECS Approaches. Algorithm 5.1 is designed to be applied specifically to the pricing model in Section 5.3.2. Although it cannot be compared with alternative existing schemes other than [86, Alg. 2] (of which Algorithm 5.1 is a nontrivial generalization), it can be easily adjusted to accommodate other DSM approaches within said pricing model: this adaptability represents a remarkable feature of our framework. In particular, we extend Algorithm 5.1 to incorporate ECS, perhaps the most popular among the plethora of DSM techniques (see, e.g., [51, 72, 73]), into the day-ahead bidding process. In the following, we provide a comparison between ECS and DS: the former consists in shifting flexible load to off-peak hours (as discussed in Section 5.1), whereas the latter allows to store cheap energy during off-peak hours for later use.

[7] This can be easily implemented by forcing the value of τ in [86, Th. 4(b.1)] and $\boldsymbol{\lambda}^{(i)} = \mathbf{0}$ until the optimal strategies without Constraint 1 are reached.

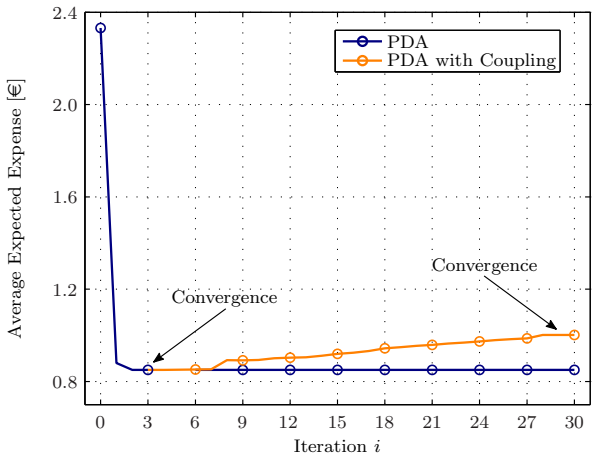

Figure 5.5: Comparison between [86, Alg. 2] (PDA) and Algorithm 5.1 (PDA with Coupling) with $L^{(\min)} = 385$ kWh and $L^{(\max)} = 600$ kWh, $\forall h$: Convergence in terms of average expected expense.

Again, we consider $N = 100$ active users and $P = 900$ passive users with the same average consumption curves used above; furthermore, we impose Constraint 1 with $\left\{L^{(\min)}(h)\right\}_{h=1}^{H} = 415$ kWh and $\left\{L^{(\max)}(h)\right\}_{h=1}^{H} = 675$ kWh. We assume that ECS enables each active user to shift 4 kWh from peak-hours, i.e., during $h = 16, \ldots, 24$, to other time-slots; on the other hand, we consider the same setup in Table 5.1 for the energy storage (note that the amount of shiftable load and the storage device's capacity are the same). Observing Fig. 5.6(a), it is evident that Algorithm 5.1 allows to achieve similar aggregate load curves with ECS and DS. Nonetheless, from Fig. 5.6(b), it emerges that the expected expense obtained with ECS is slightly lower than that resulting from DS (23.6% and 16.9%, respectively, less than when no DSM approach is used). This difference can be mainly ascribed to the leakage of the storage device, which is only partially compensated by the fact that the stored energy can be sold to the grid during peak hours. On the other hand, the discomfort produced by the rescheduling of activities and the capital costs associated to controllable appliances and storage devices have not been considered here, although they are important issues to be taken into account when comparing the two methods.

5.6.2 Real-Time Adjustments of the Production and Storage Strategies

After implementing the day-ahead optimization based on Algorithm 5.1, we test the real-time adjustments of the production and storage strategies described in Section 5.5. Here, the less uncertainty about the users' consumption corresponds to a reduced standard deviation with respect to that characterizing the day-ahead optimization. The standard deviation perceived by user n at each hour h for the upcoming time-slots $t = h + 1 \ldots H$ is thus modeled as $\sigma_{n,h}(t) = 0.75\sqrt{(t-h)/H}\left|\bar{e}_n(t)\right|$, with $h = 0$ corresponding to the day-ahead.

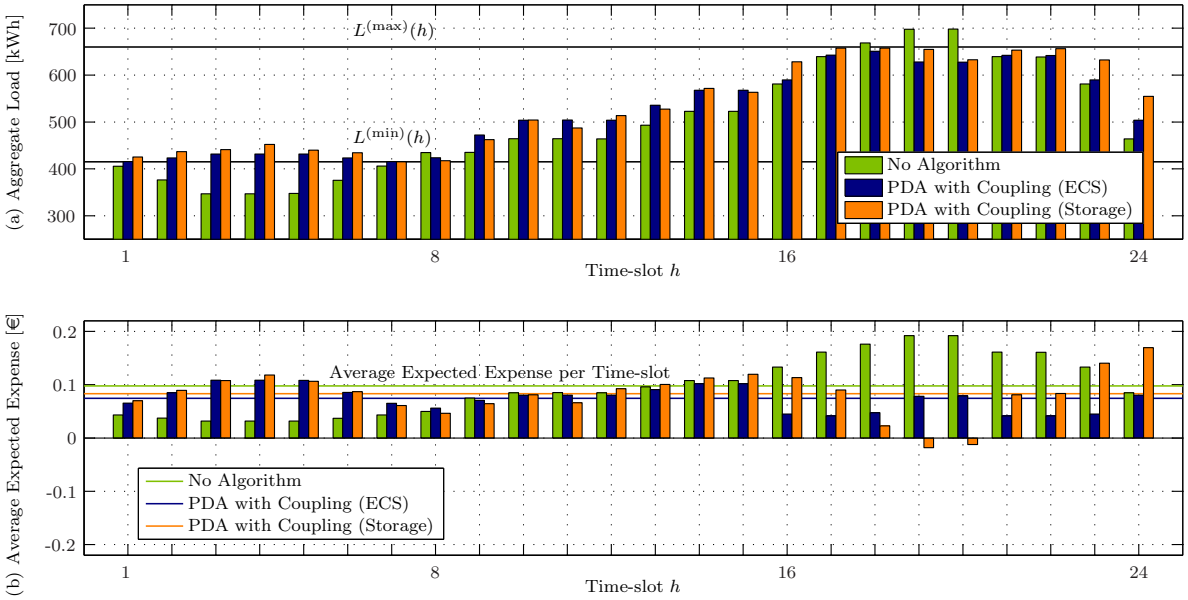

Figure 5.6: Algorithm 5.1 (PDA with Coupling) applied to ECS and DS, with $L^{(\min)} = 415$ kWh and $L^{(\max)} = 675$ kWh, $\forall h$: (a) Aggregated bid energy loads; (b) Average per-slot expected expenses.

We use the Monte Carlo method and simulate 1000 normally distributed random consumption curves of a generic active user. Hence, in Fig. 5.7 we plot the histogram of the cumulative expenses obtained through the real-time adjustments and we compare these results with the case where the user simply follows his day-ahead production and storage strategies. In this case, the average expense decreases from €1.07 to €0.96 (i.e., 10.3% less); on the other hand, the associated variance (i.e., the risk intended as a dispersion measurement [34, Ch. 4.3.1]), decreases from 0.114 to 0.088 (i.e., 22.8% less). Observe that this procedure can be even more beneficial in a practical case, where the consumption statistics are estimated by the user and they do not accurately match the actual distribution.

5.7 Conclusions

In this paper, we propose a noncooperative DSM mechanism based on a pricing model with real-time penalties, which optimizes the users' bidding, production, and storage strategies at two different time granularities, i.e., day-ahead and real-time. In the day-ahead, we consider coupling constraints on the aggregate load: the grid optimization is thus formulated as a generalized Nash equilibrium problem and its main properties are studied using the general framework of variational inequality. We devise a distributed algorithm that allows to compute the variational solutions of the GNEP with limited information exchange between the central unit and the demand-side of the grid. Furthermore, in real-time, the users exploit the reduced uncertainty about their energy consumption and renewable generation to adjust their strategies, alleviating

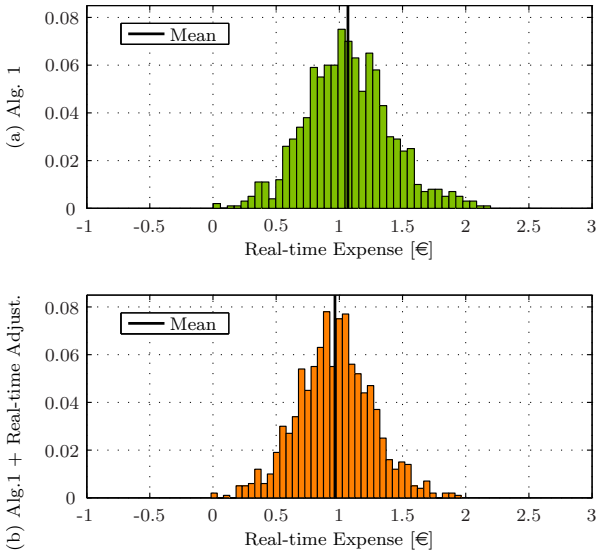

Figure 5.7: Histogram of the cumulative expenses of a generic user: (a) With day-ahead strategies from Algorithm 5.1; (b) With additional real-time adjustments.

the impact of their real-time deviations with respect to the day-ahead schedule. Numerical results show that our day-ahead DSM method consistently diminishes the users' expected monetary expenses while fulfilling the global constraints. On the other hand, the real-time adjustments reduce both the average value and the variance of the user's actual monetary expense.

5.A Energy Cost and Pricing Model

5.A.1 Energy Pricing for Passive Users

In order to stimulate the demand-side users to participate in the day-ahead bidding process, passive users may be penalized with respect to the active ones by paying an overprice κ_h on the purchased energy as

$$\mathsf{p}_n^{(\mathcal{P})} \triangleq \sum_{h=1}^{H} \kappa_h K_h \tilde{L}(h) l_n(h), \quad n \in \mathcal{P} \tag{5.33}$$

where $l_n(h) > 0$ for users $n \in \mathcal{P}$, since we assume that only active users are allowed to sell energy to the grid.

A procedure to calculate the overprice parameter κ_h is to guarantee that $\mathsf{E}\{\mathsf{p}_n^{(\mathcal{P})}\}$ is greater than the expected cumulative expense when user $n \in \mathcal{P}$ resembles an active user who simply bids his expected loads $\{\bar{l}_n(h)\}_{h=1}^{H}$. It is not difficult to show that this condition holds whenever

$$\kappa_h > 1 + \alpha_h + \beta_h. \tag{5.34}$$

5.A.2 Expected Cost Minimization: Proof of Lemma 5.1

The expected cumulative expense of active user $n \in \mathcal{N}$, with per-slot bid energy loads $\tilde{\mathbf{l}}_n$, is given by (5.18), where $\phi_{e_n(h)}\big(\mathbf{x}_n(h)\big)$ is defined in (5.15) and developed as

$$\begin{aligned}\phi_{e_n(h)}\big(\mathbf{x}_n(h)\big) &= \bar{e}_n(h) - g_n(h) + s_n(h) \\ &\quad + \alpha_h \int_{\tilde{e}_n(h)}^{\infty} \big(t - \tilde{e}_n(h)\big) f_{e_n(h)}(t)dt + \beta_h \int_{-\infty}^{\tilde{e}_n(h)} \big(\tilde{e}_n(h) - t\big) f_{e_n(h)}(t)dt \end{aligned} \quad (5.35)$$

with $\bar{e}_n(h) = \mathsf{E}\{e_n(h)\}$. Finally, using $G_{e_n(h)}(x)$ defined in (5.17) and observing that

$$\int_x^{\infty} t f_{e_n(h)}(t)dt = \bar{e}_n(h) - G_{e_n(h)}(x) \quad (5.37)$$

the expression for $\phi_{e_n(h)}\big(\mathbf{x}_n(h)\big)$ in (5.16) readily follows. □

5.B Day-Ahead DSM for Expected Cost Minimization

5.B.1 Proof of Lemma 5.2

The lemma follows from the application of the results in [74, 116, 117] to the specific GNEP $\mathscr{G} = \big\langle \Theta_{\mathbf{x}}, \mathbf{f} \big\rangle$ in (5.21). More specifically, a solution of the VI($\Theta_{\mathbf{x}}, \mathbf{F}$) is a solution of the GNEP if the following conditions hold [74, Lem. 4.2], [116]: (a) the strategy sets $\Omega_{\mathbf{x}_n}$ in (5.5) are closed and convex; (b) the objective functions $\mathsf{f}_n(\mathbf{x}_n, \tilde{\mathbf{l}}_{-n})$ in (5.18) are convex on $\Omega_{\mathbf{x}_n}$ for any feasible $\tilde{\mathbf{l}}_{-n}$; (c) the coupling function $\mathbf{q}(\mathbf{x})$ is (jointly) convex in $\mathbf{x}$. Condition (a) is immediately satisfied if the sets $\Omega_{\mathbf{g}_n}$ and $\Omega_{\mathbf{s}_n}$ are closed and convex (note that $\Omega_{\tilde{\mathbf{e}}_n}$ in (5.2) is convex by definition). Likewise, condition (c) is also fulfilled for $\mathbf{q}^{(\min)}(\mathbf{x})$ and $\mathbf{q}^{(\max)}(\mathbf{x})$ defined as in (5.18). Hence, we only need to verify (b), i.e., the convexity of $\mathsf{f}_n(\mathbf{x}_n, \tilde{\mathbf{l}}_{-n})$.

Observe that its Hessian matrix $\mathbf{H}_{nn}(\mathbf{x})$ is obtained as

$$\mathbf{H}_{nn}(\mathbf{x}) = \mathrm{Diag}\big(\mathbf{H}_{nn}\big(\mathbf{x}(h)\big)\big)_{h=1}^{H} \quad (5.38)$$

with block elements $\mathbf{H}_{nn}\big(\mathbf{x}(h)\big) \triangleq \nabla^2_{\mathbf{x}_n(h)\mathbf{x}_n(h)} \mathsf{f}_n(\mathbf{x}_n, \tilde{\mathbf{l}}_{-n})$ given by

$$\mathbf{H}_{nn}\big(\mathbf{x}(h)\big) = K_h \begin{pmatrix} 2\phi'_{e_n(h)}\big(\tilde{e}_n(h)\big) + \tilde{L}(h)\phi''_{e_n(h)}\big(\tilde{e}_n(h)\big) & -\phi'_{e_n(h)}\big(\tilde{e}_n(h)\big) - 1 & \phi'_{e_n(h)}\big(\tilde{e}_n(h)\big) + 1 \\ -\phi'_{e_n(h)}\big(\tilde{e}_n(h)\big) - 1 & 2 + W''_n\big(g_n(h)\big) & -2 \\ \phi'_{e_n(h)}\big(\tilde{e}_n(h)\big) + 1 & -2 & 2 \end{pmatrix} \quad (5.39)$$

with $\phi_{e_n(h)}(x)$ defined in (5.16), and

$$\phi'_{e_n(h)}(x) \triangleq \frac{d\phi_{e_n(h)}(x)}{dx} = (\alpha_h + \beta_h)F_{e_n(h)}(x) - \alpha_h \tag{5.40}$$

$$\phi''_{e_n(h)}(x) \triangleq \frac{d^2\phi_{e_n(h)}(x)}{dx^2} = (\alpha_h + \beta_h)f_{e_n(h)}(x). \tag{5.41}$$

Hence, $\mathsf{f}_n(\mathbf{x}_n, \tilde{\mathbf{l}}_{-n})$ is convex if the partial Hessian matrices $\big\{\mathbf{H}_{nn}\big(\mathbf{x}(h)\big)\big\}_{h=1}^{H}$ are positive semidefinite. Assuming that $W_n(x)$ is convex, i.e., that $W''_n(x) \geq 0$, the smallest eigenvalue of $\mathbf{H}_{nn}(\mathbf{x}(h))$ (disregarding the null eigenvalue) is given by

$$\frac{K_h}{2}\big(2\phi'_{e_n(h)}\big(\tilde{e}_n(h)\big) + \tilde{L}(h)\phi''_{e_n(h)}\big(\tilde{e}_n(h)\big) + 4\big) - \frac{K_h}{2}\Big(2\big(2\phi'_{e_n(h)}\big(\tilde{e}_n(h)\big) + 2\big)^2 + \big(2\phi'_{e_n(h)}\big(\tilde{e}_n(h)\big) + \tilde{L}(h)\phi''_{e_n(h)}\big(\tilde{e}_n(h)\big) - 4\big)^2\Big)^{1/2}. \tag{5.42}$$

It thus follows that $\mathbf{H}_{nn}\big(\mathbf{x}(h)\big) \succeq 0$ if

$$2\tilde{L}(h)\phi''_{e_n(h)}\big(\tilde{e}_n(h)\big) \geq \big(\phi'_{e_n(h)}\big(\tilde{e}_n(h)\big) - 1\big)^2. \tag{5.43}$$

Finally, since $-\alpha_h \leq \phi'_{e_n(h)}(x) \leq \beta_h$ and $\tilde{L}(h) \geq L^{(\min)}(h)$ (see Constraint 1), (5.43) is satisfied whenever $\chi_n^{(\min)}$ and $\chi_n^{(\max)}$ are chosen as in Lemma 5.2(c). □

5.B.2 Bidding Strategy Set for Multimodal Distributions

When the pdf of the per-slot net energy consumption is multimodal, there may be multiple intervals in which Lemma 5.2(c) is satisfied. In this appendix, we present a heuristic method to determine the best values of $\chi_n^{(\min)}(h)$ and $\chi_n^{(\max)}(h)$, while guaranteeing the convexity of the bidding strategy sets.

Let us assume that user $n \in \mathcal{N}$ is a price taker, i.e., his load profile does not significantly affect the resulting energy prices [114]. Under this premise, the only variable term in $\mathsf{f}_n(\mathbf{x}_n, \mathbf{l}_{-n})$ in (5.18) is given, at each time-slot h, by $\phi_{e_n(h)}(x)$ in (5.16), where we have omitted the production and storage strategies. It is straightforward to see that $\phi_{e_n(h)}(x)$ is convex $\forall x$ and has a minimum at $\tilde{e}_n^{(0)}(h)$, where $\tilde{e}_n^{(0)}(h)$ is such that $F_{e_n(h)}\big(\tilde{e}_n^{(0)}(h)\big) = \alpha_h/(\alpha_h + \beta_h)$. At this point, we either have that: i) $f_{e_n(h)}\big(\tilde{e}_n^{(0)}(h)\big)$ satisfies condition (5.23), and $\chi_n^{(\min)}(h)$ and $\chi_n^{(\max)}(h)$ are chosen as the limit points around $\tilde{e}_n^{(0)}(h)$ that fulfill (5.23); or ii) $f_{e_n(h)}\big(\tilde{e}_n^{(0)}(h)\big)$ does not satisfy condition (5.23), and $\chi_n^{(\min)}(h)$ and $\chi_n^{(\max)}(h)$ can be found heuristically by searching intervals in the neighborhood of $\tilde{e}_n^{(0)}(h)$ such that (5.23) holds. In this case, when $\bar{e}_n(h) \geq 0$, it can be easily shown that $\mathsf{f}_n(\mathbf{x}_n, \mathbf{l}_{-n})$ increases for any $\tilde{e}_n(h) \geq \tilde{e}_n^{(0)}(h)$ and, hence, it is always better to chose the interval on the right-hand side of $\tilde{e}_n^{(0)}(h)$. Unfortunately, when $\bar{e}_n(h) < 0$, we do not have such clue.

5.B.3 Proof of Theorem 5.1

The proof of the convergence of Algorithm 5.1 is based on the connection between the augmented NEP (5.24) and VIs, and on recent results on monotone VIs [76]. Next, we first establish the connection with VIs, and then we prove the theorem.

In the setting of Lemma 5.2, the NEP (5.24) is equivalent to the partitioned VI($\Theta_{\mathbf{x},\boldsymbol{\lambda}}, \mathbf{F}_{\boldsymbol{\lambda}}$), with $\Theta_{\mathbf{x},\boldsymbol{\lambda}} \triangleq \prod_{n=1}^{N} \Omega_{\mathbf{x}_n} \times \mathbb{R}_+^{2H}$ and $\mathbf{F}_{\boldsymbol{\lambda}}(\mathbf{x}, \boldsymbol{\lambda})$ defined as

$$\mathbf{F}_{\boldsymbol{\lambda}}(\mathbf{x}, \boldsymbol{\lambda}) \triangleq \begin{pmatrix} \mathbf{F}(\mathbf{x}) + \boldsymbol{\lambda}^{\mathrm{T}} \nabla_{\mathbf{x}} \mathbf{q}(\mathbf{x}) \\ -\mathbf{q}(\mathbf{x}) \end{pmatrix}. \tag{5.44}$$

Solving the NEP is then equivalent to solving the VI($\Theta_{\mathbf{x},\boldsymbol{\lambda}}, \mathbf{F}_{\boldsymbol{\lambda}}$). Since, in the above setup, the VI($\Theta_{\mathbf{x},\boldsymbol{\lambda}}, \mathbf{F}_{\boldsymbol{\lambda}}$) is monotone, we can hinge on distributed regularization techniques for monotone partitioned VIs [76]. More specifically, instead of solving the original VI directly, one can more easily solve, in a distributed fashion, a sequence of regularized strongly monotone VIs in the form $\mathrm{VI}\big(\Theta_{\mathbf{x},\boldsymbol{\lambda}}, \mathbf{F}_{\boldsymbol{\lambda}} + \tau(\mathbf{I} - \mathbf{z}^{(i)})\big)$ with $\mathbf{z}^{(i)} \triangleq (\mathbf{x}^{(i)}, \boldsymbol{\lambda}^{(i)})$. In fact, Algorithm 5.1 is an instance of the PDA algorithm in [86, Alg. 1] applied to the aforementioned sequence of strongly monotone regularized VIs. According to [74, Th. 4.3], its convergence is guaranteed if the following conditions are satisfied: (a) the mapping function $\mathbf{F}_{\boldsymbol{\lambda}}(\mathbf{x}, \boldsymbol{\lambda})$ in (5.44) is monotone on $\Theta_{\mathbf{x},\boldsymbol{\lambda}}$; (b) the regularization parameter τ is chosen such that the $(N+1) \times (N+1)$ matrix

$$\bar{\boldsymbol{\Upsilon}}_{\mathbf{F},\tau} \triangleq \begin{pmatrix} \boldsymbol{\Upsilon}_{\mathbf{F}} + \tau \mathbf{I}_N & -\mathbf{w} \\ -\mathbf{w}^{\mathrm{T}} & \tau \end{pmatrix} \tag{5.45}$$

is a P-matrix [74, Cor. 4.2], where $\boldsymbol{\Upsilon}_{\mathbf{F}}$ is given by

$$[\boldsymbol{\Upsilon}_{\mathbf{F}}]_{nm} \triangleq \begin{cases} \upsilon_n^{(\min)}, & \text{if } n = m \\ -\upsilon_{nm}^{(\max)}, & \text{if } n \neq m \end{cases} \tag{5.46}$$

$$\upsilon_n^{(\min)} \triangleq \min_{\mathbf{x} \in \Omega_{\mathbf{x}}} \lambda_{\min}\big\{\bar{\mathbf{J}}_{nn}(\mathbf{x})\big\} \tag{5.47}$$

$$\upsilon_{nm}^{(\max)} \triangleq \max_{\mathbf{x} \in \Omega_{\mathbf{x}}} \big\|\bar{\mathbf{J}}_{nm}(\mathbf{x})\big\| \tag{5.48}$$

where $\lambda_{\min}\{\cdot\}$ denotes the smallest eigenvalue of the matrix argument, $\bar{\mathbf{J}}_{nn}(\mathbf{x})$ and $\bar{\mathbf{J}}_{nm}(\mathbf{x})$ are the partial Jacobian matrices defined next in (5.50) and (5.51), respectively, and $\mathbf{w} \triangleq \big(\sup_{\mathbf{z}_n \in \Omega_{\mathbf{x}_n}} \|\nabla_{\mathbf{x}_n} \mathbf{q}_n(\mathbf{z}_n)\|_2\big)_{n=1}^{N}$; (c) $\rho^{(i)}$ is chosen such that $\{\rho^{(i)}\} \subset [R_m, R_M]$, with $0 < R_m < R_M < 2$.

Proof of Theorem 5.1(a): The mapping function $\mathbf{F}_{\boldsymbol{\lambda}}(\mathbf{x}, \boldsymbol{\lambda})$ is monotone on $\Theta_{\mathbf{x},\boldsymbol{\lambda}}$ if $\mathbf{F}(\mathbf{x})$ is so on $\Omega_{\mathbf{x}}$ [74, Prop. 4.4].

We have that $\mathbf{F}(\mathbf{x})$ is monotone on $\Omega_{\mathbf{x}}$ if the symmetric part of its Jacobian $\mathsf{J}\mathbf{F}(\mathbf{x})$ is positive

semidefinite on $\Omega_{\mathbf{x}}$, i.e., $\frac{1}{2}\big(\mathsf{J}\mathbf{F}(\mathbf{x})+\mathsf{J}\mathbf{F}^{\mathrm{T}}(\mathbf{x})\big) \succeq 0$, $\forall \mathbf{x} \in \Omega_{\mathbf{x}}$. We write the symmetric part of $\mathsf{J}\mathbf{F}(\mathbf{x})$ as

$$\bar{\mathbf{J}}(\mathbf{x}) \triangleq \frac{1}{2}\big(\mathsf{J}\mathbf{F}(\mathbf{x}) + \mathsf{J}\mathbf{F}^{\mathrm{T}}(\mathbf{x})\big) = \big(\bar{\mathbf{J}}_{nm}(\mathbf{x})\big)_{n,m=1}^{N} \tag{5.49}$$

with block elements given by

$$\bar{\mathbf{J}}_{nn}(\mathbf{x}) \triangleq \nabla^2_{\mathbf{x}_n\mathbf{x}_n} \mathsf{f}_n(\mathbf{x}_n, \tilde{\mathbf{I}}_{-n}) = \mathrm{Diag}\big(\mathbf{H}_{nn}\big(\mathbf{x}(h)\big)\big)_{h=1}^{H} \tag{5.50}$$

$$\bar{\mathbf{J}}_{nm}(\mathbf{x}) \triangleq \frac{1}{2}\big(\nabla^2_{\mathbf{x}_n\mathbf{x}_m} \mathsf{f}_n(\mathbf{x}_n, \tilde{\mathbf{I}}_{-n}) + \nabla^2_{\mathbf{x}_m\mathbf{x}_n} \mathsf{f}_m(\mathbf{x}_m, \tilde{\mathbf{I}}_{-m})^{\mathrm{T}}\big) = \mathrm{Diag}\big(\bar{\mathbf{J}}_{nm}\big(\mathbf{x}(h)\big)\big)_{h=1}^{H}, \quad n \neq m \tag{5.51}$$

where $\mathbf{H}_{nn}\big(\mathbf{x}(h)\big)$ is given in (5.39) and $\bar{\mathbf{J}}_{nm}\big(\mathbf{x}(h)\big)$ is defined as

$$\bar{\mathbf{J}}_{nm}\big(\mathbf{x}(h)\big) \triangleq \frac{K_h}{2} \begin{pmatrix} \phi'_{e_n(h)}\big(\tilde{e}_n(h)\big) + \phi'_{e_m(h)}\big(\tilde{e}_m(h)\big) & -\phi'_{e_n(h)}\big(\tilde{e}_n(h)\big) - 1 & \phi'_{e_n(h)}\big(\tilde{e}_n(h)\big) + 1 \\ -\phi'_{e_m(h)}\big(\tilde{e}_m(h)\big) - 1 & 2 & -2 \\ \phi'_{e_m(h)}\big(\tilde{e}_m(h)\big) + 1 & -2 & 2 \end{pmatrix}. \tag{5.52}$$

In order to guarantee that $\mathbf{z}^{\mathrm{T}}\bar{\mathbf{J}}(\mathbf{x})\mathbf{z} \geq 0, \forall \mathbf{z} \in \mathbb{R}^{3HN}$, we decompose the vector $\mathbf{z}$ as $\mathbf{z} \triangleq \big(\mathbf{z}(h)\big)_{h=1}^{H}$, where $\mathbb{R}^{3N} \ni \mathbf{z}(h) \triangleq \big(\mathbf{z}_n(h)\big)_{n=1}^{N}$ and $\mathbf{z}_n(h) \triangleq \big(z_{\tilde{e},n}(h), z_{g,n}(h), z_{s,n}(h)\big)$; then, we can write $\mathbf{z}^{\mathrm{T}}\bar{\mathbf{J}}(\mathbf{x})\mathbf{z}$ as

$$\mathbf{z}^{\mathrm{T}}\bar{\mathbf{J}}(\mathbf{x})\mathbf{z} = \sum_{h=1}^{H} \mathbf{z}^{\mathrm{T}}(h)\bar{\mathbf{J}}\big(\mathbf{x}(h)\big)\mathbf{z}(h) \tag{5.53}$$

with $\bar{\mathbf{J}}\big(\mathbf{x}(h)\big) \triangleq \big(\bar{\mathbf{J}}_{nm}\big(\mathbf{x}(h)\big)\big)_{n,m=1}^{N}$. Now, the proof reduces to ensuring that $\mathbf{z}(h)^{\mathrm{T}}\bar{\mathbf{J}}\big(\mathbf{x}(h)\big)\mathbf{z}(h) \geq 0$, $\forall \mathbf{z}(h) \in \mathbb{R}^{3N}$, $\forall h$.

For the sake of notation, in the following we omit the time-slot index h in the components of the auxiliary variable $\mathbf{z}(h)$. After some manipulations, it holds that

$$\begin{aligned} &\big(1/K_h\big)\mathbf{z}^{\mathrm{T}}(h)\bar{\mathbf{J}}\big(\mathbf{x}(h)\big)\mathbf{z}(h) \\ &\quad= \Big(\sum_{n\in\mathcal{N}} z_{gs,n}\Big)^2 + \sum_{n\in\mathcal{N}} \Big(\tilde{L}(h)\phi''_{e_n(h)}\big(\tilde{e}_n(h)\big) - \frac{1}{4}\big(\phi'_{e_n(h)}\big(\tilde{e}_n(h)\big) - 1\big)^2\Big) z^2_{\tilde{e},n} \\ &\qquad+ \Big(\sum_{n\in\mathcal{N}} \big(\phi'_{e_n(h)}\big(\tilde{e}_n(h)\big) + 1\big) z_{\tilde{e},n}\Big)\Big(\sum_{m\in\mathcal{N}} z_{gs,m}\Big) + \Big(\sum_{n\in\mathcal{N}} \phi'_{e_n(h)}\big(\tilde{e}_n(h)\big) z_{\tilde{e},n}\Big)\Big(\sum_{m\in\mathcal{N}} z_{\tilde{e},m}\Big) \\ &\qquad+ \sum_{n\in\mathcal{N}} \Big(\frac{1}{2}\big(\phi'_{e_n(h)}\big(\tilde{e}_n(h)\big) + 1\big) z_{\tilde{e},n} + z_{gs,n}\Big)^2 + \sum_{n\in\mathcal{N}} W''_n\big(g_n(h)\big) z^2_{g,n} \end{aligned} \tag{5.54}$$

where we have introduced $z_{gs,n} \triangleq z_{s,n} - z_{g,n}$. Recall that, under Lemma 5.2(b), $W''_n\big(g_n(h)\big) \geq 0$, $\forall n \in \mathcal{G}$, so that the term $\sum_{n\in\mathcal{N}} W''_n\big(g_n(h)\big) z^2_{g,n} \geq 0$ can be ignored.

Now, observe that $-\alpha_h \leq \phi'_{e_n(h)}(x) \leq \beta_h$, which implies $\big|\phi'_{e_n(h)}(x)\big| \leq 1$, and let us define

$$\varphi_n^{(\min)}(h) \triangleq \min_{\chi_n^{(\min)}(h)\leq x\leq \chi_n^{(\max)}(h)} \phi'_{e_n(h)}(x) \geq -\alpha_h \tag{5.55}$$

$$\varphi_n^{(\max)}(h) \triangleq \max_{\chi_n^{(\min)}(h)\leq x\leq \chi_n^{(\max)}(h)} \phi'_{e_n(h)}(x) \leq \beta_h \tag{5.56}$$

$$\varphi_n^{(\mathrm{abs})}(h) \triangleq \max\big(\big|\varphi_n^{(\min)}(h)\big|, \big|\varphi_n^{(\max)}(h)\big|\big) \tag{5.57}$$

and the sets $\mathcal{N}^+ \triangleq \Big\{n \ : \ z_{\tilde{e},n}\Big(\sum_{m\in\mathcal{N}} z_{gs,m}\Big) \geq 0\Big\}$ and $\mathcal{N}^- \triangleq \Big\{n : z_{\tilde{e},n}\Big(\sum_{m\in\mathcal{N}} z_{gs,m}\Big) < 0\Big\}$. Hence, it holds that

$$\begin{aligned}
&\Big(\sum_{n\in\mathcal{N}} \big(\phi'_{e_n(h)}\big(\tilde{e}_n(h)\big)+1\big) z_{\tilde{e},n}\Big)\Big(\sum_{m\in\mathcal{N}} z_{gs,m}\Big) \\
&\quad \geq \big(\varphi_n^{(\min)}(h)+1\big)\Big(\sum_{n\in\mathcal{N}^+} z_{\tilde{e},n}\Big)\Big|\sum_{m\in\mathcal{N}} z_{gs,m}\Big| - \big(\varphi_n^{(\max)}(h)+1\big)\Big(\sum_{n\in\mathcal{N}^-} |z_{\tilde{e},n}|\Big)\Big|\sum_{m\in\mathcal{N}} z_{\tilde{e},m}\Big| \qquad (5.58)\\
&\quad \geq \big(\varphi_n^{(\min)}(h) - \varphi_n^{(\max)}(h)\big)\Big(\sum_{n\in\mathcal{N}} |z_{\tilde{e},n}|\Big)\Big|\sum_{m\in\mathcal{N}} z_{\tilde{e},m}\Big| \qquad (5.59)
\end{aligned}$$

and

$$\begin{aligned}
\Big(\sum_{n\in\mathcal{N}} \phi'_{e_n(h)}\big(\tilde{e}_n(h)\big) z_{\tilde{e},n}\Big)\Big(\sum_{m\in\mathcal{N}} z_{\tilde{e},m}\Big) &\geq -\varphi_n^{(\mathrm{abs})}(h)\Big(\sum_{n\in\mathcal{N}} |z_{\tilde{e},n}|\Big)\Big|\sum_{m\in\mathcal{N}} z_{\tilde{e},m}\Big| \qquad (5.60)\\
&\geq -\varphi_n^{(\mathrm{abs})}(h)\Big(\sum_{n\in\mathcal{N}} |z_{\tilde{e},n}|\Big)^2. \qquad (5.61)
\end{aligned}$$

Now, if $\Big|\sum_{n\in\mathcal{N}} z_{gs,n}\Big| \leq \sum_{n\in\mathcal{N}} |z_{\tilde{e},n}|$, we obtain

$$\begin{aligned}
&\big(1/K_h\big)\mathbf{z}^{\mathrm{T}}(h)\bar{\mathbf{J}}\big(\mathbf{x}(h)\big)\mathbf{z}(h) \\
&\quad \geq \Big(\sum_{n\in\mathcal{N}} z_{gs,n}\Big)^2 + \sum_{n\in\mathcal{N}} \Big(\tilde{L}(h)\phi''_{e_n(h)}\big(\tilde{e}_n(h)\big) - \frac{1}{4}\big(\phi'_{e_n(h)}\big(\tilde{e}_n(h)\big)-1\big)^2 \\
&\qquad - N\big(\varphi_n^{(\mathrm{abs})}(h) + \varphi_n^{(\max)}(h) - \varphi_n^{(\min)}(h)\big)\Big) z_{\tilde{e},n}^2 + \sum_{n\in\mathcal{N}} \Big(\frac{1}{2}\big(\phi'_{e_n(h)}\big(\tilde{e}_n(h)\big)+1\big) z_{\tilde{e},n} + z_{gs,n}\Big)^2.
\end{aligned} \tag{5.62}$$

Consequently, $\mathbf{z}^{\mathrm{T}}(h)\bar{\mathbf{J}}\big(\mathbf{x}(h)\big)\mathbf{z}(h) \geq 0$ if

$$\tilde{L}(h)\phi''_{e_n(h)}\big(\tilde{e}_n(h)\big) \geq \frac{1}{4}\big(\varphi_n^{(\min)}(h)-1\big)^2 + N\big(\varphi_n^{(\mathrm{abs})}(h)+\varphi_n^{(\max)}(h)-\varphi_n^{(\min)}(h)\big), \quad \forall n \in \mathcal{N}. \tag{5.63}$$

Otherwise, if $\Big|\sum_{n\in\mathcal{N}} z_{gs,n}\Big| > \sum_{n\in\mathcal{N}} \big|z_{\tilde{e},n}\big|$, we have that

$$\begin{aligned}
&\big(1/K_h\big)\mathbf{z}^{\mathrm{T}}(h)\bar{\mathbf{J}}\big(\mathbf{x}(h)\big)\mathbf{z}(h)\\
&\geq \sum_{n\in\mathcal{N}} \Big(\tilde{L}(h)\phi''_{e_n(h)}\big(\tilde{e}_n(h)\big) - \frac{1}{4}\big(\phi'_{e_n(h)}\big(\tilde{e}_n(h)\big)-1\big)^2 - N\varphi_n^{(\mathrm{abs})}(h)\Big) z_{\tilde{e},n}^2\\
&\quad + \big(1-\varphi_n^{(\max)}(h)-\varphi_n^{(\min)}(h)\big)\Big(\sum_{n\in\mathcal{N}} z_{gs,n}\Big)^2 + \sum_{n\in\mathcal{N}}\Big(\frac{1}{2}\big(\phi'_{e_n(h)}\big(\tilde{e}_n(h)\big)+1\big)z_{\tilde{e},n} + z_{gs,n}\Big)^2 \qquad (5.64)
\end{aligned}$$

and, therefore, $\mathbf{z}^{\mathrm{T}}(h)\bar{\mathbf{J}}\big(\mathbf{x}(h)\big)\mathbf{z}(h) \geq 0$ if both the following conditions are fulfilled, $\forall n \in \mathcal{N}$:

$$\tilde{L}(h)\phi''_{e_n(h)}\big(\tilde{e}_n(h)\big) \geq \frac{1}{4}\big(\varphi_n^{(\min)}(h)-1\big)^2 + N\varphi_n^{(\mathrm{abs})}(h) \qquad (5.65)$$

$$\varphi_n^{(\max)}(h) - \varphi_n^{(\min)}(h) \leq 1. \qquad (5.66)$$

Note that condition (5.63) is more restrictive than (5.65) and, since $\tilde{L}(h) \geq L^{(\min)}(h)$ (from Constraint 1), we readily obtain the lower bound in (5.26). On the other hand, the condition in Theorem 5.1(a.3) comes from substituting the definitions (5.55)–(5.57) into (5.66). □

Proof of Theorem 5.1(b): Here, we determine the value of τ that ensures the P-matrix property of $\bar{\boldsymbol{\Upsilon}}_{\mathbf{F},\tau}$ in (5.45).

In Appendix 5.B.1, we have shown that, under the conditions of Lemma 5.2, $\mathsf{f}_n(\mathbf{x}_n, \tilde{\mathbf{l}}_{-n})$ is convex on $\Omega_{\mathbf{x}_n}$: this implies that $\bar{\mathbf{J}}_{nn}(\mathbf{x}) \succeq 0$, $\forall \mathbf{x}_n \in \Omega_{\mathbf{x}_n}$ and $\forall n \in \mathcal{N}$. Hence, we can already state that $\upsilon_n^{(\min)} \geq 0$ (c.f. (5.47)). Let us thus examine $\upsilon_{nm}^{(\max)} = \max_{\mathbf{x}\in\Omega_{\mathbf{x}}} \big\|\bar{\mathbf{J}}_{nm}(\mathbf{x})\big\|$, with $\bar{\mathbf{J}}_{nm}(\mathbf{x}) = \mathrm{Diag}\big(\bar{\mathbf{J}}_{nm}\big(\mathbf{x}(h)\big)\big)_{h=1}^{H}$ and $\bar{\mathbf{J}}_{nm}\big(\mathbf{x}(h)\big)$ defined as in (5.52): it holds that

$$\max_{\mathbf{x}\in\Omega_{\mathbf{x}}} \big\|\bar{\mathbf{J}}_{nm}(\mathbf{x})\big\| \leq \max_h \Big(\max_{\mathbf{x}\in\Omega_{\mathbf{x}}} \lambda_{\max}\big\{\bar{\mathbf{J}}_{nm}\big(\mathbf{x}(h)\big)\big\}\Big) \qquad (5.67)$$

where $\lambda_{\max}\{\cdot\}$ denotes the largest eigenvalue of the matrix argument. Hence, we have that

$$\begin{aligned}
\lambda_{\max}\big\{\bar{\mathbf{J}}_{nm}\big(\mathbf{x}(h)\big)\big\} &= K_h\Big(1 + \frac{1}{4}\Big(\phi'_{e_n(h)}\big(\tilde{e}_n(h)\big) + \phi'_{e_m(h)}\big(\tilde{e}_m(h)\big)\Big)\\
&\quad + \frac{1}{4}\Big(\phi'_{e_n(h)}\big(\tilde{e}_n(h)\big)^2 + \phi'_{e_m(h)}\big(\tilde{e}_m(h)\big)^2 + 10\phi'_{e_n(h)}\big(\tilde{e}_n(h)\big)\phi'_{e_m(h)}\big(\tilde{e}_m(h)\big) + 24\Big)^{1/2}\Big) \qquad (5.68)
\end{aligned}$$

with $\phi'_{e_n(h)}(x)$ defined in (5.40), and, using (5.56)–(5.57), we obtain

$$\begin{aligned}
(5.68) \leq& K_h\Big(1 + \frac{1}{4}\Big(\varphi_n^{(\max)}(h) + \varphi_m^{(\max)}(h)\Big)\\
&+ \frac{1}{4}\Big(\varphi_n^{(\mathrm{abs})}(h)^2 + \varphi_m^{(\mathrm{abs})}(h)^2 + 10\varphi_n^{(\mathrm{abs})}(h)\varphi_m^{(\mathrm{abs})}(h) + 24\Big)^{1/2}\Big) \qquad (5.69)\\
\leq& K_h\Big(1 + \frac{\alpha_h}{2} + \frac{\sqrt{3}}{2}\big(\max(\alpha_h,\beta_h)^2 + 2\big)^{1/2}\Big) < 3K_h. \qquad (5.70)
\end{aligned}$$

Therefore, combining the previous results, we have that

$$\upsilon_n^{(\min)} \geq 0 \tag{5.71}$$

$$\upsilon_{nm}^{(\max)} < 3\big(\max_h K_h\big). \tag{5.72}$$

Now, observe that $\big(-\mathbf{q}^{(\min)}(\mathbf{x})\big)^+ \perp \big(-\mathbf{q}^{(\max)}(\mathbf{x})\big)^+$, where $\mathbf{a} \perp \mathbf{b}$ means $\mathbf{a}^{\mathrm{T}}\mathbf{b} = \mathbf{0}$, with $\mathbf{q}^{(\min)}(\mathbf{x})$ and $\mathbf{q}^{(\max)}(\mathbf{x})$ defined as in (5.18). Now, let us introduce $\boldsymbol{\omega} \triangleq (-\boldsymbol{\omega}^{(\min)}, \boldsymbol{\omega}^{(\max)}) \otimes \boldsymbol{\delta}$, where $\boldsymbol{\omega}^{(\min)}$ and $\boldsymbol{\omega}^{(\max)}$ are H-dimensional vectors with elements

$$[\boldsymbol{\omega}^{(\min)}]_h \triangleq \begin{cases} 0 & \text{if } \big[\mathbf{q}^{(\min)}(\mathbf{x})\big]_h \leq 0 \\ 1 & \text{if } \big[\mathbf{q}^{(\min)}(\mathbf{x})\big]_h > 0 \end{cases} \tag{5.73}$$

$$[\boldsymbol{\omega}^{(\max)}]_h \triangleq \begin{cases} 0 & \text{if } \big[\mathbf{q}^{(\max)}(\mathbf{x})\big]_h \leq 0 \\ 1 & \text{if } \big[\mathbf{q}^{(\max)}(\mathbf{x})\big]_h > 0. \end{cases} \tag{5.74}$$

Since $\boldsymbol{\omega}^{(\min)} \perp \boldsymbol{\omega}^{(\max)}$, we have that $[\mathbf{w}]_n = \sqrt{\boldsymbol{\omega}^{\mathrm{T}}\boldsymbol{\omega}} \leq \sqrt{3H}$. Hence, we can state that $\bar{\boldsymbol{\Upsilon}}_{\mathbf{F},\tau} \succeq \widetilde{\boldsymbol{\Upsilon}}_{\mathbf{F},\tau}$, where

$$\big[\widetilde{\boldsymbol{\Upsilon}}_{\mathbf{F}}\big]_{nm} \triangleq \begin{cases} \tau, & \text{if } n = m \\ -3\max_h K_h, & \text{if } n \neq m \text{ and } n, m \neq N+1 \\ -\sqrt{3H}, & \text{otherwise.} \end{cases} \tag{5.75}$$

By [74, Prop. 4.3], the matrix $\widetilde{\boldsymbol{\Upsilon}}_{\mathbf{F},\tau}$, and thus $\bar{\boldsymbol{\Upsilon}}_{\mathbf{F},\tau}$, is a P-matrix if, for some $w > 0$, the following conditions hold:

$$\tau > 3(N-1)\max_h K_h + w\sqrt{3H} \tag{5.76}$$

$$\tau > N\frac{1}{w}\sqrt{3H}. \tag{5.77}$$

Evidently, the value of w that minimizes τ satisfies

$$3(N-1)\max_h K_h + w\sqrt{3H} = N\frac{1}{w}\sqrt{3H}. \tag{5.78}$$

and, substituting the obtained w back into (5.76), the value of τ in (5.27) follows, as stated in Theorem 5.1(b). □

6

Concluding Remarks

This dissertation has focused on the analytical evaluation of DSM methods in smart grid contexts where the demand-side is a multiuser system of interacting active consumers. Particular emphasis has been placed on DSM approaches based on dispatchable DG and DS, for which the current literature does not provide adequate theoretical insights. In contrast to invasive and onerous centralized solution methods, we have developed efficient distributed schemes, with an eye to key issues such as convergence speed, information exchange, scalability, and privacy. Analytical studies of these approaches from an optimization perspective have determined the conditions ensuring the existence of optimal solutions and the convergence of the proposed algorithms. Lastly, numerical results are reported to corroborate the outlined DSM methodologies in practical situations, providing concrete incentives for the active and voluntary participation of the end users in the optimization of the demand-side.

6.1 Summary of Results

Let us give a detailed summary of the main results contained in this PhD thesis.

i) We have devised accurate demand-side models that constitute a guideline for representing realistic DSM scenarios where dispatchable DG and DS are employed and for studying their impact at the level of the end users and on the whole electricity infrastructure: this will hopefully pave the way for a more extensive deployment of dispatchable DG and DS under the DSM paradigm.

ii) For competitive market environments, we have tackled the demand-side optimization from a user-oriented perspective: we have formulated the DSM optimization problem using non-cooperative game theory (NEPs and GNEPs), whose solution analysis has been addressed

building on the more general variational inequality framework.

iii) For externally regulated market environments, we have adopted a holistic-based design, allowing some cooperation among the end users: the objective of the whole demand-side has been expressed as a nonconvex sum-utility function and its solution analysis has been addressed building on decomposition methods based on partial linearizations.

iv) The distributed algorithms resulting from both approaches do not require each user to know the individual strategies of the others, thus preserving the privacy and limiting the overall communication overhead; furthermore, despite being specifically designed for optimizing the dispatchable DG and DS strategies, they are very general and can accommodate other DSM techniques (such as ECS).

v) The noncooperative schemes can be totally asynchronous, can incorporate global constraints, but generally require slightly more restrictive (sufficient) convergence conditions than the cooperative ones; the latter, in turn, allow to achieve a better, or at least equal, performance but are characterized by a parallel strategy update and need to be externally regulated so as to avoid selfish deviations by the users.

vi) We have defined and examined deterministic day-ahead and stochastic day-ahead/real-time energy market models. For both formulations, we have used specific energy cost functions, whereas the former has also been analyzed under a generalized pricing model.

vii) Simulations on realistic scenarios have shown that the proposed day-ahead DSM mechanisms consistently diminish the users' (actual or expected) monetary expenses while fulfilling the relative (local and global) constraints: at a higher level, this results in a flattened load curve, which lowers the generation costs and enhances the robustness of the whole network; on the other hand, the real-time DSM methods reduce both the average value and the variance of the user's real-time monetary expense.

6.2 Future Research Lines

The signal processing community has already made a great research effort towards the accomplishment of the envisioned smart grid by investigating DSM and fomenting its implementation. Still, there are many open issues that need further investigation. This dissertation illustrates just some of many challenging problems related to DSM paradigm that call for advanced signal processing and distributed optimization techniques. In the following, we list some future research lines that would complement nicely the presented work.

i) This thesis, as most works in the smart grid literature, assumes that the real-time energy demand is always guaranteed by the supply-side. Neglecting this simplification, i.e., imposing that the demand must follow the supply precisely, means involving global constraints on the real-time aggregate load that are constantly changing (so as to follow the actual availability of renewable energy production) and that must be rapidly satisfied in order to comply with

the real-time market requirements.

ii) Including risk-aversion (e.g., by minimizing measures such as variance, value-at-risk, conditional value-at-risk, etc.) in energy trading problems in order to avoid high losses/dissatisfaction of the grid agents (both on the demand- and supply-side) is quite a common practice. Nonetheless, the uncertainty in the day-ahead bidding process affects the users' feasible sets the same way it does their objectives. Therefore, a further step would be to consider day-ahead DSM problems with stochastic strategy sets, with the users aiming at obtaining a day-ahead strategy that is also feasible in real-time with a certain probability, in order to limit the extent of eventual real-time adjustments.

iii) After thoroughly investigating day-ahead DSM approaches, the evolution of energy trading suggests focusing more on real-time market scenarios. In such context, the prices of electricity change rapidly and are not fully predictable even shortly before the dispatch time, thus introducing a further degree of uncertainty in the demand-side optimization. In addition, depending on the time granularity of the price updates, the amount of signaling can be significant and the users might receive corrupted price signals from the market regulator with high probability. These issues call for risk-averse and robust real-time DMS mechanisms that adequately exploit the responsive properties of dispatchable DG and DS devices.

References

[1] European Regulators Group for Electricity and Gas, "Position paper on smart grids: An ERGEG conclusions paper," Tech. Rep., June 2010.

[2] E. Santacana, G. Rackliffe, L. Tang, and X. Feng, "Getting smart," *IEEE Power Energy Mag.*, vol. 8, no. 2, pp. 41–48, Mar.-Apr. 2010.

[3] P. Varaiya, F. Wu, and J. Bialek, "Smart operation of smart grid: Risk-limiting dispatch," *Proc. IEEE*, vol. 99, no. 1, pp. 40–57, Jan. 2011.

[4] J. Fan and S. Borlase, "The evolution of distribution," *IEEE Power and Energy Mag.*, vol. 7, no. 2, pp. 63–68, 2009.

[5] X. Fang, S. Misra, G. Xue, and D. Yang, "Smart grid – The new and improved power grid: A survey," *IEEE Comm. Surveys Tutor.*, vol. 14, no. 4, pp. 944–980, 2012.

[6] G. Li, J. Shi, and X. Qu, "Modeling methods for GenCo bidding strategy optimization in the liberalized electricity spot market–A state-of-the-art review," *J. Energy*, vol. 36, no. 8, pp. 4686–4700, 2011.

[7] H. A. Hejazi, A. R. Araghi, B. Vahidi, S. H. Hosseinian, M. Abedi, and H. Mohsenian-Rad, "Independent distributed generation planning to profit both utility and DG investors," *IEEE Trans. Power Syst.*, vol. 28, no. 2, pp. 1170–1178, May 2013.

[8] N. Hatziargyriou, H. Asano, R. Iravani, and C. Marnay, "Microgrids," *IEEE Power Energy Mag.*, vol. 5, no. 4, pp. 78–94, July 2007.

[9] R. Lasseter, "Smart distribution: Coupled microgrids," *Proc. IEEE*, vol. 99, no. 6, pp. 1074–1082, 2011.

[10] G. W. Arnold, "Challenges and opportunities in smart grid: A position article," *Proc. IEEE*, vol. 99, no. 6, pp. 922–927, June 2011.

[11] Y. Atwa, E. El-Saadany, M. Salama, and R. Seethapathy, "Optimal renewable resources mix for distribution system energy loss minimization," *IEEE Trans. Power Syst.*, vol. 25, no. 1, pp. 360–370, Feb. 2010.

[12] M. Alizadeh, L. Xiao, W. Zhifang, A. Scaglione, and R. Melton, "Demand-side management in the smart grid: Information processing for the power switch," *IEEE Signal Process. Mag.*, vol. 29, no. 5, pp. 55–67, Sept. 2012.

[13] M. Ventosa, A. Baillo, A. Ramos, and M. Rivier, "Electricity market modeling trends," *Energy Policy*, vol. 33, no. 7, pp. 897–913, 2005.

[14] G. B. Giannakis, V. Kekatos, N. Gatsis, S. Kim, H. Zhu, and B. Wollenberg, "Monitoring and optimization for power grids: A signal processing perspective," *IEEE Signal Proc. Magazine, IEEE*, vol. 30, no. 5, pp. 107–128, Sept 2013.

[15] K. Mostafa, "Capturing the breadth of our activities," *IEEE Signal Process. Mag.*, vol. 27, no. 3, p. 4, May. 2010.

[16] H. Gharavi, A. Scaglione, M. Dohler, and X. Guan, "Special Section–Signal Processing Techniques for the Smart Grid," *IEEE Signal Process. Mag.*, vol. 29, no. 5, Sept. 2012.

[17] Y. F. Huang, S. Kishore, V. Koivunen, D. Mandic, and L. Tong, "Special Issue–Signal Processing in Smart Electric Power Grid," *IEEE J. Sel. Topics Signal Process.*, Dec. 2014 (to be published).

[18] N. Golmie, A. Scaglione, L. Lampe, and E. M. Yeh, "Special Issue–Smart Grid Communications," *IEEE J. Sel. Areas Comm.*, vol. 30, no. 6, July 2012.

[19] N. Golmie, A. Scaglione, L. Lampe, E. M. Yeh, S. Smith, and L. Tong, "Special Issue–Smart Grid Communications," *IEEE J. Sel. Areas Comm.*, vol. 31, no. 7, July 2013.

[20] L. Lampe, A. M. Tonello, and D. Shaver, "Special Section–Power Line Communications for Automation Networks and Smart Grid," *IEEE Comm. Mag.*, vol. 49, no. 12, Dec. 2011.

[21] J. Lloret, P. Lorenz, and A. Jamalipour, "Special Section–Communication Protocols and Algorithms for the Smart Grid," *IEEE Comm. Mag.*, vol. 50, no. 5, May 2012.

[22] R. Q. Hu, Y. Qian, H. Chen, and H. T. Mouftah, "Special Section–Cyber Security for Smart Grid Communications: Part I," *IEEE Comm. Mag.*, vol. 50, no. 8, Aug. 2012.

[23] ——, "Special Section–Cyber Security for Smart Grid Communications: Part II," *IEEE Comm. Mag.*, vol. 51, no. 1, Jan. 2013.

[24] J. N. De Souza, P. Lorenz, and A. Jamalipour, "Special Section–Ultimate Technologies and Advances for Future Smart Grid: UTASG," *IEEE Comm. Mag.*, vol. 51, no. 1, Jan. 2013.

[25] Y. Yan, Y. Qian, H. Sharif, and D. Tipper, "A survey on smart grid communication infrastructures: Motivations, requirements and challenges," *IEEE Comm. Surveys Tutor.*, vol. 15, no. 1, pp. 5–20, First 2013.

[26] Z. Fan, P. Kulkarni, S. Gormus, C. Efthymiou, G. Kalogridis, M. Sooriyabandara, Z. Zhu, S. Lambotharan, and W. H. Chin, "Smart grid communications: Overview of research challenges, solutions, and standardization activities," *IEEE Comm. Surveys Tutor.*, vol. 15, no. 1, pp. 21–38, First 2013.

[27] Z. M. Fadlullah, M. M. Fouda, N. Kato, A. Takeuchi, N. Iwasaki, and Y. Nozaki, "Toward intelligent machine-to-machine communications in smart grid," *IEEE Comm. Mag.*, vol. 49, no. 4, pp. 60–65, April 2011.

[28] S. Galli, A. Scaglione, and Z. Wang, "For the grid and through the grid: The role of power line communications in the smart grid," *Proc. IEEE*, vol. 99, no. 6, pp. 998–1027, June 2011.

[29] Y. Huang, S. Werner, J. Huang, N. Kashyap, and V. Gupta, "State estimation in electric power grids: Meeting new challenges presented by the requirements of the future grid," *IEEE Signal Process. Mag.*, vol. 29, no. 5, pp. 33–43, Sept 2012.

[30] G. Mateos and G. B. Giannakis, "Robust nonparametric regression via sparsity control with application to load curve data cleansing," *IEEE Trans. Signal Process.*, vol. 60, no. 4, pp. 1571–1584, Apr. 2012.

[31] ——, "Load curve data cleansing and imputation via sparsity and low rank," *IEEE Trans. Smart Grid*, vol. 4, no. 4, pp. 2347–2355, Dec. 2013.

[32] J. Yin, P. Sharma, I. Gorton, and B. Akyoli, "Large-scale data challenges in future power grids," in *IEEE Int. Symp. Service Oriented Syst. Eng. (SOSE)*, Mar. 2013, pp. 324–328.

[33] S. Chan, K. Tsui, H. Wu, Y. Hou, Y.-C. Wu, and F. Wu, "Load/price forecasting and managing demand response for smart grids: Methodologies and challenges," *IEEE Signal Process. Mag.*, vol. 29, no. 5, pp. 68–85, Sept. 2012.

[34] A. J. Conejo, M. Carrión, and J. M. Morales, *Decision making under uncertainty in electricity markets.* New York, NY, USA: Springer-Verlag Inc., 2010.

[35] J. P. Luna, C. Sagastizábal, and M. Solodov, "Complementarity and game-theoretical models for equilibria in energy markets: Deterministic and risk-averse formulations," in *Complementarity Modeling in Energy Markets.* New York, NY, USA: Springer-Verlag Inc., 2012.

[36] Y. Zhang, N. Gatsis, and G. B. Giannakis, "Robust energy management for microgrids with high-penetration renewables," *IEEE Trans. Sustain. Energy*, vol. 4, no. 4, pp. 944–953, Oct 2013.

[37] C. Gellings, "The concept of demand-side management for electric utilities," *Proc. IEEE*, vol. 73, no. 10, pp. 1468–1470, Oct. 1985.

[38] D. Weers and M. Shamsedin, "Testing a new direct load control power line communication system," *IEEE Trans. Power Delivery*, vol. 2, no. 3, pp. 657–660, July 1987.

[39] J. Chen, F. Lee, A. Breipohl, and R. Adapa, "Scheduling direct load control to minimize system operation cost," *IEEE Trans. Power Syst.*, vol. 10, no. 4, pp. 1994–2001, Nov 1995.

[40] S. Kim and G. B. Giannakis, "Scalable and robust demand response with mixed-integer constraints," *IEEE Trans. Smart Grid*, vol. 4, no. 4, pp. 2089–2099, Dec 2013.

[41] C. Triki and A. Violi, "Dynamic pricing of electricity in retail markets," *A Quart. J. Operat. Res. (4OR)*, vol. 7, no. 1, pp. 21–36, 2009.

[42] L. P. Qian, Y. J. A. Zhang, J. Huang, and Y. Wu, "Demand response management via real-time electricity price control in smart grids," *IEEE J. Sel. Areas Comm.*, vol. 31, no. 7, pp. 1268–1280, July 2013.

[43] F. Rahimi and A. Ipakchi, "Demand response as a market resource under the smart grid paradigm," *IEEE Trans. Smart Grid*, vol. 1, no. 1, pp. 82–88, June 2010.

[44] H. Lee Willis and L. Philipson, *Understanding Electric Utilities and De-Regulation.* Boca Raton, FL, USA: CRC Press, 2005.

[45] M. A. A. Pedrasa, T. D. Spooner, and I. F. MacGill, "Coordinated scheduling of residential distributed energy resources to optimize smart home energy services," *IEEE Trans. Smart Grid*, vol. 1, no. 2, pp. 134–143, Sept. 2010.

[46] G. Carpinelli, G. Celli, S. Mocci, F. Mottola, F. Pilo, and D. Proto, "Optimal integration of distributed energy storage devices in smart grids," *IEEE Trans. Smart Grid*, vol. 4, no. 2, pp. 985–995, June 2013.

[47] P. Vytelingum, T. D. Voice, S. D. Ramchurn, A. Rogers, and N. R. Jenning, "Agent-based micro-storage management for the smart grid," in *Int. Conf. on Auton. Agents and Multiagent Syst. (AAMAS)*, May 2010.

[48] K. Clement-Nyns, E. Haesen, and J. Driesen, "The impact of charging plug-in hybrid electric vehicles on a residential distribution grid," *IEEE Trans. Power Syst.*, vol. 25, no. 1, pp. 371–380, Feb. 2010.

[49] A. Kwasinski and A. Kwasinski, "Signal processing in the electrification of vehicular transportation: Techniques for electric and plug-in hybrid electric vehicles on the smart grid," *IEEE Signal Process. Mag.*, vol. 29, no. 5, pp. 14–23, Sept. 2012.

[50] B. G. Kim, S. Ren, M. Van Der Schaar, and J. W. Lee, "Bidirectional energy trading and residential load scheduling with electric vehicles in the smart grid," *IEEE J. Sel. Areas Comm.*, vol. 31, no. 7, pp. 1219–1234, July 2013.

[51] A.-H. Mohsenian-Rad, V. Wong, J. Jatskevich, R. Schober, and A. Leon-Garcia, "Autonomous demand-side management based on game-theoretic energy consumption scheduling for the future smart grid," *IEEE Trans. Smart Grid*, vol. 1, no. 3, pp. 320–331, Dec. 2010.

[52] A.-H. Mohsenian-Rad and A. Leon-Garcia, "Optimal residential load control with price prediction in real-time electricity pricing environments," *IEEE Trans. Smart Grid*, vol. 1, no. 2, pp. 120–133, Sept. 2010.

[53] M. Alizadeh, A. Scaglione, and R. Thomas, "From packet to power switching: Digital direct load scheduling," *IEEE J. Sel. Areas Comm.*, vol. 30, no. 6, pp. 1027–1036, July 2012.

[54] N. Gatsis and G. B. Giannakis, "Decomposition algorithms for market clearing with large-scale demand response," *IEEE Trans. Smart Grid*, vol. 4, no. 4, pp. 1976–1987, Dec. 2013.

[55] M. Albadi and E. El-Saadany, "Demand response in electricity markets: An overview," in *IEEE Power Eng. Soc. Gen. Meet.*, June 2007, pp. 1–5.

[56] A. J. Conejo, J. M. Morales, and L. Baringo, "Real-time demand response model," *IEEE Trans. Smart Grid*, vol. 1, no. 3, pp. 236–242, Dec. 2010.

[57] J. H. Chow, W. De Mello, and K. W. Cheung, "Electricity market design: An integrated approach to reliability assurance," *Proc. IEEE*, vol. 93, no. 11, pp. 1956–1969, Nov. 2005.

[58] A.-H. Mohsenian-Rad, V. Wong, J. Jatskevich, and R. Schober, "Optimal and autonomous incentive-based energy consumption scheduling algorithm for smart grid," in *IEEE Inn. Smart Grid Technol. (ISGT)*, Jan. 2010, pp. 1–6.

[59] P. Samadi, H. Mohsenian-Rad, R. Schober, and V. W. S. Wong, "Advanced demand side management for the future smart grid using mechanism design," *IEEE Trans. Smart Grid*, vol. 3, no. 3, pp. 1170–1180, 2012.

[60] P. Samadi, H. Mohsenian-Rad, V. W. S. Wong, and R. Schober, "Tackling the load uncertainty challenges for energy consumption scheduling in smart grid," *IEEE Trans. Smart Grid*, vol. 4, no. 2, pp. 1007–1016, June 2013.

[61] N. Li, L. Chen, and S. H. Low, "Optimal demand response based on utility maximization in power networks," in *IEEE Power Eng. Soc. Gen. Meet.*, July 2011, pp. 1–8.

[62] S. Boyd and L. Vandenberghe, *Convex Optimization*. New York, NY, USA: Cambridge University Press, 2004.

[63] R. Rockafellar, *Convex Analysis*. Princeton, NJ, USA: Princeton University Press, 1970.

[64] D. P. Bertsekas, *Convex Analysis and Optimization*. Belmont, MA, USA: Athena Scientific Press, 2003.

[65] M. J. Osborne and A. Rubinstein, *A Course in Game Theory*. Cambridge, MA, USA: MIT Press, 2004.

[66] G. Scutari and D. P. Palomar, "MIMO cognitive radio: A game theoretical approach," *IEEE Trans. on Signal Process.*, vol. 58, no. 2, pp. 761–780, Feb. 2010.

[67] G. Scutari, D. P. Palomar, and S. Barbarossa, "Optimal linear precoding strategies for wideband noncooperative systems based on game theory—Part I & II: Nash Equilibria & Algorithms," *IEEE Trans. on Signal Process.*, vol. 56, no. 3, pp. 1230–1249 & 1250–1267, Mar. 2008.

[68] ——, "Competitive design of multiuser MIMO systems based on game theory: A unified view," *IEEE J. Sel. Areas Comm.*, vol. 26, no. 7, pp. 1089–1103, Sept. 2008.

[69] ——, "The MIMO iterative waterfilling algorithm," *IEEE Trans. on Signal Process.*, vol. 57, no. 5, pp. 1917–1935, May 2009.

[70] W. Saad, H. Zhu, H. Poor, and T. Basar, "Game-theoretic methods for the smart grid: An overview of microgrid systems, demand-side management, and smart grid communications," *IEEE Signal Process. Mag.*, vol. 29, no. 5, pp. 86–105, Sept. 2012.

[71] Z. M. Fadlullah, Y. Nozaki, A. Takeuchi, and N. Kate, "A survey of game theoretic approaches in smart grid," in *IEEE Int. Conf. Wireless Comm. and Signal Process. (WCSP)*, Nov. 2011, pp. 1–4.

[72] C. Ibars, M. Navarro, and L. Giupponi, "Distributed demand management in smart grid with a congestion game," in *IEEE Int. Conf. Smart Grid Comm. (SmartGridComm)*, Oct. 2010, pp. 495–500.

[73] C. Chen, S. Kishore, and L. Snyder, "An innovative RTP-based residential power scheduling scheme for smart grids," in *IEEE Int. Conf. Acoust., Speech, Signal Process. (ICASSP)*, May 2011, pp. 5956–5959.

[74] G. Scutari, D. P. Palomar, F. Facchinei, and J.-S. Pang, "Monotone games for cognitive radio systems," in *Distributed Decision-Making and Control*. New York, NY, USA: Springer-Verlag Inc., 2011.

[75] F. Facchinei and C. Kanzow, "Generalized Nash equilibrium problems," *A Quart. J. Operat. Res. (4OR)*, vol. 5, no. 3, pp. 173–210, Sep. 2007.

[76] G. Scutari, F. Facchinei, J.-S. Pang, and D. P. Palomar, "Real and complex monotone games," *IEEE Trans. Inf. Theory*, 2014, to be published.

[77] F. Facchinei and J.-S. Pang, *Finite-Dimensional Variational Inequalities and Complementarity Problems*. New York, NY, USA: Springer-Verlag Inc., 2003.

[78] ——, "Nash equilibria: the variational approach," in *Convex Optimization in Signal Processing and Communication*. London, UK: Cambridge University Press, 2009, ch. 11, pp. 443–493.

[79] G. Scutari, D. P. Palomar, F. Facchinei, and J.-S. Pang, "Convex optimization, game theory, and variational inequality theory," *IEEE Signal Process. Mag.*, vol. 27, no. 3, pp. 35–49, May 2010.

[80] D. P. Palomar and M. Chiang, "Alternative distributed algorithms for network utility maximization: Framework and applications," *IEEE Trans. Automatic Control*, vol. 52, no. 12, pp. 2254–2269, Dec. 2007.

[81] C. Sagastizábal, "Divide to conquer: decomposition methods for energy optimization," *Mathematical Programming*, vol. 134, no. 1, pp. 187–222, 2012.

[82] G. Scutari, F. Facchinei, P. Song, D. P. Palomar, and J.-S. Pang, "Decomposition by partial linearization: Parallel optimization of multiuser systems," *IEEE Trans. Signal Process.*, vol. 62, no. 3, pp. 641–656, Feb. 2014.

[83] G. Scutari, D. P. Palomar, F. Facchinei, and J.-S. Pang, "Distributed dynamic pricing for MIMO interfering multiuser systems: A unified approach," in *5th Int. Conf. on Netw. Games, Control and Optimiz. (NetGCooP)*, Oct. 2011, pp. 1–5.

[84] I. Atzeni, L. G. Ordóñez, G. Scutari, D. P. Palomar, and J. R. Fonollosa, "Demand-side management via distributed energy generation and storage optimization," *IEEE Trans. Smart Grid*, vol. 4, no. 2, pp. 866–876, June 2013.

[85] ——, "Noncooperative and cooperative optimization of distributed energy generation and storage in the demand-side of the smart grid," *IEEE Trans. Signal Process.*, vol. 61, no. 10, pp. 2454–2472, May 2013.

[86] ——, "Day-ahead bidding strategies for demand-side expected cost minimization," in *IEEE Int. Conf. Smart Grid Comm. (SmartGridComm)*, Nov. 2012, pp. 91–96.

[87] ——, "Cooperative day-ahead bidding strategies for demand-side expected cost minimization," in *IEEE Int. Conf. Acoust., Speech, Signal Process. (ICASSP)*, May 2013, pp. 5224–5228.

[88] ——, "Noncooperative day-ahead bidding strategies for demand-side expected cost minimization: A GNEP approach," *IEEE Trans. Signal Process.*, vol. 62, no. 9, pp. 2397–2412, May 2014.

[89] T. Orfanogianni and G. Gross, "A general formulation for LMP evaluation," *IEEE Trans. Power Syst.*, vol. 22, no. 3, pp. 1163–1173, 2007.

[90] J.-S. Pang and M. Fukushima, "Quasi-variational inequalities, generalized Nash equilibria, and multi-leader-follower games," *Comput. Manag. Sci.*, vol. 6, no. 3, pp. 373–375, Aug. 2009.

[91] K. Kubota and M. Fukushima, "Gap function approach to the generalized Nash equilibrium problem," *J. Optimiz. Theory, Appl.*, vol. 144, pp. 511–531, 2010.

[92] Communication from the Commission to the European Parliament, the Council, the European Economic and Social Committee, and the Committee of the Regions, "Smart grids: From innovation to deployment," European Commission, Tech. Rep., Apr. 2011.

[93] IEA Demand Side Management Programme, "Integration of demand side management, distributed generation, renewable energy sources and energy storages," International Energy Agency, Tech. Rep., 2008.

[94] P. Samadi, A.-H. Mohsenian-Rad, R. Schober, V. W. S. Wong, and J. Jatskevich, "Optimal real-time pricing algorithm based on utility maximization for smart grid," in *IEEE Int. Conf. Smart Grid Comm. (SmartGridComm)*, Oct. 2010, pp. 415–420.

[95] M. Roozbehani, M. Dahleh, and S. Mitter, "Dynamic pricing and stabilization of supply and demand in modern electric power grids," in *IEEE Int. Conf. Smart Grid Comm. (SmartGridComm)*, Oct. 2010, pp. 543–548.

[96] S. Suryanarayanan, F. Mancilla-David, J. Mitra, and Y. Li, "Achieving the smart grid through customer-driven microgrids supported by energy storage," in *IEEE Int. Conf. on Ind. Techn. (ICIT)*, Mar. 2010, pp. 884–890.

[97] A. Mohd, E. Ortjohann, A. Schmelter, N. Hamsic, and D. Morton, "Challenges in integrating distributed energy storage systems into future smart grid," in *IEEE Int. Symp. Ind. Electron. (ISIE)*, July 2008, pp. 1627–1632.

[98] C. Kwang-Cheng, Y. Ping-Cheng, H. Hung-Yun, and C. Shi-Chung, "Communication infrastructure of smart grid," in *Int. Symp. Comm., Control and Signal Process. (ISCCSP)*, Mar. 2010, pp. 1–5.

[99] Department of Energy and Climate Change, "Sub-national Electricity Consumption Data," Tech. Rep., 2009. [Online]. Available: http://www.decc.gov.uk/en/content/cms/statistics/regional/electricity/electricity.aspx

[100] ——, "Energy Price Statistics," Tech. Rep., 2009. [Online]. Available: http://www.decc.gov.uk/en/content/cms/statistics/prices/prices.aspx

[101] R. Walt, "The BioMax™: A new biopower option for distributed generation and CHP," in *IEEE Power Eng. Soc. Gen. Meet.*, vol. 2, June 2004, pp. 1653–1656.

[102] Biomass Energy Centre, "Fuel Costs per kWh," Tech. Rep., 2011. [Online]. Available: http://www.biomassenergycentre.org.uk

[103] C. Mi, L. Ben, D. Buck, and N. Ota, "Advanced electro-thermal modeling of lithium-ion battery system for hybrid electric vehicle applications," in *IEEE Veh. Power and Prop. Conf. (VPPC)*, Sept. 2007, pp. 107–111.

[104] A. Papalexopoulos and H. Singh, "Alternative design options for a real-time balancing market," in *IEEE Int. Conf. Power Ind. Comp. Appl. (PICA)*, May 2001, pp. 272–277.

[105] H. Miao, S. Murugesan, and Z. Junshan, "Multiple timescale dispatch and scheduling for stochastic reliability in smart grids with wind generation integration," in *IEEE INFOCOM*, Apr. 2011, pp. 461–465.

[106] G. Scutari, D. P. Palomar, and S. Barbarossa, "Competitive optimization of cognitive radio MIMO systems via game theory," in *Convex Optimization in Signal Processing and Communication.* London, UK: Cambridge University Press, 2009, ch. 11.

[107] S. Bu, F. R. Yu, and P. X. Liu, "Stochastic unit commitment in smart grid communications," in *IEEE INFOCOM Workshops*, Apr. 2011, pp. 307–312.

[108] G. M. Masters, *Renewable and Efficient Electric Power Systems.* New York, NY, USA: John Wiley & Sons, Inc., 2005.

[109] D. P. Bertsekas and J. N. Tsitsiklis, *Parallel and Distributed Computation: Numerical Methods*, 2nd ed. Belmont, MA, USA: Athena Scientific Press, 1989.

[110] M. Abramowitz and I. A. Stegun, *Handbook of Mathematical Functions, with Formulas, Graphs, and Mathematical Tables.* Dover, 1972.

[111] S.-E. Fleten and E. Pettersen, "Constructing bidding curves for a price-taking retailer in the Norwegian electricity market," *IEEE Trans. Power Syst.*, vol. 20, no. 2, pp. 701–708, May 2005.

[112] W. Zhongping and F. Heng, "Bidding strategy for day-ahead and real-time markets based on newsvendor method in electricity markets," in *IEEE Int. Conf. Inf. Sci., Manag. Eng. (ISME)*, vol. 2, Aug. 2010, pp. 310–313.

[113] A. Baillo, S. Cerisola, J. Fernandez-Lopez, and R. Bellido, "Strategic bidding in electricity spot markets under uncertainty: a roadmap," in *IEEE Power Eng. Soc. Gen. Meet.*, 2006, pp. 1–8.

[114] R. Herranz, A. Munoz San Roque, J. Villar, and F. Campos, "Optimal demand-side bidding strategies in electricity spot markets," *IEEE Trans. Power Syst.*, vol. 27, no. 3, pp. 1204–1213, Aug. 2012.

[115] J. Contreras, O. Candiles, J. De La Fuente, and T. Gómez, "Auction design in day-ahead electricity markets," *IEEE Trans. Power Syst.*, vol. 16, no. 1, pp. 88–96, Feb. 2001.

[116] F. Facchinei, A. Fischer, and V. Piccialli, "On generalized Nash games and variational inequalities," *Operat. Res. Letters*, vol. 35, no. 2, pp. 159–164, 2007.

[117] P. T. Harker, "Generalized Nash games and quasi-variational inequalities," *Eur. J. Operat. Res.*, vol. 54, no. 1, pp. 81–94, 1991.